UTS UNIVERSITY OF TECHNOLOGY SYDNEY

Optimising Landfill Settlement Prediction to Cater for Transport Infrastructure on Closed Landfills

by Michael Vinod

Thesis submitted in fulfilment of the requirements for the degree of

Doctor of Philosophy

under the supervision of Prof Hadi Khabbaz
A/Prof Behzad Fatahi

University of Technology Sydney
Faculty of Engineering and Information Technology

March 2023

Certificate of Original Authorship

I, Michael Vinod, declare that this thesis is submitted in fulfilment of the requirements for the award of Doctor of Philosophy, in the School of Civil and Environmental Engineering for the Faculty of Engineering and Information Technology at the University of Technology Sydney.

This thesis is wholly my own work unless otherwise referenced or acknowledged. In addition, I certify that all information sources and literature used are indicated in the thesis.

This document has not been submitted for qualifications at any other academic institution.

This research is supported by the Australian Government Research Training Program.

Production Note:
Signature removed prior to publication.

Michael Vinod
06 March 2023

Acknowledgement

I would like to sincerely thank Professor Hadi Khabbaz for his guidance over the past four years. His patience, availability and encouragement helped me develop throughout the PhD journey. It has been a great pleasure working with my co-supervisor Associate Professor Behzad Fatahi. His invaluable suggestions and attention to detail assisted in improving the quality of the work significantly. I am thankful to both for making this an enjoyable learning experience, which I can carry throughout my career as a geotechnical engineer.

I would like to thank Dr Lam Nguyen and Hossein Haddad for their support in the laboratory with setting up tests, brainstorming, monitoring and problem solving.

Thank you to Dr Jeff Hsi and Idy Li from EIC Activities (member of the CIMIC group) for both their technical guidance and financial support throughout the course of the PhD.

Special thanks to Ben Scott, Hamish Ford, Colin Archambault and Charles Ferlat from Geomotion Australia for their support over the past 3 years from assisting with planning the instrumentation to installation and long term monitoring.

Thank you to all the friends who supported me throughout the PhD journey. The encouragement really helped me to get across the finish line.

Finally, the greatest thanks goes to my mother, father, sister and brother in-law for their constant support from the very beginning. It would not have been possible to undertake 4 days of full time work and 3 days of part time PhD without their special care and support throughout the intense months, which gave me the ultimate focus. Thanks for inspiration to finish this thesis by my sister and the occasional gaming sessions to calm my mind with my brother in-law.

Journal Publications in the Pipeline

- Vinod, M., Haddad, H. Khabbaz, H., Fatahi, B., Li, I., Hsi, J. 2022. Field Investigation for Redevelopment Projects on Closed Landfill Sites with Reference to a Landfill in Sydney. (under review)

- Vinod, M. Khabbaz, H., Fatahi, B., Hsi, J. 2022. Measuring Strength and Compressibility Characteristics of Landfill Waste Using Multistage Consolidated-Drained Triaxial Test (under review)

- Vinod, M. Khabbaz, H., Fatahi, B., Hsi, J. 2022. Undisturbed versus disturbed response of landfill in multistage triaxial testing considering creep. (under review)

- Vinod, M. Khabbaz, H., Fatahi, B., Hsi, J. 2022. Small strain to large strain correlation using Hall Effect gauge in unconsolidated undrained test (under review)

- Vinod, M. Khabbaz, H., Fatahi, B., Hsi, J. 2022. Landfill settlement prediction and monitoring with reference to a landfill in Sydney. (under review)

It can be noted that due to the lengthy process for getting industry approval, publishing the papers has been delayed.

Table of Contents

List of Figures

List of Tables

Nomenclature

Greek letters

$\frac{\Psi}{v_0}$	creep index measured in natural logarithm scale of time
γ_d	dry unit weight of waste
γ_i	unit weight of lift
ε_a	axial strain
ε_b	strain due to biodegradation
ε_c	strain due to creep
ε_i^c	time-dependent creep strain
ε_i^d	degradation induced strain
ε_i^e	elastic strain
ε_i^p	plastic strain
ε_p	strain due to instantaneous loading
ε_r	radial strain
ε_{sh}	shear strain
ε	Total strain
$\varepsilon(t)_{dec}$	total compression strain due to biodegradation
$\varepsilon(t)_{mec}$	mechanical creep strain
$\frac{\lambda}{b}$	rate of secondary compression
λ_j	first-order kinetic constant for the jth group
ρ	density of the landfill
ρ_d^0	initial global dry density
ρ_{so}^0	initial solid organic dry density
ρ_w	density of water
σ_0	existing overburden pressure at the middle of the waste layer
σ_0	average normal stress below the plate
σ_{0max}	maximum normal stress below the plate
ΔH	total settlement
$(\Delta H)_b$	biodegradation induced settlement

$(\Delta H)_m$	mechanical compression
ΔM	mass of organics biodegraded from the beginning of placement (i. e. $\Delta M = M_o - M(t)$)
Δq	increase in overburden pressure acting at the middle of the layer
ϕ'	Effective friction angle
k	recompression index
v	Poisson's ratio
δ	average plate settlement
λ	compression ratio

Latin letters

A_{cp}	influence area for each location (square root of the grid spacing)
a_0, a_1, a_2	constants calculated from the plate pressure vs settlement curve using the fitting method proposed in the DIN standard
a	primary compressibility index
b	secondary compressibility index
C	gas produced per unit mass of organic material biodegraded
C^*	compressibility parameter
C_c	primary compression ratio
C'_c	$\frac{C_c}{1+e_0}$
c	secondary mechanical compression rate
c	initial gravimetric solid organic content
c'	Effective cohesion
c_k	permeability change index
C_u	coefficient of uniformity
C_v	coefficient of consolidation
C_α	creep coefficient $\frac{\Delta e}{\Delta(Log t)}$
$C_{\alpha f}$	final creep
$C_{\alpha\varepsilon M}$	total secondary compression ratio $\frac{C_\alpha}{1+e_0}$
C_β	biodegradation creep
D	depth of influence

D	plate diameter
D_{10}	diameter through which 10% of soil can pass through
D_{90}	diameter through which 90% of the grout mass passes
d	secondary biodegradation compression rate
E_{dg}	total compression due to waste degradation
E_{max}	small strain Young's modulus
E_{ref}	reference secant Young's modulus
E_s	elastic modulus of waste material
E_s	Young's Modulus
E_s	secant Young's modulus
E_{v1}	strain modulus during the first loading cycle
E_{v2}	strain modulus during unloading /reloading cycles
e	void ratio
e_0	initial void ratio
f_{sj}	initial solids fraction for each waste
$G\ (t)$	volume of gas produced for the entire landfill at time t
G_0	small strain shear modulus
G_{max}	small strain shear modulus
G_{sj}	specific gravity of jth group of waste solids
g	gravitational acceleration
h	drop height
H_o	initial waste thickness
K	bulk viscosity of the solid waste
k	gas generation rate
k	weighted biodegradation rate
k	hydraulic conductivity
k_0	initial coefficient of permeability
k_m	biodegradation rates for moderately biodegradable materials
k_r	biodegradation rates for readily biodegradable materials
k_s	biodegradation rates for slowly biodegradable materials
L_o	methane gas generation potential

M	frictional constant
M	gradient of failure envelope
$M\ (t)$	mass of biodegradable landfill (tonnes) remaining at time t
M_o	initial biodegradable mass of landfill (tonnes) at time t = 0
m	percentage of moderately biodegradable materials
m_v	coefficient of volume change
N	number of drops
N	groutability of the soil
N'	rate of compression
n	empirical coefficient factor combining soil composition and water table
n, m	constants depending on the material
OCR	overconsolidation ratio
OW	organic waste content
P	number of passes
P_g	gas pressure
P_l	liquid pressure
p'	mean effective stress
p'_f	Mean effective stress at failure
p_0	initial settlement rate
p'_0	pre-consolidation pressure
p_{ref}	reference mean effective stress
q	deviatoric stress
q_f	Deviatoric stress at failure
Q	applied load at centre of plate
R_α	stress relaxation parameter
r	percentage of readily biodegradable materials
r	plate radius
S_g	gas phase saturation
S_i	initial settlement
S_l	liquid phase saturation
S_{ult}	ultimate settlement

s	percentage of slowly biodegradable materials
t''	time elapsed since waste disposal
t_1	time for completion of primary settlement
t_2	ending time period
t_{oB}	start of biodegradation time
t_{oM}	initial time when primary compression is finished
V_p	primary wave (P-wave) velocity
V_s	shear wave (S-wave) velocity
$^{w}/_{c}$	water to cement ratio of the grout
w	block weight
Y	vertical strain rate

Acronyms and Abbreviations

Abbreviation	Term
CD	Consolidated drained triaxial test
CP	Confining pressure
CPT	Cone Penetration Test
CU	Consolidated undrained triaxial test
EPA	Environmental Protection Agency
FLAC	Fast Lagrangian Analysis of Continua
GPR	Ground Penetrating Radar
HEIC	High Energy Impact Compaction
HPD	High Pressure Dilatometer
InSAR	Interferometric Synthetic Aperture Radar
IPCC	Inter-governmental Panel on Climate Change
LiDAR	Light Detection and Ranging
LL	Liquid Limit
LLT	lateral load test pressuremeter
LVDT	Linear Variable Displacement Transducer
MASW	Multi-channel Analysis of Surface Waves
MSW	Municipal solid waste
NGER	National Greenhouse and Energy Reporting
PBP	pre-bored pressuremeter
PI	Plasticity Index
PIP	push-in pressuremeter
PL	Plastic Limit
PSD	Particle size distribution
PVD	Prefabricated Vertical Drains
RCPTu	Resistivity Cone Penetration Test with pore pressure
RIC	Rapid Impact Compaction
SASW	Spectral Analysis of Surface Waves

SBP	self-boring pressuremeter
SCPTu	Seismic Cone Penetration Test with pore pressure
SMDT	Seismic Dilatometer test
SPT	Standard Penetration Test
VSP	Vertical Seismic Profiling
WCI	Waste compressibility index

Abstract

As urban development increases in major cities, there is an increasing trend in development above closed landfill sites. Waste mechanics and properties have been studied for decades by many researchers, and the current approach by practicing geotechnical engineers is heavily reliant on assuming parameters from the literature. However, due to the heterogeneous nature of waste, age, stiffness, climatic conditions, compaction, composition and variability among different landfill sites, the application of research studies towards assessing settlement from structures built above landfills is complex.

This research is focussed on developing a practical and consistent approach utilising site investigation techniques and geotechnical laboratory testing to reasonably predict landfill settlement. The research is supported by a case study at a landfill in Sydney. The key field investigations undertaken included the collection of over 90 m of 100 mm diameter sonic drilling cores, test pitting over 5 tonnes of landfill, undisturbed and disturbed sampling for further testing in the laboratory, plate load testing, multi-channel analysis of surface waves (MASW), LIDAR and vertical seismic profiling.

In this study, waste material, estimated to be aged between 18-31 years old, was collected from a landfill at a depth of 8 - 10 m using the sonic drilling technique. A multistage consolidated drained (CD) triaxial test was undertaken on a reconstituted sample to obtain design parameters for settlement prediction including friction angle, cohesion, modulus, compression indices (λ and κ), pre-consolidation pressure, over-consolidation ratio, permeability and long-term creep through constant stress creep and stress relaxation methods for the waste material.

To demonstrate the benefits of undertaking site specific testing, settlement predictions were undertaken using existing 1D settlement prediction models and PLAXIS 2D. Predictions were validated with an embankment at the landfill that was instrumented using settlement cells and extensometers and monitored for a period of 2 years. Satellite monitoring using interferometric synthetic aperture radar (InSAR) was undertaken using the European Space Agency's (ESA) Sentintel-1 satellite. The InSAR technique proved to be a

low cost and effective method for long-term measurement of landfill settlement. Comparison of the settlement predictions using the field monitoring data and laboratory testing data exhibited a sound correlation with field monitoring data when initial settlement was corrected.

Chapter 1 – Introduction

1.1 Overview

The management of solid waste has become a global issue due to increasing populations and rapid urbanisation resulting in higher waste production. The current and most common method for waste disposal is through landfilling. With increasing the waste generation rates, there is a growing need for high capacity landfill areas in close proximity to urban areas.

Figure 1.1 Landfill in Western Sydney (photo taken by the Author)

The availability of space in urban areas is becoming scarce resulting in development above or adjacent to old landfills in urban areas. However, development above or adjacent landfills is challenging due to the relatively complex behaviour of waste material including its heterogeneous nature and presence of organic matter. Accordingly, it is critical to quantify and assess geotechnical and environmental considerations prior to prevent failure of infrastructure above or adjacent to landfill. Key issues related to failure of infrastructure can include differential settlement, stability, leachate and gas generation, creep settlement and waste behaviour under loading.

1.2 Problem statement

Many landfills both closed and operational are located near urban areas as shown in Figure 1.2. These landfills often consume large areas and pose as a prime opportunity for

redevelopment upon landfill closure. However, the geotechnical properties of landfill material is variable leading to complex behaviour. Common issues that are encountered at a landfill site include differential settlement, creep, biodegradation and long term environmental issues including generation of leachate and gas.

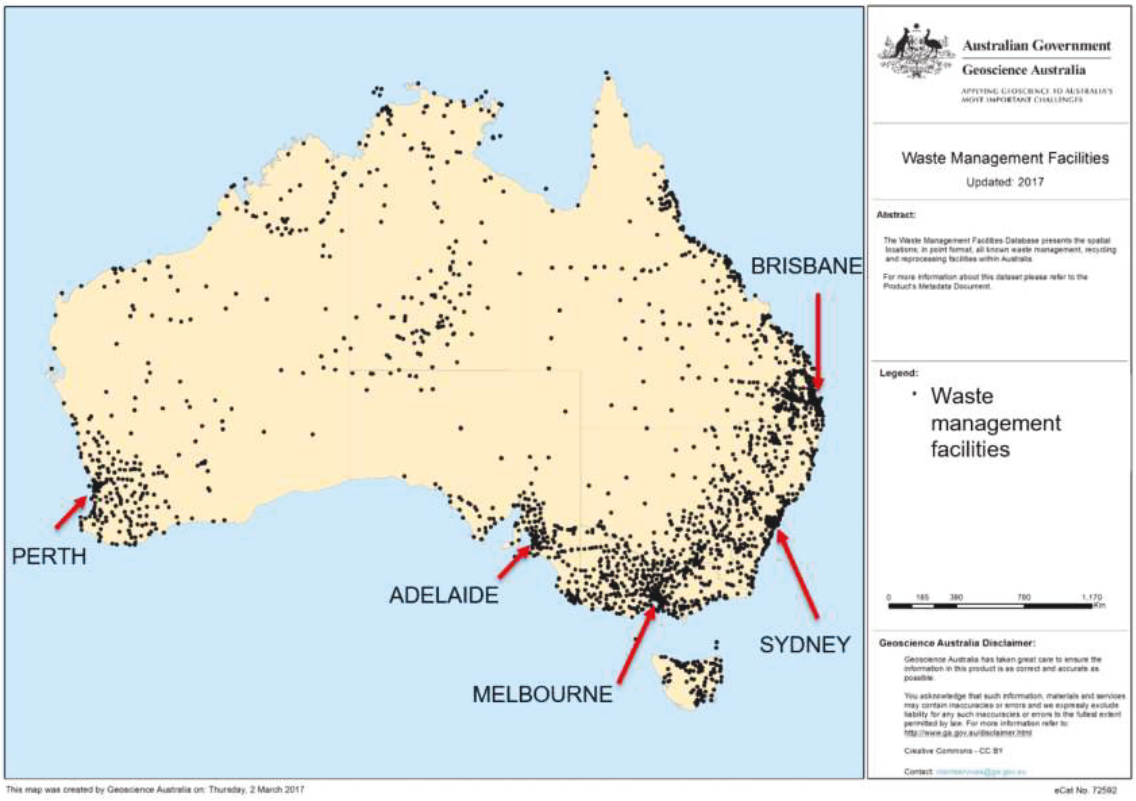

Figure 1.2 Waste management facilities across Australia (Geoscience Australia, 2017)

The complex behaviour of waste material in landfills poses as a significant issue for redevelopment above closed landfills. The current procedure adopted by practicing engineers include referencing published consolidation parameters for prediction of settlement, without adequate site specific field testing. These consolidation parameters are dependent on a number of factors, which can include geographical location, climate, waste composition and waste thickness. As a result of this desktop study approach, the landfill settlement prediction is often overly conservative and requires extensive ground improvement measures to mitigate this potential settlement.

The existing settlement models adopted by practicing engineers is very simplified for landfill material. These settlement models do not incorporate a number of factors such as

settlement under self-weight, surcharge and traffic loading. The current models do not include a number of critical parameters that are known to effect landfill settlement, including the moisture content, the landfill gas, the saturation condition of waste, the creep rare, and the biodegradation of putrescible materials.

The current state for waste generated by the Australian households is that all non-recyclable materials are disposed in landfills. Therefore, there is a growing need for more landfills for waste disposal until an alternative waste disposal procedure is discovered. With this demand for high capacity landfills close to urban areas, redevelopment post-closure above or adjacent to closed / operational landfills is becoming increasingly common.

As a result, it is necessary to establish proper approaches for practicing geotechnical engineers to design foundations of structures and infrastructure on closed landfills through development of meticulous field investigation procedures, where parameters are used in a more thorough settlement prediction model.

1.3 Objectives and scope of research

1.3.1 Research objectives

The main goal of the project is to be able to predict closed landfills settlement under transport infrastructure loading and obtain landfill properties. Research objectives are summarised into three categories including numerical modelling, field investigation and monitoring, and laboratory testing. The research objectives for the project include:

a) Understanding waste behaviour and obtaining waste properties (strength and compressibility)
b) Predicting landfill settlement using parameters obtained
c) Developing guidelines and an approach to design above or adjusted to closed landfills using planned site investigation that inputs into the predictive models

1.3.2 Scope of work

The scope for the project includes:

a) Undertaking site investigation and field monitoring (settlement cells and extensometers) as well as satellite monitoring of settlement through InSAR at a landfill in Sydney. This forms the case study for this project.
b) Laboratory testing through multistage triaxial testing to determine strength and compressibility properties of landfill material extracted from a landfill in Sydney.
c) Use of parameters obtained from laboratory testing in the prediction of landfill settlement as well as back calculation from field data. This includes employing existing settlement models as well as PLAXIS 2D software to predict settlement. This shall be compared against the field data collected.

1.4 Outline of thesis

This thesis comprises of eight chapters, which are structured as follows:

- Chapter 1 – brief introduction about issues associated with constructing infrastructure above closed landfills along with the objectives and scope of this study
- Chapter 2 – presents a comprehensive literature review on landfills and associated aspects with construction above closed landfills including site investigation techniques, available landfill settlement models and ground improvement techniques
- Chapter 3 – details findings from the site investigation and sample collection at the case study location at a landfill in Sydney. Site investigation techniques discussed in this chapter include test pitting, downhole geophysics, multi-channel analysis of surface waves, LiDAR, gas pumping trial and plate load testing. Field testing results are translated into critical design parameters including unit weight, moisture content, organic content, small strain shear modulus, small strain Young's modulus, biodegradation rate and age of waste. Sample collection includes undisturbed sampling with push tubes within test pits taken from the surface of the landfill.
- Chapter 4 – compressibility and strength parameters of reconstituted landfill material obtained from a depth of 8-10m below the landfill surface through a multi-stage consolidated drained triaxial test.
- Chapter 5 – a comparison between compressibility and strength of undisturbed and reconstituted landfill material obtained from the landfill surface is described through a multi-stage consolidated undrained triaxial tests.

- Chapter 6 – findings from unconfined compressive strength (UCS) testing with Hall Effect testing on relatively undisturbed material from various landfill depths is presented. The combination of UCS and Hall Effect testing allows for determination of the ratio between small strain parameters typically obtained from field geophysics to the large strain parameter (Young's modulus) that is required for landfill settlement prediction.
- Chapter 7 – provides validation of the need for site specific testing to predict landfill settlement with reasonable accuracy. 1-D landfill settlement models and PLAXIS 2D are used to predict the landfill settlement with inputs from site-specific laboratory tests. 1D and 2D predictions are compared with data obtained over a 2-year period from field monitoring equipment comprising of settlement cells and extensometers installed at the case study site of a landfill in Sydney. Furthermore, remote satellite monitoring through use of interferometric synthetic aperture radar (InSAR) is validated with the settlement cells to provide a cost-effective monitoring technique.
- Chapter 8 – a summary of the thesis is provided along with the conclusions and recommendations for further research.

Chapter 2 – Literature Review

This chapter describes aspects of construction above closed landfills including site investigation techniques, available landfill settlement models and ground improvement techniques.

2.1 Landfill types, components and waste composition

2.1.1 Landfill types

Landfills are engineered waste disposal facilities. These facilities are built in compliance with government regulations and are monitored to ensure environmental contamination (leachate and gas) is not an issue. There are a few types of landfills, each varying based on the type of waste accepted for disposal. EPA(USA) (2018) describes three main types of landfills including:

- Municipal solid waste landfills – solid waste landfills
    - Bioreactor landfills – accelerated decomposition of organic waste
- Industrial waste landfills
    - Construction and demolition waste landfills – construction materials including brick, concrete, wood etc.
    - Coal combustion residual landfills – residual waste from coal combustion and coal ash
- Hazardous waste landfills – laboratory waste, chemical waste, radiological waste and other special waste

Note that some landfills combine municipal solid waste with construction waste. Hazardous waste landfills cannot accept municipal solid waste since these landfills are specially designed to contain only hazardous waste.

2.1.2 Waste classification

Landva & Clark (1986b) were the pioneers for waste classification. They provided a split for classification of landfill material based on dry unit weight and material type. These three categories included inorganic non-degradable material (soil, bricks, concrete, glass and

metal), non-putrescible organic (wood, timber, plastic, textile, foam, rubber) and putrescible (paper, organic material, anything unidentifiable). This provided a classifying waste material for landfill settlement calculation.

The residual biodegradation process is dependent on the age of the landfill material. This can be completed using aerial imagery and historical information from landfill operators. Landfill operators should maintain accurate records for waste composition for all landfills to ensure accurate information is available for design above closed landfills.

Current methods make determination of landfill material based on visual assessment only, with limited testing on the landfill material for composition by dry weight. Part of this is understandably due to the cost of testing and paperwork required for transportation of landfill material to a laboratory, however for the accurate calculation of settlement it is necessary to undertake such testing similar to any other soil / rock from a geotechnical perspective.

2.1.3 Waste composition and properties

Landfills are biologically active for a period of at least 20-25 years following completion of landfilling. Biological activity refers to the generation of landfill gas. Van Impe & Bouazza (1996) compiled statistics on the type of waste material forming landfills. Referring to Table 2.1, the components of waste is variable between cities and countries, which emphasises the importance of undertaking site specific testing for landfill infrastructure projects.

Table 2.1 Waste composition percentage for domestic landfills (after Van Impe & Bouazza, 1996)

Component	Cities																		
	1	**2**	**3**	**4**	**5**	**6**	**7**	**8**	**9**	**10**	**11**	**12**	**13**	**14**	**15**	**16**	**17**	**18**	**19**
Metals	1	1	2	3	3	2	-	5	1	1	3	2	5	3	3	4	1	-	3
Paper/cardboard	25	5	8	12	33	8	14	22	9	20	22	10	24	31	9	19	2	12	16
Leather, wood, rubber	-	1	4	5	-	7	-	-	8	11	8	3	4	10	4	7	3	-	20
Textiles	3	-	1	-	10	1	-	-	4	4	-	3	4	5	5	-	-	-	-
Putrescible material	44	45	81	74	15	79	56	20	72	23	52	61	50	28	45	59	71	59	58
Glass	1	1	2	4	10	2	-	6	1	7	4	1	5	9	1	2	1	-	2
Others	19	46	1	2	22	1	30	46	5	30	9	14	8	11	33	5	21	-	1

Note: 1. Bangkok, Thailand; 2. Peking, China; 3. Vicosa, Brazil; 4. Nairobi, Kenya; 5. Hong Kong; 6. Bandun City, Indonesia; 7. Madras, India; 8. New York, USA; 9. Algiers, Algeria; 10. Zagreb, Croatia; 11. Meruelo, Spain; 12. Istanbul, Turkey; 13. Beirut, Lebanon; 14. Geneva, Switzerland; 15. Dakar, Senegal; 16. Athens, Greece; 17. Cochabamba, Bolivia; 18. Moscow, Russia; 19. Wollongong, Australia.

Van Impe & Bouazza (1996) noted that the duration of waste decay is highly variable and affected by climate. Whereby, in arid conditions waste decomposition is slower than in areas where rainfall is prevalent. When waste is compacted, there is less available room for air and water, thus decomposition is slower than in porous waste.

Considering the majority of the settlement models are validated using landfill material from countries other than Australia there is a gap in the testing regime. Climate conditions have a significant impact of the biodegradation of waste, therefore testing and validation using the settlement methods is an area that needs further refinement in Australia.

2.2 Field site investigation techniques

The subsurface conditions are critical for the design of any infrastructure project. A sound geotechnical investigation will reveal ground conditions and potential issues. However, for landfill sites, the heterogeneous nature of waste makes geotechnical investigations in these area quite difficult. Generally, they are not needed on landfill sites since in most cases the end use of the landfill is for open space with no load application above ground. In some instances for construction above landfills including for landfill expansion including vertical height or piggyback landfill cells, they are undertaken to better understand waste properties and behaviour. This section briefly summarises field based geotechnical investigation techniques utilised for landfill applications.

2.2.1 Geophysical methods

Geophysics refers to the use of physics principles to study ground conditions. There are many geophysical methods for underground investigations. However, this section briefly describes only multichannel analysis of surface waves, electrical resistivity, cross hole seismic tomography and ground penetrating radar as these are considered as the most commonly used geophysical methods.

Multichannel analysis of surface waves (MASW)

This is a non-intrusive method introduced by Park et al. (1999) whereby geophones (sensors) are spaced equally on the ground surface and a seismic source is struck producing a surface wave (Rayleigh wave). The seismic source can either be a vibrational source or a weight (such as 10 kg sledgehammer) that is struck onto the ground surface, refer to Figure 2.1 for equipment setup. The geophones then record the wave motion as a function of time. The data is then converted using either the phase shift or the swept frequency approach (Park & Lee, 1997) to create a dispersion curve which plots the wavelength against the phase velocity. The shear wave velocity profile can then be found by inversion of the dispersion curve. The shear wave velocity profile plots the depth against the shear wave velocity. Shear wave velocity is a key parameter that can be used to determine the elastic moduli and density of soil as well as create a geologic profile.

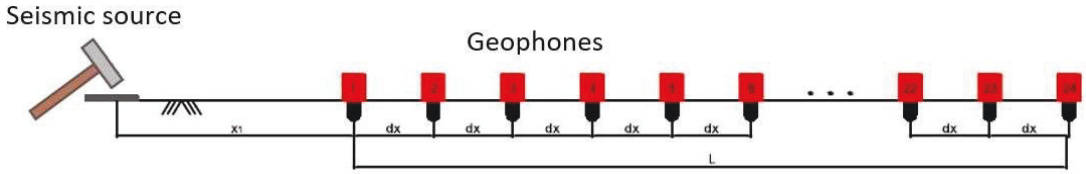

Figure 2.1 MASW field set up (after Ólafsdóttir, 2014)

Spectral analysis of surface waves (SASW) was the older version of the MASW method. The MASW is faster with only one strike required per sampling location, compared to repeated shots required for the SASW method.

The depth of investigation can range up to a depth of 30 m from the ground surface. This value can be higher if the seismic source is higher such as a crane.

Electrical Resistivity

This method involves the introduction of a current into the ground surface between multiple electrodes. The difference in electrical potential generated between the two electrodes allows for the resistivity of the subsurface conditions to be determined. There are two methods for measuring electrical resistivity, including vertical electrical sounding (Figure 2.2) and the dipole-dipole method (Figure 2.3). Increasing the spacing allows for increasing the depth of the investigation. These methods are useful for determining the presence of metallic ores, groundwater table and contaminants.

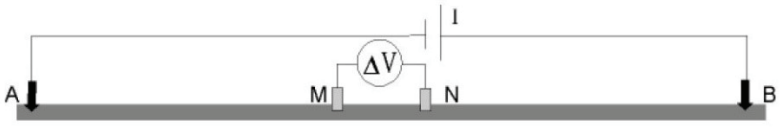

Figure 2.2 Electrical resistivity vertical sounding (after Okpoli, 2013)

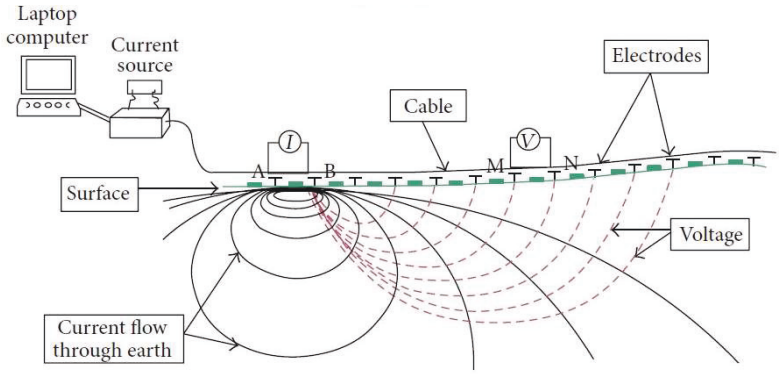

Figure 2.3 Electrical resistivity dipole-dipole field setup (after Okpoli, 2013)

Cross hole seismic tomography

Cross hole seismic tomography involves the use high frequency pulses between two boreholes. The system comprises of two boreholes, one source and one receiver borehole. A seismic device is lowered into the first borehole and a geophone into the receiver borehole. Multiple points within each of the source borehole and receiver borehole are used to produce a detailed profile of subsurface conditions between the boreholes (Figure 2.4). The process of converting the amplitude and travel time from the receiver borehole is similar to the aforementioned methods.

This method has significant advantage if boreholes are already constructed. The depth of effectiveness is dependent on the depth of the source and receiver boreholes.

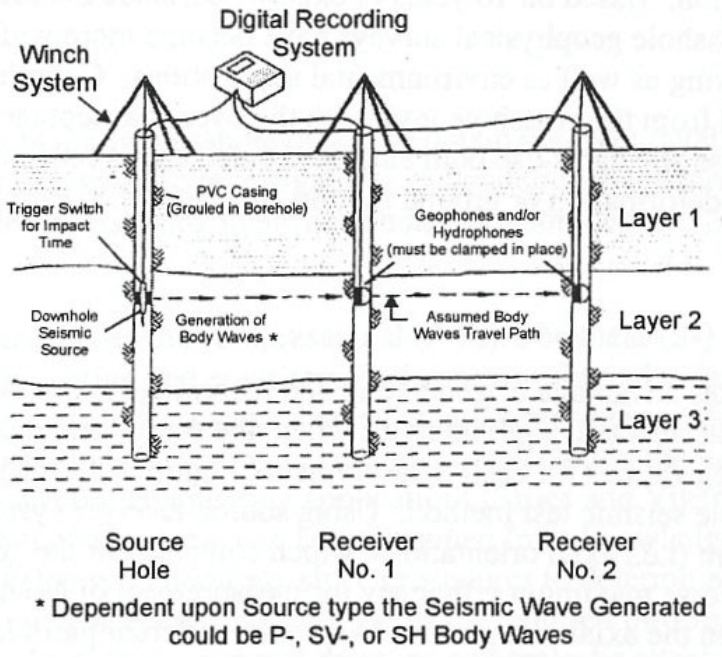

Figure 2.4 Cross hole seismic tomography (EPA(USA), 2016)

Ground penetrating radar (GPR)

This method involves the use of a high frequency electromagnetic impulse wave that is generated at the surface level. The waves produced travel through the soil and are reflected, the time taken and amplitude are recorded and are used to produce a velocity depth model. A geological profile can be created based off this data.

Application on landfills

The application of geophysics for landfills is quite commonly used particularly since most of the geophysical methods are non-intrusive. The need to excavate and dispose of waste is an expensive venture, and so non-intrusive geotechnical investigation methods are preferred over traditional site investigation methods.

The use of electrical resistivity for landfills is widely used for environmental applications. Carlo et al. (2013) describe the use of this method to determine the extent of a municipal solid waste landfill base and detect the presence of leachate. The electrical resistivity method proved to be effective to a depth of 40 m below the landfill surface.

A combination of electrical resistivity and MASW were utilised for an old dumping ground in Singapore. Yin et al. (2017) have recently used the combination of techniques to characterise the dumping ground. The authors noted that MASW technique was more accurate in determining the extent of landfill compared to the electrical resistivity method. However, limited boring was recommended to confirm the findings of the geophysical investigation.

Acworth & Jorstad (2006) utilised the cross borehole seismic tomography method on a landfill site to detect the presence of leachate. This method was coupled with electrical resistivity to confirm the accuracy of the cross borehole method in a landfill site. The authors describe this method as efficient for conducting a large scale geotechnical investigation on landfills.

Splajt et al. (2003) describe the use of GPR to be effective for mapping shallow depths (generally < 4 m) for landfills. The authors describe this method to be 'fast and cost-effective' for assisting in monitoring leachate breakout points in the landfill. Note that this method is appropriate for determining boundaries within waste; however, it does not capture critical data for geotechnical design including waste density or shear strength.

Benefits and limitations

Table 2.2 Benefits and limitations of geophysical geotechnical investigation methods

Benefits	Limitations
• Suitable for landfill application with numerous supporting case studies • Effective for a range of depths including shallow and deep (50 – 100 m) applications • Non-invasive method, resulting in cost savings since excavated waste disposal not required	• Costly equipment requires specialist geophysics contractor • Interpretation of results can be difficult and time consuming • May require boreholes (cross hole seismic tomography)

2.2.2 Boreholes

The use of boreholes is a traditional method for geotechnical site investigations. The method involves drilling a hole through the investigation area to a designed depth. A geotechnical engineer or geologist logs the material as it is extracted from the ground. Samples collected

from the process includes rock core samples and soil samples. These samples can be sent to the laboratory for further testing of geotechnical properties, however logging techniques on site often provide general guidance for soil or rock classification. This method is useful for defining landfill waste material, gas concentrations, groundwater levels and collecting samples for laboratory testing of geotechnical design parameters, such as shear strength and moisture content.

Traditional methods for borehole construction utilise a rotary drill bit that is driven by torque and downward pressure to create a hole within the ground surface. Recently, the advances with the sonic drilling have seen this as a fast and more commercially viable alternative to the traditional borehole construction methods. Lianggang et al. (2014) describe the drilling speed for sonic drilling to be five times faster than traditional methods. The key aspect of this method is the use of vibration frequency in combination with a variable rotation speed and downward pressure to efficiently core through soil and rock strata. Burlingame et al. (2007) points out the unit costs for sonic drilling are higher than traditional drilling methods, typically due to the cost of drilling technology. However, this is offset by the increased efficiency and penetration rates.

Application on landfills

The use of boreholes on landfills is a common method for geotechnical investigation. The heterogeneous nature of waste requires physical sampling of landfill waste to accurately determine its geotechnical properties. Numerous case studies have been documented for this method and some have been briefly described below.

Note the methodology for logging of waste material extracted from a borehole is relatively difficult. Waste is heterogeneous comprising of a range of materials, which can be difficult to visually assess and separate. The current industry practice for this is to send representative samples to a laboratory for physical testing and percentage composition by dry weight.

Chiampo et al. (1996) used boreholes to characterise waste properties of a landfill. The key outcome was the ability to determine the presence of water lenses within the landfill. This is critical to assess the prediction of the landfill waste biodegradation rate and associated

settlement. The authors do note that this was a relatively expensive method for collection of this data. Modern non-intrusive methods are able to determine similar information without the cost of drilling and waste disposal.

Sonic drilling experiences on landfills have recently been shared by Burlingame et al. (2007) for landfill characterisation. The method was effective for drilling through a range of landfill materials including putrescible material and building waste. No significant correlations were found between the depth of landfill material and unit weight. However, there was a link between the composition of the waste material and the unit weight.

Benefits and limitations

Table 2.3 Benefits and limitations of boreholes

Benefits	Limitations
• Suitable for landfill application with numerous supporting case studies • Effective till borehole depth top of base liner of landfill • Effective for physical sample collection at various depths (can be tested for actual geotechnical properties of landfill material in laboratory conditions)	• Costly for specialised drilling equipment • Potential difficulty drilling through waste • Waste disposal of landfill samples can be costly • Investigation depth limited to above the base liner of the landfill (to prevent damage to integrity of landfill lining system) • Potential contamination between pockets of landfills can be created by boreholes • Samples collected can be difficult to classify visually

2.2.3 Test pits

Test pits are an effective commonly used geotechnical investigation method. It involves the use of either hand tools or more typically an excavator or backhoe to dig a trench within the ground. From the surface, geologists or geotechnical engineers can then examine the soil / rock surface and log a cross section of material whilst collecting samples for material testing. Once test pit data is collected, the test pit is backfilled and compacted in layers to return the ground close to its original condition.

The dimension of a test pit vary, they are wide enough to allow a person to see the side walls of the trench. Once the desired width of the trench is selected, the excavator bucket

is selected accordingly. One excavator bucket width is selected for trench constructability and efficiency purposes. Trench depth is limited by the reachability of the excavator and also the trench slope stability. Benching can be employed for deeper test pit investigations, however is not considered as cost-effective due to significant amounts of excavation. This method is most useful for shallow investigations of soil up to depths of approximately 3 m.

Application on landfills

The application of test pits on landfills is a common method for geotechnical investigation. However, this is often coupled with other investigation methods as it is limited to investigation of the landfill surface. The heterogeneous nature of waste is not often captured by this investigation of method alone, but rather serves to add reliability to data collected in other methods and also as a source for collecting physical landfill samples.

Seneversa (2012) described the use of test pits to characterise waste at a landfill site. The range of effectiveness was typically between 0.6 m – 1 m below ground level, with a maximum depth of 2.2 m below the ground surface. During the investigation the geotechnical engineers on site were able to define a thin cover layer of soil placed above waste. The use of test pits were coupled with a series of boreholes to better define the waste material with depth as well as to determine landfill gas and groundwater levels.

Benefits and limitations

Table 2.4 Benefits and limitations of test pits on landfills

Benefits	Limitations
• Suitable for landfill application with numerous supporting case studies • Relatively cheap and fast method of collecting physical samples from landfill surface (up to approximately 3 m from landfill surface) • Cross section of landfill can be logged and assessed by geotechnical engineer • Effective for physical sample collection at various depths (can be tested for actual geotechnical properties of landfill material in laboratory conditions)	• Potential difficulty excavating waste material • Waste disposal of landfill samples can be costly • Investigation depth is shallow and needs to be coupled with other geotechnical investigation methods i.e. geophysical or boreholes • Difficult to visually assess in-situ waste from test pit cross section • Benching or shoring required if deeper test pit investigation required, which can be costly • Depth of investigation limited by test pit slope stability and excavator reach length • Samples collected are unlikely to provide a representative sample for the entire landfill as they are primarily from the surface

2.2.4 Standard Penetration Test (SPT)

Standard penetration tests involve are a cheap testing method conducted simultaneously to borehole construction. The method utilises a hammer with weight of 63.5 kg, driving a tube into the base of the borehole. The number of hammer blows to drive the tube into the ground by 150 mm is recorded until a depth of 450 mm. The number of blows can be correlated to a density and friction angle. The vertical spacing between SPT tests can vary, but is typically 1 m or for every point of change in soil strata. This enables data collection for the entire length of the borehole. After reaching the 450 mm penetration, the tube sample is extracted from the ground and can be tested in laboratory conditions.

Application on landfills

The application of this method for landfill investigation has been documented in some recent case studies. Although the authors do note there are some disadvantages to SPT use on a landfill.

Gomes et al. (2013) analysed the use of SPT testing for determining the shear strength of waste at a landfill site. The friction angle obtained is similar to results obtained by the

triaxial test for low strain (less than 15%), however for higher strain levels the results are too high. If triaxial testing is able to provide sufficient and accurate data for shear strength analysis, then the use of SPT during borehole construction can be considered as an unnecessary additional test. The construction of the borehole means that core samples are likely to be extracted and tested, removing the need for SPT as it will slow down the process. It may however be useful for justifying the results obtained during triaxial testing.

Rogers (2006) describes some downsides to the use of the SPT method. A key downside is the returned sample is highly disturbed, meaning any laboratory testing conducted on extracted samples are unlikely to be representative of the in situ material. The heterogeneous nature of waste means that the SPT tube may not capture some landfill waste, and in some instances may record a high blow count or refusal presented by an obstruction. This method is most effective for cohesionless soils, for landfill material where moisture is present and cohesion, there may be some issues with obtained data. Potential errors during data collection include miscounting the number of blows and inconsistent setting of the SPT tube on the base of the borehole.

Benefits and limitations

Table 2.5 Benefits and limitations of SPT testing on landfills

Benefits	Limitations
• Suitable for landfill application with some case studies • Relatively cheap and fast method of collecting physical samples from range of depths below landfill surface • Can be conducted at same time as borehole construction • Samples collected can be tested in laboratory conditions	• Requires borehole (costly) and may interrupt the efficiency if only drilling is required • Refusal / high blow count recorded randomly (may be due to obstruction in waste) • Waste disposal of landfill samples can be costly • Samples collected are unlikely to provide a representative sample for the entire landfill • Samples collected are highly disturbed and difficult to analyse • Lack of reliable correlation charts (data) between SPT number and shear/strength.

2.2.5 Cone Penetrometer Test (CPT)

The cone penetration test (CPT) is a common method for geotechnical investigation of cohesive soils. It involves the use of a special cone, which measure tip resistance and sleeve friction as it penetrates into the ground. The equipment can vary from being mounted on a truck and tracks for investigation areas, which are difficult to access. A hydraulic arm is responsible for driving the cone into the ground normally at a standard rate, although this can be adjusted by the field technician.

Various modifications to the CPT method have included the use of a piezocone (CPTu) and resistivity piezocone (RCPTu). The piezocone in addition to tip resistance and sleeve friction measures pore pressure, allowing for detection of ground water or perched water pockets. The resistivity cone piezocone in addition to the aforementioned also measures the electrical resistance of current flow in the ground. Mondelli et al. (2012) states that other attachments can include sensors for pH and temperature, these are particularly useful for environmental applications. Seismic piezocone (SCPTu) can also be utilised to determine shear wave velocity and shear modulus of material within a close range of the probe. With all these potential sources of information gained from a single invasive probe into the ground, data collection is simple and cost effective.

Application on landfills

Although the use of CPT is mainly for cohesive material and fine grained soils, the application is currently used for landfill applications. The effectiveness of the method is variable due to the heterogeneous nature of landfills. The presence of obstructions within the landfill waste is likely to cause shallow depth refusals which can be time consuming and costly if reoccurring. If however, a significant depth can be reached without obstruction, this investigation method is likely to provide very useful information for geotechnical parameters of the landfill.

For landfills, the presence of obstructions within the waste may significantly deviate the probe. The inclinometer within the probe is able to detect the tit angle. Mondelli et al. (2012) states that vertical deviation of the CPT probe beyond a 90 degree tilt angle may not

be recoverable. This effect is likely to occur and may significantly vary across the landfill site due to its heterogeneous nature.

The use of RCPTu was successful used and documented by Mondelli et al. (2007). The method was able to successfully detect small changes in waste strata and assisted in mapping the leachate levels present within the landfill. Geophysical methods confirmed the accuracy of the test results. The justification of doing the RCPTu over the regular CPT or CPTu is strongly beneficial with little relative additional cost.

Benefits and limitations

Table 2.6 Benefits and limitations of CPT testing on landfills

Benefits	Limitations
• Suitable for landfill application with significant supporting case studies • Relatively cheap and fast method of collecting critical geotechnical information • Attachments such as resistivity, pH and temperature can be useful for collecting information in one ground penetration • Results are immediately received • No waste disposal issues	• Refusal at shallow depths if reoccurring may be costly (may be due to obstruction in waste) • No physical samples collected, may need to be coupled with another investigation method • Limited suitability to cohesive soils and fine grained soils

2.2.6 Seismic Dilatometer test (SMDT)

The seismic dilatometer test (SMDT) is an effective method for measurement of shear wave velocity of in-situ material and the maximum shear modulus of the ground conditions. The method consists of drilling a seismic module into the ground and creating a shear wave on ground surface. The seismic module consists of two receivers spaced at 0.5 m along the longitudinal plane of the module. The source generation consists of a single hammer blow at

surface. The time taken to receive the signal is recorded for each receiver. A hammer blow and readings are recorded every 0.5 m along the depth of the hole.

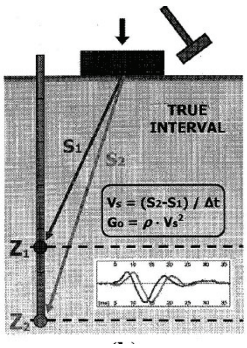

Figure 2.5 SMDT configuration (after Marchetti et al., 2008)

Application on landfills

SMDT is a relatively new technique for the characterisation of landfill waste. Limited literature is available for the use of this technique in landfill applications.

Castelli & Maugeri (2014) attempted to use the method for characterising geotechnical properties of landfill waste. The results obtained showed good reliability with laboratory testing methods including the direct shear test. The average friction angle obtained (33°) showed good reliability with previous literature for landfill waste. Note this comparison is difficult to conclude particularly due to the heterogeneous nature of waste and the range of friction angles obtained was between 27 – 41°. The findings in this paper require further research and reliability testing to confirm the claimed conclusions.

Benefits and limitations

Table 2.7 Benefits and limitations of SMDT testing on landfills

Benefits	Limitations
• Relatively cheap and fast method of collecting critical shear velocity and maximum shear modulus of landfill waste • No waste disposal issues	• Limited available literature for use in landfill applications • No physical samples collected, need to be coupled with another investigation method • Difficult to interpret data obtained from testing

2.2.7 Pressuremeter test

There are multiple forms of the pressuremeter test that can be used to determine in-situ geotechnical properties. Likitlersuang et al. (2013), describe four pressuremeter methods

including the pre-bored pressuremeter (PBP), self-boring pressuremeter (SBP), push-in pressuremeter (PIP) and lateral load test (LLT) pressuremeter. Three of the methods have been illustrated in Figure 2.6. The only difference between the LLT and the other methods is the use of a monocell probe instead of a tricell probe. The tricell probe is less likely to be damaged due to guarded edges when inflated compared to the monocell probe.

The procedure for the pressuremeter test involves lowering the cylindrical probe into a hole of slightly larger diameter. Once at the required depth, the probe is pressurised and expands against the borehole walls and volume change is measured. The shear strength, shear modulus and horizontal stresses can be interpreted from the results using complex mathematical theory.

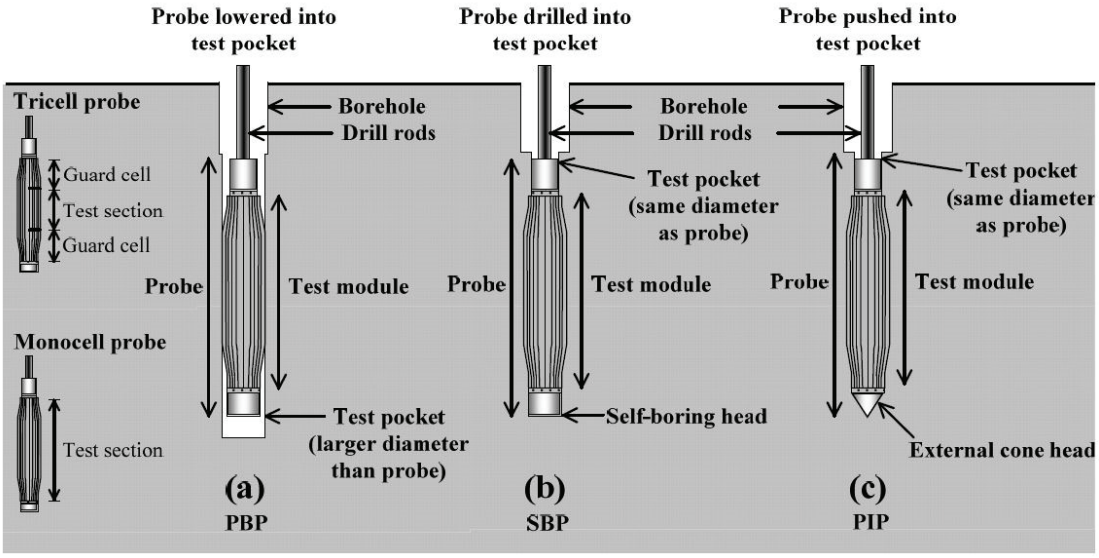

Figure 2.6 Pressuremeter test configurations (a) PBP (b) SBP (c) PIP Likitlersuang et al. (2013)

Application on landfills

The use of pressuremeter tests for landfill applications is quite common. Dixon & Jones (2005) used the pressuremeter test to determine the in-situ stresses and shear stiffness in municipal solid waste. Their experimental program comprised of conducting tests to a depth of 17 m below ground level. Testing was conducted across a range of landfill sites, with test results in general agreement between each site. Although the authors did not have access at the time to previous literature to validate the results.

Dixon & Jones (2005) were able to optimise the use of SBP and high pressure dilatometer (HPD) for in-situ measurement of shear stiffness. Issues with sample disturbance meant that shear strength, a critical geotechnical parameter for design, was not able to be accurately determined. The range of test data obtained ranged from 4 – 20 m below ground level.

More recently, Lapeña et al. (2013) utilised PBP tests to determine waste stiffness properties. The authors identified some issues with the method including membrane failure during pressuremeter extraction primarily due to waste 'sticking' to the pressuremeter membrane causing excess deformation. Results obtained have limited previous literature for validation.

Benefits and limitations

Table 2.8 Benefits and limitations of pressuremeter testing on landfills

Benefits	Limitations
• Can accurately determine shear stiffness of waste material • No waste disposal issues	• Limited available literature for use in landfill applications • No physical samples collected, need to be coupled with another investigation method • Difficult to interpret data obtained from testing • Pressuremeter membrane tears during extraction – time consuming and costly for repair

2.2.8 Summary of geotechnical investigation techniques

Appendix A summarises key landfill geotechnical investigation techniques with benefits, limitations, effective depths and parameters obtained.

2.3 Landfill settlement

2.3.1 Landfill settlement phases

Numerous studies have been undertaken to understand the phases of landfill settlement (Sowers (1973), Bjarngard & Edgers (1990), Wall & Zeiss (1995)). As depicted in Figure 2.7, authors concluded there are three main phases for landfill settlement comprising of:

- Initial settlement
- Primary settlement
- Secondary settlement

Sowers (1973) describes initial settlement to occur instantaneously as an external load is placed on waste material. This is due to expulsion of air voids and immediate compaction of highly deformable waste material. Initial settlement can be calculated using the measured elastic modulus of waste as per the equation below.

$$S_i = \frac{\Delta q H_o}{E_s} \qquad \textit{Eq. 2.1}$$

where: S_i = initial settlement in m, Δq = increase in overburden pressure acting at the middle of the layer, H_o = initial waste thickness and E_s = elastic modulus of waste material (N/m^2). Note the elastic modulus of waste varies depending on the depth and type of waste.

Primary settlement is a result of physical and mechanical compression of waste, this is a slow but short process. Note that gas production continues for the lifecycle of the landfill since gas is a by-product of the biodegradation process. Secondary settlement (long term) forms a large portion of the total settlement, based on the biological breakdown of waste. As a result, volume of waste material is reduced causing additional settlement over time.

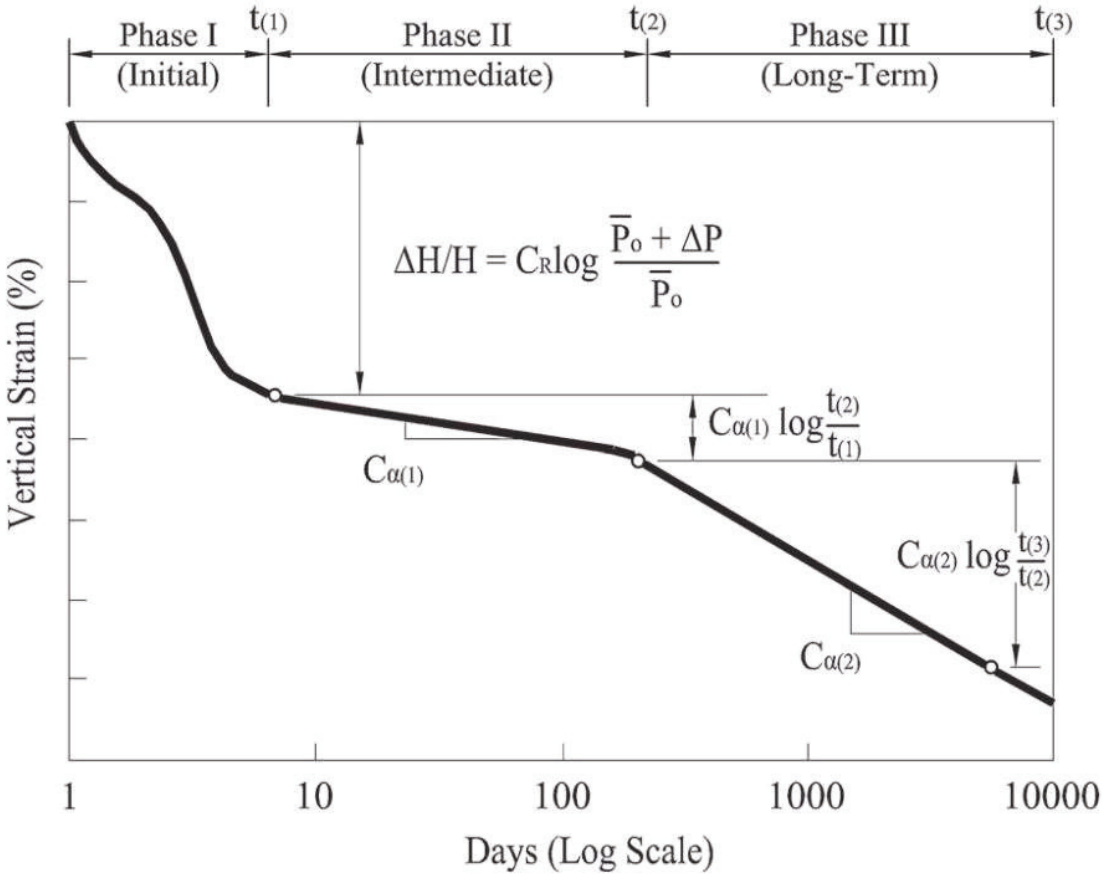

Figure 2.7 Phase period vs vertical strain (after Wong et al., 2013)

Grisolia et al. (1995) have since split the settlement process into further sub-stages as presented in Figure 2.8. This process can be summarised as follows:

- Stage I Initial settlement (few days) – instant mechanical compression due to compression of highly deformable waste material
- Stage II Primary settlement (up to 3 months) – mechanical compression due to waste slippage and particle rearrangement
- Stage III Secondary settlement (1 to 3 years) – mechanical deformation due waste creep and commencement of organic waste decomposition
- Stage IV Decomposition settlement (10 to 30 years) – biological degradation of waste
- Stage V Residual settlement (indefinitely) – mechanical settlement over time and minor decomposition settlement over long period of time

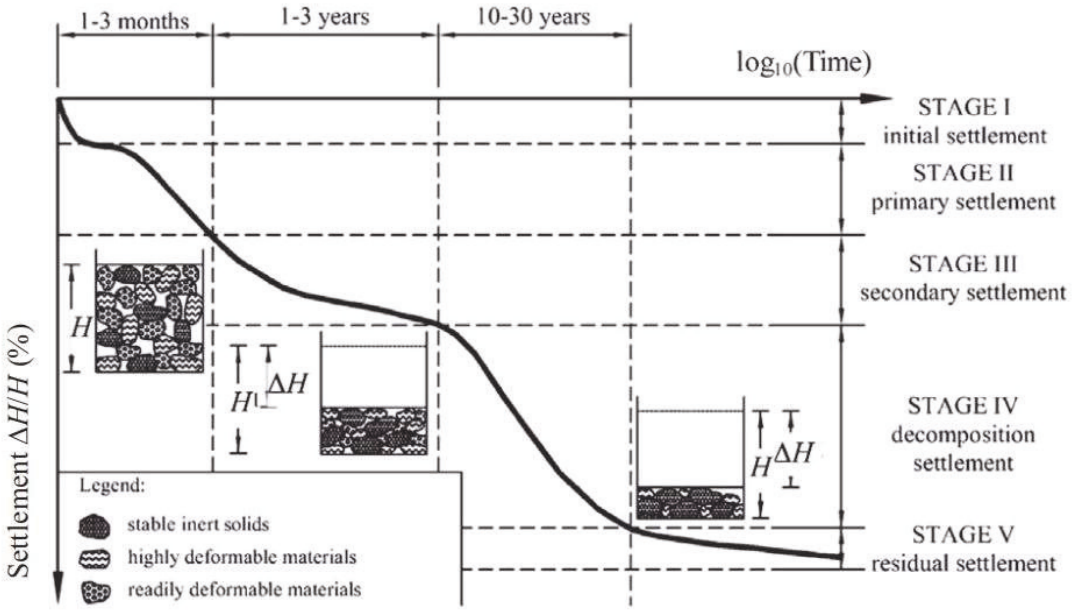

Figure 2.8 Landfill time settlement curve (after Grisolia et al. 1995)

Stages I and II are not critical since they both occur relatively quickly, and can occur concurrently to construction of infrastructure above landfills. The most critical stages for construction of infrastructure above landfills is stages III, IV and V where current knowledge is unable to consistently predict long term settlement.

2.3.2 Contributing factors to landfill settlement

Sivakumar Babu et al. (2010) states the attributes of municipal solid waste settlement to comprise of the following:

1. Physical and mechanical processes – similar soil behaviour including particle rearrangement and collapse of voids
2. Chemical processes – combustion and oxidation
3. Dissolution processes – formation of leachate from waste combined with landfill water
4. Decomposition of waste – aerobic/anaerobic biological breakdown of waste over time

Leonard et al. (2000) described the high contributors for landfill settlement to include decomposition of waste combined with long-term physical creep. The rate of decomposition is highly variable and dependent on a number of factors, including pH, temperature, presence of biological organisms, moisture content, organic content of waste and the type of waste.

With a significant number of contributing factors, the settlement induced by biological decay is difficult to be captured in settlement models. Physical creep refers to the movement of particles and rearrangement following biological decay. As waste is decomposed, the volume reduces creating voids within the landfill; and physical movement of landfill waste particles into these voids causes additional settlement.

2.3.3 Existing landfill settlement theories and models

Sivakumar Babu et al. (2010) has compiled a consolidated list of landfill settlement prediction models, and has grouped them into four types including:

- Soil mechanics based models
- Empirical models
- Rheological models
- Biodegradation models

Liquid and gas generation models and constitutive models can be included as further categories branching from biodegradation models.

2.3.3.1 Soil mechanics based models

Sowers model

Sowers (1973), created the following formula to predict landfill settlement. The model considers primary and secondary settlement over time. Compression indices from MSW landfills were reported to be within 0.163 – 0.205 and 0.015 – 0.350, for primary and secondary settlement respectively. One particular downfall is the variability of compression ratios, which can lead to significantly different settlement predictions. This model also does not consider biodegradation exclusively; as a result, this can underestimate predicted settlement.

$$\Delta H = HC_c \, log\left(\frac{\sigma_0+\Delta\sigma}{\sigma_0}\right) + HC_\alpha \, log\left(\frac{t_2}{t_1}\right) \qquad \textit{Eq. 2.2}$$

where: ΔH = total settlement; H = initial waste layer thickness; C_c = primary compression ratio; σ_0 = existing overburden pressure at the middle of the waste layer; $\Delta\sigma$ = increment of overburden pressure in middle of waste layer from construction of additional waste layer

above; C_α = secondary compression ratio; t_2 = ending time period for which long term settlement is desired and t_1 = time for completion of primary settlement.

Bjarngard & Edgers (1990), furthered the original sowers equation by separating the secondary settlement into intermediate and final secondary settlement. Sowers (1973) model considered a consistent secondary compression ratio; however, this value was not the same for all secondary settlement stages. The Bjarngard & Edgers model was able to separate this by adding secondary compression ratios for different heights being more realistic of landfilling scenarios. Although there is difficulty in obtaining an accurate secondary compression ratio. Their equation is summarised below:

$$\Delta H = HC_c \, log\left(\frac{\sigma_0+\Delta\sigma}{\sigma_0}\right) + H_{t(1)}C_\alpha \, log\left(\frac{t_2}{t_1}\right) + H_{t(2)}C_{\alpha(2)} \, log\left(\frac{t_{(n+1)}}{t_2}\right) \qquad \textit{Eq. 2.3}$$

where: ΔH = total settlement; H = initial waste layer thickness; C_c = primary compression ratio; σ_0 = existing overburden pressure at the middle of the waste layer; $\Delta\sigma$ = increment of overburden pressure in middle of waste layer from construction of additional waste layer above; C_α = secondary compression ratio; $C_{\alpha(2)}$ = long term compression ratio; $t_{(n+1)}$= total time period considered in modelling; t_2 = ending time period for which intermediate settlement is desired and t_1 = time for completion of primary settlement.

Hossain & Gabr (2005), provided insight into secondary settlement. This does not consider primary settlement, which needs to be calculated separately and combined to produce the total settlement. Gas generation as a by-product from the biodegradation process is the basis for this model. The amount of gas generated in the landfill is dependent on landfill composition, which is variable between landfill sites. The large amount of factors that feed into the equation is likely to result in a large amount of assumptions and make this method quite difficult for application without significant ground investigation and available landfill data. The authors' equation is presented below:

$$\frac{\Delta H}{H} = C_{\alpha i} \log\left(\frac{t_2}{t_1}\right) + C_\beta \log\left(\frac{t_3}{t_2}\right) + C_{\alpha f} \log\left(\frac{t_4}{t_3}\right) \qquad \textit{Eq. 2.4}$$

where: $C_{\alpha i}$ = compression index (stress level and degree of decomposition), t_1 = time for completion of initial compression, t_2 = duration for which compression is to be evaluated,

C_β = biodegradation index, t_3 = duration for biological compression completion, $C_{\alpha f}$ = creep index and t_4 = end time of biological degradation.

2.3.3.2 Empirical models

There are three main empirical equations for landfill settlement, based on basic mathematical functions include the logarithmic function, the power creep model, hyperbolic equation and the attenuation equation. Using these mathematical concepts and data collected from landfill sites, the formulas can be used to roughly estimate landfill settlement. These models are all significantly generalised and are not considered accurate for site-specific applications.

Logarithmic function

The logarithmic function (Yen & Scanlon, 1975) is expressed as:

$$\Delta H = H_0 \left[\alpha + \beta \log\left(t - \frac{t_c}{2}\right)\right] \qquad \textit{Eq. 2.5}$$

where: ΔH = total settlement; H_0 = initial height of landfill waste; $\alpha = 0.00035H_f + 0.00969$; $\beta = 0.00035H_f + 0.00501$; t = time since beginning of filling and t_c = construction period.

Power creep model

The power creep model (Edil et al., 1990) represents time-dependent deformation under a constant stress. This can be represented as:

$$\Delta H = H_0 \Delta\sigma M' \left(\frac{t}{t_f}\right)^{N'} \qquad \textit{Eq. 2.6}$$

where: ΔH = total settlement; H_0 = initial height of landfill waste; $\Delta\sigma$ = compressive stress depending on landfill waste height, density and external loading; M' = reference compressibility (1.6 x 10^{-5} to 5.8 x 10^{-5} / kPa); t = time since load application; t_f = reference time - typically 1 day (El-Fadel et al., 1999) and N' = rate of compression (0.50 – 0.67).

The parameter M' takes into account site-specific waste compressibility, which is variable based on the age of the landfill and waste placement conditions.

Hyperbolic equation

Ling et al. (1998) proposed the following equation to determine the landfill settlement at a given time. This equation relies on the final settlement to be known.

$$\Delta H = \frac{t}{(1/p_0)+(t/S_{ult})} \quad \textit{Eq. 2.7}$$

where: ΔH = total settlement; t = time since load application; p_0 = initial settlement rate and S_{ult} = ultimate settlement.

Attenuation equation

Coumoulos & Koryalos (1997) created a useful equation for comparison between landfill sites and settlement using an approximated straight line. The straight line is determined as a function of the logarithmic method as a function of time. The model is expressed in the following equation:

$$Y = \frac{d(\Delta H/H)}{dt} = \frac{0.434C_{\alpha}}{t_c+(\frac{t}{2})} \quad \textit{Eq. 2.8}$$

where: Y = vertical strain rate (expressed as a percent per month or per year); C'_{α} = coefficient of secondary compression (0.20 – 0.25); t_c = filling time (assumed as 1 month) and t = time elapsed in months or years.

This model does not consider primary settlement and is heavily reliant on the coefficient of secondary compression.

2.3.3.3 Rheological models

Based on the contributions of Gibson & Lo (1961) for peaty soils experiencing secondary settlement, Edil et al. (1990) were able to apply a similar principle to landfill waste settlement. The principle behind this method can be represented with the analogy of a spring, where compression of the spring represents primary settlement and the pistons and springs represent slow deformation. The equation is represented as:

$$\frac{\Delta H}{H} = \Delta\sigma a + \Delta\sigma b(1 - e^{-\left(\frac{\lambda}{b}\right)t}) \quad \textit{Eq. 2.9}$$

where: ΔH = settlement; H = initial height of waste; $\Delta\sigma$ = compressive stress depending on waste height, density and external loading; a = primary compressibility index (1×10^{-4} to 8×10^{-5} kPa); b = secondary compressibility index (2×10^{-3} to 1.6×10^{-2} kPa); $\frac{\lambda}{b}$ = rate of secondary compression (1.4×10^{-4} to 9.0×10^{-4} / day) and t = time since load application.

Again, the secondary compressibility index is significantly variable between each landfill site. An accurate method for determining this factor is yet to be found.

2.3.3.4 Biodegradation models

The consideration of biodegradation is critical for landfill settlement calculations. This can account for a large portion of the long-term landfill settlement. The following models attempt to utilise more site-specific landfill parameters to more accurately predict landfill settlement.

Park and Lee model

Park & Lee (1997) created a model based on time-dependent biodegradation of waste. This model is founded on the assumption that settlement is directly related to the available amount of soluble solids. Organic material solubilisation is based on first order kinetics. However, determining these factors is quite difficult due to the variability of organics across landfill sites. The equations proposed include:

$$\varepsilon(t)_{mec} = C_{\alpha}\log\left(\frac{t_2}{t_1}\right) \qquad \textit{Eq. 2.10}$$

$$\varepsilon(t)_{dec} = \varepsilon_{tot\_dec}(1 - e^{-k_1}) \qquad \textit{Eq. 2.11}$$

where: C_{α} = rate of secondary compression; ε_{tot_dec} = total amount of compression that will occur due to biodegradation of waste (6.1 to 7.2%); k_1 = first order decompression strain rate constant / time (1.35 to 2.37/year) and $\varepsilon(t)_{mec} + \varepsilon(t)_{dec} =$ total settlement.

Hettiarachchi model

Hettiarachchi et al. (2009) similar to Park & Lee (1999) also developed a settlement model based on first order kinetics. The model is expressed as:

$$(\Delta H)_b = H_i\left[\frac{M_{si}}{\rho_w}\sum_{j=1}^{4}\frac{f_{sj}}{G_{sj}}(1 - exp^{-\lambda_j t})\right] \qquad \textit{Eq. 2.12}$$

$$(\Delta H)_m = H_i C^* \log\left(\frac{\sigma' + \Delta\sigma'}{\sigma'}\right) \quad \textit{Eq. 2.13}$$

$$H_f = H_i - (\Delta H)_b - (\Delta H)_m \quad \textit{Eq. 2.14}$$

where: $(\Delta H)_m$ = mechanical compression; $(\Delta H)_b$ = biodegradation induced settlement; C^* = compressibility parameter (0.174 to 0.205); H_i = initial waste thickness; ρ_w = density of water; λ_j = first-order kinetic constant for the jth group (0 - 0.001 /day); f_{sj} = initial solids fraction for each waste (0.15 to 0.35); G_{sj} = specific gravity of jth group of waste solids (1 to 3); σ' = effective stress and $\Delta\sigma'$ = difference in effective stress.

There are significant difficulty in obtaining the factors required for this equation. Guidance for selection of these parameters require detailed reference to the authors' original journal article.

Marques 2001 model

Marques (2001) incorporated waste degradation to primary settlement, with the observation that secondary settlement is linear for void ratio curves as a function of the applied stress logarithm. The model is represented by the following equation:

$$\frac{\Delta H}{H} = C'_c \log\left(\frac{\sigma_0 + \Delta\sigma}{\sigma_0}\right) + \Delta\sigma \cdot b \cdot \left(1 - e^{-ct'}\right) + E_{dg} \cdot \left(1 - e^{-ct''}\right) \quad \textit{Eq. 2.15}$$

where: ΔH = settlement; H = initial height of waste; C'_c = primary compression ratio; σ' = effective stress; $\Delta\sigma'$ = difference in effective stress; σ' = effective stress; b = coefficient of secondary mechanical compression; c = secondary mechanical compression rate; E_{dg} = total compression due to waste degradation; d = secondary biodegradation compression rate; t' = time elapsed since loading application and t'' = time elapsed since waste disposal.

Marques 2003 model

Marques et al. (2003) furthered the compressibility model by incorporating lift thickness. Since landfills are filled slowly over a number of years, the lift thickness does impact the effective stresses and settlement of the landfill waste material. This model combines instantaneous responses to load, mechanical creep and degradation. After all landfill lifts have been completed the settlement at any given time can be determined using total strain. The total strain is represented by:

$$\varepsilon = \varepsilon_p + \varepsilon_c + \varepsilon_b \qquad \textit{Eq. 2.16}$$

Instantaneous loading (ε_p) is not time dependent, however both creep (ε_c) and waste degradation (ε_b) strains are time dependent. As a result the settlement at any given time is:

$$\Delta H = \sum_{i=1}^{N} H_i\left[\varepsilon_{pi} + \varepsilon_{ci}(t) + \varepsilon_{bi}(t)\right] \qquad \textit{Eq. 2.17}$$

where: N = number of landfill lifts; H_i = initial compacted lift thickness; ε_{pi} = strain in lift i as response from overlying lifts; $\varepsilon_{ci}(t)$ = creep strain at time t due to self-weight and weight of overlying lifts and $\varepsilon_{bi}(t)$ = strain at time t due to biological decomposition of lift i.

$$\varepsilon_{pi} = C'_c \log\left(\frac{0.5\gamma_i H_i + \sum_{j=i+1}^{N} \Delta\sigma_{ij}}{0.5\gamma_i H_i}\right) \qquad \textit{Eq. 2.18}$$

$$\varepsilon_{ci}(t) = b\left[0.5\gamma_i H_i\left(1 - e^{-c(t-t_i)}\right) + \sum_{j=i+1}^{N} \Delta\sigma_{ij}\left(1 - e^{-c(t-t_j)}\right)\right] \qquad \textit{Eq. 2.19}$$

$$\varepsilon_{bi}(t) = E_{DG}(1 - e^{-d(t-t_i)}) \qquad \textit{Eq. 2.20}$$

where: $t - t_i > 0$ & $t - t_j > 0$, since t is after all landfill lifts are completed; C'_c = compression ratio (0.0732 to 0.320); γ_i = unit weight of lift i; $\Delta\sigma_{ij}$ = change in vertical stresses impost by lift j ($j = i + 1$) on lift i, calculated using Boussinesq theory; t_i & t_j= time at which lift i and j were placed, respectively; E_{DG} = total amount of strain that can potentially occur due to decomposition (0.131 to 0.214); b = coefficient of mechanical creep (2.92×10^{-4} to 7.26×10^{-4}); c = mechanical creep rate (9.69×10^{-4} to 2.55×10^{-3} / day) and d = biological decomposition rate (6.77×10^{-4} to 2.57×10^{-3}).

Significant information is required for accurate calculation of landfill settlement. However, this method is supported with large-scale landfill specific test results. The combination of theory and practice has developed this method to be a rough guide to landfill settlement whilst considering a range of factors.

Similar methods (Liu et al. 2006; Oweis 2006) were developed to capture the effects of gas generation on settlement and to further findings from Marques (2003).

Chakma model

Chakma & Mathur (2013) were able to consider additional factors in their model to biodegradation induced landfill settlement including pH, temperature and moisture content of landfill waste. This is based on the Park and Lee biodegradation model and follow first order equations created by Young (1989). The authors also conducted a sensitivity analysis to determine the effect of each variable on landfill settlement. It was found that pH, temperature and moisture content have an impact on landfill settlement. Mechanical compression is calculated separately from biodegradation settlement and added together to get the total settlement.

Gourc model

Gourc et al. (2010) produced a model for secondary settlement of MSW based on mechanical and biochemical settlement. This analytical method is a simplified version of the biodegradation element presented by McDougall (2007). The development of the Gourc (2010) model included using existing biodegradation models including LANDGEM (used by the USA EPA) and SWAMA (Cossu et al., 1996). These biodegradation models are based on first order decay and are used to predict landfill gas generation. The total secondary strain is presented in the equation below, the first portion of the equation addresses mechanical settlement whilst the latter is biochemical settlement.

$$\varepsilon_2 = C_{\alpha\varepsilon M} log_{10}\left(\frac{t}{t_{oM}}\right) + \frac{\rho_d^0}{\rho_{so}^0} c(1 - e^{-k(t-t_{oB})}) \qquad \textit{Eq. 2.21}$$

where: ε_2 = total secondary strain, $C_{\alpha\varepsilon M}$ = total secondary compression ratio, t = time from start of test, t_{oM} = initial time when primary compression is finished, ρ_d^0 = initial global dry density, ρ_{so}^0 = initial solid organic dry density, c = initial gravimetric solid organic content, k = gas generation rate and t_{oB} = start of biodegradation.

This model does appear to correlate well with experimental data. However, a key limitation for this model is the difficulty in predicting the secondary compression ratio, which is reliant on a number of factors. This model also does not consider a number of biological contributors including temperature, pH and moisture in the biodegradation aspect of the equation; albeit

the authors commented that the assessment of biogas could be sufficient for settlement calculations.

Bareither model

Bareither et al. (2013b) dismissed other models stating that 'no single waste characteristic was found to consistently influence C_c'. Instead, the authors combined critical factors found to influence waste compressibility to form the waste compressibility index (WCI) presented in the equation below.

$$WCI = w_d \cdot (\frac{\gamma_w}{\gamma_d}) \cdot (\frac{OW}{100-}) \quad \textit{Eq. 2.22}$$

where: γ_w = unit weight of water, γ_d = dry unit weight of waste and OW = organic waste content (%).

The WCI can then be used to determine the compressibility of waste using the following equation:

$$C_c' = 0.26 + 0.058 \cdot log_{10}(WCI) \quad \textit{Eq. 2.23}$$

Note the authors claim the accuracy of this method to be approximately $\pm$ 0.087 for a given WCI. Although this is a step forward in prediction of waste compressibility, this method still requires further refinement for infrastructure loading above landfills. The level of impact of other critical landfill components such as waste lift thickness proven by other research (Marques et al., 2003) has not been considered in this model, perhaps over simplifying the solution to landfill settlement.

2.3.3.5 Liquid and gas generation models

El-Fadel & Khoury (2000) provided critical commentary on existing landfill settlement models at the time, stating that an integrated model considering all solid, liquid and gas phases should be considered for accurate representation of landfill settlement. Many models that have considered gas and liquid generation are for the purposes of recovery / disposal rather than the effect on settlement. Similarly, most of the models consider the landfill to be rigid during landfill settlement. Further studies considering a deforming landfill is required to more accurately calculate landfill settlement.

Durmusoglu et al. (2005) produced a 1D numerical model to simulate vertical settlement using liquid and gas flows in a settling MSW landfill. The model assumes the worst case scenario, where the landfill waste material is completely saturated to stimulate biodegradation and resultant gas generation. The stress, porosity and strain rate are also calculated. Collaboration between this mathematical model and real-life landfill examples is required to confirm findings. The authors utilised Maxwell's body instead of the Hookean Spring to represent the viscoelastic nature of an MSW landfill to capture time-dependent deformation of the solid matrix. The strain rate is defined as per the following equation.

$$\frac{\partial \varepsilon}{\partial t} = m_v \frac{\partial \sigma'}{\partial t} + \frac{1}{k}\sigma' \qquad \textit{Eq. 2.24}$$

where: ε = strain, m_v = coefficient of volume change, σ' = effective stress and K = bulk viscosity of the solid waste. m_v and σ' are defined as:

$$m_v = \frac{(1+v)(1-2v)}{E(1-v)} \qquad \textit{Eq. 2.25}$$

$$\sigma' = \sigma_T + S_l P_l + S_g P_g \qquad \textit{Eq. 2.26}$$

where: v = Poison's ratio, E = Young's modulus, σ_T = total stress (compressive stresses are negative), S_l = liquid phase saturation, P_l = liquid pressure, S_g = gas phase saturation and P_g = gas pressure.

McDougall (2007) created the Hydraulic, Biological and Mechanical (HBM) model. This model captured the relationship between the void volume changes and waste degradation. The hydraulic flow utilises the unsaturated hydraulic flow model, in which the primary variables are the pressure head and moisture content. The bio-degradation model is a two-stage anaerobic model, which utilises volatile fatty acid and methanogenic biomass concentrations as the main variables. The mechanical model is a combination of load, creep and biodegradation to create a total landfill settlement as per the equation below:

$$\varepsilon_i = \varepsilon_i^e + \varepsilon_i^p + \varepsilon_i^c + \varepsilon_i^d \qquad \textit{Eq. 2.27}$$

where: ε_i = strain vector, ε_i^e = elastic strain, ε_i^p = plastic strain, ε_i^c = time-dependent creep and ε_i^d = degradation induced strain. Further field testing is required to confirm the accuracy of this prediction model.

2.3.3.6 Constitutive models

Constitutive models aim to define a stress-strain relationship for MSW. Development in this area commenced with Machado et al. (2002) aiming to model MSW using fundamental concepts of soil mechanics. Triaxial compression and confined compression of MSW were the key laboratory tests undertaken to create the framework of the model. The authors postulated two different effects for MSW behaviour including behaviour of MSW paste with fibres using elasto-plastic framework and MSW paste (without fibres) using critical state framework. Considering this was one of the first constitutive models, key limitations included refinement of the degradation aspect, consideration of shear strength losses over time and supporting large-scale field studies to support the findings. Some developments were made to this model (Machado et al., 2008).

Machado et al. (2017) furthered the original equation by also considering the compressibility of waste particles and the concepts of Skempton's equation for the effective stress. This model considers the drained case whilst the 2002 model addressed undrained loading conditions. The fibrous materials consider plastics and textiles, whilst the paste component considers organic material and glass, rubber and water. It should be noted this model maintains the same assumptions as the original 2002 model. There is a significant amount of parameters required, however these can be obtained quite easily from triaxial and oedometer tests, thus can be considered practical. This model is promising for prediction due to validation with lab testing data, however further validation is required using large scale field testing.

In a separate attempt, Sivakumar Babu et al. (2010) derived a constitutive equation considering mechanical compression and biological decomposition based on the Gibson & Lo (1961) and Park & Lee (1997) models. The proposed model is an extension of the modified cam clay model. The yield surface for the derived equation has been presented below.

$$q = Mp'\sqrt{\left\{\left[\left(\frac{p_0'}{p'}\right)^{\lambda}\exp\left\{\left[\frac{(e_0-e)}{1+e_0}+b\Delta p' e^{-ct}+E_{dg}e^{-dt}\right](1+e)\right\}\right]^{\frac{1}{\lambda-k}}-1\right\}} \qquad \textit{Eq. 2.28}$$

where: M = frictional constant, p' = mean effective stress, p'_0 = pre-consolidation pressure, e_0 = initial void ratio, e = void ratio after load increment, b = coefficient of mechanical creep, c = rate constant for mechanical creep, E_{dg} = total amount of strain that can occur due to biological decomposition, d = rate constant for biological decomposition, t = time since filling, λ = compression ratio and k = recompression index.

Validation of this model in terms of the stress strain response was completed by conducting one-dimensional compression and triaxial consolidated undrained shear experiments on three different types of municipal solid waste (MSW). The test results were in good agreement with the model predictions. However, the tests for determining the mechanical creep and biodegradation were based on short term experimental data, where in reality landfill settlement occurs over a long period of time. Although this model has correlation to existing predicting models and experimental results, it requires further validation for predicting actual field landfill settlement data.

Chouskey & Sivakumar Babu (2015) extended the simplistic model to consider more critical landfill settlement parameters for drained conditions of MSW settlement. Key considerations included developing an equation that considered elastic, plastic, creep and biodegradation elements based on critical state of soil framework. The amended yield surface equation from the 2010 model is presented below.

$$q = Mp'\sqrt{\left(\frac{p'_0}{p'}\right)\exp\left\{\left[\frac{(e_0-e)}{1+e_0} + b\sigma'_{11}(1-e^{-ct}) + E_{dg}e^{-dt}(1-e^{-ct})\right]\frac{1+e_0}{\lambda}\right\}}$$

Eq. 2.29

In addition, the model also considers plastic and elastic deviatoric strains to calculate the total volumetric strain as per the strain hardening rule. The results of the predictive model show good agreement with field experiments and previous literature. It should be noted although this model is relatively simple for the intent of practical use, it still does not consider some parameters known to be critical for landfill settlement. Once again, further validation using large scale landfill testing is required for confirming this generalised procedure.

One of the more recent models include an extension of the HBM model originally created by McDougall (2007). Reddy & Kumar (2018) created a model combining a

hydraulic model, biodegradation model and mechanical model to simulate behaviour of municipal solid waste in bioreactor landfills. Bioreactor landfills refer to landfills where leachate reinjection occurs to increase the rate of biodegradation and induce related settlement at a faster rate than a conventional landfill. Fast Lagrangian Analysis of Continua (FLAC) was used for creating the mathematical framework. The hydraulic model comprised of two elements, two-phase flow according to Darcy's law and saturated-unsaturated MSW behaviour based on soil-water retention model. Mechanical settlement was based on the Mohr-Coulomb constitutive model, whilst waste biodegradation was modelled via first order decay kinetics. The model was validated against experimental and field data provided by previous literature.

The model as highlighted by the authors has some critical limitations. The use of Mohr-Coulomb model simplifies mechanical settlement of MSW, since there is a reduced number of input parameters. A key element to note for all of the biodegradation models is the use of a single parameter, the decay constant. Biodegradation in landfills is based on a large number of factors, although it is difficult to capture all of these in a practical manner, the authors suggested the incorporation of temperature and pH as they have a significant effect on microbial activity.

2.3.3.7 Comparison between landfill settlement models

Sivakumar Babu et al. (2010) conducted a comparison between each of the prediction models available at the time to gauge the variation in total settlement. The landfill conditions and parameters were the same for each model and are summarised in Table 2.9 below. The variation for total settlement considering both primary and secondary settlement ranges from 6.54 m to 20.18 m. This creates issues during prediction of landfill waste settlement and data validation. Refer to Appendix B for a summary of the settlement prediction models.

Table 2.9 Comparison on landfill settlement models (adapted from Sivakumar babu et al. 2010)

Settlement model	Primary / Secondary Settlement	Total settlement (m)
Soil mechanics-based models		
Soil mechanics-based model (Sowers 1973)	Primary and secondary settlement	6.54
Bjarngard and Edgers model (Bjarngard and Edgers 1990)	Primary and secondary settlement	15.34
Hossain and Gabr (2005)	Secondary settlement only	3.65
Empirical models		
Logarithmic function (Yen and Scanlon 1975)	Secondary settlement only	2.35
Power creep function (Edil et al. 1990)	Primary and secondary settlement	9.92
Hyperbolic function (Ling et al. 1998)	Primary and secondary settlement	0.53
Attenuation equation (Coumoulos and Koryalos 1997)	Secondary settlement only	1.33
Rheological model		
Gibson and Lo model (Gibson and Lo 1961)	Primary and secondary settlement	14.84
Settlement models incorporating biodegradation		
Long-term biodegradation model (Park and Lee 1997)	Secondary settlement only	0.242
Hettiarachchi et al. (2009)	Primary and secondary settlement	20.18
Composite rheological model (Marques 2001)	Primary and secondary settlement	10.45
Composite compressibility model (Marques et al. 2003)	Primary and secondary settlement	8.97
Mechanical and decomposition (Oweis 2006)	Primary and secondary settlement	19.74
Liu et al. (2006)	Secondary settlement only	6.31
Sivakumar babu et al. (2010)	Primary and secondary settlement	9.09

2.4 Ground improvement techniques on landfills

2.4.1 Dynamic compaction

Dynamic compaction is a technique that utilises dropping a heavy weight onto the ground surface to improve the mechanical properties of granular soil. Bo et al. (2009) describe the repeated impacts of dropping the heavy weight over short intervals to cause rearrangement of soil particles into a denser state forming craters in the ground surface. Multiple passes are undertaken to compact the soil uniformly. Typically, the second pass occurs at a central location between points of the first pass. After each pass, the craters are backfilled with available material on site generally clean fill material. Alternatively, dynamic replacement methods involve backfilling the craters with rock to strengthen in-situ material. The number of drops can be calculated to achieve the minimum void ratio in the in-situ soil mass. Beyond this maximum amount of drops, there is minimal increase in the density of landfill material.

Theory

When the heavy weight impacts with the ground surface the impact energy generated from the drop height and mass of the block is converted into seismic radiation and transferred to the soil mass. Hamidi et al. (2011) describe the seismic energy as body waves, shear waves and compression waves that propagate radially outward from the heavy weight point of impact with the soil surface along a hemispherical front as shown in Figure 2.9. Similarly, the Rayleigh waves (R-waves) travel radially along a cylindrical wave front. Energy losses in the soil create a damping effect for the wave and limit the densification of the soil. A shear window is created by the interaction between the body waves and compression waves against the horizontal R-waves.

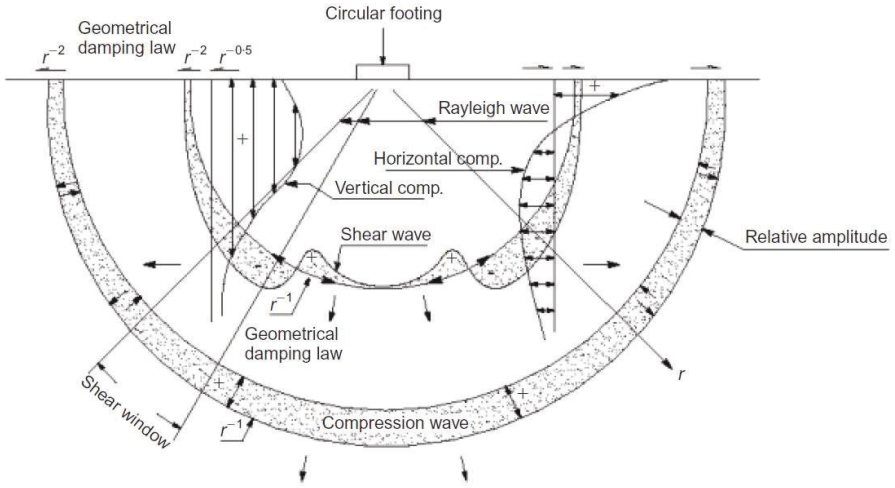

Figure 2.9 Wave propagation due to dynamic compaction (after Woods, 1968)

Depending on the saturation of the soil, the effect of dynamic compaction is variable. Within dry granular soils, Bo et al. (2009) describe the compressive and shear waves induced by the impact of the heavy weight to overcome the interlocking soil stresses decreasing the presence of voids. Within saturated soils, the impact of the heavy weight results in an increase in the pore pressure resulting in a state of temporary liquefaction. The shear waves and R-waves travel slower than the compression waves, and combined with the state of temporary liquefaction cause the soil particles to increase in density.

Known factors that affect the level of compaction achieved in soil masses include the pattern of compaction, spacing between drops, number of drops, drop height and mass of the heavy weight. Menard & Broise (1975) created the following equation for predicting the depth of influence of heavy weight impact on soil as:

$$D = (w \times h)^{0.5} \qquad \textit{Eq. 2.30}$$

where D = depth of influence, w = block weight in tonnes and h = drop height. However, Lukas (1986) developed a more acceptable version of the equation as:

$$D = n(w \times h)^{0.5} \qquad \textit{Eq. 2.31}$$

where n is the empirical coefficient factor combining soil composition and water table considerations, this value varies between 0.3 and 1.0. Leonards et al. (1980) proposed an n vale of 0.5 for granular soils based on field data under varying conditions.

Van Impe (1994) determined that the shape of weight and impact surface area both effect the depth of influence. Lukas (1986) stated that multi-tamping allowed for only improving the zone of influence rather than the depth of influence. Mayne et al. (1984) correlated the depth of the crater created by the impact of the weight against the number of drops $(Dc/(WH)^{0.5})$.

Chow et al. (1992) used numerical modelling methods to predict the crater depth produced by the impact of the weight with the ground surface using a wave equation model. This is a well-validated prediction justified by two case studies. This is useful in calculating the required backfill material volume for filling the craters produced by the impact of the weight.

Zekkos et al. (2013) describes the applied energy (AE) refers to the total energy introduced into the ground divided by the area of improvement. This is defined by the following equation:

$$AE = \frac{N.w.h.P.g}{A_{cp}} \qquad Eq.\ 2.32$$

where N is the number of drops per location, P is the number of passes, g is the gravitational acceleration and A_{cp} is the influence area for each location (square of the grid spacing).

Van Impe & Bouazza (1996) determined the value of empirical factor n for dynamic compaction of municipal solid waste landfills is highly variable, but can be assumed to be within the range of 0.3 and 0.65 as depicted in Figure 2.10. This is dependent on the age of the landfill, where younger landfills (less than 15 years old) show higher enforced settlement during dynamic compaction thus the value of n is closer to 0.65. For older landfills (greater than 15 years to approximately 20 to 25 years) the value of n is approximately 0.35 and behaves similarly to soil. Older landfills will have typically decomposed and experienced most of its settlement, thus the amount of enforced settlement would be limited since any remaining material would likely to be inert and chemically inactive.

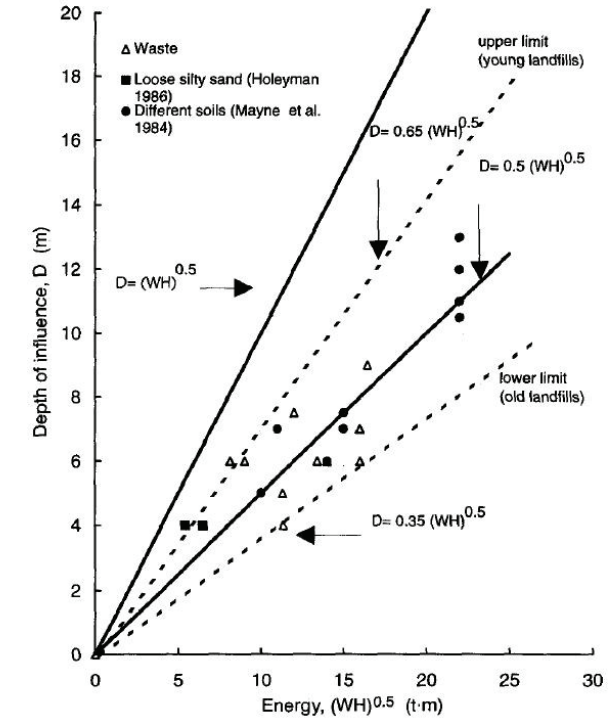

(a)

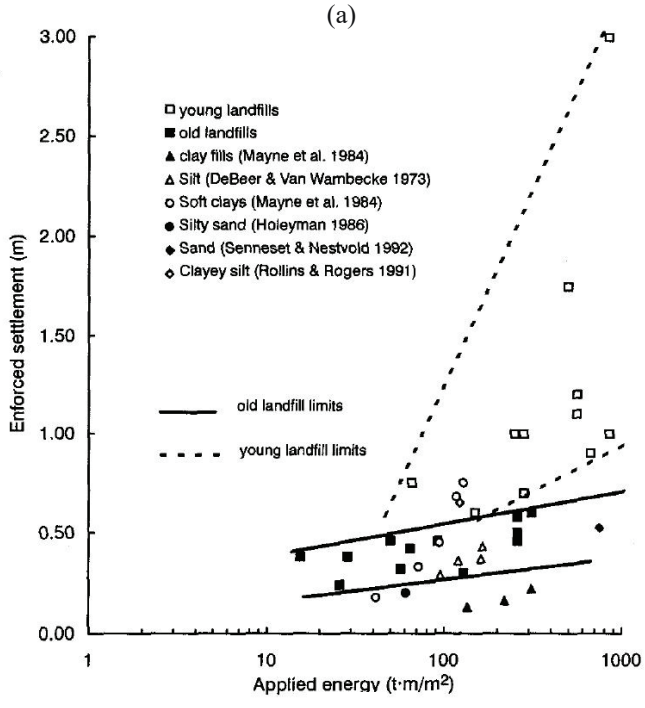

(b)

Figure 2.10 (a) Maximum depth of improvement vs scaled energy and (b) enforced settlement vs applied energy (right) after Van Impe & Bouazza (1996)

Applications on landfills

Zekkos et al. (2013) compiled a list of 56 test sites comprising of 33 municipal solid waste landfills that have utilised the dynamic compaction technique between 1979 and 2006. This does not include recent examples of dynamic compaction that have not been documented in the technical literature.

Dynamic compaction on solid waste landfills has additional difficulties in evaluating the depth of influence. This is primarily due to the heterogeneous nature of waste and the technology available to measure the depth of improvement. Only more recent investigations (post-1990s) have been able to measure the effective depth of influence.

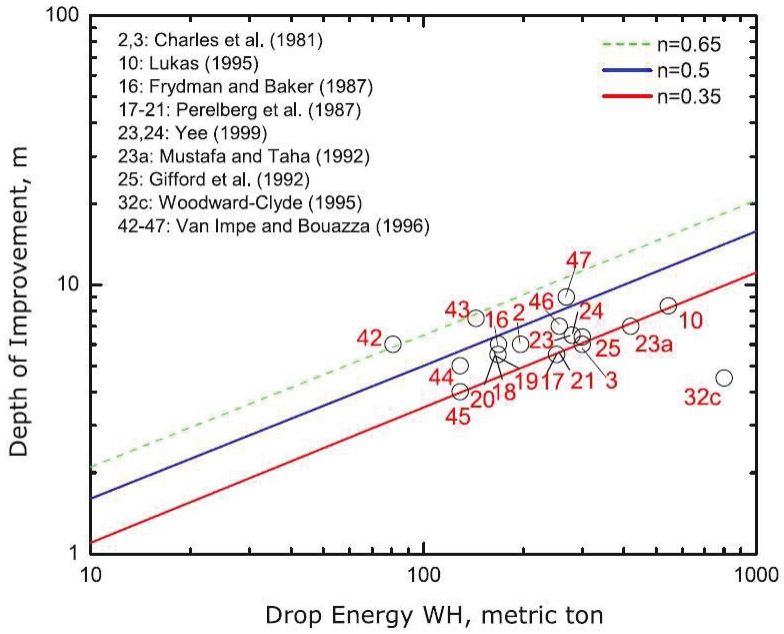

Figure 2.11 Relationship between the depth of improvement and drop energy after Zekkos et al. (2013)

From the case studies presented the depth of influence for use of dynamic compaction on municipal solid waste landfills ranges between 4 m and 9 m. This is very dependent on the thickness of the landfill waste, age of the landfill and applied energy for dynamic compaction.

More recently, the use of heavy compaction equipment ranging between 10 t and 40 t including sheepsfoot rollers and vibratory rollers have reduced the need for deep

compaction. The development of filling plans and limiting the height of waste placement has increased the effectiveness of the rollers in daily compaction of landfill waste at shallower depths. However, deep compaction methods can still be used at higher lift levels to induce settlement at a faster rate and to increase the available waste capacity of landfills.

Benefits vs limitations

The benefits and limitations of the use of dynamic compaction on solid waste landfills has been summarised in Table 2.10 below.

Table 2.10 Benefits and limitations of dynamic compaction

Benefits	Limitations
• Suitable for landfill application • Effective at depths between 4 – 9 m depending on applied energy for landfills Zekkos et al. (2013) • Most effective in unsaturated conditions • Cost effective (only backfilling with soil compared to other chemical methods)	• Time consuming to achieve compaction in saturated conditions • Environmental pollution (dust, noise and shock waves) to surrounding areas • Not suitable/effective for shallow depths (<2m) • Effect of dynamic compaction on geosynthetics are not known

2.4.2 Rapid impact compaction (RIC)

Rapid impact compaction (RIC) is a newer form of dynamic compaction developed in the 1990s. This method drops a pounder repeatedly (between 40 – 50 blows per minute) from a height between 1.2 – 1.5 m (above ground level) onto a steel plate. The steel plate is always in contact with the ground. Technology on board the RIC rig (refer Figure 2.12) can record the amount of blows, the energy input, the penetration per blow and cumulative settlement. The rig will continue to operate on a single location typically until either the amount of blows is completed for the set or the penetration reaches a certain depth.

One particular advantage of having the steel plate in continuous contact with the ground is the impact load is evenly distributed to the ground. For dynamic compaction, contact with a rock or heterogeneous material can result in load being transferred in a non-uniform manner.

Figure 2.12 Rapid Impact Compaction rig (after Serridge and Synac, 2006)

Theory

Applies the same theoretical concepts as dynamic compaction to improve soil density. Refer Section 2.4.1 for details.

Applications on landfills

Serridge & Synac (2006) compiled case studies for the use of RIC in a range of applications including landfills. Watts & Charles (2002) undertook a field trial for the use of RIC in loose building waste at Waterbeach in the United Kingdom. The building waste was piled and spread on top of a natural clay deposit in 1 m lifts to a total depth of 6.5 m. Groundwater was located approximately 4.5 m below the final surface level of the building waste.

The RIC method was employed utilising a 7 tonne rig with drop height of 1 m onto a 1.5 m diameter steel plate. Grid spacing was 1.5 m between adjacent RIC locations. Average energy input for the RIC locations was approximately 150 t.m/m^2. The settlement at the surface was on average 0.3 m across the site. The depth of influence was observed to be approximately 4 m below the initial surface level. Measurement methods to determine the effectiveness of the RIC was using SASW analysis.

This case study demonstrated the application of RIC to building waste material with induced settlement results. It is assumed that the application to domestic waste will produce a similar effect to that of dynamic compaction as the methodology is very similar. Although the depth of influence is known to be less for the use of RIC methods than the use of dynamic compaction methods.

Benefits vs limitations

The benefits and limitations of the use of rapid impact compaction on solid waste landfills has been summarised in Table 2.11 below.

Table 2.11 Benefits and limitations of RIC

Benefits	Limitations
• Suitable for landfill application – domestic waste and inert building waste • Effective at depths between 2 – 4 m • Most effective in unsaturated conditions • Cost effective (only backfilling with soil compared to other chemical methods) • Faster than dynamic compaction since drop height is reduced and more blows per minute • Ability to work in close proximity to buildings since peak particle velocity is less than dynamic compaction • Size of equipment is smaller than dynamic compaction equipment	• Not suitable for saturated conditions • Environmental pollution (dust, noise and shock waves) to surrounding areas • Not suitable/effective for deep compaction • Effect on underlying geosynthetics are not known

2.4.3 Preloading

Preloading involves placing an external load typically an embankment or stockpile of material for a long duration to accelerate the consolidation process.

Theory

Mohamad (2008) describes the process of preloading as a simple form of inducing settlement to limit post construction settlement. To construct an embankment, the preloading process consists of placing the final embankment height worth of fill material along with an additional height of material known as surcharge load above the final level as shown in Figure 2.13.

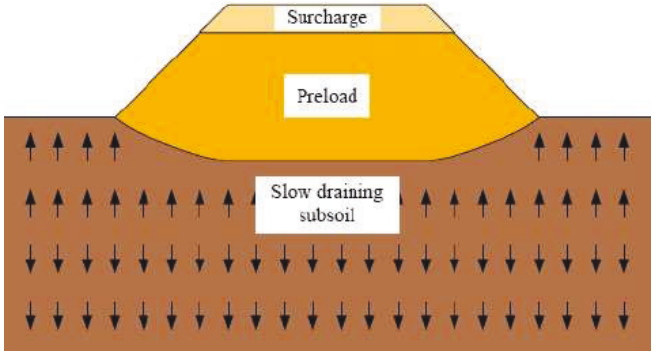

Figure 2.13 Preloading technique

The embankment and surcharge loads are applied over a period typically ranging between 3 months and 12 months inducing settlement. At the end of this preloading period, the surcharge load is removed causing the underlying material to be unloaded, this will significantly reduce or completely eliminate the post-construction settlement of the final embankment. As a result of preloading, the material underlying the embankment will become stiffer and over consolidated.

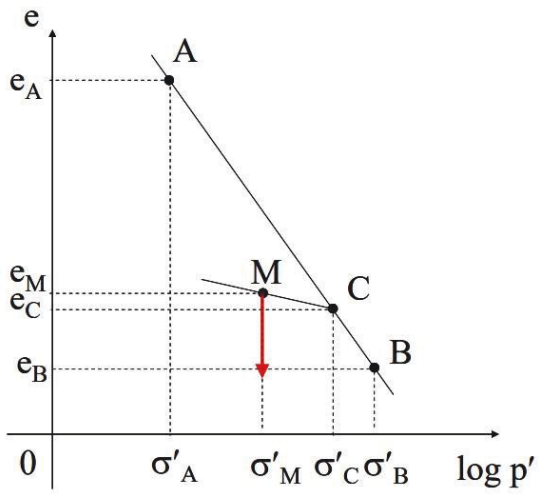

Figure 2.14 e-log p' relationship after Balasubramaniam et al. (2010)

Balasubramaniam et al. (2010) presented an e-log p' relationship as shown in Figure 2.14 to create a better understanding of the loading and unloading effects on the void ratio and stress of clay material. Point A is representative of the initial conditions where the initial void ratio is high. Point B depicts the void ratio following placement of the embankment and

surcharge loads, where this is the maximum stress the clay has achieved at any point in its lifetime. Just prior to unloading, Point C lies along the line AB prior to removal of the surcharge load. Point M is the swelling line following removal of the surcharge load, placing the clay in a largely over consolidated state.

The application of prefabricated drains (PVD) can typically be used for accelerating the consolidation process. However, the use of PVD application for landfills is not a feasible solution due to installation difficulties and due to creation of potential flow paths for gas and leachate to transfer to outside the landfill. Potential contamination of preloading material (including the portion of material in direct contact with waste material) is likely if PVDs are utilised for landfill material.

Application on landfills

For preloading works on landfills, the heterogeneous nature of waste presents a major obstacle for prediction of settlement, in particular secondary settlement. Research into this has been relatively limited since the construction on top of landfills for either road or rail applications is quite rare and is generally avoided due to construction difficulty. Recent ground improvement on landfill has seen preloading as a simple and common method due to its cost and easy installation.

The most recent documented use of preloading techniques was in 2012 at Fresh Kills landfill on Staten Island, New York. de Melo et al. (2012) describe the use of preloading for construction of a road embankment above the landfill. The waste type was classified as a mixture of municipal solid waste and building waste. Field records indicated that primary settlement occurred within 30 days of first placement of stockpile material above the landfill. This is consistent with the general theory where primary consolidation is to occur within 10 to 100 days according to Dunn (1995) or within the first month as suggested by Wall & Zeiss (1995). Secondary settlement was assumed to be any settlement beyond the first month up until 132 days (end of the monitoring period).

Settlement ranges as presented by de Melo et al. (2012) for the Fresh Kills landfill included:

- For primary settlement range 0.06 - 0.65 m during the first month including stockpile placement
- For secondary settlement range 0.05 - 0.37 m over 132 days

de Melo et al. (2012) was unable to collect information regarding construction details of the stockpiles and could not correlate this information to primary settlement. The authors were able to back-calculate the compression ratio using the settlement data obtained for primary and secondary settlement. The values for the modified primary compression index and modified primary recompression index were 0.23 and 0.023 respectively. The secondary compression index ranged between 0.016 and 0.026.

Lewis et al. (2004) similarly describes a case at Tinton Falls landfill in New Jersey, USA. This site employed both dynamic compaction and preloading techniques to treat the landfill prior to construction of the road. Based on this site, the authors back calculated the compression index using the available settlement data. The secondary compression index ranged between 0.0529 and 0.0817. This is significantly different to the range outlined by de Melo et al. (2012) and requires further investigation and validation.

One significant point also outlined by Lewis et al. (2004) is the long-term settlement of dynamic compaction compared against preloading on landfills. The observed settlement was greater for preloading areas than the dynamic compaction areas. However, long-term observations of road surface indicated that the preloaded areas showed significant signs of differential settlement whilst the dynamic compaction areas only showed minimal settlement effects.

Benefits vs limitations

The benefits and limitations of the use of preloading on solid waste landfills has been summarised in Table 2.12.

Table 2.12 Benefits and limitations of preloading

Benefits	Limitations
• Suitable for landfill application – domestic waste • Non-intrusive ground improvement method – no excavation into waste required • Effective for deep compaction • Effective in both saturated and unsaturated conditions • Cost effective (if surcharge and embankment material available onsite) • Specialised equipment not required • No major environmental concerns	• Time consuming – 3 months to 12 months depending on surcharge and final load conditions • Requires monitoring to measure effects of preloading • Not suitable for inert building waste since this material is not compressible under purely surcharge loads • Effect on underlying geosynthetics are not known

2.4.4 High energy impact compaction

Compaction machinery for standard applications typically comprises of static rollers or vibratory rollers to achieve a higher strength material. This method includes passing over the material multiple times in an effort to increase the density of the underlying material. Although this is effective in standard construction applications, these methods are not efficient in compaction beyond a certain depth because they have inadequate energy to transfer deep within the material.

High Energy Impact Compaction (HEIC) is a refined version of the traditional compaction method that allows for faster compaction with a greater amount of energy transferred deeper within the material. HEIC impact rollers (refer to Figure 2.15) consist of non-circular modules that are typically attached to the back of a tractor and rolled in multiple passes across the area requiring compaction. The non-circular module can vary in shape from 3 sided, 4 sided, 5 sided and polygonal. Clifford (1976) stated the development of the HEIC dated back to the 1930s; however, its practical implementation commenced in the late 1960s in South Africa.

As the non-circular module is towed by the tractor, it rotates and reaches a point where gravitational force causes it to fall and impact the ground surface. Hamidi et al. (2011) describe the tractor speed to range between 8 – 11 km/hr, beyond this speed there is risk that the non-circular module will skip along the ground surface and if at a greater speeds will act

similar to a conventional circular roller reducing the depth of influence. Note the speed of the impact roller also provides kinetic energy to increase the force of impact with the ground surface.

Figure 2.15 HEIC 3 sided roller (after Landpac, 2016)

Theory

Impact compaction is similar to dynamic compaction in that the impact of the weight with the ground surface causes a compaction. However, as Hamidi et al. (2011) states, there are some major differences between these methods including:

- Drop height of impact roller non-circular module is considerably less than dynamic compaction as a result there is a reduction in the depth of influence
- Frequency of impact with ground surface is greater for impact rollers than dynamic compaction
- Application of impact rollers is typically for surface compaction with depth less than 2 m, whilst dynamic compaction targets compaction of deeper strata ranging between 4 – 9 m for landfills

Pinard (1999) argues that theory behind impact compaction is based on the amplitude and frequency of the impacts similar to the laboratory tests such as Proctor and modified AASHTO tests. Vibratory or static compaction is based on delivering low amplitude waves at a high frequency whereas impact compaction is high amplitude low frequency waves for deeper compaction. This concept has been depicted in Figure 2.16. In addition, Pinard (1999) describe that HEIC requires less moisture conditioning than conventional compaction

methods. This allows for thicker lifts of material placement with less moisture conditioning, making this a cost effective solution for fill placement for embankments.

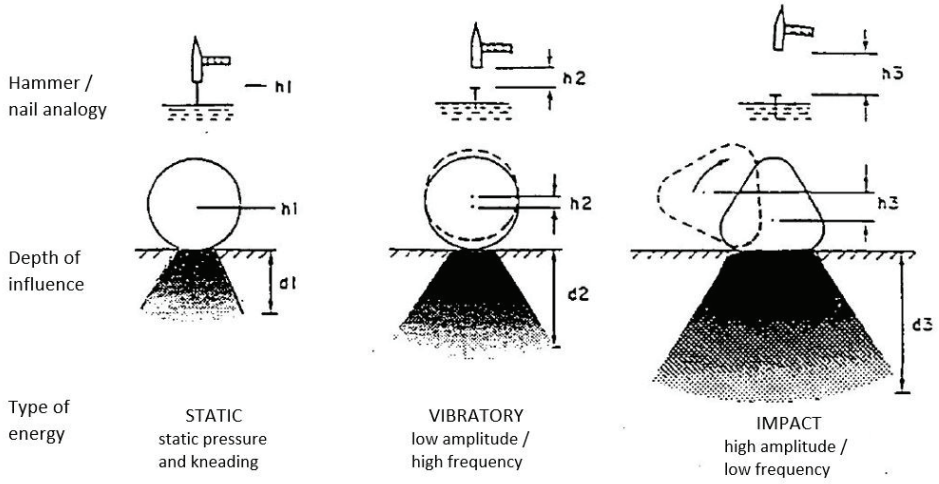

Figure 2.16 Comparison between static, vibratory and impact compaction methods (after Pinard, 1999)

Landpac (2016) has presented Figure 2.17, which demonstrates the large variation in the depth of influence between conventional compaction and HEIC.

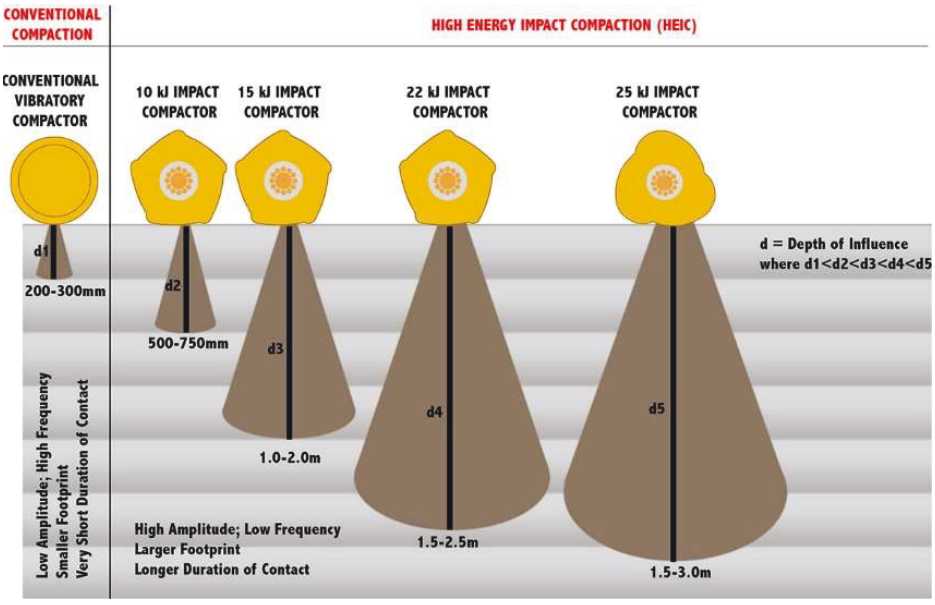

Figure 2.17 Conventional compaction vs HEIC depth of influence after Landpac (2016)

Application on landfills

HEIC has been utilised as a ground improvement technique for landfill applications. However, there is little current literature on the prediction of settlement and effectiveness of this technique specifically for landfill applications on new landfills (with age less than 15 years).

Avalle & McKenzie (2005) described the successful application of a square impact roller on an old landfill site in Victoria, Australia. The landfill site was mainly filled with domestic waste, and was closed in the late 1970s, making the landfill approximately 25 years of age. The landfill was capped, so the capping system was removed (clay cap), HEIC completed, surcharge placed and then cap reinstated prior to construction of residential infrastructure above the area. Waste thickness in the area was approximately 3-4 m thick.

Dynamic compaction was considered for this application, however due to cost, environmental issues and potential for damage to the capping system HEIC method was considered more appropriate. The HEIC method was continued for the site until no further measurable settlement could be completed. Settlement surveys were conducted at intervals in between passes of the HEIC roller to determine the average settlement and if no changes were observed, the HEIC roller would cease compaction. Figure 2.18 presents the average settlements across five grid lines and the overall average settlement for the site. Note the settlement is not constantly increasing, the authors observed heave in some locations as other points settled and explain this to be due to ‘rebound’ phenomenon of waste material.

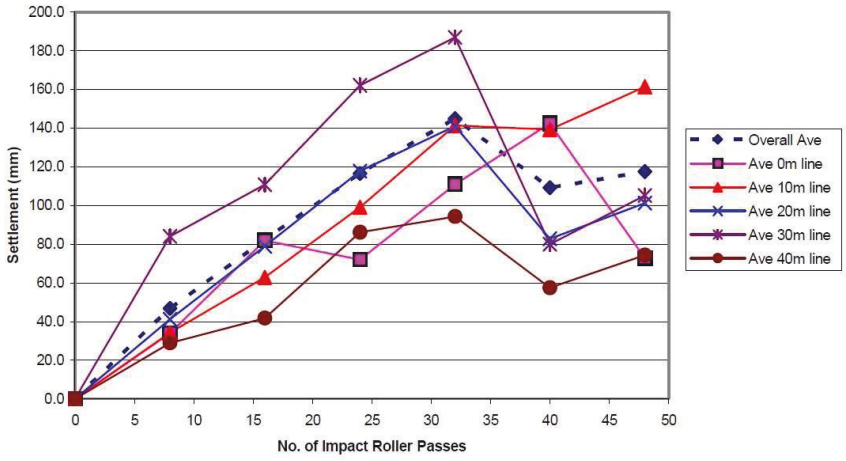

Figure 2.18 Average settlement during HEIC (after Avalle & McKenzie 2005)

Continuous surface wave methods (CSWS) were used to test the ground improvement effectiveness and depth improvement was found to be approximately 2 m from ground surface. Further surcharging on the site was completed for one month and settlement was observed to be on average 2 mm, with a maximum value of 4 mm.

Bouazza & Avalle (2006) confirmed the effectiveness of the HEIC ground improvement technique for this same site was approximately 2 m below the surface, which included a thin layer of clay capping system and waste material. They both deem the method as acceptable for this shallow compaction acceptable and cost effective.

Note the age of the landfill is determined to be relatively old, and almost all primary settlement and secondary settlement would have been completed. The waste thickness was also very shallow so further settlement observations would be limited. Settlement observations beyond this period would typically be due to creep or remaining secondary settlement, a period of one month of observation is unlikely to be sufficient for determining its long term effectiveness especially considering the area was not loaded.

Benefits vs limitations

The benefits and limitations of the use of HEIC on solid waste landfills has been summarised in Table 2.13 below.

Table 2.13 Benefits and limitations of HEIC

Benefits	Limitations
• Suitable for landfill application – domestic waste up to depths of 2 m • Limited influence depth can limit interaction with landfill capping or base lining systems • Non-intrusive ground improvement method – no excavation into waste required • Cost effective and fast method of compaction • No major environmental concerns	• Does not address secondary settlement and creep related issues • Limited to depth of 2 m, may not be suitable for deep applications • Application on building waste not currently known • Effect on underlying geosynthetics are not known

2.4.5 Vibro compaction and vibro replacement

Vibro compaction involves the penetration of a vibrating probe into the ground typically in conjunction with either water or air jets to increase the density of in-situ material. Vibro replacement involves placing material typically rock into the void created by vibro compaction, creating a zone of high strength material (i.e. stone column construction).

The use of vibro compaction or vibro replacement is not considered as a practical form of ground improvement on landfills. The main reason as Woodward (2005) describes is due to the presence of obstructions including building waste or large domestic waste in landfills that is highly likely to cause damage to the vibrating probe as it penetrates the ground surface. Without the ability to reach deep depths without obstruction from potential metal scraps or building rubble, this technique cannot adequately perform to its potential as it would in other soil types.

2.4.6 Chemical stabilisation

Chemical stabilisation refers to the mechanical mixing of chemical additives to soil to improve its geotechnical properties. Limiting ground settlement, creating groundwater barriers and providing support during excavations are some of the geotechnical properties improved from chemical stabilisation methods. Raj (2011) states that chemical additives can

include cement, lime, fly ash, bitumen, asphalt, polymers and other chemicals. Generally, this method is most effective for granular material where voids are present.

Theory

The aim of each of the chemical stabilisation methods and processes vary slightly for each type of additive used for ground improvement. This section briefly outlines the theory behind the main chemical additives.

Raj (2011) describes there to be three types of grouting methods utilising a combination of cement, sand and water include compaction grouting, permeation grouting and hydro fracturing as depicted in Figure 2.19. Permeation grouting refers to the use of a low-pressure grout pumped through pores and voids in the soil and rock material. Compaction grouting uses a high-pressure grout that exerts an outward pressure on the soil, with the grout remaining in mainly one solid mass. Hydro fracturing applications is specifically for use in rock systems with large voids, where the grout pressure is sufficiently high to travel through rock fractures.

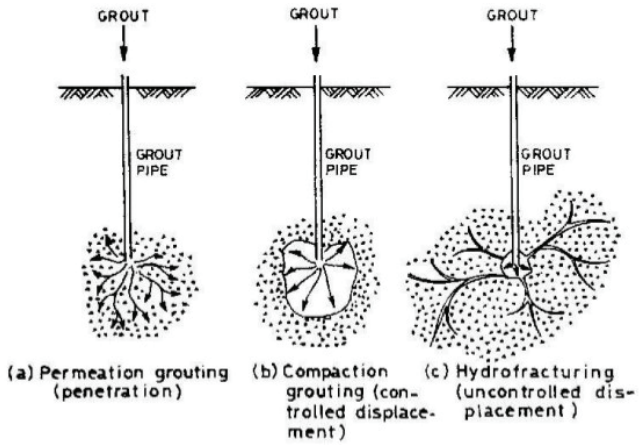

Figure 2.19 Types of grouting methods (after Raj, 2011)

There are a few formulas for calculating the groutability of granular material. One recommended method is explained by Incecik & Ceren (1995) in the equation below:

$$N = \frac{D_{10}(soil)}{d_{90}(grout)} \qquad \textit{Eq. 2.33}$$

where N is the groutability of the soil, D_{10} is the diameter through, which 10% of soil can pass through and d_{90} is the diameter through, which 90% of the grout mass passes. If the value of N is greater than 10, then grouting is suitable for the soil.

Akbulut & Saglamer (2002) proposed a new approach for estimating the ability to grout granular soils. This is presented in equation below:

$$N = \frac{D_{10}(soil)}{d_{90}(grout)} + k_1 \frac{w/c}{FC} + k_2 \frac{P}{D_r} \qquad Eq.\ 2.34$$

where k_1 is a constant (0.5), k_2 is a constant (0.01) in 1/kPa, w/c is the water to cement ratio of the grout, FC is the content of soil material passing through a 0.6 mm sieve, D_r is the relative density of the soil sample and P is the grouting pressure. D_{10}, D_{90} and N have been previously described. These values were obtained from analysis of experimental data.

The use of cement is an expensive choice for stabilising material, especially considering the large volume required for landfill application. Horpibulsuk et al. (2011) suggested that an alternative cost effective and environmentally friendly solution is the use of lime, fly ash or as more recently discovered a combination of both lime and fly ash.

Prakash & Sridharan (1989) were one of the first to document research on the use of lime products for soil stabilisation. Lime products can include quicklime (CaO), hydrated lime (calcium hydroxide – $Ca(OH)_2$) or a lime slurry. This chemical stabilisation process is most effective on clay. Graymont (2004) explains the chemical process to consist of three processes:

1) Drying – hydration of the quicklime causes a chemical reaction that releases heat. This heat then causes subsequent evaporation and drying of the soil
2) Modification – the calcium ions from quicklime migrate to the soil surface and cause displacement of water and other ions. This increases the ability to compact the material as it displays brittle behaviour. This process is known as flocculation and agglomeration, taking a few hours for the process to complete.
3) Stabilisation – lime increases the pH of the soil, causing some clay material to break down. During the break down process for reactive soils, silica and alumina are release and react with the calcium from the lime. This create calcium silica hydrates (CSH)

and calcium aluminate hydrates (CAH) which are both cementitious products. This increases the strength of the material. This process commences within a few hours of addition of the quick lime and can continue for a long period.

Graymont New York Materials (2004) states that for lime stabilisation to be effective in step 3 (above), the soil is to be reactive where it contains the silica and alumina. However, these circumstances can be uncommon and are not uniform across a large site such a highway. Instead, the use of fly ash in combination with the lime can assist in providing the silica and alumina for the long-term stabilisation of the material.

Qubain et al. (2000) utilised the technique of lime stabilisation for construction of a highway pavement on clayey material. The results indicated that the clay material strength increased significantly, leading to cost savings as pavement thickness was reduced. Similarly, other researchers have noted strength improvements in various soils including Ismail (2004) and Ampera & Aydogmus (2005).

Abmaruzzaman (2010) describes that fly ash is the planet's fifth largest raw material resource. Fly ash is a waste byproduct from energy production at coal-fired power plants. The use of fly ash for ground improvement allows for both a method of disposal of this waste product whilst providing soils with strength improvement.

FHWA (2016) describes two typical fly ash products used for construction include Class C and Class F fly ash. Class C fly ash has self-cementing properties allowing it to be used by itself. Class F fly ash has little or no cementing value by itself and is used in combination with lime or other additives.

Fly ash chemically reacts with water to form a mixture with cementitious properties. Andreas et al. (2003) states the mixture hardens within a few hours of injection into the soil body. Note the strength is not as high as Portland cement.

Edil et al. (2002), Acosta (2002), Senol et al. (2002) and Thomas & White (2003) have documented the use of fly ash as a ground stabilisation method. The outcomes of the use of fly ash included an increase in the unconfined compressive strength and increase in stiffness of the soil material. Note these cases were all for subgrade ground improvement for road construction.

The combined use of fly ash and lime together allow for further increasing the maximum unconfined compressive strength of the soil Sahoo et al. (2010). Note that the optimum moisture content is increased to achieve this maximum unconfined strength of soil.

Application on landfills

The application of chemical stabilisation methods are quite uncommon, however some case studies have been found and are summarised below.

Naveen et al. (2014) describes the use of fly ash mixed with water to stabilise landfill waste. This procedure involved collection of domestic waste samples from the Mavallipura landfill and testing in laboratory conditions. The sample was then mixed with 20% fly ash and water to achieve the optimum moisture content of 22%. Direct shear and California bearing ratio (CBR) tests were undertaken to determine the effectives of the addition of fly ash to the waste material. The results indicated shear strength of the waste increased, but is still not sufficient to support a flexible road pavement. The CBR value of the stabilised waste dump was found to be 1.2%, however the CBR of the subgrade soil is required to be 4%. This method alone was not found to provide an effective solution for waste stabilisation.

Andreas et al. (2003) investigated the use of fly ash injection into the Tveta sanitary landfill in Sweden. This was a large-scale investigation whereby 100 tonnes of fly ash was mixed with water and pumped into the landfill. At the landfill site, perforated pipes were installed to a depth of 9 m below the surface of the landfill (the top 3 m of the pipe were solid wall pipe). The landfill itself was a mixture between domestic waste and industrial waste at a ratio of 1:2. This landfill two years of age at the time of fly ash injection with an estimated porosity of 30-40%. The authors determined the degree of filling to be in the range of 22-29% in the landfill body. Key findings from this investigation included the ash hardening occurs within a few days of injection creating hard but brittle lumps, the ash-water-slurry flows through the waste voids easily and can spread some distance from the injection location. Note the effectiveness of this method and ability to predict the amount of fly ash required has been classed as ‘unpredictable’ for landfills due to its heterogeneous nature.

Figure 2.20 Fly ash mixture with the injection hose and hydraulic hose (Fatahi, 2012)

Khabbaz & Fatahi (2012) compared the compaction, permeability and shear strength properties of municipal solid waste with and without the use of Class F fly ash combined with lime. Samples were taken from a landfill in Sydney and tested in laboratory conditions simulating deep soil mixing techniques. The results indicated by mixing 13.4% fly ash and lime with the MSW samples, the maximum dry density of the waste increase by 70 kg/m^3 and OMC decreased by 2%. When 6.7% of fly ash and lime was mixed with waste, the permeability decreased rapidly, however if curing time was extended and fly ash and lime content increased, no significant changes in the permeability was observed. Unconfined compressive strength was also observed to increase in the order of 150%, with a 20% fly ash and lime mixture. Overall, the application of fly ash and lime mixture to municipal solid waste appears to be effective in providing strength gain, reducing permeability and increasing the density of waste material. Note the application of the chemical stabilisation method has been thoroughly examined in laboratory setting; however the application for real world landfills has been limited.

Benefits vs limitations

The benefits and limitations of the use of chemical stabilisation on solid waste landfills has been summarised in Table 2.14.

Table 2.14 Benefits and limitations of chemical stabilisation

Benefits	Limitations
• Suitable for landfill application, although practical applications are limited • Environmentally friendly for fly ash solution (using waste by product of coal) • Potentially suitable for deeper applications, however this is dependent on the landfill • No major environmental concerns	• Applications on landfills is limited • Can be costly compared to other traditional ground improvement techniques • Potential to clog leachate pipework systems at the base of the landfill • Existing studies have not addressed secondary settlement and creep related issues • Existing studies have not established a potential depth of improvement. It is however reliant on installation of perforated vertical pipes through the landfill which may cause some difficulty • Effect on underlying geosynthetics are not known

2.4.7 Summary of ground improvement techniques on landfills

A summary of the ground improvement techniques on landfills with benefits, limitations, depth of effectiveness are presented in Appendix C.

2.5 Gap identification

The literature review reveals that there is a lack of guidance for practicing engineers to undertake geotechnical design of infrastructure above closed landfills. Whilst there are cases where design has been undertaken above closed landfills, the input parameters used for settlement prediction are heavily reliant on literature rather than employing site-specific landfill testing. Furthermore, landfill settlement prediction is a complicated procedure and with decades of research undertaken, it is still unclear which models should be utilised as a standardised and proven approach. Therefore, the following research gaps have been identified:

1. There is a lack of a standardised approach to geotechnical design for infrastructure above closed landfills
2. Site investigation and laboratory testing methods to obtain critical landfill settlement parameters are unclear

3. An appropriate settlement prediction model to utilise the parameters obtained from site investigation and laboratory testing which has been validated with field monitoring data is not available in existing literature
4. Models/studies that address decomposition settlement and residual settlement

Chapter 3 – Site Investigation at a landfill in Sydney

This chapter details the findings acquired from the site investigation and sample collection at the case study location at a landfill in Sydney, Australia. Site investigation techniques, discussed in this chapter, include test pitting, downhole geophysics, multi-channel analysis of surface waves, LiDAR, gas pumping trial and plate load testing. Field testing results are translated into critical design parameters, including the unit weight, the moisture content, the organic content, the small strain shear modulus, the small strain Young's modulus, the biodegradation rate and the age of waste. Sample collection includes undisturbed sampling with push tubes within test pits taken from the surface of the landfill.

3.1 Introduction

As urban development increases in major cities globally, there is an increasing trend in development above closed landfill sites. Within Sydney alone, there are currently a number of major infrastructure projects that are in progress or have been constructed directly above landfill sites such as Westconnex M8 - St Peters Interchange (AUD $4.6 billion), Moorebank Intermodal Terminal Project (AUD$1.7 billion) and Sydney Gateway (AUD $2.6 billion). Waste properties and mechanics in both short term and long-term have been studied for decades by many researchers (Sowers, 1973; Landva & Clark, 1986b; Kavazanjian et al., 1995; Gourc et al., 2010; Zekkos et al., 2010; Bareither et al., 2013b; Machado et al., 2017; Bonaparte et al., 2020; Rakic et al., 2020). However due to the heterogeneous nature of waste and variability among different sites, the application of these valuable research studies towards assessing the performance of structures built on landfill sites is still quite difficult for practicing engineers. Given that landfills are typically filled in lifts of 2 - 3m over decades, there are significant variations in properties with depth, which are also constantly changing over time due to physical, mechanical, chemical and biological processes.

The current approach undertaken by a large number of practicing geotechnical engineers is to simply assume design parameters based on information available in literature or to adopt an observational approach relying on post-construction monitoring results. The issue with use of data available in literature is that each landfill is unique with properties and behaviours dependent on a large number of interrelated factors such as composition,

compaction processes, unit weight, biodegradation, stiffness, age of waste, and climate conditions (El-Fadel & Khoury, 2000; McDougall, 2007; Powrie et al., 2019), which can lead to potential problems in designs and risk in construction, particularly when stringent long term settlement or stability requirements need to be satisfied. Whilst the post-construction observational approach is a practical approach, it often results in uncertainty in construction timeframe and is likely to involve long-term intervention periods to repair or readjust levels, which will increase cost and risk for clients. There are currently no internationally accepted standards or guidelines for field investigations, testing and sampling for landfill sites, which once available will be the solution for standardising the industry approach to geotechnical site investigation and design for infrastructure above closed landfills.

It should be noted that the landfill type has a significant influence on the behaviour of waste materials. According to EPA (2016), there are three main types of landfills including municipal solid waste landfills, industrial landfills and hazardous waste landfills. Municipal solid waste landfills accept household waste, which may include paper, plastics, organic material and other non-hazardous waste (Burnley, 2007). Industrial landfills accept large bulky waste including concrete, bricks, timber, metals and glass. Hazardous landfills include radiological waste, medical waste and other contaminated material. Tchobanoglous & Kreith (2002) presented a detailed list of operational records that landfill owners should be maintaining including approximate landfill composition, waste tonnages, filling plans, as-built records of base lining, leachate pipework, groundwater levels and under liner collection systems. For older landfills, these records may not be available, however understanding the existing landfill condition is critical for geotechnical design and reducing environmental impact.

Nearly all landfill researchers (Oweis & Khera, 1986; Dixon & Jones, 2005; Zekkos et al., 2006; Cirone & Park, 2020) identified and investigated unit weight and moisture content as the critical parameters for geotechnical characterisation of solid waste landfills. Indeed, the unit weight of the material is directly related to both the compaction effort at the time of waste placement and the material composition. The key limitations of research available in current literature is the limited depth of investigation into the landfill since test pits were adopted or there were practicality issues in undertaking test pitting and drilling on

landfill sites (Landva & Clark, 1986b; Zekkos et al., 2006). On the other hand, the measurement of moisture content allows determination of the dry unit weight and identification of potentially perched leachate between landfill waste lifts. Since waste is typically placed in lifts with intermediate cover soils, there is potential formation of a layered profile affecting permeability and creating perched leachate (Bella et al., 2012; Trapani et al., 2015).

Obtaining material stiffness parameters (e.g. compression modulus) is a critical step since these parameters are required in any numerical modelling undertaken for deformation calculations. Gomes et al. (2014) completed in-situ CPT testing, collected samples from adjacent boreholes and undertook triaxial and oedometer tests in the laboratory for a municipal solid waste landfill with waste comprising of mainly plastic and textiles. Testing conditions for oedometer and triaxial tests were simulated to match effective stress conditions obtained from the CPT tests at different depths. As a result, correlations were proposed to obtain stiffness using CPT data. However, CPT tests in landfills often encounter refusal when in contact with large and hard particles, are limited to localized vertical profiles and may not capture the variability of the landfill unless a large number of both in-situ and laboratory tests are undertaken. Instead other researchers (Bouazza & Kavazanjian, 2000; Zekkos et al., 2011) had success with use of geophysical testing namely multichannel analysis of surface waves (MASW) and vertical seismic profiling (VSP) to obtain shear wave (S-wave) velocity and determine the in-situ small strain stiffness. MASW is able to capture a 2D stiffness with depth allowing for detection of landfill variability. Indeed, VSP in addition to shear wave velocity also measures compression wave (P-wave) velocity, which allows for calculation of the shear modulus for seismic analysis and the Poisson's ratio for anisotropic waste. Although similar to CPT there is a limitation of only obtaining a 1D profile with depth and so a large amount of testing needs to be undertaken to capture spatial variability.

The interrelated organic content and biodegradation rate are major contributors to the long-term settlement of landfill material (Durmusoglu et al., 2005; Liu et al., 2006; Fei & Zekkos, 2013; Babu & Lakshmikanthan, 2015). There is some ambiguity around the best method for estimation of the biodegradation rate, as it is difficult to evaluate this in the laboratory due to the required large scale test setup and results in overestimating field

measurements by orders of magnitude (Lamborn, 2012; Fei et al., 2016). The reason for overestimation is that in a landfill not all of the organic matter is subject to microbial degradation (Park et al., 2018), whilst in a laboratory test the whole sample undergoes degradation. Landfill gas measurement in the field is also difficult as installation of monitoring wells and long-term measurements are required. However, field testing adopting gas generation rates (Sormunen et al., 2013; Park et al., 2018) can be considered as a reasonable first pass estimate especially if a landfill gas extraction system is available as a landfill closure and long term monitoring procedure.

The collection of samples for laboratory testing is critical for obtaining landfill specific parameters including strength, compressibility and permeability, which are necessary for any landfill performance analysis. Although undisturbed sampling via push tubes is recommended (Dixon & Jones, 2005), it can be difficult to obtain representative samples of the landfill material due to refusal during pushing of tubes into landfill and localised sampling with small sample size. The representativeness can be assessed visually and through confirmation of unit weight of the collected sample with the bulk unit weight measured in a deep test pit. Since the unit weight of collected samples is related directly to the landfill composition, a reasonable assumption would be that if the unit weight of the sample is roughly the same as the bulk unit weight of the test pit, then the sample could be considered as reasonably representative. There may still be underlying issues with representativeness in terms of particle size, however testing reconstituted material (Kavazanjian et al., 1995; Bray et al., 2009; Machado et al., 2017) is at least considered better than assumptive values from limited existing literature. With advances in technology, collection of samples from different depths can be completed with the use of sonic drilling (Burlingame et al., 2007), while this may not be feasible for some types of waste that have little to no cohesion (e.g. plastic waste). Moreover, while acceptance of landfill material into commercial geotechnical laboratories can also be a hindrance, visual observation to detect and clear hazardous materials (e.g. asbestos and medical wastes) followed by chemical testing to identify the level of contamination can facilitate laboratory testing.

This study provides guidance for standardised geotechnical site investigations on closed landfill sites to obtain critical design parameters with reference to a landfill in Sydney,

Australia as a supporting case study. This major infrastructure project involved the construction of a complex series of bridges and pavements supported by over 3000 m of driven piles directly built on top of landfill materials. The proposed practical site investigation techniques in this study incorporates recent advances in technology piloted at a landfill in Sydney, including test pits with laser scanning, sonic drilled boreholes, plate load testing, multichannel analysis of surface waves (MASW), vertical seismic profiling (VSP) and sample collection for laboratory testing. Design parameters identified and discussed in this study include unit weight, moisture content, organic content, stiffness parameters and biodegradation rate. While this thesis focuses on field investigation aspects, the other set of critical design parameters, obtained from laboratory testing (e.g. large triaxial testing, and Rowe cells) including strength, compressibility and permeability parameters shall be discussed in a separate paper to follow.

3.2 Case study of the landfill and proposed field investigation methods

3.2.1 Overview of the case study

The supporting case study was undertaken at a landfill in Sydney. The history of the landfill is summarised in Table 3.1. Landfill composition primarily consisted of food, paper, cardboard, wood waste and inert construction waste prior to 2002. Post 2002, the waste primarily consisted of construction waste and wood waste. Although a base lining system was not present, a leachate collection system was present for the deeper portion of the landfill. Further detail regarding the age of waste is presented in the next section. The surrounding geology of the landfill included in order of increasing age, Quaternary Sediments (Botany sands), Quaternary Clay, Class IV and V Weathered Ashfield Shale, Class I to III Ashfield Shale and Hawkesbury Sandstone based on the Pells classification method (Pells, 1999).

Table 3.1 Historical land use for the landfill

Date range	Activity
1908 – 1962	Quarry and brick works facility
1962 – 1988	Abandoned facility
1988 – 2002	General solid waste landfill
2002 – 2014	Non-putrescible waste landfill
2014 – 2015	Non-operational landfill
2016 – 2020	Construction above landfill

A detailed site investigation was undertaken at a landfill in Sydney to obtain critical parameters influencing the behaviour of this closed landfill site subject to loads from redevelopment structures. Table 3.2 summarises the critical parameters that are common and can be practically obtained for performance analysis. In addition, a summary of the techniques and corresponding parameters obtained is also presented in Table 3.3. It should be noted that the scoping of site investigations should be considered to obtain sufficient coverage of the landfill site to minimise risk, which is different for each individual project. Details of the proposed and adopted field investigation techniques piloted at the landfill are explained in the following sections.

Table 3.2 Key closed landfill parameters required for performance analysis in redevelopment projects

	Landfill Performance Analysis		
Critical parameters	**Settlement**	**Stability**	**Seismic**
Density	✓	✓	✓
Moisture content	✓	✓	✓
Age of waste	✓	✓	✓
Stiffness	✓	✓	✓
Poisson's ratio	✓	✓	✓
Shear Modulus			✓
Organic content	✓		
Composition	✓		
Geometry (height and side slope)	✓	✓	✓
Groundwater level	✓	✓	✓
Formation	✓	✓	✓
Leachate and gas collection systems	✓	✓	
Lining and cover systems	✓	✓	
Biodegradation rate	✓		
Laboratory test data and site data (strength, compressibility & permeability)	✓	✓	✓

Table 3.3 Summary of investigation methods and geotechnical outputs in this study

Investigation method	Geotechnical outputs
Light detection and ranging (LiDAR)	Age of waste
Test pits	Density (surface)
Sonic drilled boreholes	Density, moisture content & organic content, top of rock level, leachate level
Plate load testing	Young's modulus (surface)
Vertical seismic profiling (VSP)	Shear wave velocity, p-wave velocity, Poisson's ratio, shear modulus and Young's modulus (single location depth)
Multichannel analysis of surface waves (MASW)	Young's modulus (large scale depth), top of rock level
Gas pumping trial	Biodegradation rate
Push tube sampling	Mechanical properties through laboratory testing (oedometer, triaxial, Rowe cell)

3.2.2 Light detection and ranging (LiDAR)

LiDAR consists of sending laser pulses in many directions using oscillating mirrors on a moving drone. The laser pulses reflect off the ground surface and return to the drone, which measures the time taken and intensity, which allows the generation of a 3D point cloud. The LiDAR drone has a built in satellite positioning system that allows the generation of coordinates for all the points measured during the scan. The 3D point cloud is then converted to a surface using Civil 3D software. LiDAR has an accuracy up to 100 mm in both vertical and lateral positions.

The current use of LiDAR has a number of applications in geotechnical engineering and waste management including site survey for the purposes of measuring landfill volume, compliance of placed material with filling plans, monitoring slope stability and undertaking deformation assessments (Mitchell et al., 2017; Lato et al., 2019). Application of LiDAR can also be undertaken for determining the age of waste if sufficient LiDAR data is available at the site. Sharma & De (2007) stated the age of the landfill provides information about the potential for biodegradation related settlement for proposed developments above landfills.

At the landfill, LiDAR surveys taken in the early 2000s were combined with more recent LiDAR drone surveys untill 2020. Surfaces were created from each LiDAR survey in Civil 3D and a section (refer Figure 3.1) was cut through these combined surfaces to see the variation in height of the landfill and its corresponding year. Waste in this landfill was determined to be placed between 1988 and 2002 (i.e. 19-33 years old from top to bottom as of 2021) as depicted in Figure 3.1. The construction of an embankment on the landfill required cutting the area in 2018 to remove the existing cap and building up to the final embankment height in 2020. Although this range is quite large and does not split the landfill into defined layers with age, it helps to narrow the age of waste. For newer landfills, there is greater availability of LiDAR surveys at low cost and so defining the variation of age of waste with depth should be much more successful.

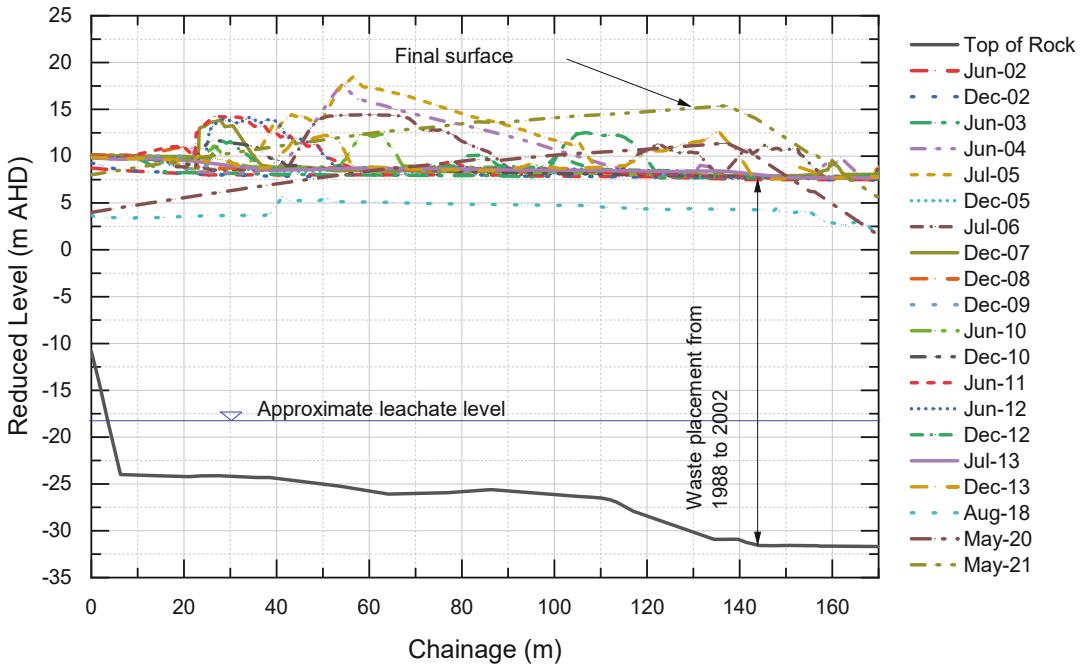

Figure 3.1 Cross Section A-A' with LiDAR survey data collected over time at the landfill from 1988 until 2021 used to determine the age of waste

3.2.3 Test pitting and sampling

Conventional test pitting is undertaken for logging excavation faces, sampling material and inspecting stockpiles of material. While the weight of materials taken from test pits can be

measured using industrial scales or weighing bridges, accurate estimation of the volume of the test pit is rather challenging. Accurate measurement of the volume of a test pit or excavated materials using modern technologies such as laser scanning can improve field practices resulting in more accurate determination of the in-situ unit weight of materials. In the pilot study at the landfill, three test pits measuring approximately 1 m^3 each were excavated in the landfill. Excavated material was loaded directly from the test pit into the back of a dump truck, and then taken to a calibrated weighbridge, which had an accuracy of ±5%. Each load of landfill material ranged from 1.6 to 2.06 tonnes, with a total combined mass of 5.5 tonnes.

Typically conventional surveying methods (e.g. total station) or the use of a tape measure can provide a rough estimate of test pit volume. However, the test pit excavation is unlikely to be a perfect cube or rectangular prism, so calculation of the test pit volume using these conventional methods is unlikely to be accurate enough for estimation of in-situ unit weight. Often the base of the test pit in landfills, especially corners and edges, are difficult to see making measurements using conventional surveying tools without entering into the test pit very challenging.

In this study, a Leica BLK-360 imaging laser scanner was utilised to capture a 360° view of the site imagery and generate a highly accurate coloured point cloud. This laser scanner was very efficient and simple to operate and could be controlled by an iPad which utilised Autodesk Recap Pro and recent Leica Cyclone Field 360 software packages. The accuracy of the adopted laser scanner was 6 mm at 10 m (99.94%) and 8 mm at 20 m (99.92%), as the distance increases the accuracy decreases. A single scan was taken immediately before excavation of each test pit. A further four scans were taken from each corner upon completion of each test pit to ensure the laser scanner had line of sight to each of the test pit corners and to capture the non-uniform base of excavation to determine an accurate test pit volume. The point clouds of each survey were overlaid to generate a 360° 3D view of the test pit excavation as shown in Figures 3a and 3b. Autodesk ReCap surveys were then put into Autodesk Civil 3D software and cropped to determine the volume of each test pit as shown in Figure 3.2.

Whilst test pits were exposed, there was an opportunity to collect landfill samples to obtain physical and mechanical properties of waste. These samples could be used for testing moisture content and organic content of materials. Moisture content and organic content measurement tests were conducted based on ASTM D 2974-87. Undisturbed samples via push tube were also collected from the exposed surfaces of the excavated landfills (Figure 3.3) and were sent to the laboratory for further testing. This method of undisturbed sample collection from within the landfill followed by laboratory testing can provide geotechnical engineers with the opportunity to directly measure a number of parameters required for the design rather than just assuming typical values available in the literature.

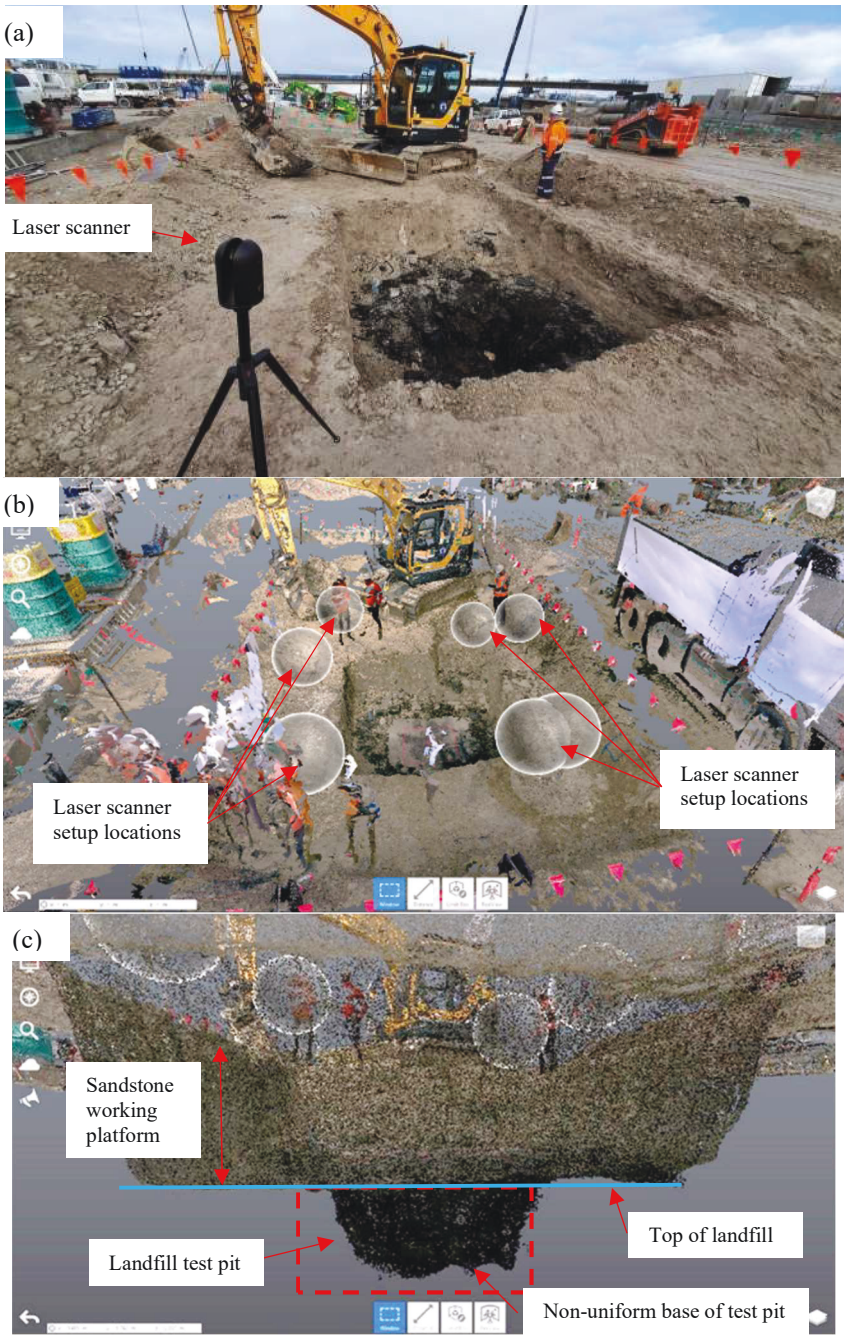

Figure 3.2 Test pitting at the landfill (a) Test pit excavation, (b) Overlayed point clouds from laser scanner viewed from Autodesk Recap software (note: white circles indicate location of laser scanner setup points to map the entire test pit, and (c) Elevation view of test pit capturing base of test pit excavation

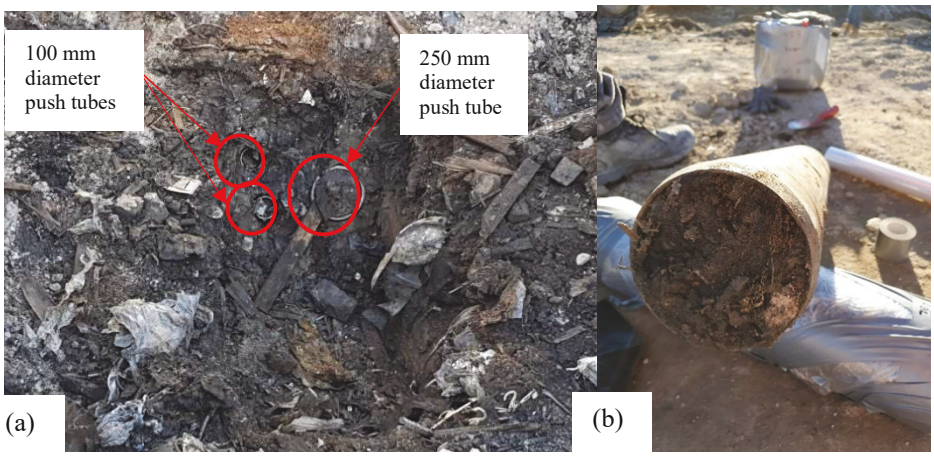

Figure 3.3 Push tube sampling (a) Two 100 mm diameter and one 250 mm diameter push tube samples taken in a test pit and (b) extracted 100 mm diameter push tube sample

3.2.4 Sonic drilling SPT testing

Sonic drilling is the preferred method for site investigation at landfill sites over conventional drilling techniques. Sonic drilling utilises rotation and axial vibration to advance the coring barrel, allowing for extraction of samples. Within landfills, sonic drilling has the capability to drill through the heterogeneous material including rocks, concrete slabs and timber at relatively faster rates of 15 - 20 m/day compared to conventional drilling methods such as wash boring.

Three boreholes with 100 mm coring diameter were drilled adjacent to test pits and each penetrated 31 - 32 m in to the landfill. In addition, SPT tests were conducted across the landfill site at 1.5m - 3m intervals at different locations following the sonic drilling done in segments. It was noted that the sample recovery from the SPT tube was very poor. This was due to nature of the landfill as the tube bounced on large timber pieces and indicated refusal on concrete blocks. The SPT blow counts were not reliable enough to be used to correlate to material properties via the correlations available in the literature for sandy or clayey soils. Figure 3.4a depicts the SPT N blow count profile with depth which can be misinterpreted without careful observation of the poor sample recovery shown in Figure 3.4b. Thus, conducting SPT is not recommended when characterising industrial waste or timber, since profiles of SPT readings with depth can easily be misinterpreted when sample recovery is poor.

Moreover, groundwater and leachate levels were obtained from piezometers installed around the landfill site. Since this is an old landfill site, there is no base lining system and therefore groundwater inflow into the landfill was observed through Botany sands and Ashfield shale leading to leachate generation (RMS, 2016). The leachate level in the landfill was found to be ranging between reduced levels of -16 m to -18 m Australian Height Datum (AHD), while groundwater levels surrounding the site ranged between -1.5 and 5 m AHD. Leachate generated was pumped out from the landfill and treated prior to discharge to sewer systems. This pumping effect created an inward gradient towards the landfill as evident from the groundwater and leachate levels presented which prevented migration of leachate and contamination offsite. To further reduce the groundwater inflow into the site for construction, a 1000 m cut-off wall with thickness of 0.8 m and hydraulic conductivity of 10^{-8} m/sec was constructed around part of the site.

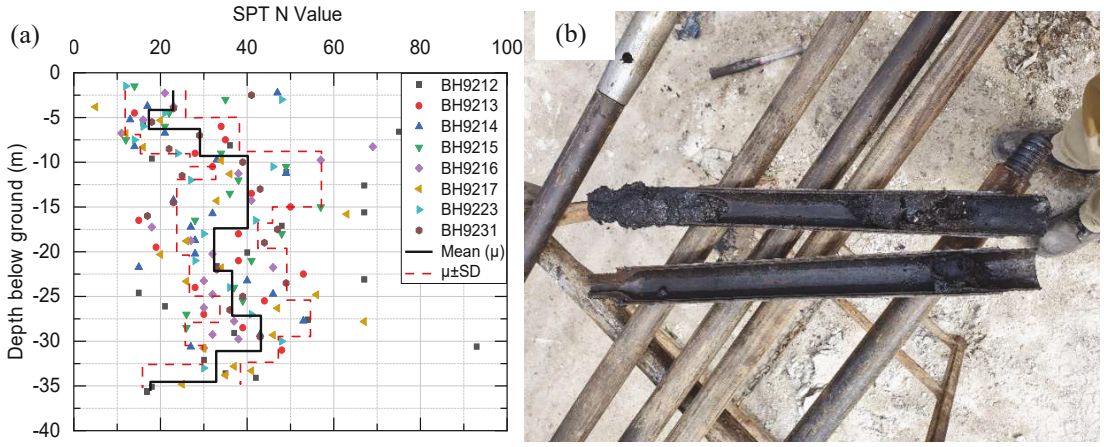

Figure 3.4 SPT testing at the landfill (a) SPT N plot with depth and (b) SPT split mould sample typical recovery

3.2.5 Geophysical testing

The non-invasiveness and large area coverage for ground profiling have been key features of conducting geophysical tests such as multi-channel analysis of surface waves (MASW) and vertical seismic profiling (VSP) (Zekkos et al., 2011; Carpenter et al., 2013; Abreu et al., 2016). In the past, geophysical methods were primarily used on landfills for the purposes of detecting voids and cavities (Park et al., 1999), depth to bedrock (Ivanov et al., 2006), assessing the extent of ground improvement (Van Impe & Bouazza, 1996; Avalle & McKenzie, 2005) in addition to characterising the landfill material (Kavazanjian et al., 1995;

Bouazza & Kavazanjian, 2000; Zekkos et al., 2014; Konstantaki et al., 2015). The following sections discuss the use of MASW and VSP undertaken at the landfill site.

Multichannel analysis of surface waves (MASW)

The use of MASW has proven to be very useful for landfill investigation applications (Bouazza & Kavazanjian, 2000; Cirone & Park, 2020). It is a fast and relatively cost effective method of collecting bulk information in a non-invasive manner. For landfills in particular, the heterogeneity can be identified, including localised pockets of higher or lower material stiffness that can be considered in performance analysis. This method is recommended to be undertaken as the first step site investigation to identify areas of the landfill where further investigation (boreholes, test pits, sampling etc.) should be targeted.

The MASW survey at the landfill involved towing a set of 24 x 4.5 Hz geophones with spacing of 2m behind a 4WD vehicle. The seismic energy source for the MASW survey was produced by hitting a metal plate with a 5kg sledge hammer. Alternatively, a rubber or plastic plate could be used in producing higher energy at a low frequency. When the hammer impacted the plate, a trigger switch attached to the hammer was initiated, and the geophones captured the vibrations. In this study, the signal was logged using a Geometrics Geode seismograph. After completion of testing in one location, the geophones, metal plate, hammer and receiver were towed 10 m in a straight line and the procedure was repeated. This process was repeated in 10 m intervals for the complete length of each MASW alignment. It should be noted that the hammer impact location was offset a distance of 8 m from the nearest geophone of the array, to prevent near-field or far-field effects (Lin & Lin, 2016).

The MASW survey was completed along 15 lines across the landfill site. Data was acquired with a sampling interval of 0.125 ms with a recording length of 2 seconds. The data was then acquired digitally on a computer and processed using Surfseis v5.0 software to generate the shear wave velocities along each of the 15 lines.

Vertical seismic profiling (VSP)

VSP or commonly known as downhole geophysics involves collecting both shear wave (S-wave) and compressive wave (P-wave) data at each borehole location allowing for calculation of a number of parameters including stiffness parameters namely shear modulus

and Poisson's ratio. This method is not as popular as MASW since one test has limited area coverage and requires drilling a borehole, which can be challenging and costly particularly for landfill sites.

In this study, the VSP survey was undertaken at the landfill site using a Geometrics Geode digital seismograph, a BHGC-1 Geophone Controller and a BHG-3 Borehole Geophone. The adopted Geophone was a 3-component 14 Hz geophone with a motor driven clamp to hold the geophone against the borehole casing. The VSP was undertaken in a cased borehole with the annulus grouted to ensure good contact between the borehole casing and the surrounding landfill material.

A metal plate was placed on the ground surface as a source of P-waves. For the S-wave source, a wooden plank was laid out a short distance from the borehole with the front two wheels of the vehicle mounted on top of the plank to ensure good contact with ground surface as shown in Figure 3.5.

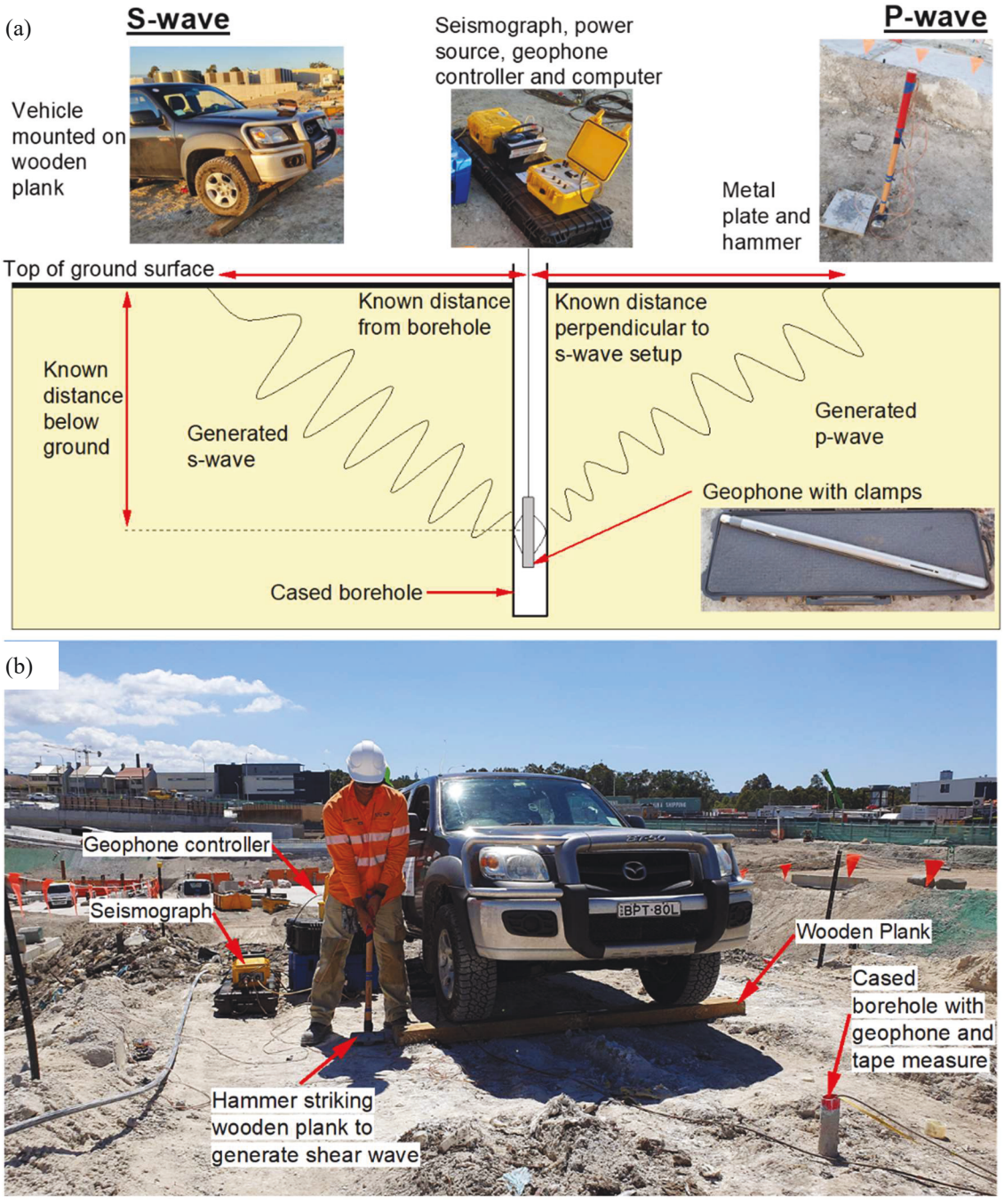

Figure 3.5 Downhole geophysics (a) test setup consisting of s-wave and p-wave measurement and (b) shear wave generation with hammer striking wooden plank under vehicle load

The geophone was then lowered down in the borehole in 0.5 m increments and clamped against the borehole wall. For each level, seismic data to generate the P-wave

component was recorded with several impacts of a sledgehammer on the metal plate, stacked in order to enhance the amplitude signal to noise ratio. On the other hand, seismic signals to generate the S-wave component was induced with multiple impacts of the sledgehammer on each side of the weighted wooden plank. Times taken for arrival of P-waves and S-waves were collected with a total recording length of 0.5 seconds with a 31.25 μs sampling interval.

S-wave and P-wave velocities were calculated from the selected P-wave and S-wave arrival times and the known distance between the signal source (sender) and receiver. Velocities, along with known material unit weight with depth obtained from sonic drilling cores were utilised to calculate small strain stiffness parameters as per the equations below (Sheriff & Geldart, 1982):

$$v = \left[2 - (V_p/V_s)^2\right]/2[1 - (V_p/V_s)^2] \qquad \textit{Eq. 3.1}$$

$$G_{max} = {V_s}^2 \rho \qquad \textit{Eq. 3.2}$$

$$E_{max} = 2G_{max}(1 + v) \qquad \textit{Eq. 3.3}$$

where v is the Poisson ratio, V_p is primary wave (P-wave) velocity, V_s is shear wave (S-wave) velocity, ρ is the density of the landfill, E_{max} is the small strain Young's modulus and G_{max} is the small strain shear modulus. Although MASW is non-intrusive, in order to estimate small strain stiffness parameters, the unit weight profile with depth is required. It should be noted that for determining the ground settlement subjected to structural loads, large strain modulus rather than small strain parameters are required. However, very limited information is available in the literature for the correlations between small strain to large strain stiffness parameters for waste material (Zekkos et al., 2008; Bray et al., 2009)

3.2.6 Gas pumping trial

The biodegradation of organic material within the landfill contributes to the generation of landfill gas and leachate as well as subsequent biodegradation induced settlement (Fei et al., 2016; Powrie et al., 2019). There are several well established first order decay models such as LandGEM developed by The US Environmental Protection Agency (Alexander et al., 2005), or NGER model by National Greenhouse and Energy Reporting (AusGov, 2020), which can use actual landfill composition, moisture data and tonnages combined with

biodegradation rates (k) which is the organic mass loss over time and methane gas generation potential (L_o) to estimate landfill gas generation rates. Gas pumping data including gas flow rates and gas composition (e.g. carbon dioxide, methane, oxygen and balance gas) may be used from sites to roughly confirm the assumed biodegradation rate and gas generation potential (Sormunen et al., 2013; Park et al., 2018).

There are existing studies to estimate the biodegradation rate (k) based on the material composition of the landfill (Arigala et al., 1995; Machado et al., 2009), which split the biodegradation rate into three classes namely (i) readily biodegradable, (ii) moderately biodegradable and (iii) slowly degradable materials. The Inter-governmental Panel on Climate Change (IPCC, 2019) documented experimental measurements, models, utilised greenhouse gas inventories and other studies to establish biodegradation rates of landfill material. This guide captures global biodegradation rates for the three classes and can be used as a reference guide to gauge first pass values for each type of waste depending on climatic conditions including mean annual temperature, mean annual precipitation and potential evapotranspiration.

Over time, the mass of each class of material within the landfill will decay at independent rates (Durmusoglu et al., 2005). A weighted biodegradation rate is calculated using the landfill mass of each class multiplied by corresponding biodegradation rates. For each year that waste is placed, the weighted biodegradation rate is used to determine the mass of landfill biodegraded, the remaining landfill mass after biodegradation and the amount of gas generated. Using the remaining landfill mass after biodegradation, the process is repeated to obtain the gas generated for each year until the final year of prediction is achieved. Using the gas generated for each year, a gas generation curve can be created and compared against field measurement of landfill gas. It should be noted that the biodegradation rate for each class of waste can be adjusted to allow fitting of the predicted gas generation curve against the actual measured landfill gas. Referring to Laquidara et al. (1987), the following formulations summarise the methodology to estimate the landfill gas generation estimate:

$$k = r \times k_r + m \times k_m + s \times k_s \qquad \textit{Eq. 3.4}$$

$$M\ (t) = M_o e^{-kt} \qquad Eq.\ 3.5$$

$$G\ (t) = C(\Delta M) \qquad Eq.\ 3.6$$

where, k is the weighted biodegradation rate (yr-1) of the entire landfill material, r, m and s are percentage of readily, moderately and slowly biodegradable materials in the landfill, respectively. k_r, k_m and k_s are the biodegradation rates for readily, moderately and slowly biodegradable materials in the landfill (yr-1), respectively, $M\ (t)$ is mass of biodegradable landfill (tonnes) remaining at time t, M_o is the initial biodegradable mass of landfill (tonnes) at time t = 0, $G\ (t)$ is the volume of gas produced for the entire landfill at time t (m^3), C is gas produced per unit mass of organic material biodegraded (m^3/kg) and ΔM is mass of organics biodegraded from the beginning of placement (i.e. $\Delta M = M_o - M\ (t)$). The sum of r, m and s should equal to 100% since this is only for the biodegradable portion of waste. The range for biodegradation rates for each class vary significantly, k_r is between 0.05 – 0.7 yr-1, k_m between 0.04 – 0.2 yr-1 and k_s between 0.01 – 0.085 yr-1 (Arigala et al., 1995; Faour et al., 2007; IPCC, 2019). The use of the landfill gas pumping data is a relatively fast method to determine an approximate biodegradation rate for a landfill. The gas pumping trial involves the measurement of the amount, quality and type of gas extracted from the landfill. Other methods using gas modelling such as using the LandGEM, and NGER (Krause et al., 2016; Park et al., 2018) may be used to compare findings and create upper and lower bound estimates. The calculated biodegradation rate can then be used in a number of reputable landfill settlement models, which require this parameter (Marques et al., 2003; Machado et al., 2009; Gourc et al., 2010; Sivakumar Babu et al., 2010; Chen et al., 2012). Due to the uncertainty associated with landfill settlement, the use of a number of models is recommended to validate the settlement result.

3.2.7 Plate load testing

The plate load test is undertaken by gradually loading a plate and measuring both the applied force and plate displacement. This method is used to obtain the compaction quality during construction, estimate foundation settlements, determine allowable bearing capacity and calculate soil stiffness of the subgrade for performance analysis and is a common in-situ test in geotechnical projects (Fu et al., 2016; Barnard, 2019). In general, the effective depth that

plate load test can evaluate is limited to a depth equivalent to twice the plate diameter (ASTM, 2003). Thus, the results can only capture the properties of very shallow waste material when used in landfill projects.

In this study, a total of eight plate load tests were undertaken at the landfill site using a 20 tonne excavator, 358 mm diameter steel plate, hydraulic loading system and 3 displacement transducers. Three tests were conducted on in-situ landfill material and five on excavated and re-compacted material, herein referred to as compacted waste in order to compare with in-situ waste. The steel plate was loaded using the hydraulic loading system and load - displacement results were recorded. Compressibility modulus was then calculated using the initial slope of the load - displacement curve using the following equation (Timoshenko & Goodier, 1951):

$$C = \frac{Q}{\delta D}(1 - v^2) \qquad \textit{Eq. 3.7}$$

where, C is compressibility modulus (MPa), Q is applied load at centre of plate (kN), δ is average plate settlement (mm), D is plate diameter and v is Poisson's ratio. This equation is denoted as the compressibility modulus since it comprises of both elastic and plastic deformation during the initial loading. Young's modulus is purely elastic and can only be obtained from the initial loading slope or unloading/reloading curves, and well established German standard (DIN 18134, 2012) was used for interpretation of plate load test results. DIN 18134 (2012) utilizes the least square curve fitting method to obtain the strain modulus during the first loading cycle (E_{v1}) and all subsequent unloading /reloading cycles (E_{v2}) as per Equation (42). The ratio between E_{v1} and E_{v2} provides an indication of the compaction level achieved. A high ratio of E_{v2}/E_{v1} indicates a larger amount of plastic deformation during initial loading, and subsequently further compaction may be required, while a low ratio represents a significant elastic deformation (Cho & Mun, 2014). The parameters obtained can also be utilized to determine the large strain Young's modulus (E_s) using the equations below for deformation predictions under structural loads (Kim & Park, 2011).

$$s = a_0 + a_1\sigma_0 + a_1{\sigma_0}^2 \qquad \textit{Eq. 3.8}$$

$$E_v = \frac{1.5r}{a_1 + a_2\sigma_{0max}} \qquad \textit{Eq. 3.9}$$

$$E_s = \frac{0.5\pi\sigma_0 r(1-v^2)}{a_0 + a_1\sigma_0 + a_1{\sigma_0}^2} \qquad \textit{Eq. 3.10}$$

where, E_v is the strain modulus (MPa), E_s is Young's Modulus (MPa), r is the plate radius (mm), a_0 (mm), a_1 (mm/MN/m2) and a_2 (mm/MN2/m4) are constants calculated from the plate pressure vs settlement curve using the fitting method proposed in the DIN standard, σ_{0max} is the maximum normal stress below the plate, σ_0 is the average normal stress below the plate and s is the average plate settlement for the loading or unloading/reloading curve analysed. The ratio of large strain Young's modulus (E_s) obtained from plate load testing can be compared with the small strain Young's Modulus (E_{max}) obtained from MASW and downhole geophysics. Establishing the ratio of small strain to large strain modulus would allow integrating the extensive small strain geophysical test results into the infrastructure design often requiring large strain modulus. It should be noted that axial strain for plate load testing was calculated based on the settlement observed over the influence zone, which was assumed to be twice of the plate diameter.

3.2.8 Additional field tests

Whilst the authors have presented a wide range of site investigation techniques for investigating closed landfill sites, there are other methods available which may also provide useful information for geotechnical design. This may include undertaking cone penetration tests with pore water pressure measurements (CPTu) and packer testing of landfill for permeability. The CPTu tests would be able to identify potential perched leachate and provide cone tip and friction resistance with depth, albeit from the authors' experience on previous landfill sites this is likely to refuse at shallow depths. Perched leachate can be detected through review of the pore pressure data, similar to how perched groundwater is detected. Packer testing when undertaking boreholes can be used to determine the permeability of the landfill material. This may be particularly useful for older landfills with high leachate levels. Pressuremeter and dilatometer tests can also be used to investigate strength properties of the landfill.

3.3 Interpretation and discussion of field results

Findings from the site investigation at the landfill are summarised below along with lessons learned and recommendations. This pilot and detailed field investigation focussed mainly on a site with an approximate plan size of 60 m × 120 m, where a new embankment was proposed to be built on the landfill. It is expected that this study can showcase detailed landfill characterisation for redevelopment projects to obtain the required design parameters.

3.3.1 In-situ unit weight of waste

Findings from the test pit unit weight comparing tape measurement (approximate) with laser scanning (accurate) are summarised in Table 3.4. The observed difference between the measured unit weight values for these two volume measurement techniques was 15-18%. The reason for this difference is due to the obvious imprecision of the tape measurements and the difficulty to access the corners of the excavation to take measurements. It should be noted that use of the laser scanner to take the measurements and processing the collected data via high performance computers was quite fast and simple and this process can be easily completed for any project. Indeed, there are a number of benefits for the use of the laser scanner against conventional surveying methods. Adopting laser scanner provides a greater reliability of volume measurement since all surfaces are surveyed in detail. In addition, it would eliminate the need to enter the excavation, providing a safer work practice. It is noted that larger test pit excavations (e.g. 5 - 10 m^3) can be considered to provide a more representative sample of landfill material to gauge the bulk unit weight. Obviously test pitting can be only done near the ground surface and resulting in unit weight measurements in shallow depths only.

Table 3.4 Comparison between tape and laser scanner measurement of test pit volume and its impact on landfill density at the landfill

Test Pit ID	Landfill mass (t)	Volume (m^3)		Unit weight (kN/m^3)		Difference (kN/m^3) (%)*
		Tape measurement	Laser scanner	Tape measurement	Laser scanner	
1	1.86	1.42	1.64	12.80	11.07	-1.73 (16)
2+	1.60	1.00	0.85	15.68	18.42	+2.74 (15)
3	2.06	1.40	1.15	14.40	17.54	+3.14 (18)
Average	1.84	1.27	1.21	14.30	15.68	+1.38 (9)

* Values in brackets indicate the % difference between tape measurement and laser scanner densities

+ Reinforced concrete sleepers observed in waste material from test pit 2, this was deducted from the mass and volume

3.3.2 Field moisture content and organic content

The moisture content and organic content of landfill materials were measured in accordance with ASTM D 2974-87. The test pits organic content and moisture content were on average 15% and 27%, respectively.

3.3.3 Stiffness characteristics of in-situ waste

Figure 3.6 shows variations of shear wave velocity, small strain shear modulus, small strain Young's modulus and Poisson's ratio with depth established based on the results obtained from vertical seismic profiling (VSP). VSP was undertaken after construction of a landfill embankment above the existing in-situ landfill material. This provided a comparison between freshly compacted landfill in the embankment (upper section) and in-situ landfill material (lower section). VSP could allow measurement of Poisson's ratio since both P-wave and S-wave velocities were measured. It should be noted that the collection of very deep data (i.e. >20 m) became difficult especially with surrounding construction activity since this caused additional noise and the geophones were unable to detect either the P-wave or S-wave data from the sledgehammer impact at the ground surface. The small strain Young's modulus was found to be on average 86 MPa for the compacted waste embankment and 98 MPa for in-situ landfill material. Whilst the compacted waste would be expected to be stiffer than the in-situ landfill waste due to controlled compaction condition, the material heterogeneity and long-term visco-plastic deformation biodegradation of in-situ landfill waste could contribute to the slightly stiffer in-situ waste compared to the compacted waste.

Referring to Figure 3.6, the measured small strain shear modulus for the embankment obtained from VSP were in the range of 24 - 60 MPa and on average was 32 MPa and appears to increase with depth. The in-situ landfill waste had similar small strain shear modulus ranging between 25 - 50 MPa with an average of 36 MPa. The measured Poisson's ratio varied between 0.2 and 0.43 with an average of 0.34 and the variations are likely to be due to variable composition with depth.

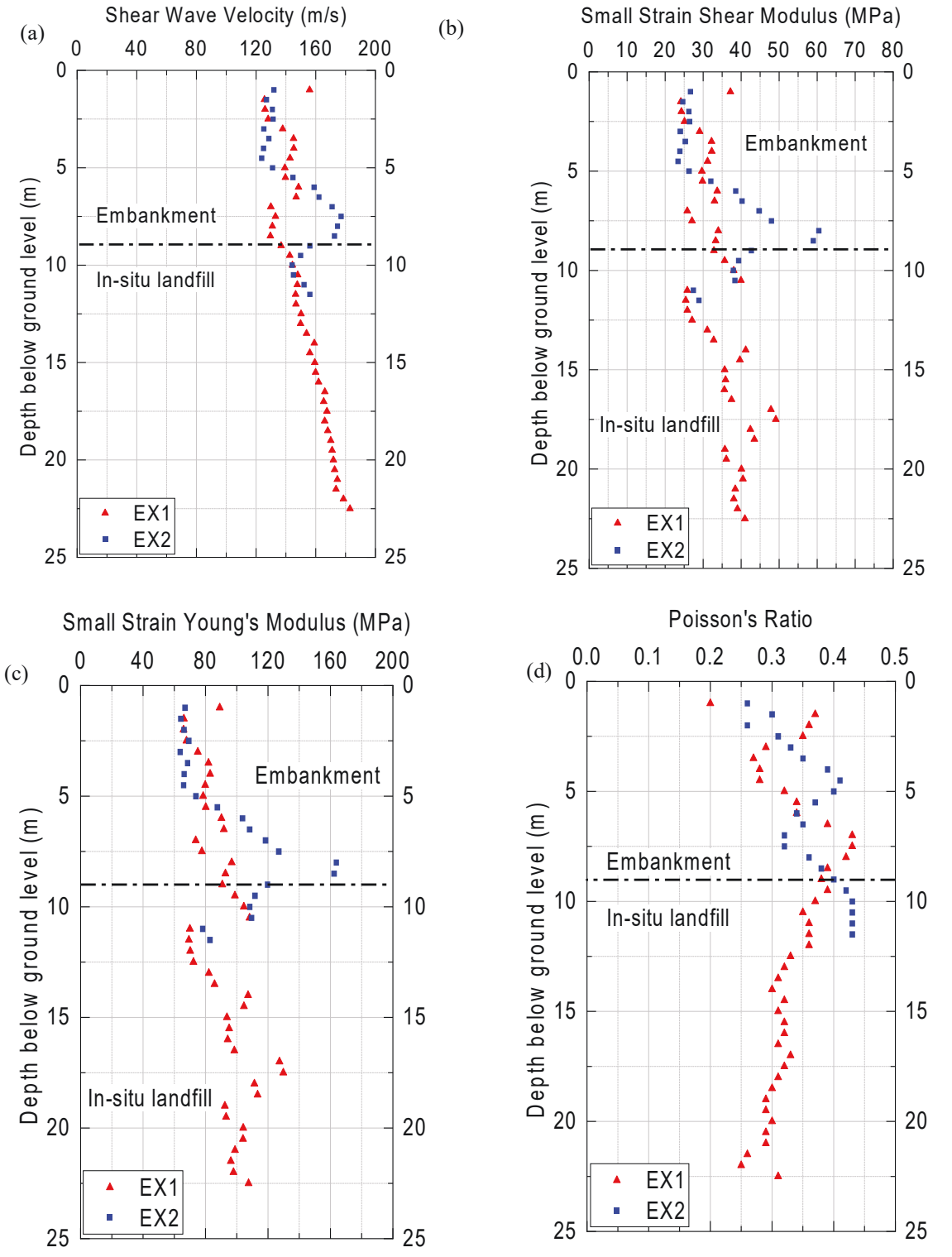

Figure 3.6 Downhole geophysics outputs (a) Shear wave velocity, (b) small strain shear modulus, (c) small strain Young's modulus and (d) Poisson's ratio with depth

Moreover, the shear wave velocity measured via multi-channel analysis of surface waves (MASW) was used to determine the small strain Young's modulus (E_{max}) based on Equation (3). Figure 3.7 shows the measured shear wave velocity at different locations for the entire landfill site, and readings from stations MASW 09_1-3 and MASW 10_1-2 are particularly related to the section of the site investigated intensively in this study. MASW 09_1-3 and MASW 10_1-2 are on the lower bound of the overall MASW readings and correspond well with the VSP results undertaken in the same area. The small strain Young's modulus of the section investigated and entire landfill was determined to be varying between 100 - 350 MPa and 75 - 400 MPa, respectively for the section investigation and the entire landfill. The stiffness follows a generally increasing trend with depth, with a sharper increase observed beyond a depth of 27m toward the base of the landfill. The average small strain Young's modulus using the entire landfill data ranged between 150 MPa and 350 MPa. The MASW method is recommended since it is cheaper than VSP since no borehole is required and provides comparable small strain stiffness results with depth.

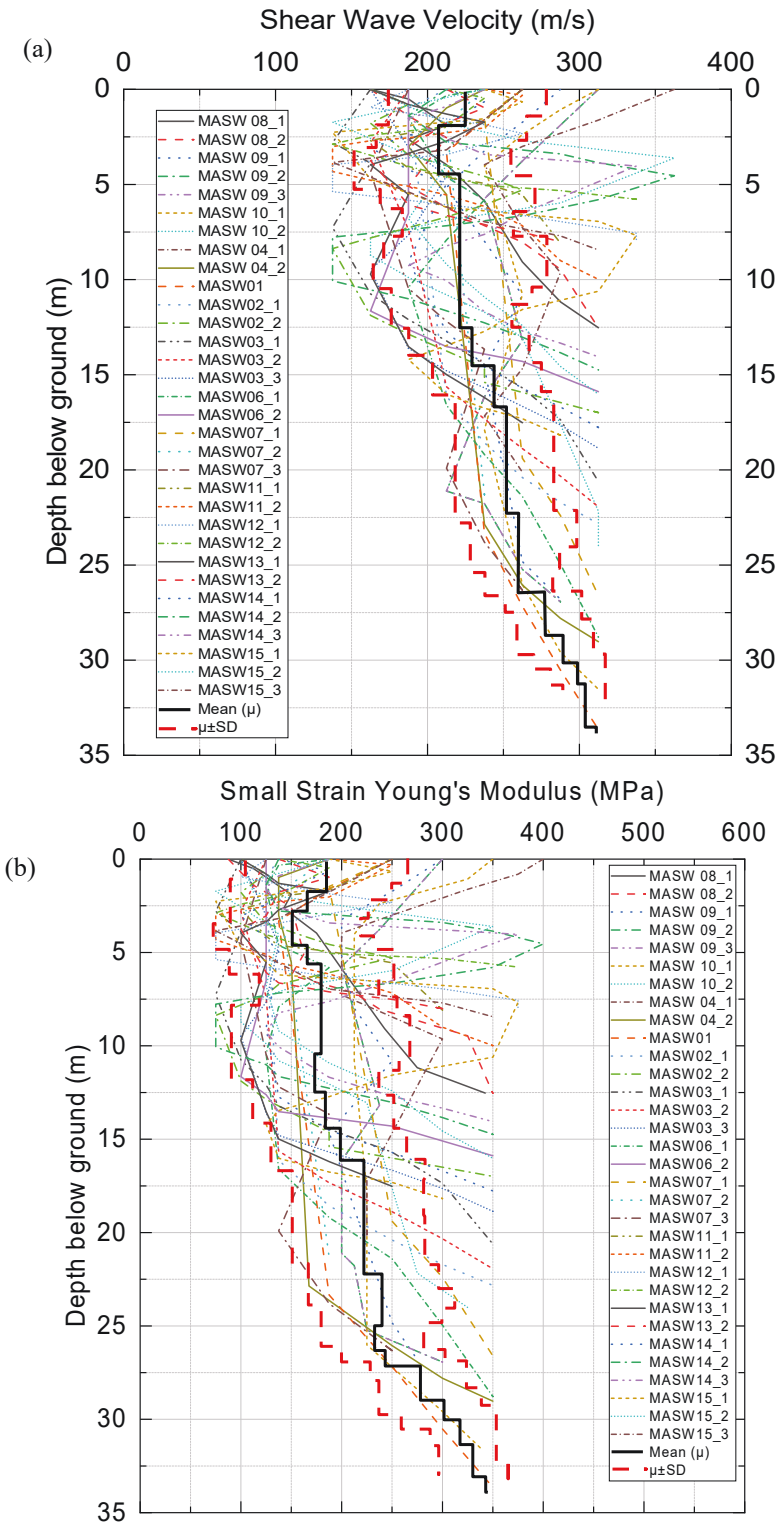

Figure 3.7 MASW outputs (a) shear wave velocity with depth and (b) small strain Young's modulus

Load – displacement curves and thus ground compressibility modulus (C) were established via plate load testing conducted at the surface for varying plate pressures on both freshly compacted landfill and in-situ landfill material as shown in Figure 3.8. A summary of the measured compressibility modulus (C), ratio of E_{v2}/E_{v1} and Young's modulus (E_s) is presented in Table 3.5. The compressibility modulus of compacted landfill was approximately double that of in-situ landfill, indicating the initial compression of in-situ landfill comprises of more plastic deformation than freshly compacted waste. Under larger loads, the Young's modulus was similar for both compacted waste and in-situ landfill. The lower ratio of E_{v2}/E_{v1} for compacted landfill (3.8-7.2) indicated that it is better compacted than the in-situ landfill (with the corresponding ratio varying between 6.3 and 9.0). It is noted that since $E_{v2}/E_{v1} > 1$ there was still an opportunity to compact the material more to reach the resilient state. By comparing the Young's modulus obtained from plate loading testing (Table 3.5) against geophysical data (refer to Figure 3.6 and Figure 3.7) the ratio between small strain and large strain stiffness (E_s/E_{max}) for the waste material was determined to be between 7 to 28, with an average of 13 when an outlier of 50 was removed. The small strain to large strain stiffness ratio allows for conversion of small strain data obtained through geophysical or small strain laboratory testing into large strain data that can be used in modelling compressive behaviour of landfill material. The standard deviation for all compacted and in-situ landfill material combined for E_s/E_{max} was found to be 5 and had a positive covariance.

Table 3.5 Summary of compressibility modulus, ratio of E_{v2}/E_{v1} and Young's modulus obtained from plate load testing on freshly compacted landfill and in-situ landfill

Parameter	**Compacted landfill**		**In-situ landfill**		**Unit**
	Range	Average	Range	Average	
Compressibility modulus (MPa)	5-22	15.7	3-12	7.2	MPa
E_{v2}/E_{v1}*	3.8-7.2	4.8	6.3-9.0	7.6	-
Young's modulus (MPa)	3-40	20.2	2-44	18.0	MPa

*E_{v1} refers to the strain modulus from initial loading and E_{v2} denotes the strain modulus for all subsequent unloading/reloading cycles

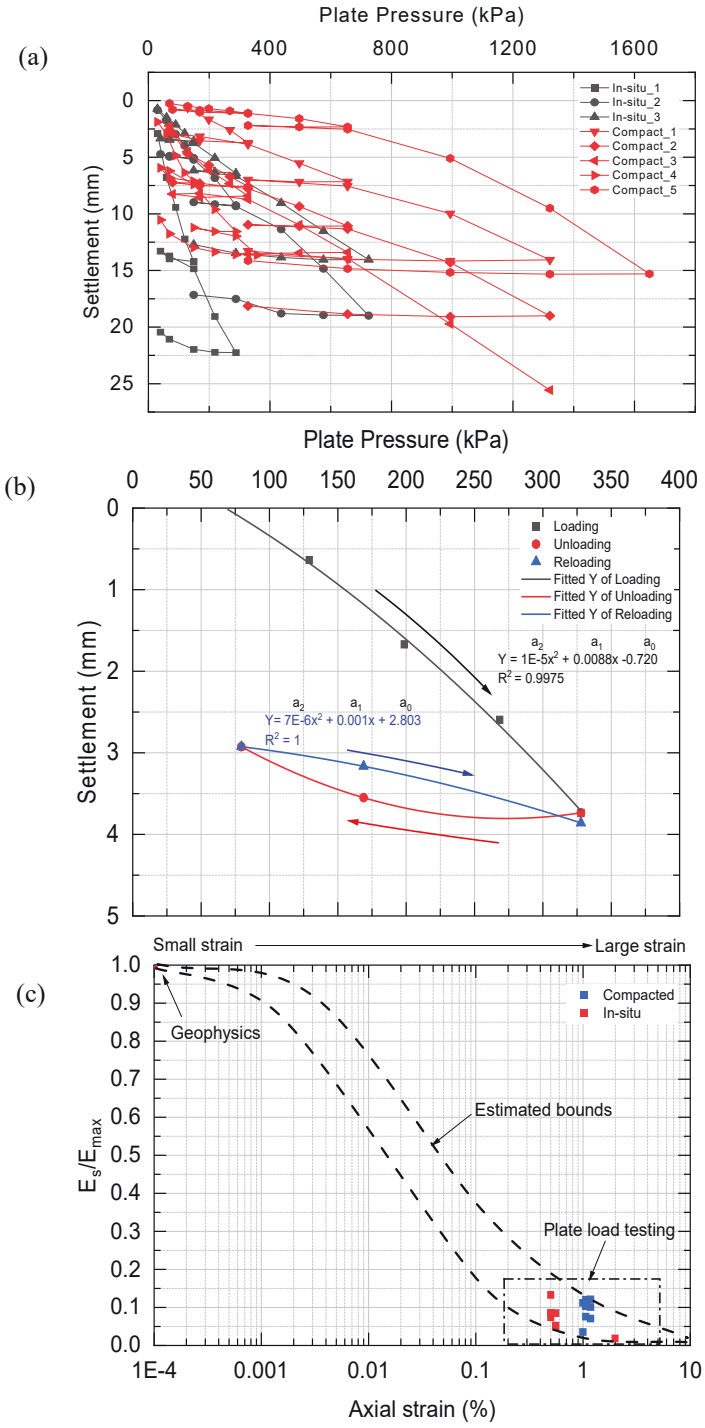

Figure 3.8 Plate load testing results (a) Compacted waste and in-situ was comparison for settlement vs plate pressure, (b) Loading, unloading and reloading curves using DIN method for calculation of coefficients a0, a1 and a2 and (c) Small strain vs large strain Young's modulus correlation determined from geophysical and plate load tests

3.3.4 Biodegradation rate

The quantity of readily, moderately and slowly biodegradable materials was available from landfill records and is presented in Table 3.6. Waste in the landfill primarily comprised of food waste between 1988 and 2002, and wood and construction waste between 2002 and 2015.

Table 3.6 Landfill waste composition and waste tonnages

Year	Waste Composition (%)				Average waste received (tonnes per year)
	Food Waste (readily biodegradable)	Paper & Vegetative Waste (Moderately biodegradable)	Other waste (wood, textiles, rubber, leather) (Slowly biodegradable)	Construction waste e.g. bricks, concrete (non-biodegradable)	
1988	10	11	51	28	94,000
1989-2001	10	11	48	31	66,000
2002-2015	1	7	21	71	79,000

Initial biodegradation rates for each class were selected based on values available from literature and these values were adjusted to match the predicted gas generation rate with the gas generation rate obtained from the pumping trial. The adjusted biodegradation rates for each class were within the IPCC (2019) ranges, presented in Table 3.7. The estimated weighted biodegradation rate reduced from 0.033 to 0.002 yr^{-1} during 1998 to 2070, respectively and the gas generation rate for the landfill reduced from 400 m^3/hr in 2002 to an estimated 20 m^3/hr in 2070. Due to higher presence of organic materials (classified as readily biodegradable) in 1988 – 2002, there was a higher gas generation rate then compared to later stages in 2002-2015 when the landfill had accept primarily construction waste. As shown in Figure 3.9, following capping and completion of landfill closure in 2020, the landfill gas generation rate was estimated to reduce slowly over time. Certainly, the availability of long-term gas monitoring data would results in more reliable prediction of variation of biodegradation rate with time, which would be a useful input in settlement models.

Table 3.7 Estimated biodegradation rates for each class of material at the landfill compared to ranges of biodegradation rates from IPCC (2019)

Parameter		Estimated Value	IPCC (2019)*	Unit
Biodegradation rate (k)	Readily biodegradable	0.170	0.05-0.2	$Year^{-1}$
	Moderately biodegradable	0.059	0.04-0.1	$Year^{-1}$
	Slowly biodegradable	0.013	0.01-0.07	$Year^{-1}$
Gas generation potential (C)		0.5	-	m^3/kg

*IPCC (2019) biodegradation rates for countries with mean annual temperature less than 20 degrees

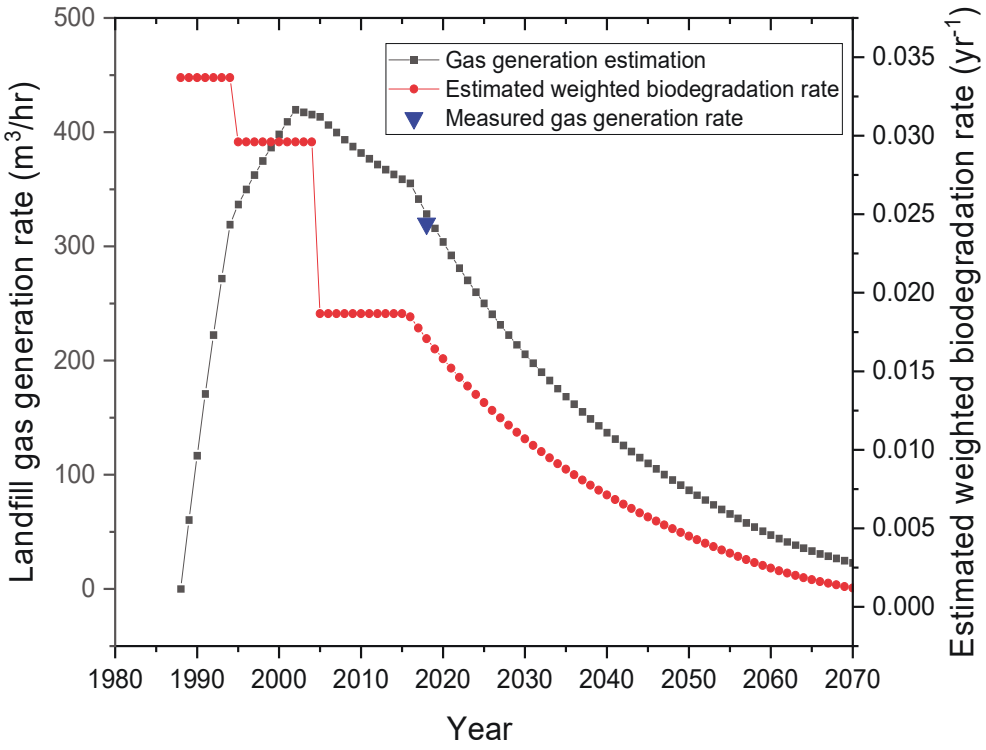

Figure 3.9 Landfill gas generation rate and estimated weighted biodegradation rate over time

3.4 Summary and conclusions

Each landfill is unique and is affected by a large number of factors. Whilst commonly adopted, applying assumed parameters from available literature fails to meet industry best practice for the design of sensitive infrastructure above closed landfill sites. Instead site specific field investigations and laboratory testing should be undertaken to understand and

obtain the critical geotechnical parameters and waste behaviour used for performance analysis, whether it be for settlement, stability or seismic calculations as currently undertaken for other problematic soils. A combination of different site investigation techniques, was used at the landfill site to obtain the required design and assessment parameters.

LiDAR technology was utilized to narrow down predictions of the waste age in the landfill, determined to be 19-33 years from top to bottom as of 2021. The use of sonic drilled boreholes at a coring rate of 18 m/day allowed for measurement of multiple properties with depth including moisture content, organic content, dry and total unit weights. As expected the variation in the total unit weight with depth was significant, with the bulk of results ranging between 10 – 15 kN/m^3. The average unit weight obtained from 90 m of 100 mm diameter core was found to be 14.5 kN/m^3 with a dry unit weight of 11.5 kN/m^3. The moisture content and organic contents were found to vary with depth with an average of 38% and 20% respectively.

Results show that conducting SPT testing on landfill sites with timber or construction waste is problematic and therefore not recommended due to issues such as bouncing, refusals and poor sample recovery, which all led to unreliable results, which could be misinterpreted. Laser scanning was used to obtain the volume of the test pit accurately, and together with measuring the weight of excavated material obtained from the test pit via trucks and weighbridge, the bulk unit weight of waste material near the surface could be determined reasonably accurately. The bulk unit weight of the landfill near the surface using the test pit and laser scanner method was on average 15.7 kN/m^3 through measurement of over 5 tonnes of waste.

For stiffness measurement, the use of geophysical tests (i.e. multichannel analysis of surface waves: MASW, and vertical seismic profiling: VSP) presented great value to establish profile of waste small strain stiffness varying spatially within the landfill. The measured small strain Young's modulus ranged between 70 and 120 MPa using VSP, and 75 - 400 MPa with MASW, while the large strain Young's modulus near the surface measured using plate load testing was on average 20 MPa. Since the VSP tests allowed measurements of both shear and compressive wave velocities, the Poisson's ratio was also quantified to vary

between 0.2 and 0.45 (with an average of 0.36). The small strain shear modulus was found to range between 24 and 60 MPa. Generally, the small strain Young's modulus and small strain shear modulus increased linearly with depth for both MASW and VSP methods. The MASW provided greater coverage of the landfill since it resulted in numerous profiles across the site, which assisted in identification of areas of lower stiffness. Through use of plate load testing and geophysical testing, the ratio between small strain and large strain stiffness (E_s/E_{max}) could be established, which was 13 on average for the entire landfill waste material. The proposed method to establish the small strain to large strain stiffness of waste only utilised field testing.

A landfill gas pumping trial was conducted on site in the landfill, and by utilising the quantity and quality of gas, landfill composition and filling records, the weighted biodegradation rate and gas generation rate could be estimated. The weighted biodegradation rate started at 0.033 yr^{-1} in 1988 and was predicted to drop to 0.002 yr^{-1} in 2070. The peak gas generation rate was estimated to be 400 m^3/hr and this was estimated to drop to 20 m^3/hr in 2070. Use of gas pumping trial is recommended as a first pass to determine biodegradation rate and it should be confirmed with other gas generation models to determine upper bound and lower bound estimates.

Chapter 4 – Reconstituted Waste Compressibility and Strength

This chapter describes the compressibility and strength parameters of reconstituted landfill material obtained from a depth of 8-10m below the landfill surface through a multi-stage consolidated drained triaxial test.

4.1 Introduction

Measurement of strength and compressibility properties of solid waste landfill materials is a complex process. Landfill materials are heterogeneous and their properties varies with time. Many factors, such as mechanical compression, chemical reactions and biological processes caused by the wastes decomposition influence their behaviour. Closed and old landfills in large cities are now being used as part of transport network more regularly. The settlement process of these landfills under traffic loads is governed by many mechanisms and the interactions among them. A large number of variables are involved in this process, including the type of waste, the organic content, the moisture content, the compaction density, the compressibility coefficients, the temperature, and the age of waste after placement. Hence, the accurate prediction of closed landfill settlement is a challenging task, particularly for those sites redeveloped to accommodate transport infrastructure. Determination of landfill settlement has been studied by many researchers experimentally, numerically and theoretically in the past decades (Bjarngard & Edgers, 1990; Edil et al., 1990; Kavazanjian et al., 1995; Wall & Zeiss, 1995; El-Fadel & Khoury, 2000; Hossain et al., 2003; Hossain & Gabr, 2005; Oweis, 2006; Zekkos et al., 2010; Tahmoorian & Khabbaz, 2020).

Recently at the suburb of Jordan Springs located in west of Sydney, Australia, there were approximately 841 homes that were built on an old closed landfill. The home owners reported property damage due to excessive settlement and after investigation this was found to be a result of poor landfill compaction (Visontay, 2020). This case study highlights the importance of understanding landfill behaviour through site investigation, laboratory testing and consideration of implementing ground improvement prior to constructing infrastructure directly above landfills. With the increasing rate of urban development and limited available space for infrastructure, there is a significant demand to allow construction directly above landfills, this is evident with projects such as Westconnex M8 – St Peters Interchange built

on the landfill, Moorebank Intermodal built on Glenfield landfill and Sydney Gateway built on Tempe landfill in Sydney.

It should be noted that both strength and compressibility parameters of landfill are the most critical for assessing landfill settlement, and these parameters can be obtained from laboratory tests such as triaxial and direct shear tests in the laboratory, and plate load test and geophysical tests in the field (Sowers, 1973; Marques et al., 2003; Machado et al., 2008; Gourc et al., 2010; Sivakumar Babu et al., 2010). In the past prominent landfill researchers have collected landfill material for reconstituted triaxial testing from typically near surface test pits and less commonly boreholes (Kavazanjian, 2001; Machado et al., 2002; Bray et al., 2009; Zekkos et al., 2010) and have undertaken single stage triaxial testing, which faces the serious challenge of collecting multiple identical or similar samples from one location. Whilst for soil undertaking single stage triaxial tests at different effective stresses is common since collecting rather similar samples are possible, for landfill material each test sample may be different in terms of composition, unit weight and compaction which may result in inconclusive or unrealistic shear strength parameters (Zekkos et al., 2013). Results of previous research studies have shown that multistage triaxial testing can be potentially used to obtain compressibility and strength characteristics of soils (Kenney & Watson, 1961; Sharma et al., 2011; Choi et al., 2018; Banerjee et al., 2020). Moreover, the use of drained multistage testing is preferred over undrained multistage testing due to the collection of volumetric strains during shearing in addition to deviatoric strains, both of which are indicators for the sample approaching the yield point, allowing progression to the following stage (Malandraki & Toll, 2000; Sharma et al., 2011). In addition, multistage triaxial testing is faster than conventional testing since sample preparation and saturation stage are only required once.

The primary consolidation behavior of waste is comparable to conventional soil behavior with loading and unloading curves; this has been expressed in terms of an expanded version of the modified Cam clay model with compression indices for virgin loading (λ) and unloading/reloading (κ) by numerous researchers (Machado et al., 2002; Machado et al., 2008; Fatahi, 2013; Chouskey & Sivakumar Babu, 2015). However, the compression indices (λ and κ) varies depending on a large number of factors particularly material composition

and compaction processes whereby large voids can form due to irregularities in landfill particle size as well as the orientation of fibres that act as reinforcement (McDougall, 2007; Powrie et al., 2019; He et al., 2021). Therefore, there is a need to undertake site specific testing to determine the compressibility of waste at each landfill.

Long-term creep behavior of waste material can be obtained through oedometer and Rowe cell testing, triaxial consolidation and triaxial stress relaxation tests. Oedometer and Rowe cell tests on landfills were undertaken by many researchers over decades (Sowers, 1973; Wall & Zeiss, 1995; Machado et al., 2002; Hossain et al., 2003; Bareither et al., 2013b; He et al., 2021) with a wide range of reported values for parameters. Undertaking oedometer testing provides 1D deformation characteristics (i.e. constrained sample), whereas triaxial testing can provide data for both volumetric and shear deformation components. As such, in a landfill setting where landfill geometry and embankment profile (e.g. crest, batterers and berms) vary, conducing test under triaxial loading conditions is more appropriate to reflect on the 3D stress state of waste (Wang et al., 2020). Consolidation within the triaxial testing framework utilises measurement of sample volume change to determine sample compression including both consolidation and creep components (Augustesen et al., 2004; Long et al., 2020). Moreover, stress relaxation is another method to measure creep characteristics of materials, where an initial stress is applied to the sample, and then stress change over time due to creep is measured while the sample deformation is prevented (Yin et al., 2014).

This chapter details a consolidated-drained multistage triaxial test undertaken on reconstituted landfill waste material extracted using the sonic drilling technique from a landfill in Sydney. Parameters obtained in this study include friction angle, cohesion, compression indices (λ and κ), pre-consolidation pressure, over-consolidation ratio, permeability and creep coefficient. The paper emphasises the need for obtaining site specific parameters through testing of landfill waste material which feed into settlement prediction models.

4.2 Sample collection and experimental plan

4.2.1 Waste sample collection from the landfill

Landfill waste was collected from a landfill in Sydney. The landfill operated as a quarry and brickworks facility from 1908-1962, then remained as an abandoned facility until in 1988 where it re-opened as a general solid waste landfill. It remained as an operational landfill until 2015 when it was closed and construction commenced for infrastructure above the landfill. The landfill composition consists of food, paper, cardboard, wood waste and inert construction waste with an average depth of 30 m. A base lining system is not present in the landfill; however, there is a deep leachate collection system.

The surrounding geology of the landfill in order of increasing age with depth (approximate thickness is indicated in brackets) includes sands (~15m), shale (~25m) and Sandstone. The groundwater surrounding the landfill flows through the Botany sands into the landfill generating leachate, however leachate has been pumped, treated and disposed creating an inward gradient groundwater flow for the site preventing contamination and migration of groundwater offsite. The leachate level was located approximately 24 m below the top of the landfill. Gas generation was measured to be at a rate of 300 m^3/hr with a landfill gas pumping trial in 2018 indicating the landfill is undergoing decomposition.

Sonic drilling was undertaken at the landfill to collect over 95 m of 100mm diameter core sealed in plastic sleeves and core boxes. Whilst the sonic drilling method uses vibration and rotation to collect samples, the material within the boreholes is predominantly poorly compacted and intact samples with sufficient length for undisturbed testing were sparse. It should be noted that the dominant materials within the sample included gravel, sand and timber. The solid waste is estimated to be placed between 1988 and 2002, based on light detection and range (LiDAR) surveys, hence the age of waste is estimated to be between 18 and 32 years.

4.2.2 Sample preparation

A length of 2 m of core was selected at a depth of 8 - 10m from Borehole 1 (BH1) within the landfill as in Figure 4.1. The section of core selected was due to the intact nature of the core collected for a sample that would be suitable dimensions for a triaxial test with

height that is two times the diameter of the sample. The average moisture content and unit weight of the full length of core from sonic drilling was 28% and 13 kN/m^3, respectively. This collected waste material was cut into particles with size less than 20 mm and mixed evenly. A representative sample in terms of composition was selected and compacted using the standard proctor compaction energy (i.e. 595 kJ/m^3) into a 100 mm diameter and 200 mm height mould in three equal layers. A moisture content test and organic content tests using representative weights of each material type was undertaken as per ASTM D2974-14 and particle size distribution (PSD) was determined as per AS 1289.3.6.2 with standard sieve sizes. Moreover, specific gravity was calculated using the average of three representative samples each weighing 120 g in the pycnometer as per AS 1289.3.5.2. The falling cone method was used to obtain the liquid limit of the sample as per AS 1289.3.9.1. Plastic limit was obtained as per the procedure outlined in AS 1289.3.2.1. Whilst the Atterberg limits are useful, these tests were undertaken on material passing the 0.425 mm sieve as per relevant testing standards and are not very representative of overall behaviour since the collected landfill sample had 80% by weight larger than this sieve size. A summary of the material properties of the collected waste sample is presented in Table 4.1.

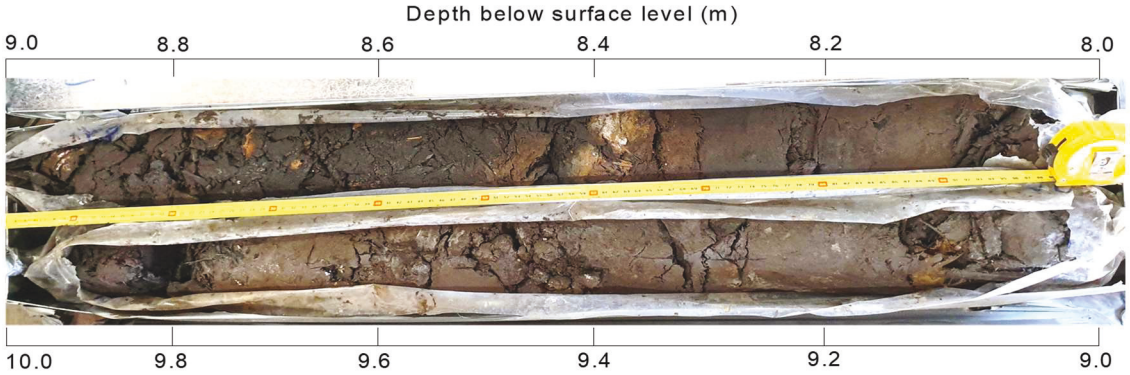

Figure 4.1 Sonic drilled borehole landfill waste sample at 8 - 10m depth below ground level

Table 4.1 Physical properties of collected landfill waste material

Sample height	Average Diameter	Moisture content	Organic content	Total Density	Dry Density	Specific gravity	LL	PI

mm	mm	%	%	t/m^3	t/m^3	-	%	%
196	103	24	22	1.28	1.03	2.1	46	N.P*

*N.P. = not plastic

4.2.3 Triaxial testing equipment and procedure

The test conducted is a multi-stage consolidated drained (CD) triaxial test on landfill waste material based on ASTM D4647. The multi-staged triaxial test is often done when collection of three rather identical samples is not feasible and thus mechanical parameter of the material need to be established from one sample. Many research studies utilised multi-stage triaxial tests to measure mechanical parameters of soil including cohesion, friction angle, and stiffness from a single sample (Kenney & Watson, 1961; Houston et al., 2008; Choi et al., 2018; Banerjee et al., 2020).

The triaxial setup used comprised of a 10 kN load frame with internal load cell, an external linear variable displacement transducer (LVDT), two 1-MPa controllers, bender elements fitted into the base and top cap and a data logger all connected to a computer as shown in Figure 4.2. Since the sample had sharp edges from timber and hard plastics, a double membrane was utilised to minimise the risk of puncture. Membrane correction factors were applied to account for the double membrane. The sample was smoothed on the edges and sharp edges were removed prior to placement of membrane. An adhesive lubricant was applied between each layer of membrane and two O-rings were used to seal the sample at the top and bottom.

After the cylindrical sample (100 mm in diameter and 200 mm in height) was prepared as explained in the previous section, it was placed in the triaxial cell and saturated using back pressure technique where the back pressure increases in stages while maintaining the consolidation pressure (i.e. cell pressure – back pressure) as 20 kPa. In this study, Skempton's B-value of 0.95 was achieved under the back-pressure of 200 kPa after 7 days.

Effective isotropic consolidation stresses of 50, 100, 200 and 400 kPa were adopted and the termination of the each consolidation stage was upon completion of primary consolidation which was deemed as the intersection between the linear fit of the steepest portion of the consolidation curve and the linear portion of the ending of the curve as

described in ASTM 2435 using the change in back volume of the sample measured over time. Additionally, the soil volumetric creep test under isotropic loading was conducted at the end of each isotropic consolidation stage based on measurement of back volume change over time. Only the 50 kPa consolidation stage was completed prior to the first shearing stage, all subsequent isotropic consolidation stages (100 kPa, 200 kPa and 400 kPa) were undertaken after a shearing stage and were therefore in a heavily overconsolidated state.

Following the completion of the isotropic consolidation, the shearing stage was conducted. Indeed, the rate of shearing is known to have a significant impact on the results (Bray et al., 2009; Karimpour-Fard et al., 2011; Zekkos et al., 2012). A slow axial strain rate of 0.3% per hour was adopted for each shearing stage based on the consolidation data as per AS 1289.6.4.2 to ensure drained conditions during shearing. Since multi-stage triaxial test needed to be conducted, a stopping criteria needed to be introduced for each shearing stage, at which the rate of deviatoric stress change was less than 1% over 5 minutes implying that the stress - strain curve had approached an asymptote prior to surpassing the failure point to avoid sample damage in multi-stage triaxial test.

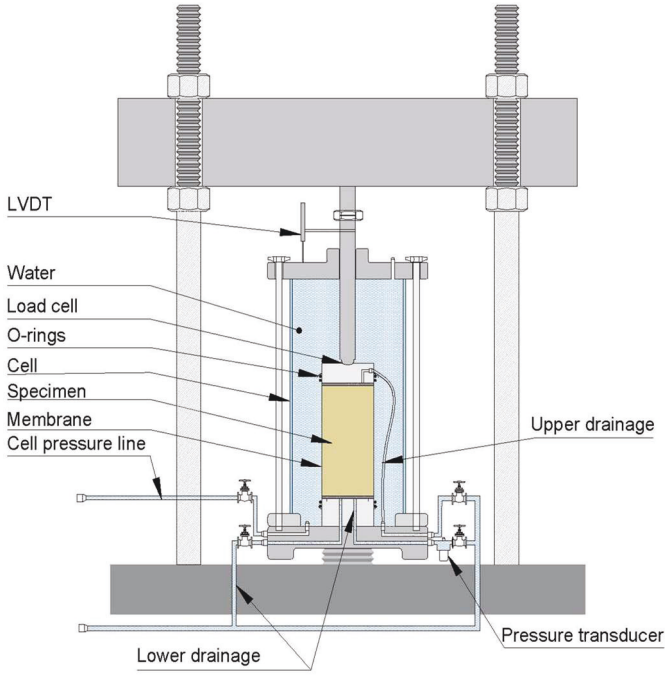

(a)

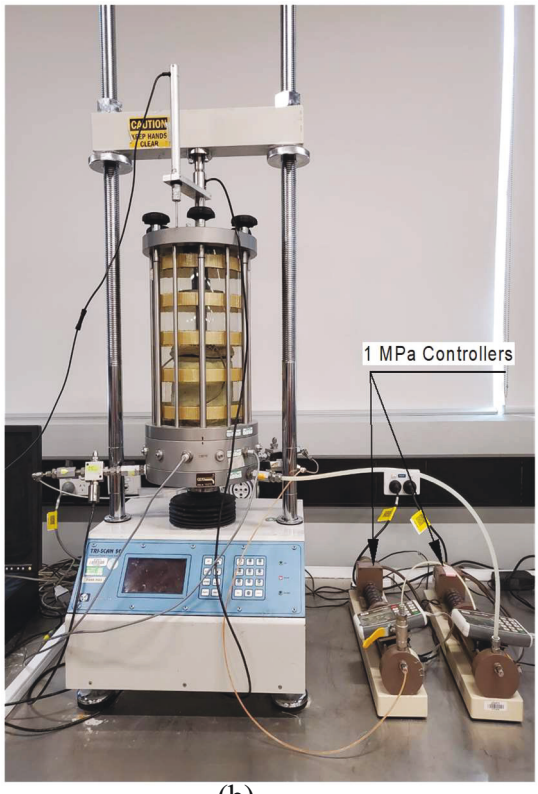

(b)

Figure 4.2 Experimental setup (a) schematic diagram and (b) triaxial test equipment used in this study

Moreover, stress relaxation was undertaken following the procedure proposed by Yin et al. (2014). Whilst this method was originally formulated for soft soils, it is a simple addition to the standard triaxial test to obtain creep parameters for other materials such as waste material used in this study. Indeed, as a result of soil creep, the stress level in the soil drops while the strain is kept constant (this is know as stress relaxation), and thus the creep rate can be determined based on the rate of reduction in the stress level. Stress relaxing stage was conducted immediately after completion of shearing, whereby the application of strain was stopped and thus continuous drop in the deviatoric load was measured over time. The stress relaxation was repeated at the end of drained shearing stages and due to the level of experienced mean effective stresses at the end of drained shearing in this study, the determined creep rates from stress relaxation tests corresponded to the normally consolidated state of the landfill waste material.

4.3 Results and discussion

4.3.1 Basic landfill material characteristics

The PSD reported in Figure 4.3 shows a relatively well graded sample, since coefficient of uniformity (Cu) was determined to be 25 while coefficient of curvature (Cc) was 1, with a low amount of fines (i.e. 4 % finer than 75 μm). The total unit weight and dry unit weight of the reconstituted compacted sample was 12.5 kN/m^3 and 10.9 kN/m^3 comparable to the in-situ unit weight of waste material obtained from sonic drilling. The specific gravity of the waste composite material based on three pycnometer tests as explained in the previous section was found to be 2.1, which is well less than the typical value of 2.55 - 2.75 adopted for soils. Material composition was assessed by visually separating the sample after PSD testing. Materials were classified into material types including glass, plastic, foam, timber, gravels, paper, fibre (clothing), sand and fines as shown in Figure 4.3. Organic content of the adopted landfill waste was determined to be 22%, which is very well in line with accumulative weight percentage of paper, fibre and timber components obtained from classification. The Atterberg limits of the sample were found to be LL = 46 (liquid limit) and non-plastic for the 17% passing the 425 μm sieve size used for this testing as per AS 1289.3.9.1. The classification of the fines was determined to be low plasticity silt (ML).

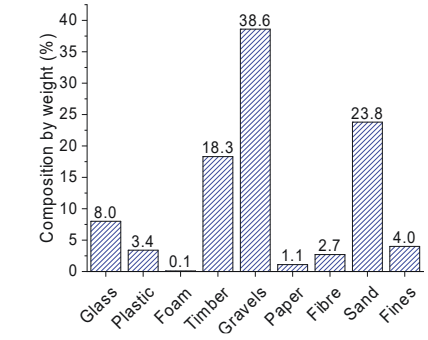

(a)

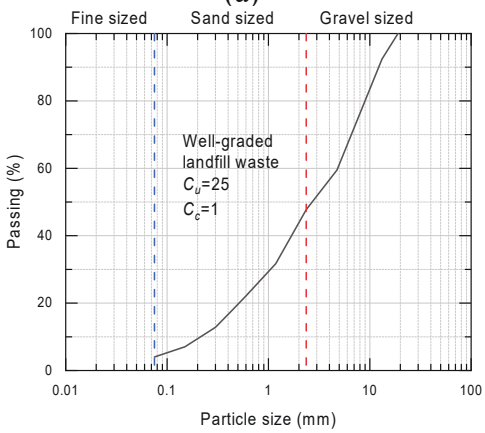

(b)

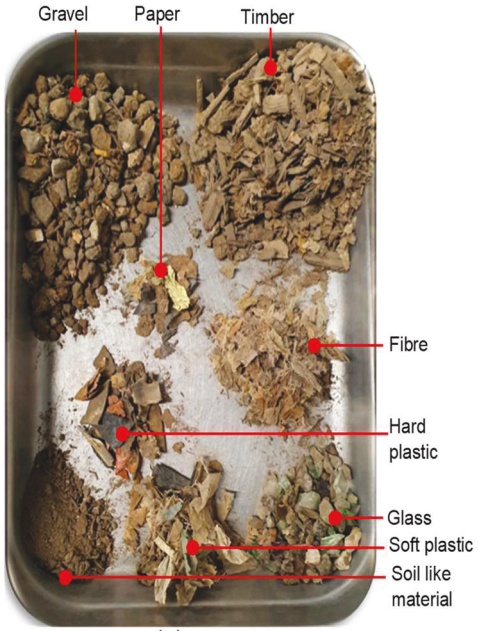

(c)

Figure 4.3 Landfill material (a) composition by weight, (b) particle size distribution and (c) photograph of segregated material after drying from sieve sizes greater than 1.18 mm

In Australia, operating landfills have stringent regulations including the placement of daily cover comprised of placing cover soil at the end of each day to reduce odour, rainfall infiltration and generation of debris (EPA, 2016). This daily cover material is usually removed the next day when the next layer of waste is placed. However, during this process, a portion of the daily cover material is lost into the waste material. A potential reason for the large portion of fine gravel and soil within the sample at this depth could potentially be due to this daily cover material mixed with waste or the presence of uncontrolled fill within the landfill. It should be noted that the daily cover placement techniques commonly used in Australia can affect waste composition compared to many other landfill waste materials reported in literature where daily cover practice did not apply (Landva & Clark, 1986b; Machado et al., 2009; Karimpour-Fard et al., 2011; Ramaiah et al., 2014). Shear wave velocity tests were undertaken with bender elements with sender and receiver attached to the top and bottom of the sample. Indeed, the shear wave velocity was utilised to measure the small strain stiffness of the reconstituted sample. The shear wave velocity of the sample was measured to be V_s = 166 m/s, corresponding to the estimated small strain shear modulus G_{max} = 35 MPa and estimated small strain Young's modulus E_{max} = 92 MPa (assuming Poisson's ratio v = 0.3).

4.3.2 Characteristics of landfill waste under shear loading

Photographs of the reconstituted sample before testing and the deformed sample after shearing are presented in Figure 4.4. Stress - strain curves for individual shearing stages of multi-stage triaxial tests based on stage axial strain and accumulated axial strains are presented in Figure 4.5. It is evident that the first shearing stage corresponding to the confining pressure CP = 50kPa resulted in quite a large axial and volumetric strains prior to the failure, whilst at CP = 100 and CP = 200 kPa less stage axial and volumetric strains were observed near the failure points. For example, referring to Figure 4.5a, the magnitude of experienced stage volumetric strain at the end of the first drained shearing stage when CP = 50 kPa was almost double that of CP =100 kPa and CP = 200 kPa stages. The significant deviatoric stresses mobilised at the large axial strains are believed to be due to the increased mean effective stresses during the drained triaxial shearing ($\frac{dq}{dp'} = 3$) in addition to the

gradual engagement of the plastic waste during sample shearing which was also reported by other researchers (Zekkos, 2005; Bray et al., 2009; Karimpour-Fard et al., 2011).

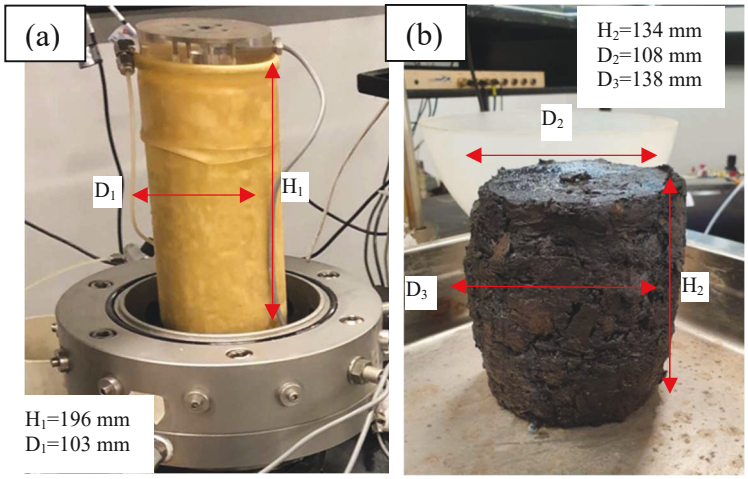

Figure 4.4 Sample (a) prior to test and (b) after test

The accumulated axial strain chart in Figure 4.5b was utilised to determine the Young's modulus of the sample. The secant Young's modulus (E_s) was found to be ranging from 3.8 MPa to 4.3 MPa, continuously increasing with the confining pressure. The equation below, originally proposed by Viggiani & Atkinson (1995) for clays, was used to estimate the constants n and m for the utilised landfill material, which can be used to estimate Young' modulus based on stress level and overconsolidation ratio.

$$E_s = E_{ref}\left(\frac{p'}{p'_{ref}}\right)^n (OCR)^m \qquad \textit{Eq. 4.1}$$

where E_s is the secant Young's modulus, E_{ref} equal to 3.8 MPa is the reference secant Young's modulus, p' is the mean effective stress, p_{ref} equal to 300 kPa is the reference mean effective stress from the 50kPa effective stress stage, OCR is the overconsolidation ratio of the sample, n and m are constants depending on the material. The values of n and m for the reconstituted landfill sample were determined to be 0.145 and 0.01 respectively.

Referring to Figure 4.5d, the apparent cohesion and friction angle of the compacted waste material in the range of stresses applied in this study were determined to be $c' = 125$ kPa and $\phi' = 39°$. Values from literature vary significantly between each landfill as shown in

Table 4.2. The high cohesion value of the sample is an interesting observation, especially given the fines were found to be non-plastic and since this is a reconstituted sample, the effects of cementation are not present. The postulated reason for the high cohesion is due to the presence of fibrous components (i.e. timber, plastic & fibres) in the waste that act like reinforcement to the sample. The maximum length of timber, plastic and fibre in the sample was 40 mm, which is large in the scale of a 100 mm diameter triaxial sample, and is likely to have prevented pull-out and allowed for binding components of the sample together similar to fibre reinforced soils. Numerous researchers in the field of fibre reinforced soils (Consoli et al., 2002; Michalowski & Cermak, 2003; Ajayi et al., 2017) as well as those presented in Table 4.2 demonstrated that increasing the fibre content and size of fibres in sandy and gravelly soils leads to a significant increase in the cohesion of the sample. Indeed, the cohesion of the fibre reinforced soils reported in the literature is comparable to the cohesion obtained from the compacted landfill waste sample in this study.

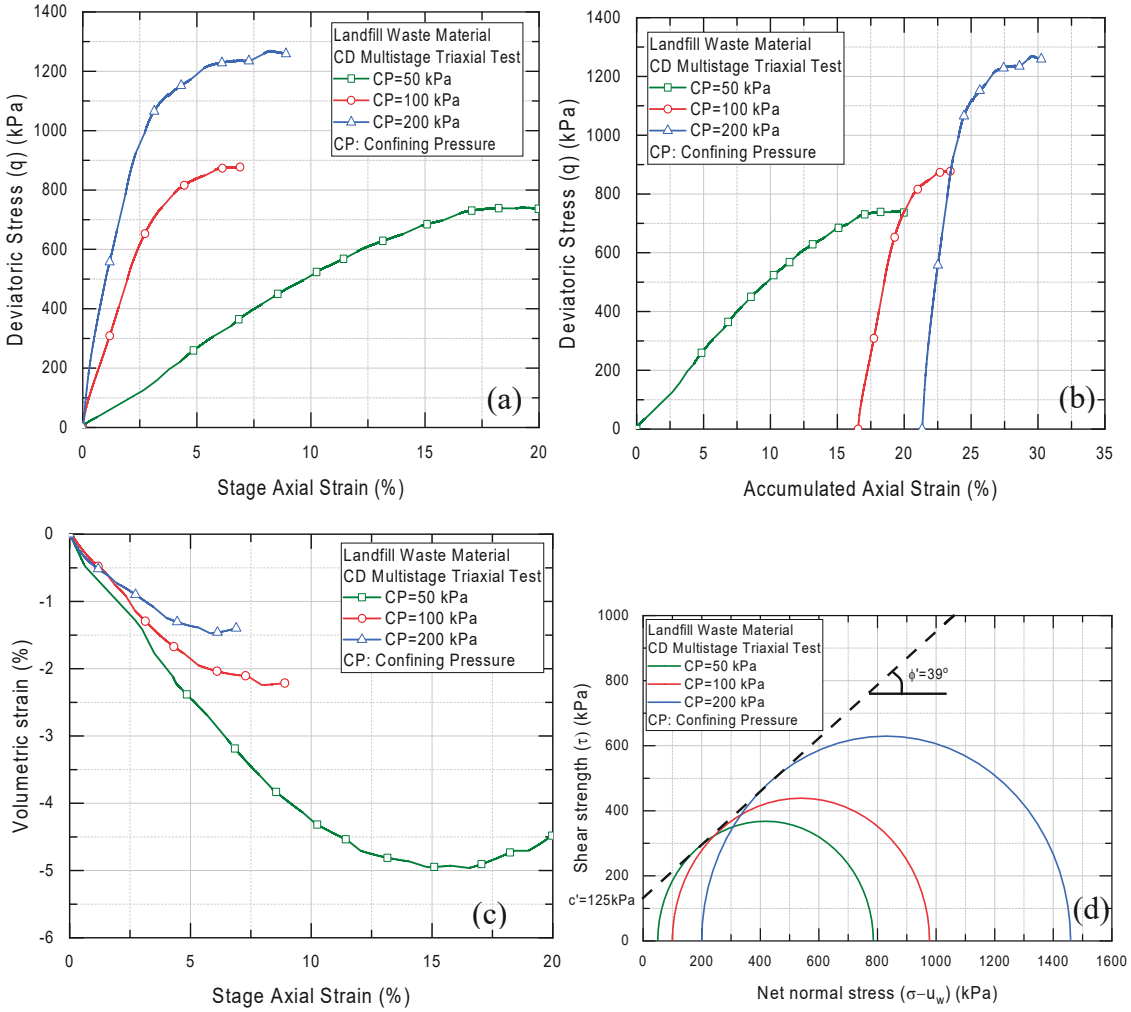

Figure 4.5 Shearing results (a) Stage axial strain vs deviatoric stress, (b) accumulated axial strain vs deviatoric stress, (c) stage axial strain vs volumetric strain and (d) net normal stress vs shear strength

Table 4.2 Landfill shear strength parameters

Landfill Types*	Primary waste constituents	Age of solid waste	c' (kPa)	ϕ (°)	Reference
M/I	Plastic and wood	Old Waste	16-23	9-41	Landva & Clark (1986a)
M	Paper and plastics	Fresh	7-28	26-42	Jessberger (1994)
S	Synthetics and wood	0-5 years old	15-20	15-35	Kölsch (1995)
M	Paper and plastics	12-16 years old	21-75	30-39	Gotteland et al. (2000)
M	Wood, paper and plastic	Variable	0-50	26-35	Pelkey et al. (2001)
M	-	Fully degraded waste	16-30	33-59	Kavazanjian (2001)
S	Metal, paper and rubber	Fresh	0-31	29-43	Dixon et al. (2008)
S	Cardboard, wood and plastic	1.5 year old	31-64	16-30	Reddy et al. (2009a)
M	Cinder, stone and plastic	15 year old waste	6-70	14-27	Machado et al. (2002)
M	Plastic, cardboard and paste	15 year old waste	2-46	9-47	Karimpour-Fard et al. (2011)
M	Cinder and organics	5 year old waste	4-55	10-19	Feng (2005)
M	Paper, plastic, wood and gravel	Fresh and old waste	0	34-48	Zekkos et al. (2012)
M	Gravels, textiles and plastic	3 year old	0-4	47-67	Ramaiah et al. (2014)
I	Fly ash and coal waste	Fresh	21-40	27-55	Gruchot & Zydro (2019)
M	Plastics, textiles and fines	2-6 years	0-40	15-48	Gomes et al. (2013)
M	Plastics and textiles	5-16 years	1-2	21-31	Keramati et al. (2020)
S	Paper and plastics	Fresh	0-65	21-32	Shi et al. (2020)
F	Unreinforced sandy soil	-	23	30	Consoli et al. (2003)
F	Plastic reinforced sandy soil	-	127	31	
F	Unreinforced sand	-	2-8	33-35	Diambra et al. (2010)
F	0.9% plastic reinforced sand	-	69-79	43-49	
F	Unreinforced sand	-	0	38	Zhao et al. (2020)
F	Plastic reinforced sand	-	110	37	
F	Sand with recycled plastic (0.1%)	-	17	30	Nolutshungu & Kalumba (2017)
F	Sand with recycled plastic (0.5%)	-	79	28	
M	Gravel, sand, timber & plastic	-	125	39	This study

*Primary landfill type: M=municipal solid waste, I=industrial, S=synthetic waste created in a laboratory, F=fibre reinforced soil

4.3.3 Compression and consolidation parameters of landfill waste material

Modified Cam Clay model (Roscoe & Burland, 1968) was used to determine the corresponding equivalent mean yield stress (i.e. p'_0) impacting the volumetric strain during loading. Indeed, the modified Cam clay model was used by many researchers for simulation of landfill waste material (Machado et al., 2008; Sivakumar Babu et al., 2010; Kumar et al., 2021). The following equation was utilised to obtain p'_0 (Muir-Wood, 1990):

$$p'_0 = \frac{q^2}{M^2 p'} + p' \qquad \textit{Eq. 4.2}$$

where p' is the mean effective stress, q denotes the deviatoric stress, M is the gradient of failure envelope (i.e. q_f/p'_f = 1.6), and p'_0 is equivalent mean yield stress known as the hardening parameter, corresponding to the mean effective stress (p') on the yield surface when q = 0 (i.e. equivalent isotropic effective stress).

According to Figure 4.6, the values of compression and recompression indices were calculated to be λ/v_0 = 0.071 and κ/v_0 = 0.007, respectively (v_0 = 1 + e_0) , and the pre-consolidation pressure was estimated to be p'_c = 730 kPa. Sharma et al. (2016) indicated that soil compacted to standard proctor energy level can be considered as over-consolidated soil with approximate preconsolidation pressure of 820 kPa as a result of compaction energy. The value of p'_c = 730 kPa was measured in this study for a unit weight of 12.5 kN/m^3 using the standard proctor energy level, which is comparable to Sharma et al. (2016) observation; the difference can be attributed to the nature of landfill material and potential energy loss during compaction. The compression indices obtained from the triaxial testing in this study is comparable to values reported in the literature ranging between 0.046-0.23 for compression (λ) and 0.0046-0.013 for recompression (κ) indices for various landfill materials (Machado et al., 2002; Machado et al., 2008; Babu & Ering, 2017).

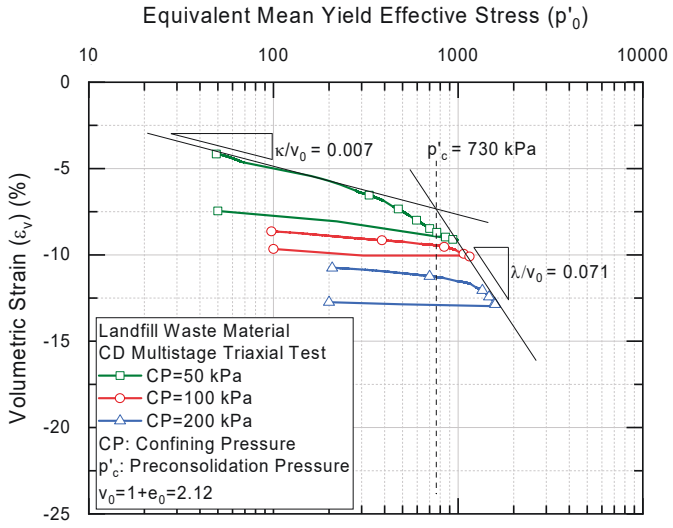

Figure 4.6 Volumetric strain vs mean effective stress

Variations of the volumetric strains with time during the isotropic consolidation stages of the tests are presented in Figure 4.7. The coefficient of consolidation (C_v) was calculated for each consolidation stage using the least square method proposed by Chan (2003). The value of C_v was determined to be in the range of 90 - 190 m^2/yr for heavily overconsolidated state of landfill with overconsolidation ratio in the range of OCR = 4 - 14. Using C_v and the coefficient of volume compressibility (m_v), the coefficient of hydraulic conductivity (k) of the reconstituted landfill sample was found to be in the range of 4.9×10^{-9} to 1.2×10^{-8} m/s, which is on the lower bound of that presented in Table 4.3. Taylor (1948) proposed Equation (4.3), to capture the variations of hydraulic conductivity of fine-grain soils with void ratio.

$$\log k = \log k_0 - \frac{e_0 - e}{c_k} \qquad \textit{Eq. 4.3}$$

where c_k is the permeability change index, k_0 is the initial coefficient of permeability corresponding to the initial void ratio e_0. Figure 4.8 plots variations of determined coefficient of permeability with void ratio measured during the sample consolidation. As evident, the sample permeability is rather low despite presence of significant gravels and sands size particles. This is due to the fact that the presence of impermeable components such as plastics as well as low permeability fines appear to impede water seepage through the composite waste contributing to rather low overall hydraulic conductivity of the sample. Xie et al. (2006) indicated that the low permeability of waste was associated with the increasing content and size of plastics as well as the swelling of organic material obstructing the flow of liquid through the sample.

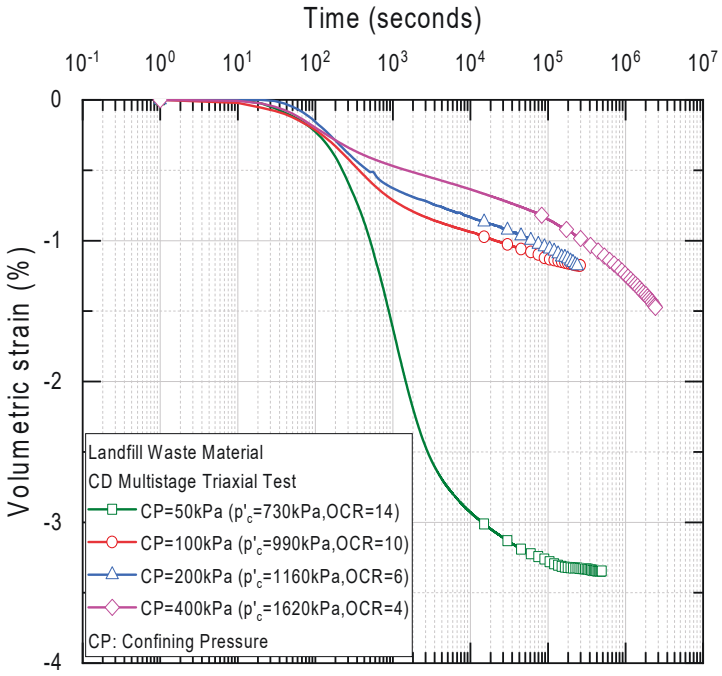

Figure 4.7 Consolidation curves at 50 kPa, 100 kPa, 200 kPa and 400 kPa

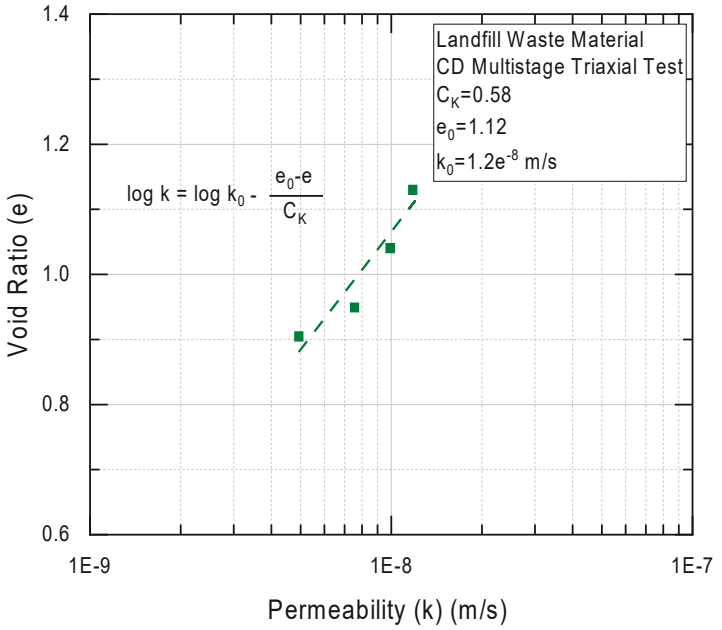

Figure 4.8 Variation of landfill permeability with void ratio

Table 4.3 Hydraulic conductivity for landfill material

Landfill type*	Primary constituents Waste	Waste age / description	Permeability (m/s)	Reference
M	Paper and plastic	Fresh	$2.3x10^{-7} – 9.5x10^{-4}$	Chen & Chynoweth (1995)
M	Cloth, paper, glass, metal	10 years	$4.7x10^{-6} – 1.24x10^{-4}$	Durmusoglu et al. (2006)
M	Glass, metal, plastic, wood	4-10 weeks	$3.3x10^{-11} – 1.8x10^{-7}$	Xie et al. (2006)
S	Paper, plastic, food waste	Fresh	$8.0x10^{-6} – 1.0x10^{-4}$	Penmethsa (2007)
M	Wood and cardboard	Fresh-1.5years	$1.0x10^{-8} – 2.0x10^{-4}$	Reddy et al. (2009b)
M	Paper, plastic, food waste	Fresh-1year	$1.0x10^{-5} – 9.0x10^{-3}$	Hossain et al. (2009)
M	Putrescible, paper, plastic	Fresh	$7.5x10^{-5} – 0.5x10^{-5}$	Staub et al. (2009)
I	Mine waste	Fresh	$3.0x10^{-9} – 6.0x10^{-6}$	Wickland et al. (2010)
M	Food, paper, plastic	Fresh	$1.1x10^{-5} – 1x10^{-4}$	Stoltz et al. (2010a)
M	Plastic, paper, glass	30 years	$1.0x10^{-9} – 6.0x10^{-5}$	Yang et al. (2016)
S	Household waste	0-18 months	$3.0x10^{-8} – 2.0x10^{-5}$	Ke et al. (2017)
S	Plastic, metal, food	Fresh	$2.5x10^{-5} – 1.2x10^{-4}$	Al-Isawi et al. (2021)
S	Household waste	Fresh	$2.0x10^{-6} – 2.0x10^{-4}$	Wang et al. (2021)
M	Gravel, sand, wood, plastic	18-32 years	$4.9x10^{-9} – 1.2x10^{-8}$	This study

*Primary landfill type: M=municipal solid waste, I=industrial, S=synthetic waste created in a laboratory

4.3.4 Creep characteristics of landfill waste material

The viscoplastic creep parameter of landfill waste was determined using two methods including constant stress creep and stress relaxation tests. Whilst these two methods provide creep coefficient of the sample, due to the sequence of testing, the constant stress creep test provided creep characteristics at over-consolidated state at low applied stress levels, whilst stress relaxation test provided creep characteristics at normally consolidated state of the waste at higher stress levels. The constant stress creep stage included the monitoring of sample volume change via back volume change with time during isotropic consolidation stages at confining pressures of 200 kPa and 400 kPa with duration of approximately 30 days each (see Figure 4.9).

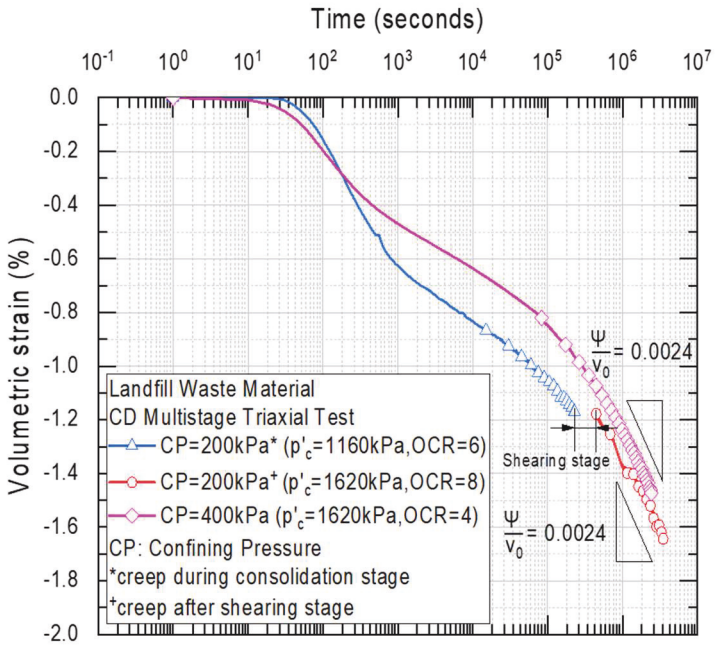

Figure 4.9 Consolidation creep curves at 200 kPa and 400 kPa

Moreover, the use of stress relaxation to determine the creep rate is an alternative method to determine the creep parameter of the landfill waste material. Following completion of the shearing stage, the sample axial straining was prevented while variation of the axial stress measured via the load cell was recorded as presented in Figures 10a. The load reduction over time is plotted in the form of variations of the normalised deviatoric stress with time (Figure 4.10b). Whilst the entire curve after commencement of stress relaxation is theoretically capturing creep effects, Bagheri et al. (2019) explained that stress relaxation is split into three components, fast relaxation, decelerating relaxation and residual relaxation. The residual relaxation corresponds to the linear portion of stress relaxation curve, which is considered as most suitable to accurately calculate the stress relaxation parameter required to obtain the creep index. Referring to (Yin et al., 2014), the following equations were used to interpret the stress relaxation test results:

$$R_\alpha = \frac{\Delta \ln (q)}{\Delta \ln (t)} \qquad \textit{Eq. 4.4}$$

$$\frac{\Psi}{v_0} = R_\alpha \frac{\lambda}{v_0} \qquad \textit{Eq. 4.5}$$

where R_α is the stress relaxation parameter (refer to Figure 4.10), q denotes the deviatoric stress, t is the time since start of relaxation, $\frac{\Psi}{v_0}$ is the creep index measured in natural logarithm scale of time, $\frac{\lambda}{v_0}$ is the slope of normal compression line reported in Figure 6 and $v_0 = e_0 + 1 = 2.12$. It should be noted that $\frac{\Psi}{v_0} = \ln(10)\, C_\alpha / v_0$, where C_α / v_0 is the conventional creep coefficient measured in decadic logarithm time scale.

By combining both constant stress creep and stress relaxation tests results, variations of creep index of the landfill waste sample with over-consolidation ratio could be determined. The creep index $\frac{\Psi}{v_0}$ in the over-consolidated stress state of the landfill waste (OCR = 4 – 14) was measured to be 0.0024 (obtained from constant stress creep test), while the corresponding values for the normally consolidated stress state obtained from stress relaxation test was in the range of 0.018-0.019. Table 4.4 summarises the range of creep coefficient for various landfill waste types reported in the literature, which are comparable with the results reported in the current research. By comparing the measured creep indices for normally consolidated and over consolidated waste at the same equivalent mean effective stress (i.e. $p'_0 \cong 400$ kPa), the secondary creep index of the over-consolidated landfill waste with OCR = 4 was 7.5 times less the corresponding value for normally consolidated state of the landfill waste.

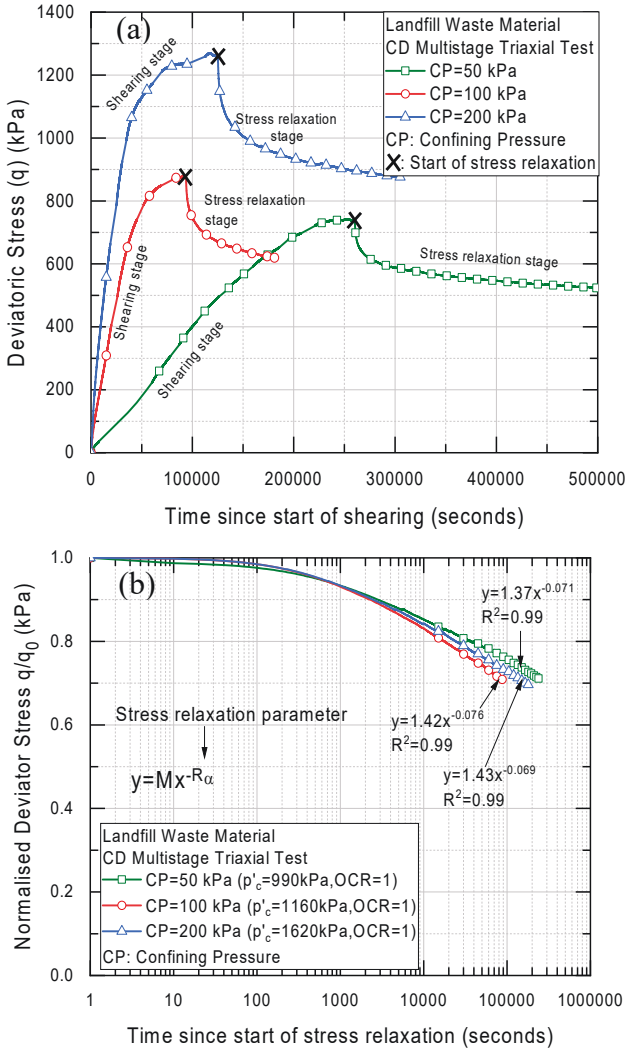

Figure 4.10 Stress relaxation results (a) shearing stage and stress relaxation with time and (b) normalised deviatoric stress relaxation with time from beginning of stress relaxation

The findings of this study highlights the importance of over consolidation ratio on creep rate, which would help to understand effectiveness of preloading for controlling the long term post-construction settlement of structures built on close landfills. The over-consolidated landfill waste material indicated a much lower creep index compared to its normally consolidated state. As such, the use of preloading would reduce long-term post-construction settlement and could be a viable improvement technique for landfill sites.

Table 4.4 Secondary creep coefficient for landfill material

Landfill type*	Primary Waste constituents+	Waste age / description	C_α X	Reference
M/I	Uncontrolled	Unlikely to decay – likely to decay	$0.03e_0$ - $0.09e_0$#	Sowers (1973)
M/I	Residential / construction	Old landfill 3-12 m deep	0.008 - 0.022	Burlingame (1985)
M	Uncontrolled	Fresh and old waste, 10-30 m deep	0.012 - 0.075	Edil et al. (1990)
M	Paper, organics and plastic	Four year old samples in test cells	0.033 - 0.056	Wall & Zeiss (1995)
M	High soil content	Old landfills	0.002 - 0.005	Oweis & Khera (1998)
M	Paper, wood, fines and plastic	Two – five year old landfill	0.01 - 0.016	Landva et al. (2000)
M	Wood, stone and plastic	15 years old landfill	0.021 - 0.044	Machado et al. (2002)
M	Organics, plastics and paper	Field monitoring of 15 year old landfill	0.015 - 0.03	Marques et al. (2003)
M	Organics, plastic, paper and stone	Fresh and four year old landfill	0.058	Machado et al. (2008)
M	Soil, gravel and paper	Fresh landfill	0.008 – 0.065	Bareither et al. (2013a)
M	Organics, soil and paper	Fresh landfill	0.034 – 0.049	Shi et al. (2016)
M	Organics, plastic, textile	Three years	0.035	He et al. (2021)
M	Gravel, sand, wood, plastic	18-32 years – over-consolidated	0.001-0.005	This study
M	Gravel, sand, wood, plastic	18-32 years – normally consolidated	0.018-0.019	This study

*Primary landfill type: M=municipal solid waste, I=industrial, S=synthetic waste created in a laboratory

+Organics typically refers to garden and food waste

X $C_\alpha = \frac{\Delta e}{\Delta(Log t)}$

e_0 is the initial void ratio of the landfill material

4.4 Summary and conclusions

In this study, a detailed investigation of landfill material collected from a landfill in Sydney at a depth of 8 - 10m below landfill surface was conducted. A consolidated drained multistage triaxial test with total duration of 5 months was undertaken on a reconstituted sample with total unit weight of 12.5 kN/m^3 at moisture content of 24%, which was saturated after compaction. The collected sample comprised of primarily gravels, sand, glass, plastic, foam, timber, paper, fibre (clothing) and fines and its initial void ratio was determined to be 1.12. Parameters identified to be critical for settlement assessment that were obtained from the

tests included friction angle, cohesion, Young's modulus, compression indices, pre-consolidation pressure, permeability and creep coefficient.

Friction angle and cohesion of the reconstituted waste sample were determined to be $\phi' = 39°$ and c' = 125 kPa, respectively. The high cohesion of the sample was attributed to the fibrous nature of timber and plastic elements acting as reinforcement to the sample. Young's modulus was found to be increasing with effective stress, ranging between 3.8 MPa and 4.3 MPa when subjected to mean effective stresses in the range of 300 - 620 kPa. Equation (1) with calibrated parameters could capture variations of the Young's modulus of the waste sample with mean effective stress and OCR.

The modified Cam clay model was utilised to obtain the equivalent mean effective stress resulting in the volumetric strain during multistage triaxial test to obtain the compression indices and pre-consolidation pressure. Compression indices were found to be $\frac{\lambda}{v_0}$ = 0.071 (compression index) and $\frac{\kappa}{v_0}$ = 0.007 (recompression/swelling index), with a pre-consolidation pressure of p'_c = 730 kPa corresponding to the compacted sample. The coefficient of consolidation of waste sample in the over consolidated state of stresses (OCR = 4 - 14) was found to be C_v = 90 - 190 m^2/yr. Moreover, sample permeability was determined to be in the range of 4.9×10-9 to 1.2×10-8 m/s with a decrease in permeability as void ratio decreased. The low permeability of the sample was attributed to the presence of plastics and swelling of organic materials impeding the water flow.

Creep deformation characteristics of the waste material was determined via two tests, namely constant stress creep and stress relaxation tests, capturing over-consolidated and normally consolidated states of the stress in the adopted multistage triaxial testing, respectively. Creep index ($\frac{\Psi}{v_0}$) obtained from constant stress creep test for the over-consolidated state of the compacted landfill waste (OCR = 4 - 14) was measured to be 0.0008-0.0024, whilst creep index ($\frac{\Psi}{v_0}$) determined from stress relaxation test corresponding to normally consolidated stress state of the landfill waste (OCR = 1) was in the range of 0.018 - 0.019. It was evident that the creep index of the waste material reduced significantly as the overconsolidation ratio increased, thus supporting the use of preloading as a ground treatment

method for closed landfill sites. Specifically, by comparing the results for the same equivalent mean effective stress, the measured secondary creep index over consolidated landfill waste with OCR = 4 was 7.5 times less than the corresponding normally consolidated index.

The results of this study show that the consolidated drained multistage triaxial test is a feasible test on landfill waste materials to obtain the required mechanical parameters for the design of redevelopment projects built on closed landfill sites, particularly since collecting three similar samples from one location in heterogeneous landfill is practically impossible. The parameters obtained from multistage triaxial test on each landfill site can be used by practicing engineer in predicting long terms settlement of new construction on closed landfill sites or design appropriate ground improvement techniques, rather than simply assuming parameters from literature, which can be very heavily variable resulting in unreliable designs. Indeed, site-specific investigation and testing schemes are likely the solution to prevent reoccurrences such as excessive settlements at Jordan Springs in Sydney.

Chapter 5 – Undisturbed Waste Compressibility and Strength

This chapter presents a comparison between compressibility and strength of undisturbed and reconstituted landfill material obtained from the landfill surface is described through a multi-stage consolidated undrained triaxial tests.

5.1 Introduction

The development of infrastructure above closed landfills is becoming increasingly popular across the globe due to the limited available space in urban areas. Within Sydney, Australia, there are a number of major infrastructure projects that are under construction or have been recently completed above landfill sites including St Peters Interchange, Moorebank Intermodal and Sydney Gateway. However, given the heterogeneous nature of landfill material, obtaining geotechnical design parameters are difficult to be able to assess long-term settlement. The current approach by geotechnical engineers is heavily reliant on design parameters from the literature, where it is known that every landfill has varying composition, unit weight and climate conditions that effect biodegradation. Therefore, site specific testing is encouraged to ensure landfill material design parameters are more reasonably captured to estimate long-term settlement.

Triaxial testing and direct shear testing have been studied over decades by many prominent landfill researchers on reconstituted and synthetic landfill material (Landva & Clark, 1986a; Kavazanjian, 2001; Machado et al., 2002; Bray et al., 2009; Zekkos et al., 2012; Zekkos & Fei, 2017). Whilst the use of reconstituted samples are practical to obtain representative properties of landfill, the quantification of the difference between results of undisturbed and reconstituted testing is very limited for both strength and compressibility. Undisturbed sampling from push tubes is recommended since landfill can highly be consist of structured material resulting from placement (Dixon & Jones, 2005). However, there are limitations including the difficulty in obtaining a push tube sample in landfill due to refusal, lack of sample representativeness, potential oversize particles, lack of cohesion in the sample to stay intact after extrusion and limited understanding of the benefits of undertaking undisturbed landfill samples by practicing geotechnical engineers.

Shear strength testing comparing intact and reconstituted samples has been undertaken on frozen municipal solid waste (Singh et al., 2009). The study included the collection of intact 150 mm diameter samples, which were frozen and tested in a triaxial apparatus and direct shear apparatus. Custom made push tubes, fabricated hydraulic extruder and a large sized deep freezer were required to collect, store and extract the landfill samples. The freeze-thaw effects on the sample and shear strength were not discussed. Unlike conventional triaxial testing where three samples can be used to obtain the Mohr-Coulomb parameters, landfill composition was different between each push tube and hence, obtaining shear strength in this manner may not be best practice. The authors concluded that reconstituted samples produce similar shear strength values to intact samples; however, the deformation of each prior to failure was different. The reconstituted samples were ductile whilst the intact samples were stiffer.

Primary consolidation behaviour of waste has been expressed in a similar way to conventional soil with loading (C_c) and unloading (C_r) curves (Chen et al., 2012; Bareither et al., 2013a; He et al., 2021). There is a large variability in literature parameters for Cc and Cr since there are a large number of factors that influence these parameters including unit weight, landfill depth, composition and compaction processes (McDougall, 2007; Powrie et al., 2019).

The long-term creep behaviour of waste material has been primarily obtained through oedometer and Rowe cell testing (Sowers, 1973; Wall & Zeiss, 1995; Machado et al., 2002; Hossain et al., 2003; Bareither et al., 2013b; He et al., 2021). The oedometer and rowe cell tests provide 1D creep due to sample confinement, whilst the use of triaxial consolidation stages and stress relaxation provides 3D creep. In a landfill setting where geometry may change due to landfill depth and embankment heights, 3D creep parameters would become necessary to capture the 3D stress state of waste (Wang et al., 2020). The triaxial consolidation stage uses the sample volume change to obtain the 3D creep (Augustesen et al., 2004; Long et al., 2020). Stress relaxation is undertaken at the end of shearing, whereby the initial stress of the sample is applied and then the stress drop over time is measured to determine the sample creep (Yin et al., 2014).

The benefit of multistage triaxial tests is the time saving on the sample preparation and saturation stage, which was only needed once rather than three separate times if the test was repeated for each effective stress condition. Other authors have proven the effects of undertaking multiple conventional triaxial tests is similar to undrained and drained multistage triaxial tests (Kenney & Watson, 1961; Houston et al., 2008; Sharma et al., 2011; Choi et al., 2018; Banerjee et al., 2020). The use of multi-stage tests reduces the limitations of the study undertaken by Singh et al. (2009), whereby the shear strength parameters are obtained from a series of single sample maintaining the same composition.

This chapter details and compares results from a consolidated-undrained multistage triaxial test undertaken on undisturbed and reconstituted landfill waste material extracted from a test pit at the landfill. Parameters obtained and compared in this study include cohesion, friction angle, coefficient of consolidation, coefficient of compression, small strain shear modulus, small strain Young's modulus, large strain Young's modulus, Poisson's ratio and creep.

5.2 Sample collection and experimental plan

5.2.1 Waste sample collection from the landfill site

Refer to Section 4.2.1 for landfill details.

Vertical push tube samples were collected from shallow tests pits within the landfill as shown in Figure 5.1a. At the time, the construction above the landfill was underway, hence there was a 1-1.5 m thick sandstone working platform above the top of the landfill. Push tubes were custom made with thicker walls (refer to Figure 5.1b) than the conventional thin walled Shelby tube samplers for clay since this was expected crumple when the excavator drives the push tube into the landfill. The area ratio of the push tube was made to be 10% in line with the requirements of literature (Gilbert, 1992) to obtain an undisturbed sample. The addition of a tapered edge assisted with the entrance of the tube to pierce through the landfill. After tubes were wrapped with multiple layers of cling wrap and sealed tightly with thick plastic wrap and duct tape (Figure 5.1c).

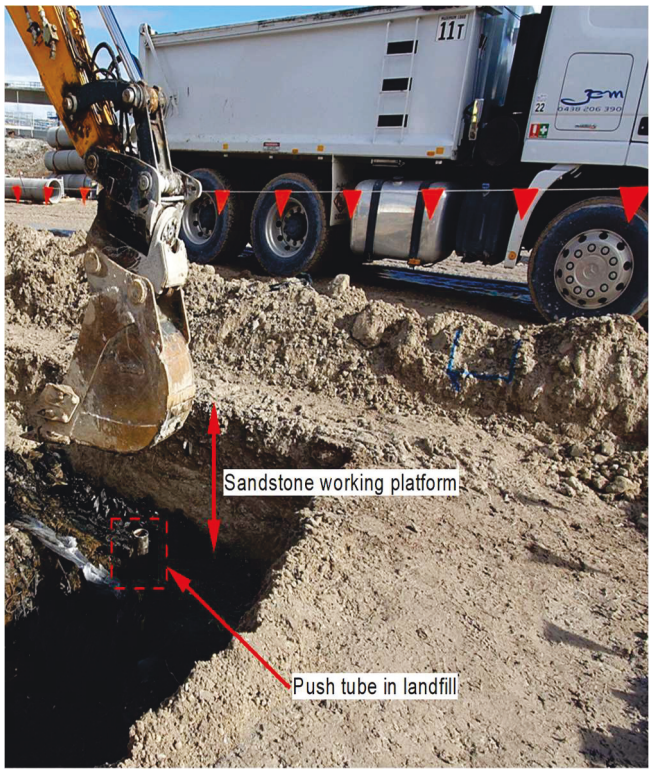

(a)

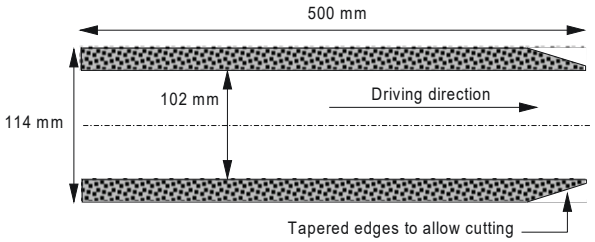

(b)

(c)

Figure 5.1 Push tube sampling (a) push tube being pushed into landfill by 20 tonne excavator, (b) sketch of custom made push tube and (c) sealed push tube samples

5.2.2 Sample preparation

Two separate tests were undertaken, one being on the undisturbed sample extracted from the push tube and the other was the same sample reconstituted to the same dry density. The first method involved extracting the undisturbed landfill sample using the extrusion process as shown in Figure 5.2. This method involved securing the push tube and pushing the sample out of the push tube using a base plate the same size as the internal diameter of the push tube. After extrusion, the sample was gently trimmed to establish a flat bottom and top of sample with a height of approximately 200 mm. A moisture content sample was taken prior to undertaking the test using ASTM D2974-14, this was used as a target moisture for the following test.

The second method involved the creation of a reconstituted sample using the sample material after completion of the undisturbed multistage test. This involved air drying the sample to remove moisture and then adding water and mixing the sample with the intent to obtain a similar dry density and total density as the initial undisturbed sample. The sample was compacted using the standard proctor compaction energy (i.e. 595 kJ/m^3) into a 100 mm diameter and 200 mm height mould in three equal layers. In this way, the reconstituted landfill sample had the same dry density, composition and moisture content as the undisturbed sample allowing them to be directly comparable.

Upon completion of both tests, an organic content test using representative weights of each material type was undertaken as per ASTM D2974-14 and particle size distribution (PSD) as per AS 1289.3.6.2 with standard sieve sizes. Specific gravity was calculated using three representative samples each weighing 120 g in the pycnometer. Atterberg limits were tested using falling cone method for liquid limit and plastic limit as per AS 1289.3.9.1 and AS 1289.3.2.1 respectively. Whilst the Atterberg limits are useful, these tests are undertaken on material passing the 0.425 mm sieve and are not very representative of overall behaviour considering that it constitutes less than 20% of the sample by weight. A summary of the material properties of the sample is presented in Table 5.1.

Table 5.1 Material properties

Sample[#]	Sample height mm	Average Diameter mm	Moisture content %	Total Density t/m^3	Dry Density t/m^3	Organic content %	Specific gravity -	LL %	PI %
U	204	104	25	1.46	1.17	10.5	2.47	35	N.P *
D	203	102	25	1.49	1.19	+	+	+	+

[#]U = undisturbed; D = disturbed

*N.P. = not plastic

[+]Only one test undertaken on sample after completion of both undisturbed and reconstituted tests

(a)

(b)

Figure 5.2 Undisturbed sample extrusion, (a) push tube extrusion process and (b) sample after extrusion and trimming

Material composition was assessed by visually separating the sample after PSD testing. Materials were classified into material types and weight including glass, plastic, timber, gravels, paper, fibre (clothing), bricks, tiles, sand and fines. The dominant materials within the sample included gravel, sand, timber and bricks. The solid waste is estimated to be placed between 1988 and 2002, based on light detection and range (LiDAR) surveys and hence, the age of waste is estimated to be between 18 years and 31 years.

5.2.3 Triaxial testing equipment and procedure

The test conducted is a multi-stage consolidated undrained (CU) triaxial test on landfill waste material based on ASTM D4647. The multi-staged triaxial test is often carried out when collection of three rather identical samples is not feasible; and thus, mechanical parameter of the material need to be established from one sample. Many research studies utilised multi-stage triaxial tests to measure mechanical parameters of soil including cohesion, friction angle, and stiffness from a single sample (Kenney & Watson, 1961; Houston et al., 2008; Choi et al., 2018; Banerjee et al., 2020).

The triaxial setup used comprised of a 10 kN load frame with internal load cell, an external linear variable displacement transducer (LVDT), two 1 MPa controllers, bender elements fitted into the base and top cap and a data logger all connected to a computer as shown in Figure 4.4. Since the sample had sharp edges from timber and hard plastics, a double membrane was utilised to minimise the risk of puncture. The sample was smoothed on the edges and sharp edges were removed prior to placement of membrane. An adhesive lubricant was applied between each layer of membrane and two O-rings were used to seal the sample at the top and bottom.

After the cylindrical sample (100 mm in diameter and 200 mm in height) was prepared as explained in the previous section, it was placed in the triaxial cell and saturated using back pressure technique where the back pressure increases in stages while maintaining the consolidation pressure (i.e. cell pressure – back pressure) as 20 kPa. In this study, Skempton's B-value of 0.95 was achieved under the back-pressure of 200 kPa after 7 days.

Effective isotropic consolidation stresses of 50, 100, 200 and 400 kPa was adopted for the test. The termination of the each consolidation stage was upon completion of primary

consolidation, which was deemed as the intersection between the linear fit of the steepest portion of the consolidation curve and the linear portion of the ending of the curve as described in ASTM 2435 using the change in back volume of the sample measured over time. Additionally, the soil volumetric creep test under isotropic loading was conducted at the end of each isotropic consolidation stage based on measurement of back volume change over time. Only the 50 kPa consolidation stage was completed prior to the first shearing stage, all subsequent isotropic consolidation stages (100 kPa, 200 kPa and 400 kPa) were undertaken after a shearing stage and were therefore in a heavily overconsolidated state.

Following the completion of the isotropic consolidation, the shearing stage was conducted. Indeed, the rate of shearing is known to have a significant impact on the results (Bray et al., 2009; Karimpour-Fard et al., 2011; Zekkos et al., 2012). A slow axial strain rate of 0.3% per hour was adopted for each shearing stage based on the consolidation data as per AS 1289.6.4.2 to ensure drained conditions during shearing. Since multi-stage triaxial test needed to be conducted, a stopping criteria needed to be introduced for each shearing stage, at which the rate of deviatoric stress change was less than 1% over 5 minutes implying that the stress - strain curve had approached an asymptote prior to surpassing the failure point to avoid sample damage in multi-stage triaxial test.

Moreover, stress relaxation was undertaken following the procedure proposed by Yin et al. (2014). Whilst this method was originally formulated for soft soils, it is a simple addition to the standard triaxial test to obtain creep parameters for other materials such as waste material used in this study. Indeed, as a result of soil creep, the stress level in the soil drops while the strain is kept constant (this is know as stress relaxation), and thus the creep rate can be determined based on the rate of reduction in the stress level. Stress relaxing stage was conducted immediately after completion of shearing, whereby the application of strain was stopped and thus continuous drop in the deviatoric load was measured over time. The stress relaxation was repeated at the end of drained shearing stages and due to the level of experienced mean effective stresses at the end of drained shearing in this study, the determined creep rates from stress relaxation tests corresponded to the normally consolidated state of the landfill waste material.

5.3 Results and discussion

5.3.1 Basic landfill material characteristics

The PSD reported in Figure 5.3 shows a relatively well graded sample, since coefficient of uniformity (Cu) was determined to be 10 while coefficient of curvature (Cc) was 0.5, with a low amount of fines (i.e. 2 % finer than 75 μm). The total unit weight and dry unit weight of the reconstituted compacted sample with 14.6 kN/m^3 and 11.6 kN/m^3, which is comparable to the undisturbed sample with 14.3 kN/m^3 and 11.5 kN/m^3. The specific gravity of the waste composite material based on three pycnometer tests as explained in the previous section was found to be 2.5, which is slightly less than the typical value of 2.55 - 2.75 adopted for soils. The higher than expected specific gravity is largely due to the presence of gravels, brick and sands which together comprise of 80% of the sample. Material composition was assessed by visually separating the sample after PSD testing. Materials were classified into material types including glass, plastic, brick, timber, gravels, paper, fibre (clothing), tiles, sand and fines as shown in Figure 5.3. Organic content of the adopted landfill waste was determined to be 10.5%, which is very well in line with accumulative weight percentage of paper, fibre and timber components obtained from classification. The Atterberg limits of the sample were found to be LL = 35 (liquid limit) and non-plastic for the 16% passing the 425 μm sieve size used for this testing as per AS 1289.3.9.1. The classification of the fines was determined to be low plasticity silt (ML).

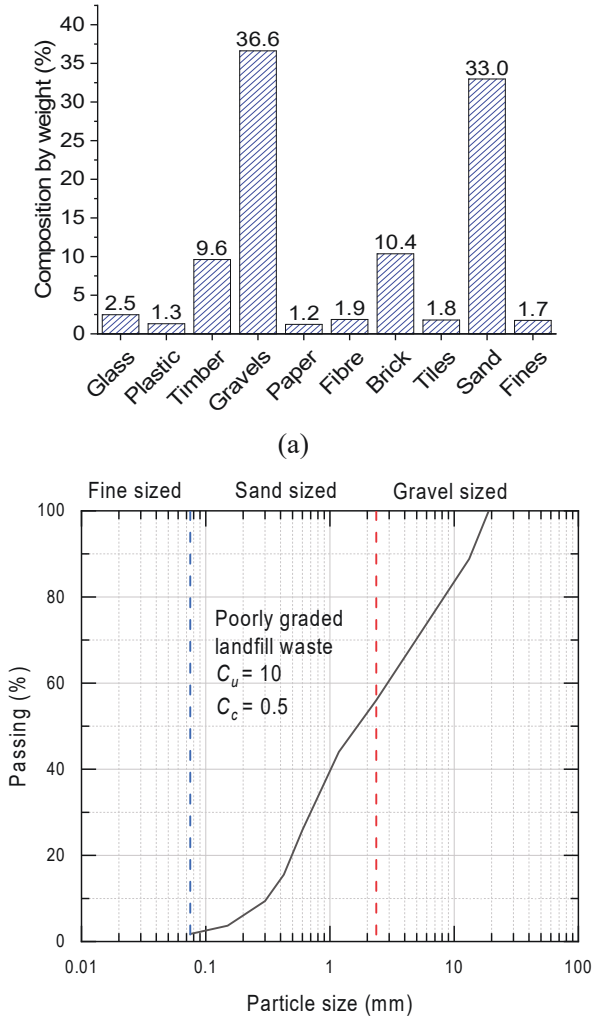

Figure 5.3 Landfill material properties (a) Material composition by weight (b) particle size distribution

It should be noted that the daily cover placement techniques commonly used in Australia can affect waste composition compared to many other landfill waste materials reported in literature where daily cover practice did not apply (Landva & Clark, 1986b; Machado et al., 2009; Karimpour-Fard et al., 2011; Ramaiah et al., 2014).

Shear wave velocity tests were undertaken with bender elements with sender and receiver attached to the top and bottom of the sample. Indeed, the shear wave velocity was utilised to measure the small strain stiffness for both the undisturbed and reconstituted samples as shown in Table 2. The results from both tests overall showed similar properties. The undisturbed sample had slightly high values for Poisson's ratio, small strain shear

modulus and small strain Young's modulus. Whilst the s-wave and p-wave velocities were measured for each stage of the entire test, after the shearing stage at 100 kPa effective stress the results appeared to rise significantly and were assumed to be erroneous. The Poisson's ratio for the sample was initially 0.29 and became approximately 0.4 for every stage after saturation for both undisturbed and reconstituted samples.

5.3.2 Characteristics of landfill waste under shear loading

Stress - strain curves for individual shearing stages of multi-stage triaxial tests based on stage axial strain and accumulated axial strains are presented in Figure 5.4. Stress strain curves including for individual shearing stages and accumulated stage strain have been presented in Figure 5.4(a) and Figure 5.4(b). The undisturbed sample achieved the same stress as the disturbed sample, except at a lower strain for all shearing stages. This stiffer behaviour in the undisturbed sample is postulated to be due to the cementation formed over decades. The first shearing stage for both disturbed and undisturbed tests had the largest axial strain of all shearing stages and each subsequent stage had reducing axial strain. This is likely due to the strain hardening effect on the sample.

As depicted in Figure 5.4c, the pore pressure response in the disturbed sample was much higher than the undisturbed sample. Singh et al. (2009) also undertook studies on intact landfill samples and observed similar pore pressure behaviour. Whilst the cause for the higher pore pressure response is postulated to be due to the cementation of the sample, the effect is important for understanding the deformation and serviceability of landfill material.

A plot of the mean effective stress (p') against the deviatoric stress is presented in Figure 5.4d. There is a noticeable difference in the stress path between the undisturbed and disturbed samples. The undisturbed sample appears to resemble a heavily overconsolidated sample, whilst the disturbed sample resembles a typical undrained test for a normally consolidated sample. This difference in behaviour is likely attributed to the presence of heavy compaction machinery during placement. The sample itself was recovered from the surface of the landfill, which may have been trafficked since landfill closure in 2016 and during construction above the landfill between 2016 and 2019. This difference in over-consolidation of the sample does emphasise the importance of undisturbed testing to capture the in-situ

stress state rather than simply assuming the sample is normally consolidated which is critical for ground improvement analysis such as preloading.

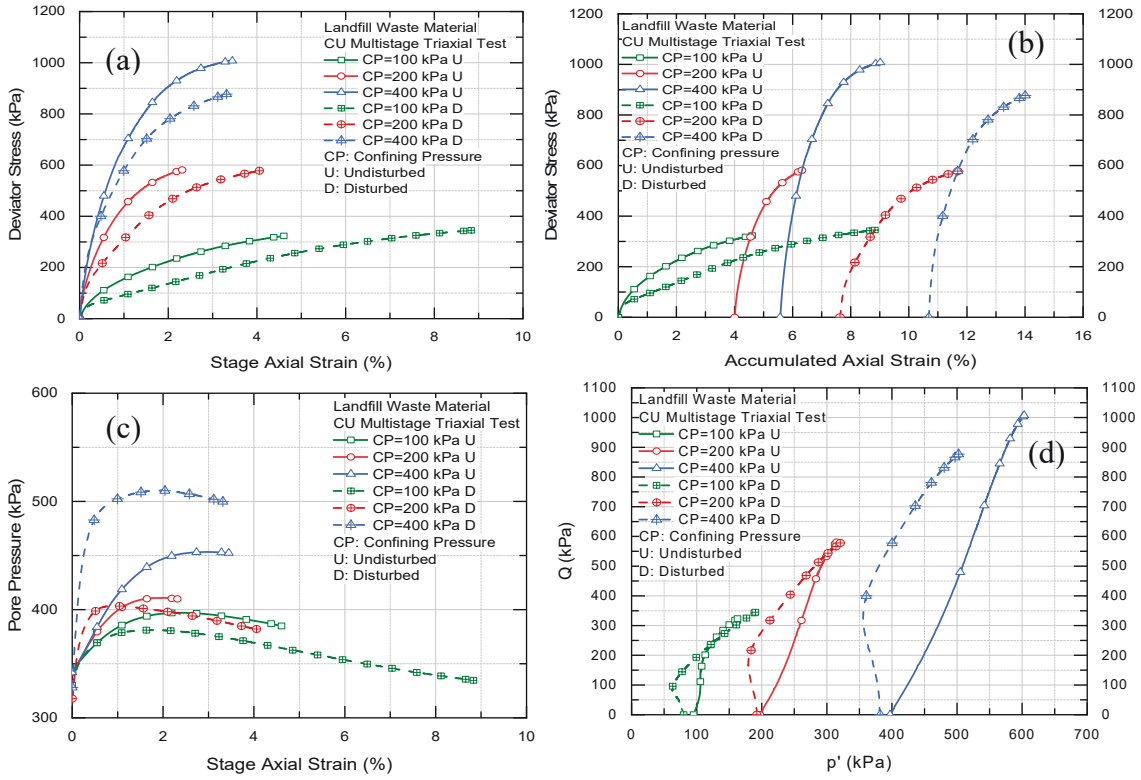

Figure 5.4 Triaxial test shearing results (a) stage axial strain vs deviatoric stress (b) accumulated axial strain vs deviatoric stress (c) stage axial strain vs pore pressure and (d) mean effective stress (p') vs deviatoric stress (q)

The accumulated axial strain chart in Figure 5.4b was utilised to determine the secant Young's modulus of the sample. The Young's modulus was found to be 7-11 MPa for the undisturbed sample and 4-6 MPa for the disturbed sample, both samples displaying increasing stiffness with increasing effective stress. Similarly from bender element testing, the small strain Young's modulus was found to be 102-349 MPa for the undisturbed sample and 82-318 MPa for the disturbed sample. Both large strain and small strain methods demonstrate the undisturbed sample behaves in a stiffer than the disturbed sample. The ratio between small strain and large strain modulus in the saturated state were found to be 30 for undisturbed material and 38 for disturbed material. When comparing the small strain obtained from the beginning of the test with the large strain Young's modulus obtained from the 100

kPa effective stress shearing stage, the ratio for was found to be 14 for undisturbed material and 20 for disturbed material.

A summary of strength parameters from literature compared to the results obtained from this study has been presented in Table 5.2. The estimated shear strength was calculated using the average values from ranges presented in literature to show the combined effect of cohesion and friction angle at different normal stresses. At low normal stresses, the standard deviation is low, however as the normal stress increases the standard deviation between the results increases. For deeper landfills or vertically expanding landfills, analysis at higher normal stresses of 500 kPa which corresponds to a depth of 40 m assuming unit weight of 12.6 t/m3 may be required (Stark et al., 2009). The values obtained for the disturbed and undisturbed tests for friction angle were 42 and 35 degrees respectively, which are both higher than the average from literature. Whilst for cohesion, the undisturbed sample had higher cohesion of 47 kPa compared to the 10 kPa for the reconstituted sample. The higher cohesion in the undisturbed sample is postulated to be attributed to the cementation that has occurred in the sample over decades after placement.

Table 5.2 Landfill shear strength parameters reported in the literature

Landfill Types[1]	Primary waste constituents	Age of solid waste	c′ (kPa)	ϕ (°)	Estimated shear strength (kPa)[2]			Reference
					σ_n=50kPa	σ_n=100kPa	σ_n=150kPa	
M/I	Plastic and wood	Old Waste	16-23	9-41	43	66	89	Landva & Clark (1986a)
M	Paper and plastics	Fresh	7-28	26-42	51	85	119	Jessberger (1994)
S	Synthetics and wood	0-5 years old	15-20	15-35	41	64	87	Kölsch (1995)
M	Paper and plastics	12-16 years old	21-75	30-39	82	117	151	Gotteland et al. (2000)
M	Wood, paper and plastic	Variable	0-50	26-35	54	84	113	Pelkey et al. (2001)
M	-	Fully degraded waste	16-30	33-59	75	127	178	Kavazanjian (2001)
S	Metal, paper and rubber	Fresh	0-31	29-43	52	88	124	Dixon et al. (2008)
S	Cardboard, wood and plastic	1.5 year old	31-64	16-30	69	90	111	Reddy et al. (2009a)
M	Cinder, stone and plastic	15 year old waste	6-70	14-27	57	75	94	Machado et al. (2002)
M	Plastic, cardboard and paste	15 year old waste	2-46	9-47	51	77	104	Karimpour-Fard et al. (2011)
M	Cinder and organics	5 year old waste	4-55	10-19	42	55	68	Feng (2005)
M	Paper, plastic, wood and gravel	Fresh and old waste	0	34-48	43	87	130	Zekkos et al. (2012)
M	Gravels, textiles and plastic	3 year old	0-4	47-67	79	156	233	Ramaiah et al. (2014)
I	Fly ash and coal waste	Fresh	21-40	27-55	74	117	161	Gruchot & Zydro (2019)
M	Plastics, textiles and fines	2-6 years	0-40	15-48	51	81	112	Gomes et al. (2013)
M	Plastics and textiles	5-16 years	1-2	21-31	26	50	75	Keramati et al. (2020)
S	Paper and plastics	Fresh	0-65	21-32	57	82	107	Shi et al. (2020)
Average from literature			23	32	56	88	121	Average of all studies
Standard deviation from literature			14	10	15	27	41	Standard deviation

[1]Primary landfill type: M=municipal solid waste, I=industrial, S=synthetic waste created in a laboratory
[2] Estimated shear strength is based on average values from friction and cohesion ranges presented

5.3.3 Compression and consolidation parameters of landfill waste material

According to Figure 5.5, the values of compression indices for undisturbed and disturbed tests were calculated to be C_c = 0.21 and C_c = 0.22, respectively. The coefficient of unloading / reloading (C_r) could not be obtained since there was insufficient points during

the initial stages of the loading curve. The compression indices obtained from the triaxial testing indicate similar results to the average of literature as shown in Table 5.3.

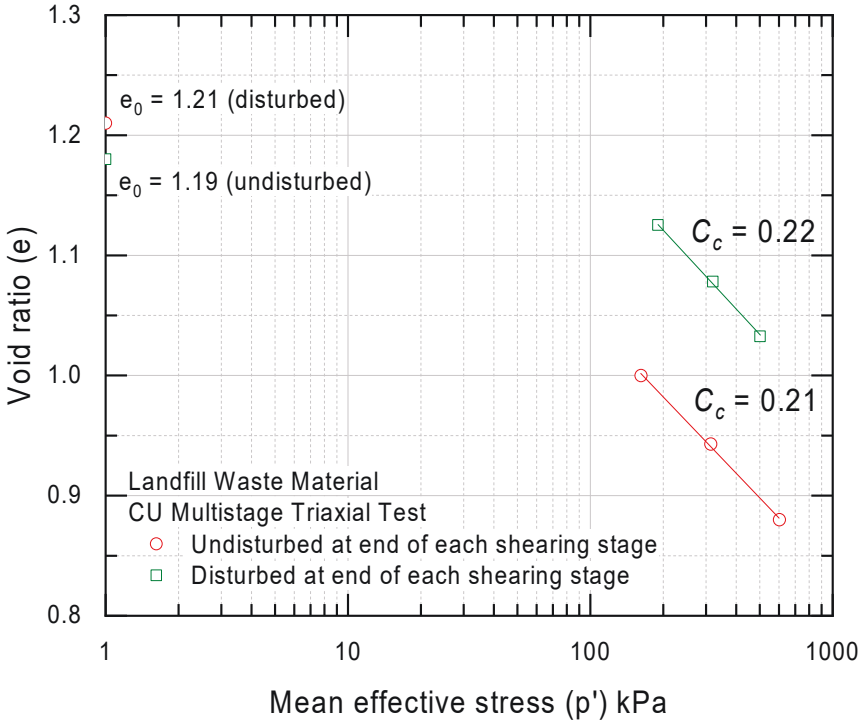

Figure 5.5 Void ratio vs mean effective stress

Table 5.3 Compression index for landfill

Landfill Type	Primary Waste Constituents	Age of solid waste	C_c	Reference
M/I	Uncontrolled	Fresh waste	0.09-0.28	Bareither et al. (2013b)
M	Organics, paper and plastic	1-11 years	0.07-0.30	Chen et al. (2009)
M	Organics, plastic, textile	Three years	0.22-0.27	He et al. (2021)
M	Paper, wood, fines and plastic	Two – five year old landfill	0.17-0.24	Landva et al. (2000)
M	Wood, stone and plastic	15 years old landfill	0.21	Machado et al. (2002)
S	Cardboard, wood and plastic	1.5 years old waste	0.19-0.24	Reddy et al. (2009a)
M/I	Uncontrolled	200 days – 2000 days	0.1-0.41	Sowers (1973)
M	Organics and plastics	1 year old waste	0.26	Stoltz & Gourc (2007)
M/I	Organics, paper and plastic	Fresh waste	0.27-0.37	Stoltz et al. (2010b)
M	Organics and plastics	15 years old waste	0.22-0.32	Vilar & Carvalho (2004)
M	Paper, organics and plastic	Four year old samples in test cells	0.21-0.25	Wall & Zeiss (1995)

Variations of the volumetric strains with time during the isotropic consolidation stages of the tests are presented in Figure 5.6. The coefficient of consolidation (C_v) was calculated for each consolidation stage using the least square method proposed by Chan (2003). The Cv range was found to be 70-190 m^2/year and 90-120 m^2/year for undisturbed and disturbed samples respectively. Using C_v and the coefficient of volume compressibility (M_v), the permeability (k) of the sample was found to have permeability in the range of 1.9×10^{-9} to 7.1×10^{-9} m/sec, which is on the lower bound of that presented in Table 5.4.

Taylor (1948) proposed Equation (3), to capture the variations of hydraulic conductivity of fine-grain soils with void ratio.

$$\log k = \log k_0 - \frac{e_0 - e}{c_k} \qquad \textit{Eq. 5.1}$$

where c_k is the permeability change index, k_0 is the initial coefficient of permeability corresponding to the initial void ratio e_0. Figure 5.7 plots variations of determined coefficient of permeability with void ratio measured during the sample consolidation. As evident, the sample permeability is rather low despite presence of significant gravels and sands size

particles. This is due to the fact that the presence of impermeable components such as plastics as well as low permeability fines appear to impede water seepage through the composite waste contributing to rather low overall hydraulic conductivity of the sample. Xie et al. (2006) indicated that the low permeability of waste was associated with the increasing content and size of plastics as well as the swelling of organic material obstructing the flow of liquid through the sample. The difference between the permeability index between the disturbed and undisturbed samples appears to be negligible.

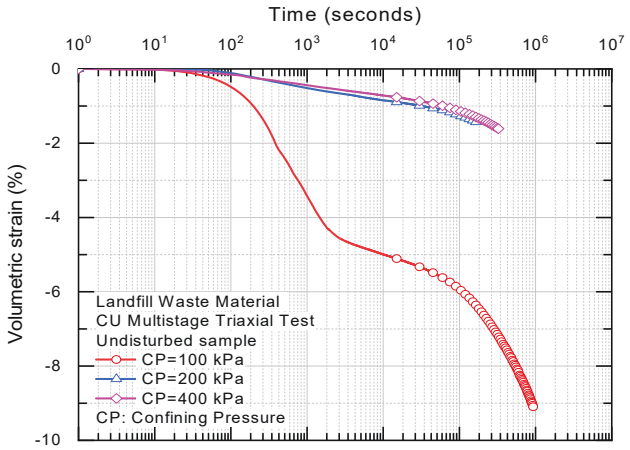

(a)

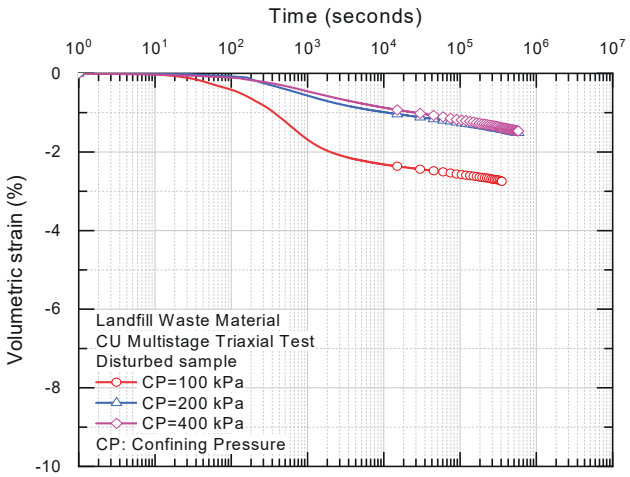

(b)

Figure 5.6 Triaxial consolidation curves, (a) undisturbed consolidation curves and (b) Reconstituted consolidation curves at 100 kPa, 200 kPa and 400 kPa

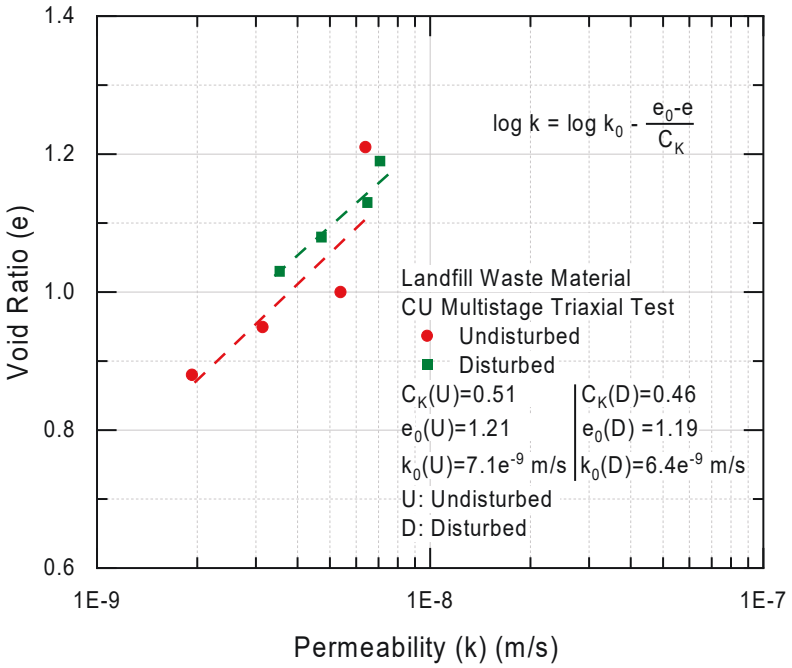

Figure 5.7 Variation of landfill permeability with void ratio

Table 5.4 Hydraulic conductivity for landfill material

Landfill type*	Primary Waste constituents	Waste age / description	Permeability (m/s)	Reference
M	Paper and plastic	Fresh	$2.3\times10^{-7} – 9.5\times10^{-4}$	Chen & Chynoweth (1995)
M	Cloth, paper, glass, metal	10 years	$4.7\times10^{-6} – 1.24\times10^{-4}$	Durmusoglu et al. (2006)
M	Glass, metal, plastic, wood	4-10 weeks	$3.3\times10^{-11} – 1.8\times10^{-7}$	Xie et al. (2006)
S	Paper, plastic, food waste	Fresh	$8.0\times10^{-6} – 1.0\times10^{-4}$	Penmethsa (2007)
M	Wood and cardboard	Fresh-1.5years	$1.0\times10^{-8} – 2.0\times10^{-4}$	Reddy et al. (2009b)
M	Paper, plastic, food waste	Fresh-1year	$1.0\times10^{-5} – 9.0\times10^{-3}$	Hossain et al. (2009)
M	Putrescible, paper, plastic	Fresh	$7.5\times10^{-5} – 0.5\times10^{-5}$	Staub et al. (2009)
I	Mine waste	Fresh	$3.0\times10^{-9} – 6.0\times10^{-6}$	Wickland et al. (2010)
M	Food, paper, plastic	Fresh	$1.1\times10^{-5} – 1\times10^{-4}$	Stoltz et al. (2010a)
M	Plastic, paper, glass	30 years	$1.0\times10^{-9} – 6.0\times10^{-5}$	Yang et al. (2016)
S	Household waste	0-18 months	$3.0\times10^{-8} – 2.0\times10^{-5}$	Ke et al. (2017)
S	Plastic, metal, food	Fresh	$2.5\times10^{-5} – 1.2\times10^{-4}$	Al-Isawi et al. (2021)
S	Household waste	Fresh	$2.0\times10^{-6} – 2.0\times10^{-4}$	Wang et al. (2021)
M	Gravel, sand, wood, plastic	18-31 years	$4.9\times10^{-9} – 1.2\times10^{-8}$	This study

*Primary landfill type: M=municipal solid waste, I=industrial, S=synthetic waste created in a laboratory

5.3.4 Creep characteristics of landfill waste material

The viscoplastic creep parameter of landfill waste was determined using two methods including constant stress creep and stress relaxation tests. Whilst these two methods provide creep coefficient of the sample, due to the sequence of testing, the constant stress creep test provided creep characteristics at over-consolidated state at low applied stress levels, whilst stress relaxation test provided creep characteristics at normally consolidated state of the

waste at higher stress levels. The constant stress creep stage included the monitoring of sample volume change via back volume change with time during isotropic consolidation stages at confining pressures of 100 kPa and 400 kPa with duration of approximately 30 days each (see Figure 5.8).

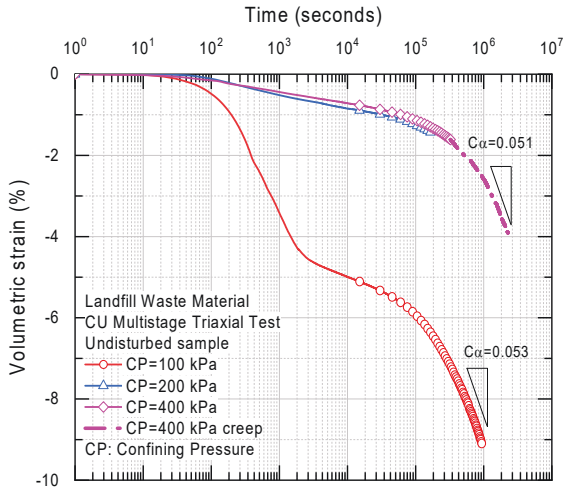

(a)

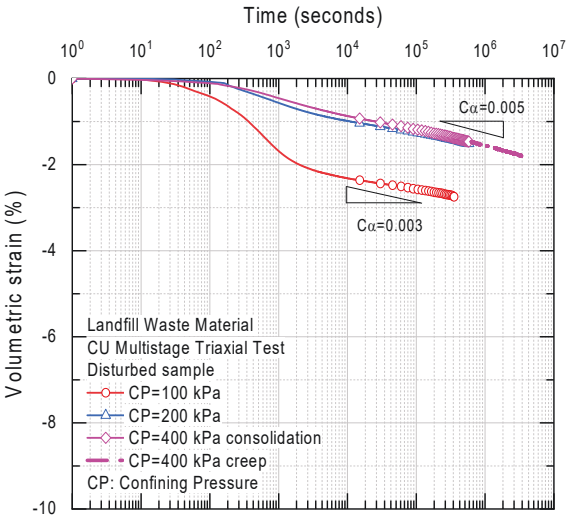

(b)

Figure 5.8 Triaxial consolidation creep and stress relaxation curves a) Undisturbed consolidation creep curves at 100 kPa, 200 kPa and 400 kPa b) Disturbed consolidation creep curves at 100 kPa, 200 kPa and 400 kPa

Moreover, the use of stress relaxation to determine the creep rate is an alternative method to determine the creep parameter of the landfill waste material. Following completion of the final shearing stage, the sample axial straining was prevented while variation of the axial stress measured via the load cell was recorded as presented in Figure 5.9a. The load reduction over time is plotted in the form of variations of the normalised deviatoric stress with time (Figure 5.9b). Whilst the entire curve after commencement of stress relaxation is theoretically capturing creep effects, Bagheri et al. (2019) explained that stress relaxation is split into three components, fast relaxation, decelerating relaxation and residual relaxation. The residual relaxation corresponds to the linear portion of stress relaxation curve, which is considered as most suitable to accurately calculate the stress relaxation parameter required to obtain the creep index. Referring to (Yin et al., 2014), the following equations were used to interpret the stress relaxation test results:

$$R_\alpha = \frac{\Delta \ln (q)}{\Delta \ln (t)} \qquad \textit{Eq. 5.2}$$

$$C_\alpha = R_\alpha C_c \qquad \textit{Eq. 5.3}$$

where R_α is the stress relaxation parameter (refer to Figure 5.9), q denotes the deviatoric stress, t is the time since start of relaxation, C_α is the secondary creep coefficient and C_c is the slope of the normal compression line. It should be noted that $C_\alpha = \Delta e / \log (t_2/t_1)$.

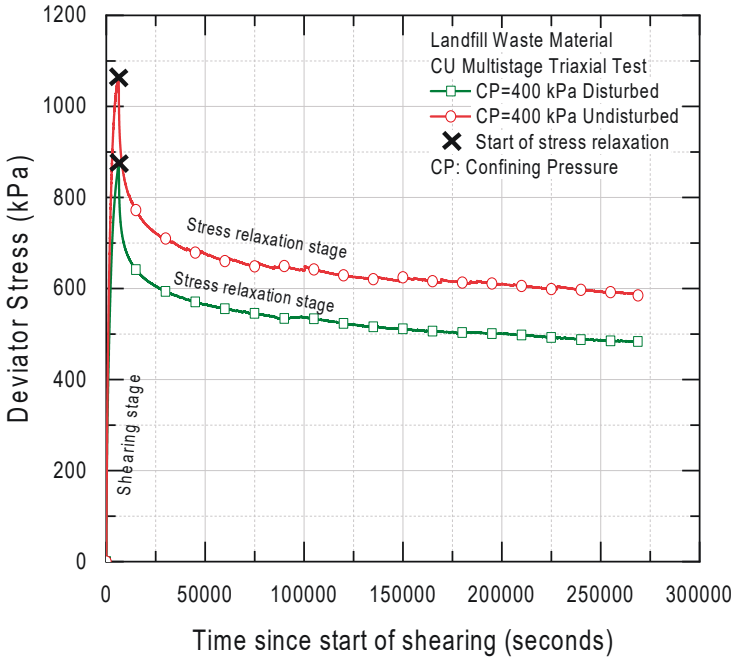

(a)

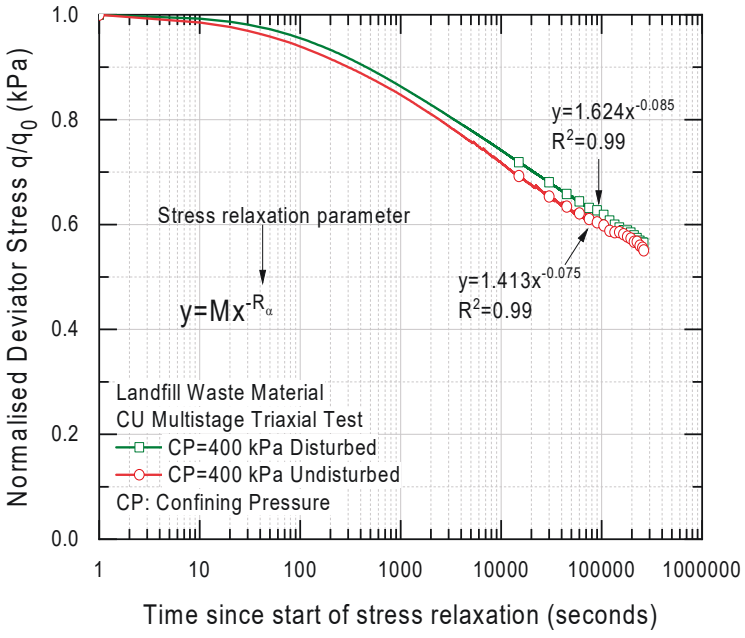

(b)

Figure 5.9 Stress relaxation results (a) Stress relaxation with time (b) Normalised deviator stress over time

The consolidated creep from the undisturbed and disturbed samples showed different behaviour. During the first consolidation stage prior to shearing, the undisturbed sample had

significantly higher creep of 0.011 compared to the disturbed sample, which had 0.003. The postulated reason for this increased creep is due to the presence of voids and non-uniform compaction of the undisturbed sample. The disturbed sample when prepared was evenly compacted in three layers and can be considered as more uniform than the undisturbed sample. For the 200 kPa and 400 kPa stages, the creep between the undisturbed and disturbed sample were similar in the range of 0.003-0.005. By this stage of the test, the samples had undergone the first shearing stage to the yield point and the effects of disturbance were no longer applicable to the sample. The results of the consolidation creep are on the lower bound of literature presented in Table 6, most comparable with Oweis & Khera (1998) where the landfill is old with a high soil content.

The creep from stress relaxation was found to be 0.015 and 0.019 from undisturbed and reconstituted samples, respectively. These creep values are undertaken at the end of shearing and are under high deviatoric stresses. Whilst the entire curve after commencement of stress relaxation is theoretically capturing creep effects, Bagheri et al. (2019) explained that stress relaxation is split into three components, fast relaxation, decelerating relaxation and residual relaxation. The residual relaxation corresponds to the linear portion of stress relaxation curve, which is considered as most suitable to accurately calculate the stress relaxation parameter required to obtain the creep index. These values of stress relaxation have been taken at very high deviator stresses (870 kPa) and are assumed to be normally consolidated. The values are not directly comparable between the undisturbed and disturbed samples since the initial stress is different for each test. Whilst the undisturbed test has a lower creep than the disturbed test, it experienced an additional 200 kPa of deviator stress prior to relaxation.

Table 5.5 Secondary creep coefficient for landfill material

Landfill type*	Primary Waste constituents+	Waste age / description	C_α X	Reference
M/I	Uncontrolled	Unlikely to decay – likely to decay	$0.03e_0$ - $0.09e_0$#	Sowers (1973)
M/I	Residential / construction	Old landfill 3-12 m deep	0.008 - 0.022	Burlingame (1985)
M	Uncontrolled	Fresh and old waste, 10-30 m deep	0.012 - 0.075	Edil et al. (1990)
M	Paper, organics and plastic	Four year old samples in test cells	0.033 - 0.056	Wall & Zeiss (1995)
M	High soil content	Old landfills	0.002 - 0.005	Oweis & Khera (1998)
M	Paper, wood, fines and plastic	Two – five year old landfill	0.01 - 0.016	Landva et al. (2000)
M	Wood, stone and plastic	15 years old landfill	0.021 - 0.044	Machado et al. (2002)
M	Organics, plastics and paper	Field monitoring of 15 year old landfill	0.015 - 0.03	Marques et al. (2003)
M	Organics, plastic, paper and stone	Fresh and four year old landfill	0.058	Machado et al. (2008)
M	Soil, gravel and paper	Fresh landfill	0.008 – 0.065	Bareither et al. (2013a)
M	Organics, soil and paper	Fresh landfill	0.034 – 0.049	Shi et al. (2016)
M	Organics, plastic, textile	Three years	0.035	He et al. (2021)
M	Gravel, sand, wood, plastic	18-31 years – undisturbed consolidation creep	0.051-0.053	This study
M	Gravel, sand, wood, plastic	18-31 years – undisturbed stress relaxation	0.015	This study
M	Gravel, sand, wood, plastic	18-31 years – disturbed consolidation creep	0.003-0.005	This study
M	Gravel, sand, wood, plastic	18-31 years – disturbed stress relaxation	0.019	This study

*Primary landfill type: M=municipal solid waste, I=industrial, S=synthetic waste created in a laboratory

+Organics typically refers to garden and food waste

X $C_\alpha = \frac{\Delta e}{\Delta(Log t)}$

e_0 is the initial void ratio of the landfill material

5.4 Summary and conclusions

The authors have undertaken a comparison of landfill strength and compressibility between material collected from the landfill in undisturbed and reconstituted states using CU multistage triaxial tests. The landfill material comprised of primarily gravels, sand, timber and bricks. Parameters determined from both tests included cohesion, friction angle,

coefficient of consolidation, coefficient of compression, small strain shear modulus, small strain Young's modulus, large strain Young's modulus, Poisson's ratio and creep.

Friction angle was found to be 42° and 35° with cohesion of 10 kPa and 47 kPa for reconstituted and undisturbed landfill materials, respectively. The higher cohesion is postulated to be due to the structured nature of undisturbed waste over decades. The difference in strength parameters has a significant impact on the shear strength of the sample particularly at higher effective stresses. During shearing stages, the undisturbed sample was stiffer with Young's modulus in the range of 7-11 MPa, whilst for the reconstituted sample Young's modulus was in the range 4-6 MPa. Similarly, from bender element testing the small strain Young's modulus of the undisturbed sample was higher than the reconstituted sample. The compression index determined from the end of each shearing stage was found to be similar between both tests with a value of 0.21-0.22.

The coefficient of consolidation was found to be in the range of 70-190 m^2/year and 90-120 m^2/year for undisturbed and reconstituted samples respectively. The undisturbed sample underwent large volume change during the 100 kPa consolidation stage. During subsequent consolidation stages at 200 kPa and 400 kPa, the volume change of both undisturbed and reconstituted samples was similar. The permeability of both samples was similar with initial permeability of 7.1×10^{-9} to 1.9×10^{-9} m/sec. The low permeability of both samples is attributed to the presence of impermeable materials throughout the sample including plastics, tiles, bricks and glass as well as low permeability fines.

Landfill creep was determined using two methods, consolidation creep and stress relaxation creep. Consolidation creep under 100 kPa effective stress was 0.011 and 0.003 for undisturbed and reconstituted samples respectively. The stress relaxation creep under higher deviatoric stress greater than 870 kPa was found to be 0.015 and 0.019 for undisturbed and reconstituted samples, respectively. Since the initial stress between the undisturbed and reconstituted sample, the stress relaxation creep is not comparable.

Overall, the use of undisturbed testing has benefits over testing on reconstituted landfill material. This includes obtaining higher creep, which captures voids and non-uniform compaction, variation in strength parameters and the more ductile behaviour for undisturbed

landfill compared to the stiffer disturbed material. There is however, limitations with the practicality of obtaining push tube samples in landfill due to refusal and consistency of the landfill material to stay in the tube. Where possible the authors recommend this testing to be undertaken, however where reconstituted samples are tested, the limitations need to be considered particularly the lower observed creep

Chapter 6 – Small Strain to Large Strain Properties for Waste

This chapter presents findings from unconfined compressive strength (UCS) testing with Hall Effect sensors and bender elements on relatively undisturbed material from various landfill depths. The combination of both large strain UCS testing and small strain Hall Effect sensors and bender elements allows for determination of the ratio between small strain parameters typically obtained from field geophysics to the large strain parameter (Young's modulus) that is required for landfill settlement prediction.

6.1 Introduction

To maximise space utilisation in urban areas, construction above closed landfills is becoming increasingly popular. This is evident in Sydney with projects such as Westconnex M8 – St Peters Interchange built on Alexandria landfill, Moorebank Intermodal on Glenfield landfill and Sydney Gateway built on Tempe landfill. However, constructing infrastructure above closed landfills is a complicated process because landfill waste is heterogeneous and their properties vary with time. In order to be able to design infrastructure to meet the long term design requirements, landfill settlement prediction is required; however a large number of variables are involved in this process, including the type of waste, the organic content, the moisture content, compaction density, compressibility parameters, temperature and age of waste. Hence, the accurate prediction of landfill settlement is a very challenging task and is especially critical for those with infrastructure built above closed landfills. Landfill settlement prediction has been undertaken by numerous authors over decades experimentally, numerically and theoretically (Bjarngard & Edgers, 1990; Edil et al., 1990; Kavazanjian et al., 1995; Wall & Zeiss, 1995; El-Fadel & Khoury, 2000; Hossain et al., 2003; Hossain & Gabr, 2005; Oweis, 2006; Zekkos et al., 2010; Tahmoorian & Khabbaz, 2020).

The use of field geophysics particularly multichannel analysis of surface wave (MASW), is a common method to obtain large scale parameters with depth in a non-intrusive manner for closed landfill waste sites (Zekkos et al., 2011; Carpenter et al., 2013; Abreu et al., 2016). The key outcome of an MASW investigation is the shear wave velocity profile with depth that can be used to develop small strain properties such as shear modulus and Young's modulus. However, for the purposes of settlement calculations in geotechnical

design and use in numerical programs such as PLAXIS 2D, the parameters required for input is large strain Young's modulus. There are two ways to obtain the large strain properties, the first incudes multiple unconfined compression tests (UCS) which would require a substantial field sample collection procedure or through conversion of the non-intrusive small strain data into large strain data. Given the variability of landfill waste, the testing procedure would require a significant number of samples to establish a 2D profile with depth, therefore the latter option of MASW provides a low cost method for obtaining large scale properties with depth. Correlations between small strain and large strain properties have been studied by numerous authors for conventional soils (Wichtmann et al., 2017; Tsai et al., 2019; Lashin et al., 2020). However, for landfill material such correlations between small strain and large strain properties have not been developed.

UCS tests as a standalone test has been undertaken on landfill material (Fatahi, 2013) in order to obtain large strain Young's modulus and UCS values. However, when the UCS test is combined with bender elements and Hall Effect sensors it can provide both small strain and large strain behaviour. Bender elements consist of a source and receiver on the top and bottom of the sample, the time taken to travel through the sample is the shear wave velocity. The shear wave velocity can then be converted into very small strain properties. Typically, Hall Effect sensors are mounted on membrane around the sample and are under confinement within the triaxial cell (Clayton & Khatrush, 1986; Jastrzębska & Kowalska, 2016; Witowski, 2019). The confinement allows for the membrane to mould around the sample and move with the sample when undergoing shearing. The use of Hall Effect sensors in an unconfined test with membrane on landfill waste material has not been documented in literature.

The shear modulus reduction curve for landfill waste has been developed through use of cyclic triaxial testing (Idriss et al., 1995; Matasovic & Kavazanjian, 1998; Zekkos & Riemer, 2006). However, the research was focussed on small strain data for seismic loading and reduction curves observed based on particle size. The particle size is difficult to assess in large scale site investigation. The range of typical strains for retaining walls, foundations, and tunnels ranges between 0.01% to 1% shear strain as shown in Figure 6.1.

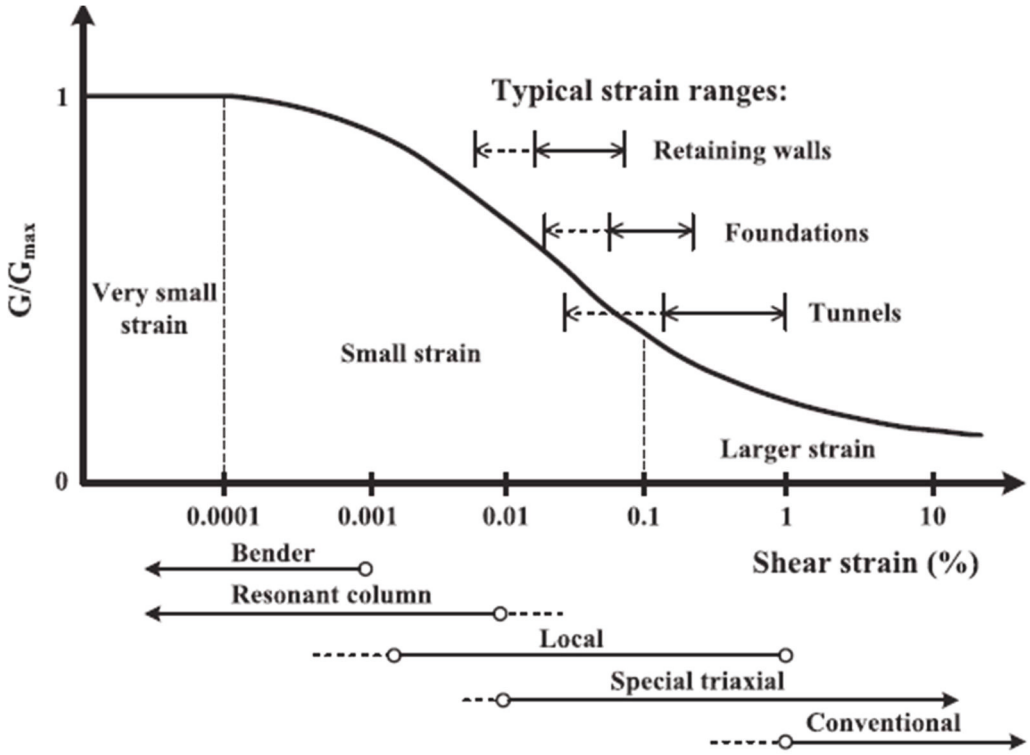

Figure 6.1 Typical shear strain ranges for structures (adapted from Atkinson & Sallfors (1991) and Mair (1993)

This chapter provides details of UCS tests combined with Hall Effect sensors and bender elements on relatively undisturbed material with varying depth extracted from the landfill. The very small, small and large strain shear modulus and Young's properties of waste material are identified and correlations with organic content, liquid limit have been presented.

6.2 Sample collection and experimental plan

6.2.1 Waste sample collection from the landfill

A total of 95m of landfill waste cores with 100 mm diameter and 1m lengths were collected from three boreholes at the landfill using the sonic drilling technique. The cores were collected from the surface of the landfill to the base, which spans over a length of 32m. The sonic drilling technique utilises high frequency vibration whilst pushing through the landfill with an outer steel casing. This is followed with a 3m long coring barrel with an internal diameter smaller than the outer casing. Once it collects 3m worth of core, with minimal use of water to flush material between the coring barrel and the outer casing, it brings the sample

to the surface where it then released from the tube in 1m lengths and placed into plastic sleeves and then into core boxes. The core boxes were then sealed and transported to the laboratory.

6.2.2 Sample preparation

The cores were inspected and intact sections of core that had the height to diameter ratio of approximately two were selected for this testing programme. Out of the 95 m worth of core only six samples were found to be intact with the required dimensions and were assumed to be in a relatively undisturbed state. The remaining cores were very loose and fell apart whilst being extracted from the core box or had insufficient height to diameter ratio.

Landfill core boxes from Borehole 1 (BH1) and Borehole 2 (BH2) containing 2m of core for the test samples are presented in Figure 6.2 to Figure 6.3. The collected intact cores were trimmed to have flat top and bottom and were ready for testing.

Figure 6.2 BH1 2-4 metres below ground core box

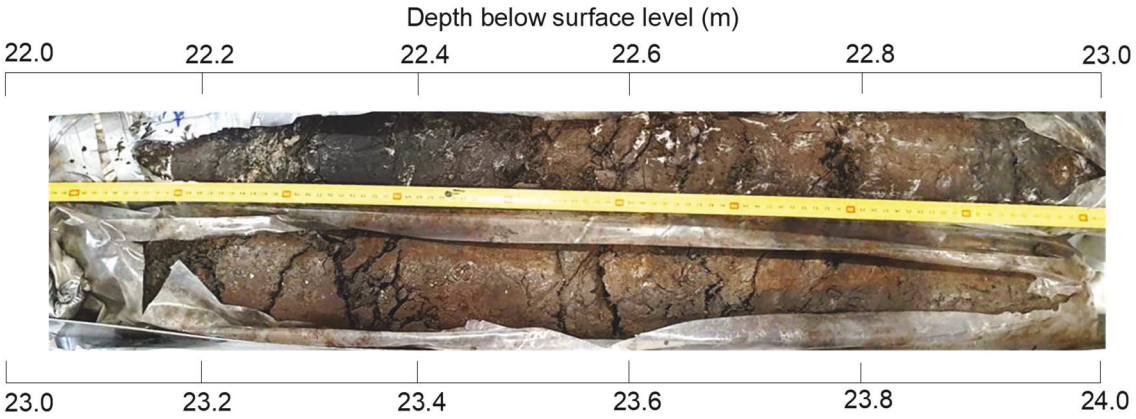

Figure 6.3 BH1 22-24 metres below ground core box

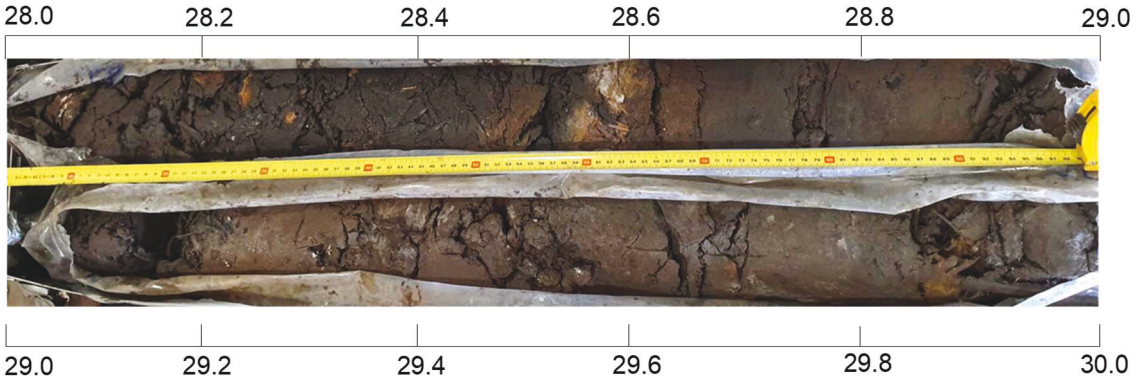

Figure 6.4 BH1 28-30 metres below ground core box

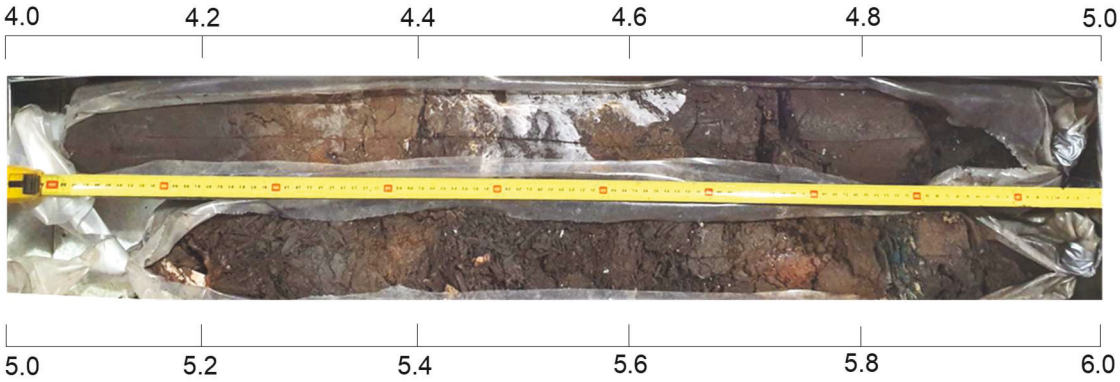

Figure 6.5 BH2 4-6 metres below ground core box

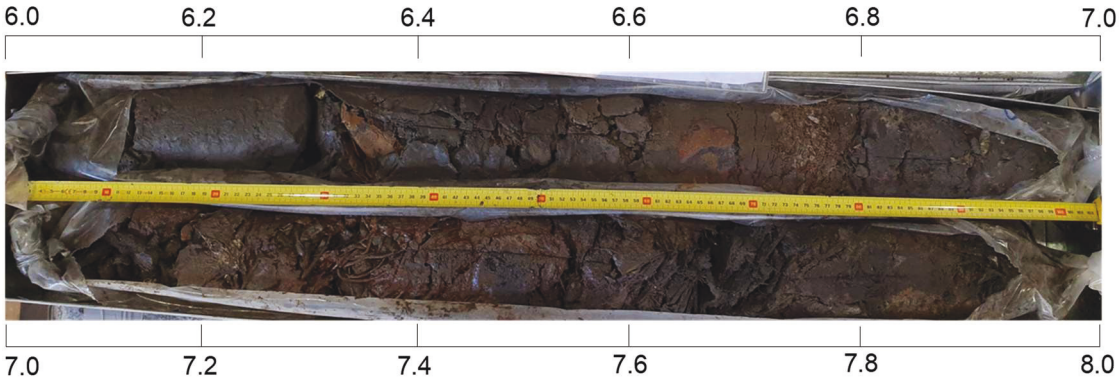

Figure 6.6 BH2 6-8 metres below ground core box

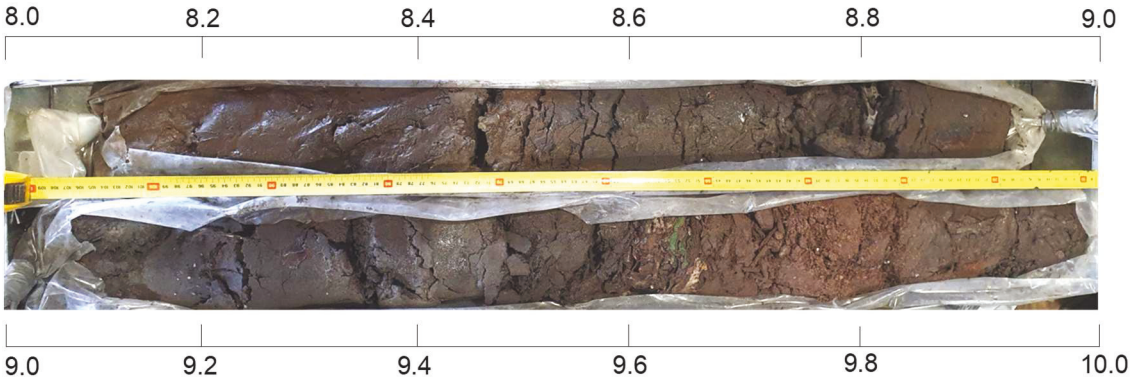

Figure 6.7 BH2 8-10 metres below ground core box

6.2.3 Test equipment and procedure

The tests conducted were unconfined compression tests (UCS) with local Hall Effect strain gauges and bender elements on landfill material. The UCS test is a simple and fast test to be able to obtain the unconfined compressive strength and Young's modulus, but when combined with local Hall Effect gauges and bender elements it can also provide small strain properties.

The test setup comprised of a 15 kN load frame with a 10 kN load cell, an external linear variable displacement transducer (LVDT), bender elements fitted into the base and top cap, Hall Effect strain gauges, a data logger and computer for the Hall Effect and bender elements and a separate data logger and computer for the UCS load cell, as shown in Figure 6.8. Typically, the Hall Effect local strain gauges are fitted on top of the membrane covering the sample and is undertaken within the triaxial cell, whereby confining pressure in the cell pushes the membrane tightly against the sample. However, in the UCS setup, since there is

no confinement, it is unclear when loading whether the membrane is moving with the sample. To address this issue, membrane patches were attached with glue to the sample at locations where the Hall Effect gauges needed to be attached as shown in Figure 6.9. The alternative option of pinning the Hall Effect gauges into the sample was attempted; however, due to the high sample stiffness and presence of gravels this was not feasible.

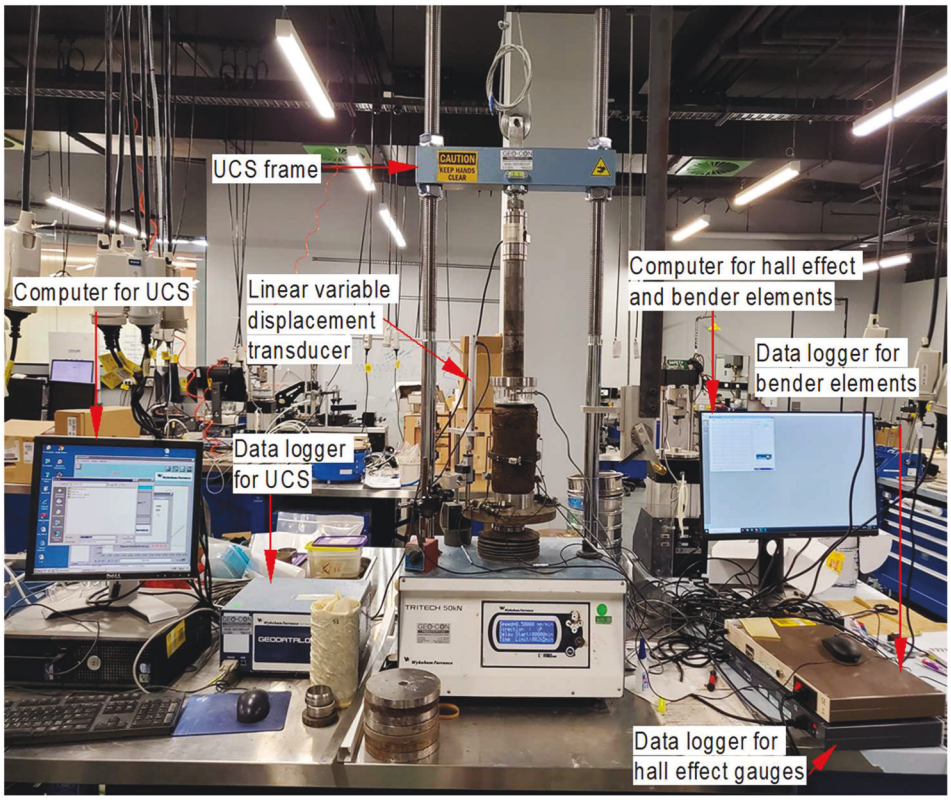

Figure 6.8 Test setup for Hall Effect and data logging

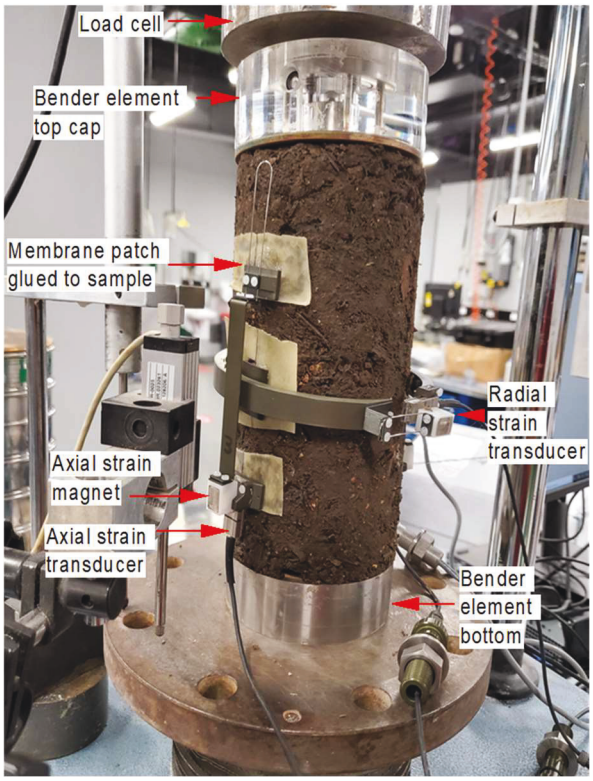

Figure 6.9 Close-up of membrane and Hall Effect sensors

Hall Effect gauges were fitted on samples as per the manufactures installation instructions, with the radial Hall Effect sensor placed at the middle of sample height and axial gauges located at one third and two thirds of sample height. After fitting the membrane and Hall Effect gauges onto the sample, the sample was mounted onto the bender elements and onto the UCS frame. Prior to shearing, bender elements were used to collected a shear wave velocity and p-wave velocity. A constant shearing rate of 0.5 mm per minute was selected for all samples to ensure the Hall Effect gauges would capture sufficient data points within the small strain range. During shearing, bender elements collected single shot shear wave data, Hall Effect readings for two axials and radial, total axial strain from the UCS frame and corresponding load were recorded every 1 second. After the sample reached the peak or 10% strain, whichever came first, the sample was unloaded at the a rate of 0.5 mm rate and reloaded.

After completion of each test, a moisture content test and organic content tests using representative weights of each material type was undertaken as per ASTM D2974-14 and particle size distribution (PSD) was determined as per AS 1289.3.6.2 with standard sieve

sizes. Moreover, specific gravity was calculated using the average of three representative samples each weighing 120 g in the pycnometer as per AS 1289.3.5.2. The falling cone method was used to obtain the liquid limit of the sample as per AS 1289.3.9.1. Plastic limit was obtained as per the procedure outlined in AS 1289.3.2.1. Whilst the Atterberg limits are useful, these tests were undertaken on material passing the 0.425 mm sieve as per relevant testing standards and are not very representative of overall behaviour since the collected landfill sample had 80% by weight larger than this sieve size. A summary of the material properties of the collected waste sample is presented in Table 6.1.

Table 6.1 Physical properties of collected landfill waste material

Sample ID	Sample height	Average Diameter	Moisture content	Organic content	Total Density	Dry Density	Specific gravity	LL	PI
	mm	mm	%	%	t/m^3	t/m^3	-	%	%
BH1 3.5	215	104	17.2	21.3	17.0	14.5	2.314	29	N.P
BH2 4.3	225	106	18.0	23.6	15.3	13.0	2.070	28	N.P
BH2 6.1	187	105	12.5	5.6	21.5	19.1	2.2652	24	12
BH2 8.4	210	109	14.2	9.1	18.4	16.1	2.554	20	8
BH1 24	187	105	11.9	13.4	19.7	17.6	2.314	26	N.P
BH1 29.7	194	110	37.9	44.6	10.0	7.3	1.9589	34	N.P

*N.P. = not plastic

6.3 Results and discussion

6.3.1 Basic landfill material properties

The particle size distribution reported in Figure 6.10 shows as expected, that each landfill sample has varying particle sizes. Sample BH2 8.4m had a fines content of 9% (i.e. 9% finer than 75 μm), which is the highest and is on average double the other samples. Samples BH1 3.5m, BH1 29.75m, BH2 4.3m and BH1 24m all had at least one particle size that was larger than 100mm in diameter. Since the sample was relatively undisturbed and extracted from sonic drilling, the composition and particle sizes prior to testing were unknown. The specific gravity was found to range in between 1.95 – 2.55 with an average of 2.19, which is well less than the typical value of 2.55 - 2.75 adopted for soils. The total unit weight and dry unit weight of the samples were on average 17 kN/m^3 and 14.6 kN/m^3, respectively, which is higher than the average unit weight from all the sonic drilled cores which was 13 kN/m^3. The higher unit weight is attributed to the sample composition, nearly all of which had a large portion of gravels. Material composition was assessed visually by separating the sample after PSD testing. Material was classified into material types including

glass, plastic, foam, timber, gravels, paper, fibres (clothing), sand, fines, GCL, metal and brick as shown in Figure 6.11. Organic content of the adopted landfill waste was determined to be on average 20%, which is very well in line with the accumulative weight percentage of paper, fibre and timber components obtained from the classification. The Atterberg limits of the samples were found on average to have a LL = 27 (liquid limit), whilst the plastic limit was only obtained for two samples for the material passing the 425 μm sieve size used for this testing as per AS 1289.3.9.1. The material classification for samples BH2 8.4 m and BH2 6.1 m were clayey SAND (SC) whilst the other samples were all silty SAND (SM).

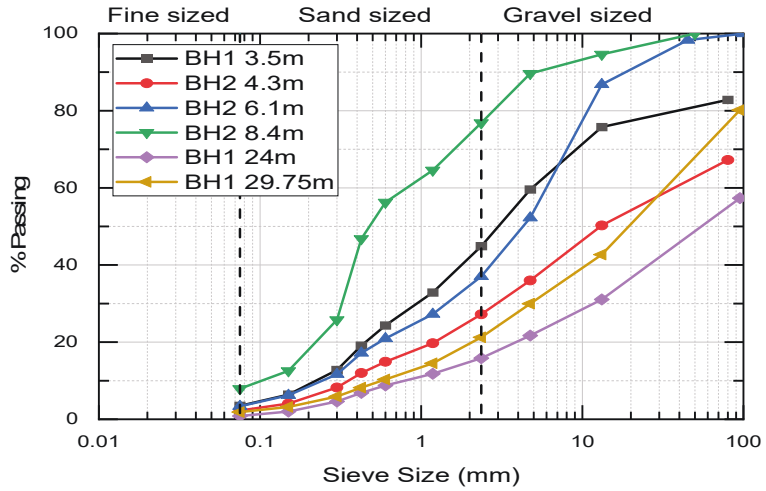

Figure 6.10 Particle size distribution for UCS tests

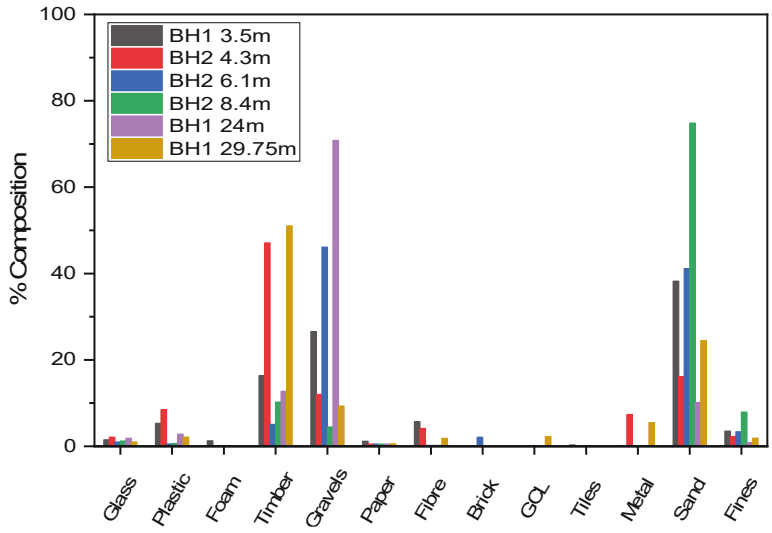

Figure 6.11 Material composition for UCS tests

Figure 6.12 Material composition for (a) BH1 29.75m, (b) BH1 24m, (c) BH2 8.4m, (d) BH2 6m, (e) BH2 4.3m and (f) BH1 3.5m

6.3.2 Characteristics of landfill waste under shear loading

Photographs of the samples before and after testing are presented in Figure 6.13. Stress strain curves for individual tests along with the Hall Effect strain gauge plots are presented in Figure 6.14. The overlayed stress strain plots from each test are presented in Figure 6.15. Samples BH1 24m and BH1 29.75m with the higher depths had the highest UCS values of 1107 kPa

and 783 kPa respectively. The UCS values for other samples ranged between 257 to 375 kPa, with sample BH2 8.4m having the lowest UCS value of 74 kPa.

(a)

(b)

(c)

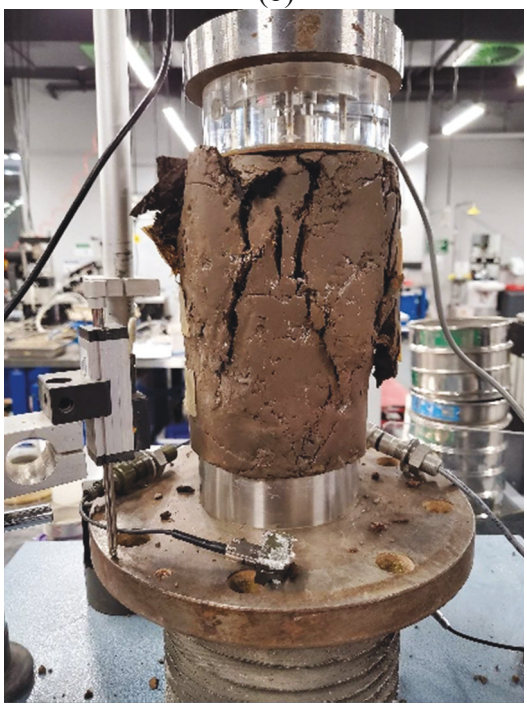

(d)

(e)

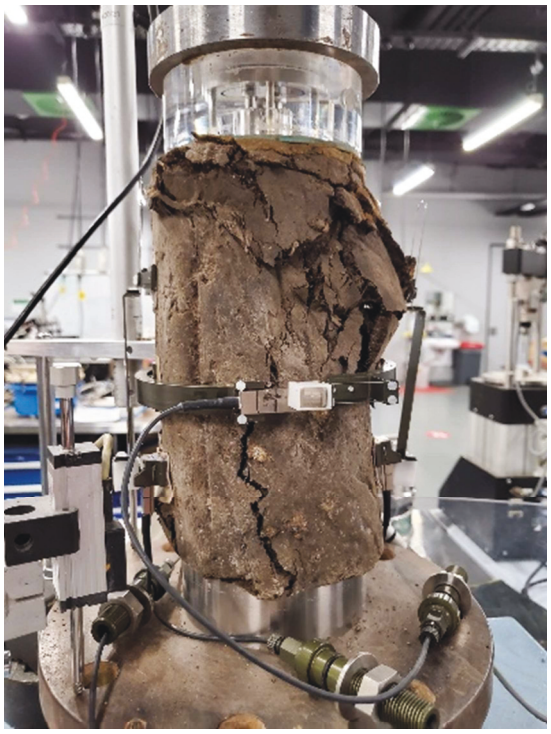

(f)

(g)

(h)

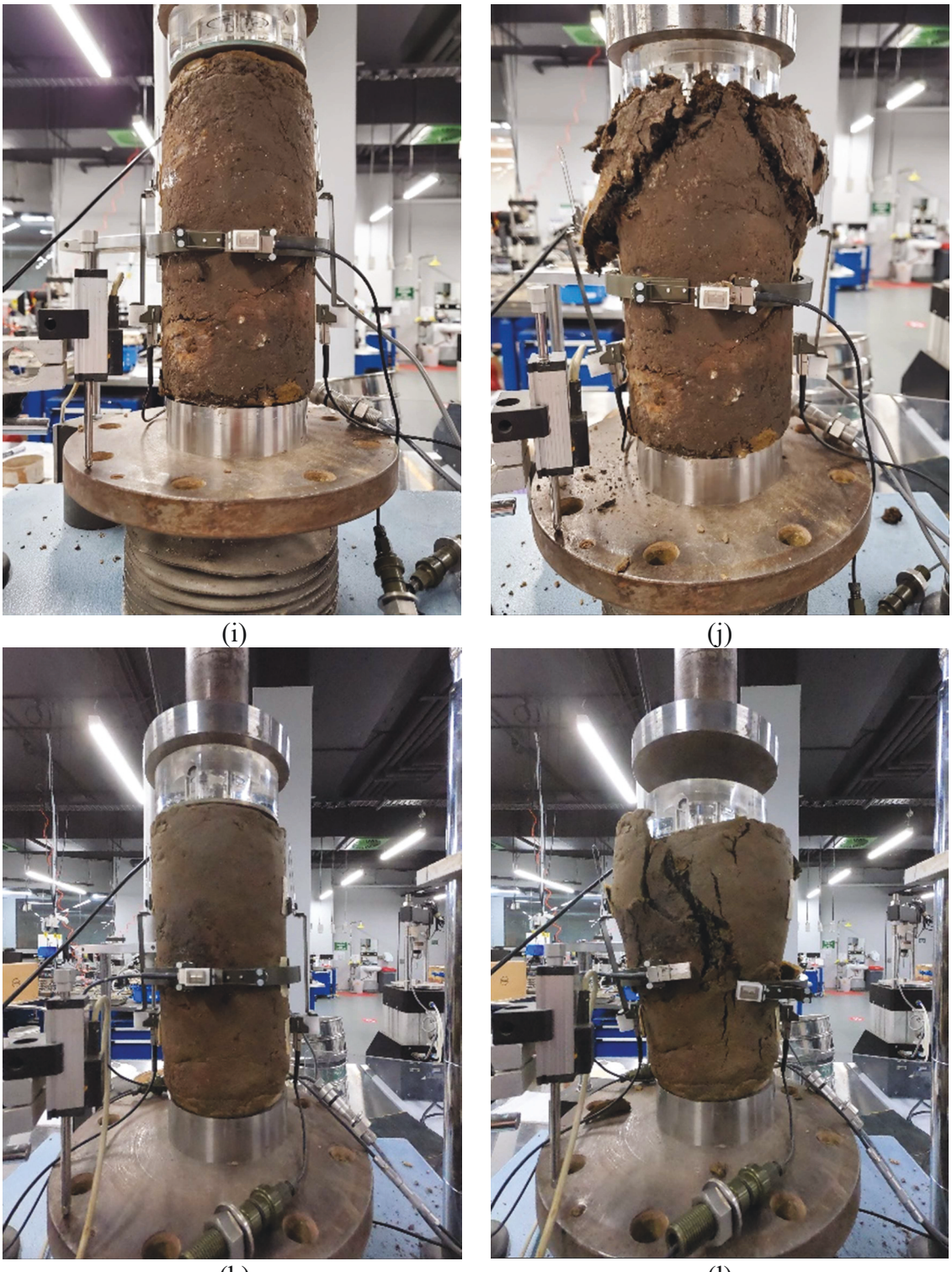

(i) (j)

(k) (l)

Figure 6.13 Photographs of tests (a) BH1 29.75m before test, (b) BH1 29.75m after test, (c) BH 2 6m before test, (d) BH 2 6m after test, (e) BH1 3.5m before test, (f) BH1 3.5m after test, (g) BH1 24m before test, (h) BH1 24m after test, (i) BH2 4.3m before test, (j) BH2 4.3m after test, (k) BH2 8.4m before test and (l) BH2 8.4m after test

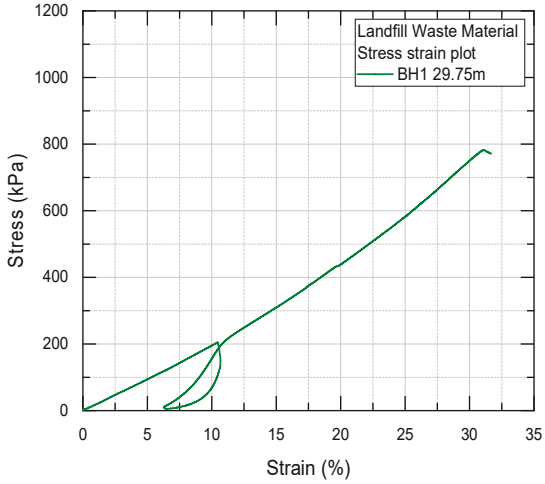
Landfill Waste Material
Stress strain plot
BH1 29.75m
Stress (kPa)
Strain (%)

(a)

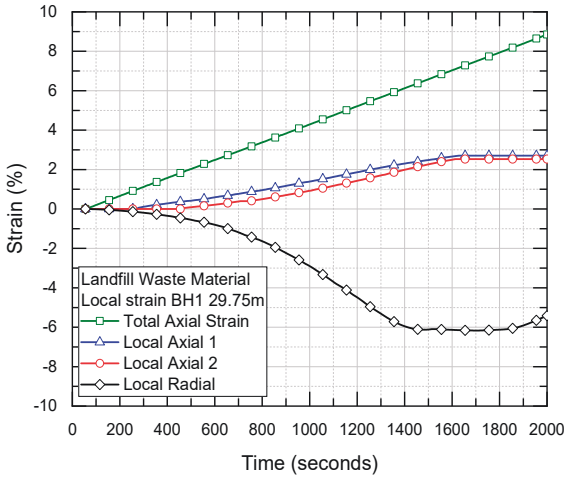
Landfill Waste Material
Local strain BH1 29.75m
Total Axial Strain
Local Axial 1
Local Axial 2
Local Radial
Strain (%)
Time (seconds)

(b)

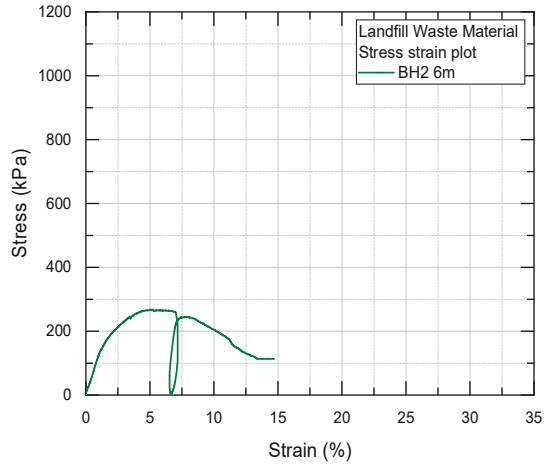
Landfill Waste Material
Stress strain plot
BH2 6m
Stress (kPa)
Strain (%)

(c)

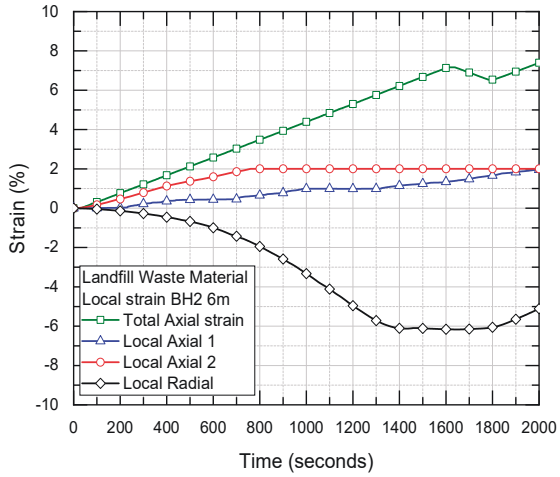
Landfill Waste Material
Local strain BH2 6m
Total Axial strain
Local Axial 1
Local Axial 2
Local Radial
Strain (%)
Time (seconds)

(d)

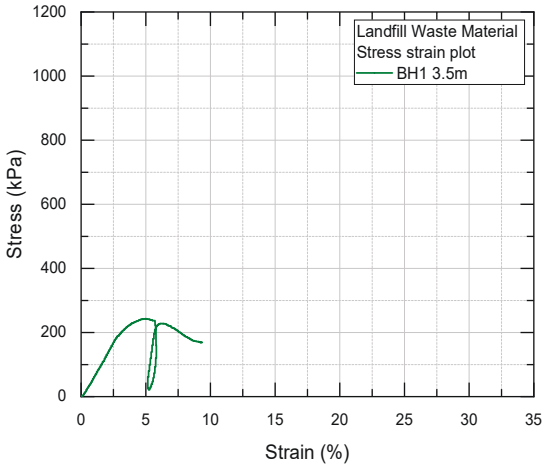
Landfill Waste Material
Stress strain plot
BH1 3.5m
Stress (kPa)
Strain (%)

(e)

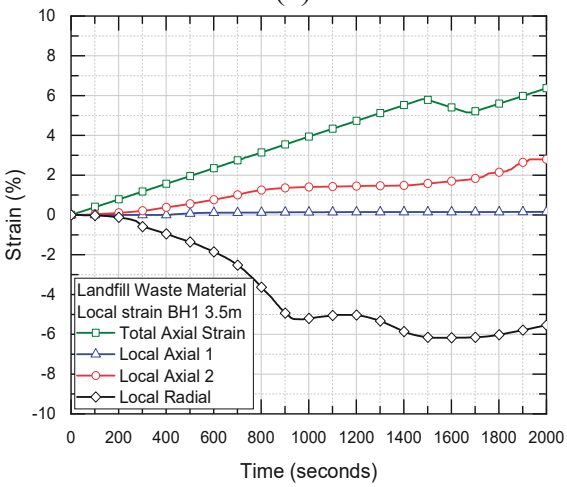
Landfill Waste Material
Local strain BH1 3.5m
Total Axial Strain
Local Axial 1
Local Axial 2
Local Radial
Strain (%)
Time (seconds)

(f)

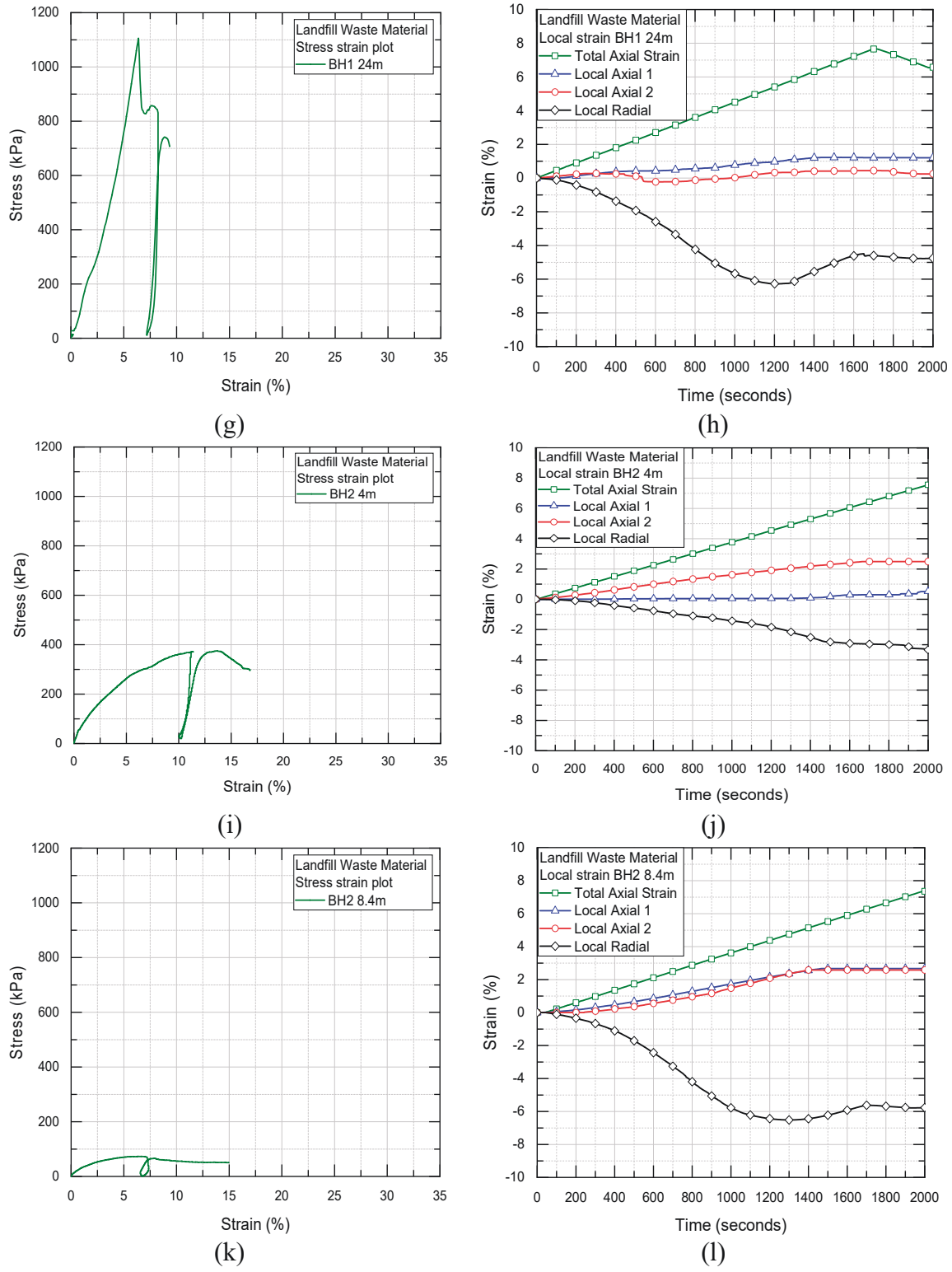

Figure 6.14 (a) Stress strain plot BH1 29.75m, (b) Strain with time BH1 29.75m, (c) Stress strain plot BH 2 6m, (d) Strain with time BH 2 6m after test, (e) Stress strain plot BH1 3.5m, (f) Strain with time BH1 3.5m, (g) Stress strain plot BH1 24m, (h) Strain with time

BH1 24m, (i) Stress strain plot BH2 4.3m, (j) Strain with time BH2 4.3m, (k) Stress strain plot BH2 8.4m and (l) Strain with time BH2 8.4m

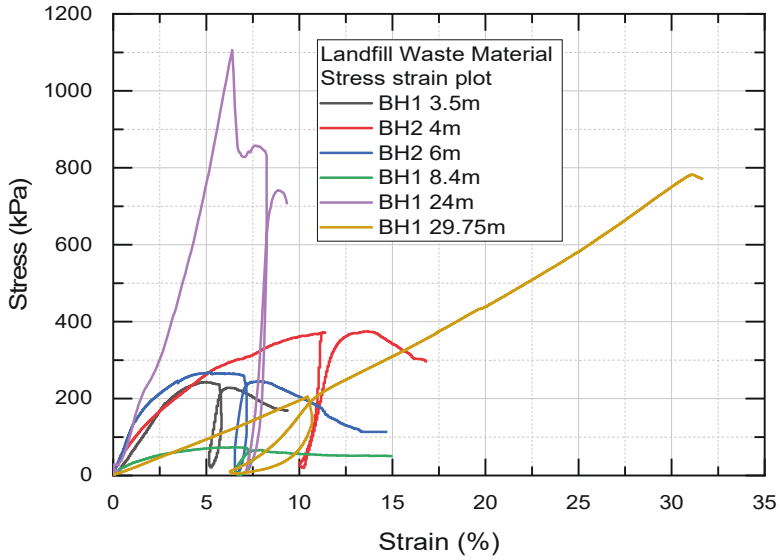

Figure 6.15 Overlayed stress strain plots from all tests

The initial Young's Modulus (E0), secant modulus at 50% of maximum strength (E50) and unloading / reloading modulus (Eur) is presented in Table 6.2. The Young's modulus ranged between 2 MPa to 14 MPa, with an average value of 7 MPa. A relationship of Young's Modulus and depth is not apparent. However, as shown in Figure 6.16, there does appear to be a logarithmic relationship between the void ratio and Young's modulus. This same trend is apparent for both organic content and liquid limit with Young's modulus. The sample BH2 8.4m appears to be an outlier with a very low value compared to other tests. The unloading / reloading modulus was generally lower for materials with higher organic content for example, BH1 29.75m had the highest organic content and rebounded very quickly, this explains why the stress strain plot shows a slow reduction. Figure 6.17 shows the trend and corresponding equation with the outlier.

Table 6.2 Young's moduli for UCS tests

Sample ID	E_0 (MPa)	E_{50} (MPa)	E_{ur} (MPa)	Void ratio
BH1 3.5	7	7	26	0.56
BH2 4.3	10	6	17	0.56
BH2 6.1	13	12	31	0.16
BH2 8.4	3	3	8	0.56
BH1 24	12	14	62	0.11
BH1 29.75	2	2	5	1.64

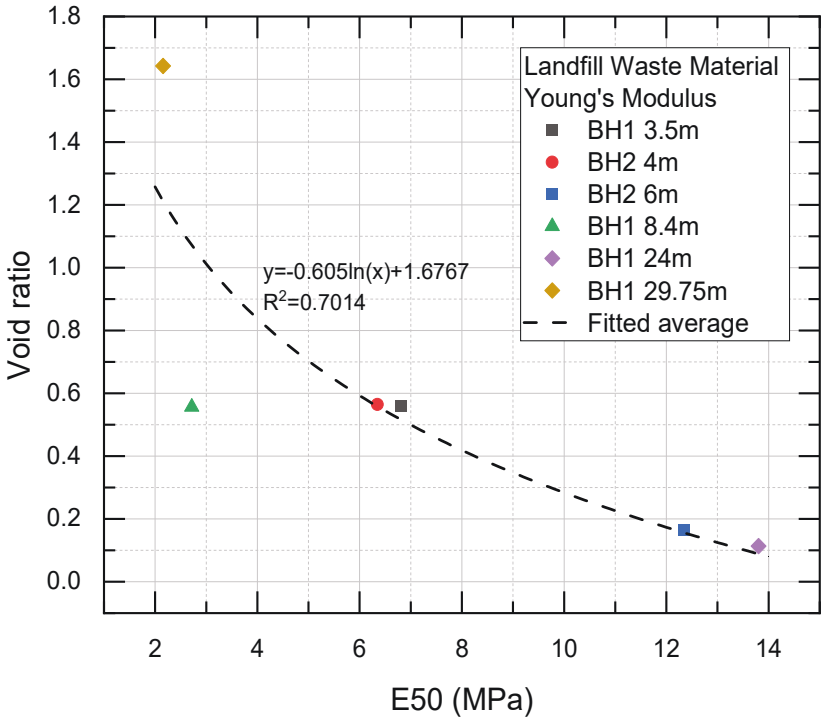

Figure 6.16 Relationship between Young's modulus and void ratio

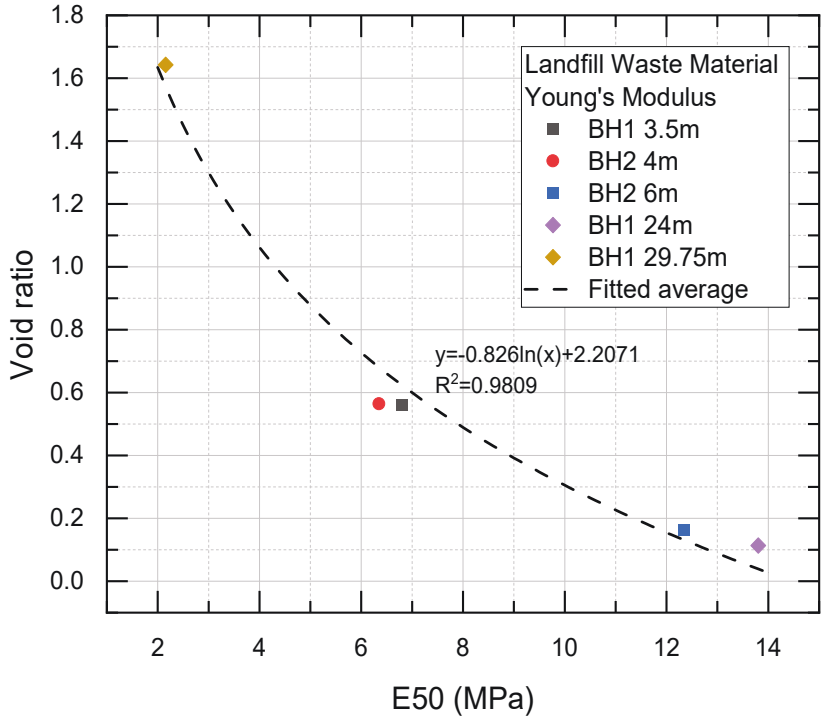

Figure 6.17 Relationship between Young's modulus and void ratio without the outlier

6.3.3 Shear modulus characteristics of waste

The shear modulus of the landfill material was calculated using the following equations (Sheriff & Geldart, 1982):

$$G_{max} = V_s^2 \rho \qquad \textit{Eq. 6.1}$$

$$\varepsilon_{sh} = 2(\varepsilon_a - \varepsilon_r)/3 \qquad \textit{Eq. 6.2}$$

$$G_0 = \Delta q/3\Delta\varepsilon_{sh} \qquad \textit{Eq. 6.3}$$

where G_{max} is the maximum small strain shear modulus, ρ is the bulk density of the sample, V_s is the shear wave velocity, ε_{sh} is the shear strain of the sample, ε_a is the axial strain, ε_r is the radial strain, G_0 is the secant shear modulus and q is the deviator stress applied to the sample.

For the large amount of shear wave data processed every 1 second during shearing, GDS BEAT software was used to batch process the shear wave velocities. The outcome of this allowed for collected of shear modulus data in the very small strain range.

The shear modulus plot for all tests is presented in Figure 6.18. The Hall Effect gauges allowed for collection of data within the 0.001% to 5% shear strain. The very small strain range data was collected through use of the bender element. The correlation between the small strain and large strain shear modulus values is dependent on the application and acceptable shear strain. The shear modulus data was then normalised (i.e. G_0/G_{max}) and trends were observed. The key trends observed in the normalised shear modulus plot is organic content and liquid limit. As the organic content increases, the shear modulus curve degrades further (refer Figure 6.19). The trend is the same for the liquid limit (refer Figure 6.20); however, this may be because the organic content and liquid limit are related. The only sample that does not comply with this trend is BH2 8.4m, however this outlier is apparent in all data sets from the PSD, composition with the highest sand and fines contents as well Young's modulus.

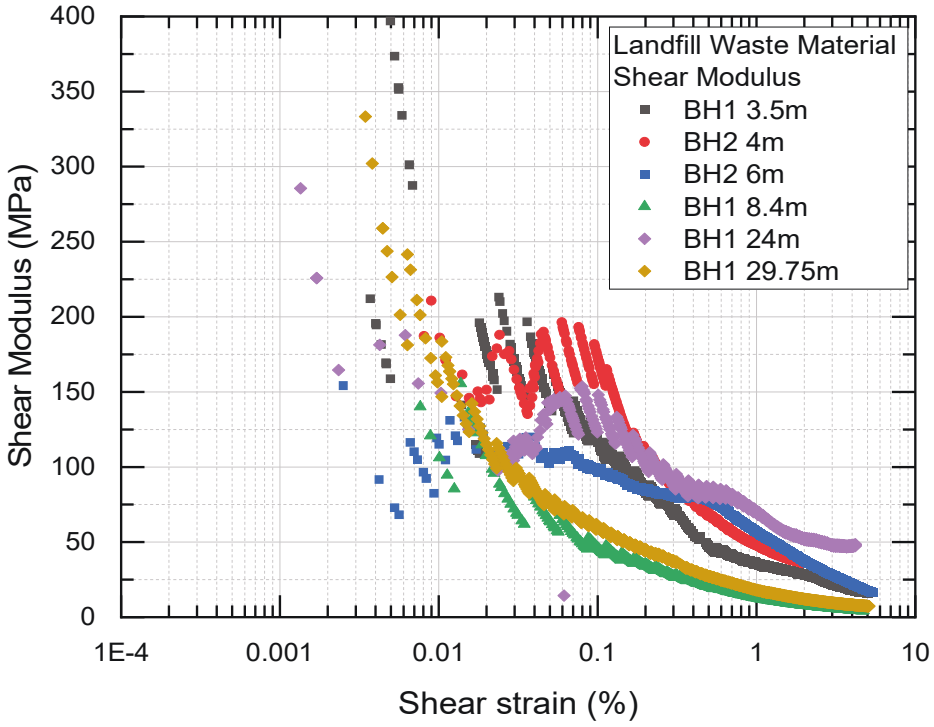

Figure 6.18 Shear modulus against shear strain for all UCS tests

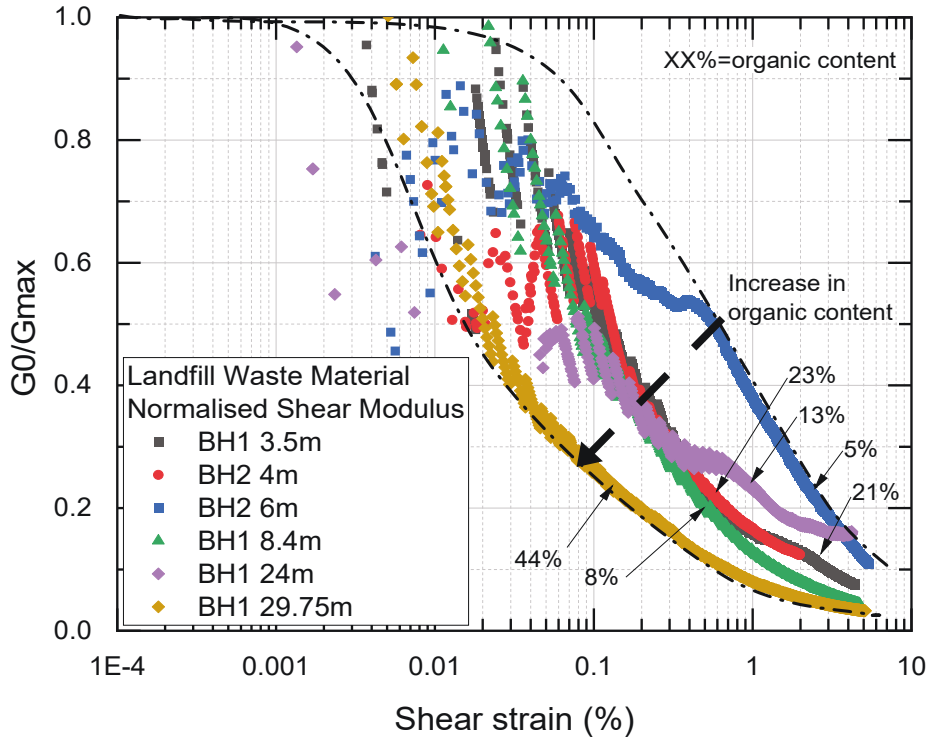

Figure 6.19 Normalised shear modulus against shear strain for all UCS tests and relationship between organic content and the degradation curve

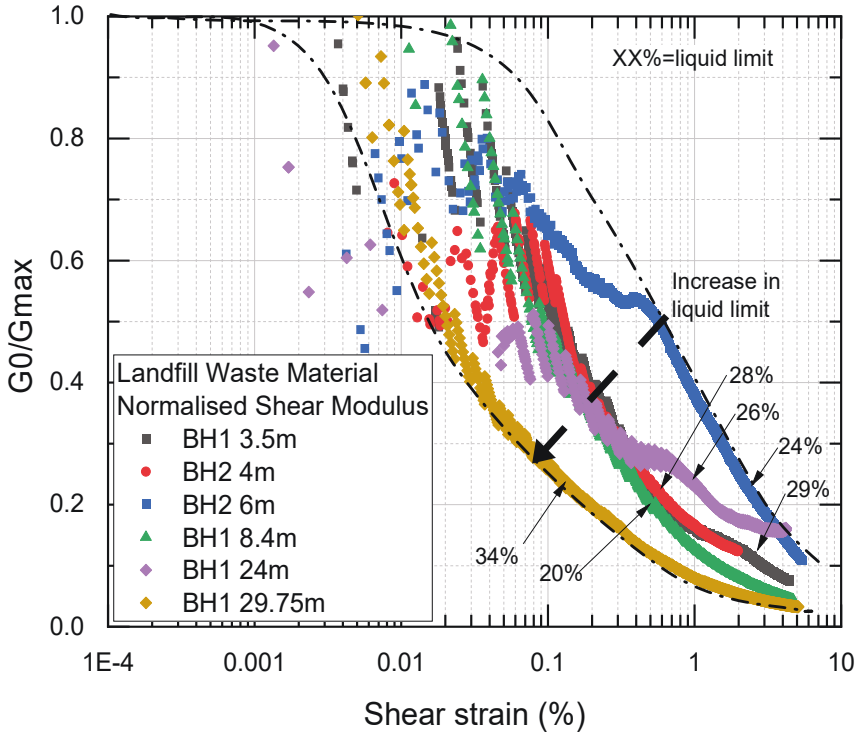

Figure 6.20 Normalised shear modulus against shear strain for all UCS tests and relationship between liquid limit and the degradation curve

6.4 Summary and conclusions

This chapter detailed the results of UCS tests coupled with Hall Effect sensors and bender elements to provide both large strain and small strain properties of landfill waste material extracted from the landfill. Landfill waste material was retrieved in a relatively undisturbed state using the sonic drilling technique. The application of small strain to large strain correlations is to be able to convert field scale geophysical small strain data into large strain data that can be used for geotechnical design and analysis.

Landfill material for the six texts undertaken comprised of varying composition consisting of predominantly timber, gravel and sand with trace elements of clothing fibre, cardboard, plastic, brick, tiles, geosynthetic clay liner, metal, glass foam and fines. There were a number of oversized particles with diameters up to 95mm present in four of the six samples. The specific gravity of the samples was found to range in between 1.95 – 2.55, with an average of 2.19, which is much less than the typical value adopted for soil. The total unit weight and dry unit weight of the samples were on average 17 kN/m^3 and 14.6 kN/m^3. The

higher than expected unit weight is attributed to the higher composition of sand and gravel. The organic content varied between the samples, ranging between 5% and 44%, with an average of 20%. The liquid limits varied between 20% and 34%. Plastic limits were only obtained from two clayey samples; and the remaining of the samples were silty and non-plastic.

UCS values for the majority of the samples varied between 257 to 375 kPa. The highest UCS values of 1107 kPa and 783 kPa corresponded to samples from the greatest depths of 24m and 29.75m. Samples BH2 8.4m had a very low UCS value of 74 kPa and was an outlier in all trends observed for other parameters. The Young's modulus of the waste material ranged between 2 MPa and 14 MPa, with an average of 7 MPa. An equation was proposed to fit the void ratio with the E50.

A plot of the shear modulus against the shear strain showed the small strain shear modulus varied largely between 150 to 250 MPa. The data was then normalised (i.e. G_0/G_{max}) to produce the degradation curve. Trends of decreasing shear modulus were observed with both organic content and liquid limit, both of which the authors believed are linked due to the moisture absorbed by the organic materials such as timber and paper. Trends were not observed with depth or with UCS values.

Chapter 7 – Settlement Prediction and Validation through Field Monitoring at the Landfill

This chapter provides validation of the need for site specific testing to predict landfill settlement with reasonable accuracy. 1-D landfill settlement models and PLAXIS 2D are used to predict the landfill settlement with inputs from site specific laboratory tests. 1D and 2D predictions are compared with data obtained over a 2-year period from field monitoring equipment comprising of settlement cells and extensometers installed at the case study site of the landfill. Furthermore, remote satellite monitoring through use of interferometric synthetic aperture radar (InSAR) is validated with the settlement cells to provide a cost-effective monitoring technique.

7.1 Introduction

Landfill settlement prediction is a complication process that has been studied for over 50 years by many experts (Sowers, 1973; Bjarngard & Edgers, 1990; Marques et al., 2003; Gourc et al., 2010; Bareither & Kwak, 2015; Chouskey & Sivakumar Babu, 2015). Given the heterogeneous waste, practicing geotechnical engineers are predominantly relying on literature to get parameters required for assessing landfill settlement where it is known that climate, unit weight and waste composition are factors that vary between every landfill. The use of values directly from literature can lead to very different settlement predictions to reality. A detailed list of settlement prediction models has been provided in Section 2.3.

Sivakumar Babu et al. (2010) undertook a study with fifteen landfill settlement models to determine the variation in landfill settlement. However, the input parameters between each of the models was different and so it is expected that there is a large variation in the predicted landfill settlement. Bareither & Kwak (2015) undertook a large scale experimental study using landfill material in a large cell and used twelve landfill settlement models (with the same input parameter values) and it was found that all the models over predicted the long term laboratory test settlement. Note the parameters used in the models were compiled from literature from a number of landfills. It was found the most practical models from this in terms of statistical matching to field monitoring data was the models by Gourc et al. (2010), Machado et al. (2008), combined model of Sowers (1973), Bjarngard &

Edgers (1990) and Hossain & Gabr (2005), Chouskey & Sivakumar Babu (2015) and Marques et al. (2003). The best model claimed was the Gourc et al. (2010) model, since it had the least parameters.

This chapter details the use of site specific laboratory testing data to obtain landfill parameters for settlement prediction rather than assuming parameters from literature whereby it is known there are a multitude of contributing factors to landfill settlement.

7.2 Prediction methodology and validation with the landfill

7.2.1 Case study background at the landfill

The history of the landfill is summarised in Table 3.1. Landfill composition primarily consisted of food, paper, cardboard, wood waste and inert construction waste prior to 2002. Post 2002, the waste primarily consisted of construction waste and wood waste. Although a base lining system was not present, a leachate collection system was present for the deeper portion of the landfill. Further detail regarding the age of waste is presented in the next section. The surrounding geology of the landfill included in order of increasing age, Quaternary Sediments (Botany sands), Quaternary Clay, Class IV and V Weathered Ashfield Shale, Class I to III Ashfield Shale and Hawkesbury Sandstone.

7.2.2 Landfill geometry

A cross section through the embankment is shown in Figure 7.1. The depth of the landfill at this location is 32 metres below the base of the embankment.

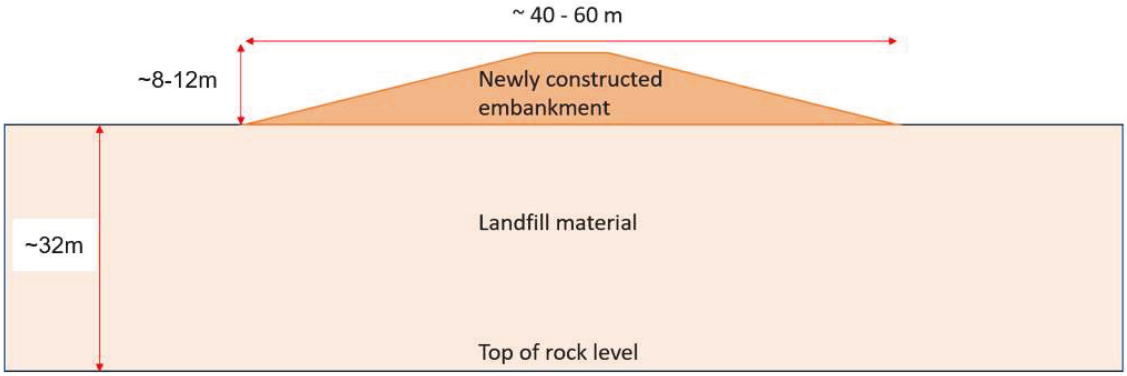

Figure 7.1 Cross section B-B′ through embankment

7.2.3 Summary of parameters obtained from site specific testing

Landfill material obtained from the landfill allowed for collection of the critical parameters necessary for prediction of landfill settlement.

Unit weight, moisture content and organic content

The unit weight, moisture content and organic of landfill found from sonic drilling and test pitting is summarised in Table 7.1, Figure 7.2 and Figure 7.3.

Table 7.1 Summary of landfill test pits

Test	Unit weight (kN/m^3)	Organic content (%)	Moisture content (%)
Test pit 1	11.07	14	28
Test pit 2	18.42	15	26
Test pit 3	17.54	18	31

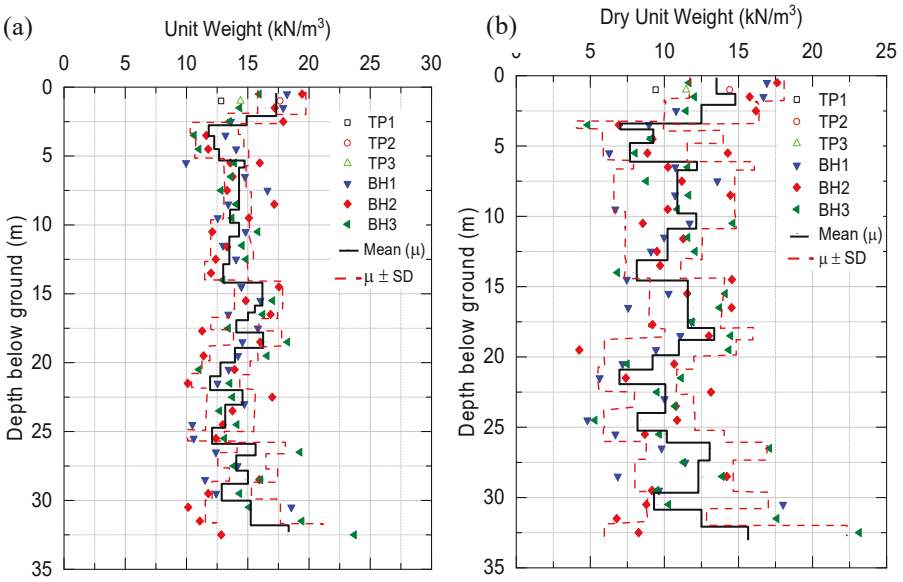

Figure 7.2 Sonic boreholes results (a) Total unit weight and (b) dry unit weight profiles of boreholes and test pits with depth

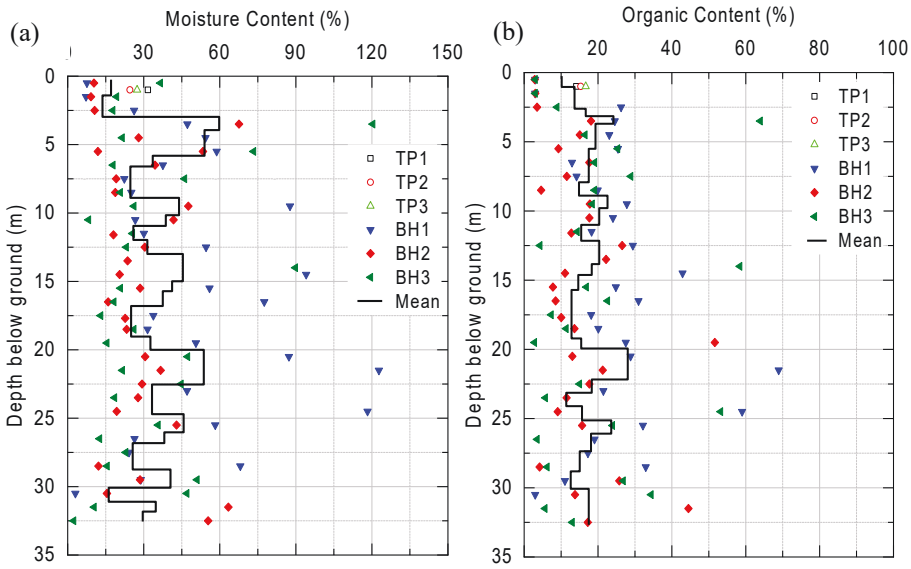

Figure 7.3 Sonic boreholes results, (a) moisture content and (b) organic content summary of boreholes and test pits

Long term creep (C_α)

A summary of creep obtained from back-calculation from a variety of site-specific laboratory tests is presented in Table 7.2.

Table 7.2 Summary of landfill C_α values

	Instrument/test	e0	$C_\alpha(\frac{\Delta e}{\Delta(Log t)})$	C_α
Laboratory testing	Rowe Cell – undisturbed	1.23	0.015-0.021	0.015-0.021 (0.053 appears to be an outlier)
	CD Triaxial – reconstituted stress relaxation	1.12	0.018-0.019	
	CU Triaxial – undisturbed consolidation creep (NC)	1.21	0.051-0.053	
	CU Triaxial – reconstituted consolidation creep (OC)	1.19	0.003-0.005	
	CU Triaxial – undisturbed stress relaxation	1.21	0.015	
	CU Triaxial – reconstituted stress relaxation	1.19	0.019	

Age of waste

The age of waste as described in Section 3.2.2 is estimated to be between 18 and 31 years old (as of 2020). The distribution of the age from the base of landfill to the surface is unknown and was assumed to be gradually ageing from 31-18 years old from the bottom of the landfill.

Biodegradation rate

The biodegradation rate obtained from the gas pumping trial described in Section 3.2.6 and 3.3.4 was found to be 0.005 and decreasing with time.

Friction angle and cohesion

The friction angle obtained from triaxial tests on material from the landfill is presented in Table 7.3.

Table 7.3 Summary of landfill effective friction angle and cohesion

Test	**Depth (mbgl)**	**ϕ (°)**	**c' (kPa)**
CD Triaxial – reconstituted	8	39	129
CU Triaxial – undisturbed	1	35	47
CU Triaxial – reconstituted	1	42	10

Young's modulus

Young's modulus is only required for the Mohr Coulomb model in PLAXIS 2D. Values from triaxial tests and plate load tests are presented in Table 7.4.

Table 7.4 Summary of landfill Young's modulus

Test	Depth (mbgl)	Young's Modulus (MPa)
CD Triaxial – reconstituted	8	3.8 – 4.3
CU Triaxial – undisturbed	1	7 – 11
CU Triaxial – reconstituted	1	4 – 6
UCS	3.5	7
UCS	4.3	10
UCS	6.1	13
UCS	8.4	3
UCS	24	12
UCS	29.75	2
Plate load tests – compacted landfill	Surface	2-44 Average = 18
Plate load tests – in-situ landfill	Surface	3-40 Average = 20.2

Coefficient of compression and recompression

A summary of coefficient of compression and recompression indices are presented in Table 7.5.

Table 7.5 Summary of landfill compression and recompression indices

Test	Depth (mbgl)	e0	$Cc\ (\frac{\Delta e}{\Delta(Log\sigma_v)})$	Cr
CD Triaxial – reconstituted	8	1.12	0.30	0.057
CU Triaxial – undisturbed	1	1.21	0.21	-
CU Triaxial – reconstituted	1	1.19	0.22	-
Rowe Cell – undisturbed	1	1.23	0.356	0.061

Permeability

A summary of the permeability coefficients obtained from laboratory testing are presented in Table 7.6.

Table 7.6 Summary of landfill permeability

Test	Depth (mbgl)	e_o	k (m/s)
CD Triaxial – reconstituted	8	1.12	4.9×10^{-9} – 1.2×10^{-8}
CU Triaxial – undisturbed	1	1.21	7.1×10^{-9} – 1.9×10^{-9}
CU Triaxial – reconstituted	1	1.19	7.1×10^{-9} – 1.9×10^{-9}
Rowe Cell – undisturbed	1	1.23	2.3×10^{-8} – 2.1×10^{-7}

7.2.4 Prediction methodology – 1D landfill settlement models

Based on the findings of Bareither & Kwak (2015), three one dimensional (1D) landfill settlement models were selected to predict landfill settlement. These models were to have the best statistical match to the field monitoring data. However, rather than 'optimising' the parameters to match the field data as undertaken by Bareither & Kwak (2015), the parameters input into each of the models is the same. A brief description of each of the models and required input parameters are presented below.

Sowers (1973), Bjarngard & Edgers (1990) and Hossain & Gabr (2005)

$$S_{TD}(t) = H_0 C'_c log\left(\frac{\sigma_{v0} + \Delta\sigma_{v0}}{\sigma_{v0}}\right) + H_{EOI}\left[C'_{\alpha M} log\left(\frac{t}{t_M}\right) + C'_{\alpha B} log\left(\frac{t}{t_B}\right) + C'_{\alpha MF} log\left(\frac{t}{t_F}\right)\right] \quad \textit{Eq. 7.1}$$

where: $S_{TD}(t)$ is the total settlement at time t, H_0 is the initial thickness of the landfill, C'_c is the primary compression index ($\frac{C_c}{1+e_0}$), σ_{v0} is the initial stress at the middle of the landfill layer, $\Delta\sigma_{v0}$ is the change in stress at the middle of the landfill layer, H_{EOI} is the height of landfill after initial compression is completed, $C'_{\alpha M}$ is the mechanical creep ($\frac{C_\alpha}{1+e_0}$), t_M is the time to transition to mechanical creep, $C'_{\alpha B}$ is the biodegradation creep, t_B is the time for transitioning from mechanical to biodegradation creep, $C'_{\alpha MF}$ is the mechanical creep after biodegradation is complete and t_F is the time for transitioning from biodedgradation creep back to mechanical creep.

Machado et al. (2008)

$$S_{TD}(t) = H_{EOI} C'_{\alpha M} log\left(\frac{t}{t_M}\right) + H_{EOI} \frac{\rho_s^* L_0 (1+w)}{\rho_p^* C_m (1+e_0)} \left\{ \left[1 + \frac{\alpha^* L_0 (1+w)}{C_m} \right] (1 - e^{-kt}) - \frac{\alpha^* L_0 (1+w)}{2C_m} (1 - e^{-kt}) \right\} \quad \textit{Eq. 7.2}$$

where: ρ_s^* is the initial specific density of solids, L_0 is the methane generation potential, w is the moisture content, ρ_p^* is the initial specific density of paste, C_m is the organic methane yield, e_0 is the initial void ratio, α^* is the rate of increase in parameter for biodegradation and k is the first order rate coefficient.

Gourc et al. (2010)

This model includes the least parameters required for

$$S_{TD}(t) = H_{EOI} \left[C'_{\alpha M} log\left(\frac{t}{t_M}\right) + \varepsilon_{BIO} (1 - e^{-k(t-t_B)} \right] \quad \textit{Eq. 7.3}$$

$$\varepsilon_{BIO} = \left(\frac{\gamma_d}{\gamma_{so}}\right) . c \quad \textit{Eq. 7.4}$$

where: ε_{BIO} is the strain due to biodegradation, γ_d is the dry unit weight at initiation of mechanical creep, γ_{so} is the dry unit weight of the solid organic fraction, c is the ratio of solid organic mass to total dry waste mass.

Adopted values for the Sowers (1973), Bjarngard & Edgers (1990) and Hossain & Gabr (2005) 1D model parameters are summarised in Table 7.7. Other parameters required for the Machado et al. (2008) and Gourc et al. (2010) models are presented in *Table 7.7* and *Figure 7.8*, respectively.

Table 7.7 Sowers (1973), Bjarngard & Edgers (1990) and Hossain & Gabr (2005) 1D model parameters

	H_0	C_c	γ_t	Δσ	$C_{\alpha M}$	t_M	$C_{\alpha B}$	t_B	$C_{\alpha MF}$	t_F
Layer	m	-	kN/m³	kPa	-	years	-	years	-	years
1	3	0.35	16.0	137.3	0.017	0.041	0.017	0.1	0.017	12
2	3	0.35	12.2	137.3	0.017	0.041	0.017	0.1	0.017	12
3	3	0.35	14.3	137.3	0.017	0.041	0.017	0.1	0.017	8
4	3	0.35	14.3	137.3	0.017	0.041	0.017	0.1	0.017	8
5	3	0.35	14.1	137.3	0.017	0.041	0.017	0.1	0.017	8
6	3	0.35	15.7	137.3	0.017	0.041	0.017	0.1	0.017	5
7	3	0.35	13.3	137.3	0.017	0.041	0.017	0.1	0.017	5
8	3	0.35	13.0	137.3	0.017	0.041	0.017	0.1	0.017	5
9	3	0.35	13.7	137.3	0.017	0.041	0.017	0.1	0.017	3
10	3	0.35	14.1	137.3	0.017	0.041	0.017	0.1	0.017	2
11	2	0.35	16.8	137.3	0.017	0.041	0.017	0.1	0.017	1

Table 7.8 Machado (2009) model parameters

	ρ_s^*	ρ_p^*	w	L_0	C_m	α^*	k	e_0
Layer	Mg/m³	Mg/m³	-	m3/Mg	m3/Mg	-	1/yr	-
1	1.17	2.47	0.25	0.21	450	20	0.005	1.23
2	1.17	2.47	0.72	0.21	450	20	0.005	1.23
3	1.17	2.47	0.28	0.21	450	20	0.005	1.23
4	1.17	2.47	0.20	0.21	450	20	0.005	1.23
5	1.17	2.47	0.45	0.21	450	20	0.005	1.23
6	1.17	2.47	0.19	0.00	450	20	0.005	1.23
7	1.17	2.47	0.28	0.00	450	20	0.005	1.23
8	1.17	2.47	0.76	0.00	450	20	0.005	1.23
9	1.17	2.47	0.24	0.00	450	20	0.005	1.23
10	1.17	2.47	0.38	0.00	450	20	0.005	1.23
11	1.17	2.47	0.06	0.00	450	20	0.005	1.23

Note: Parameters H_0, C'_c, γ_t, Δσ, $C'_{\alpha M}$, t_M are the same as presented in Table 7.7

Table 7.9 Gourc (2010) model parameters

	Organic content	ε_{BIO}
Layer	-	-
1	0.05	0.082
2	0.35	0.334
3	0.22	0.305
4	0.16	0.215
5	0.26	0.319
6	0.14	0.204
7	0.03	0.030
8	0.25	0.257
9	0.14	0.176
10	0.22	0.308
11	0.09	0.156

7.2.5 Prediction methodology – PLAXIS 2D

PLAXIS 2D is a finite element analysis program commonly used by geotechnical engineers. For landfills, some authors have used PLAXIS 2D for predicting landfill settlement. Models used for this assessment include the Mohr-Coulomb model, soft soil model and soft soil creep model. Note that both the Mohr-Coulomb and soft soil model are only useful for short-term prediction of landfill settlement, as they do not consider time dependent creep.

The methodology for use of PLAXIS 2D includes the same parameters adopted for the 1D settlement prediction discussed in 7.2.4. The model was split into 11 layers of landfill with rock below the landfill as shown in Figure 7.5. Since the landfill settlement occurs over a long time and there is inflowing groundwater, the landfill was simulated in a drained condition. The leachate level was modelled at RL -16 mAHD.

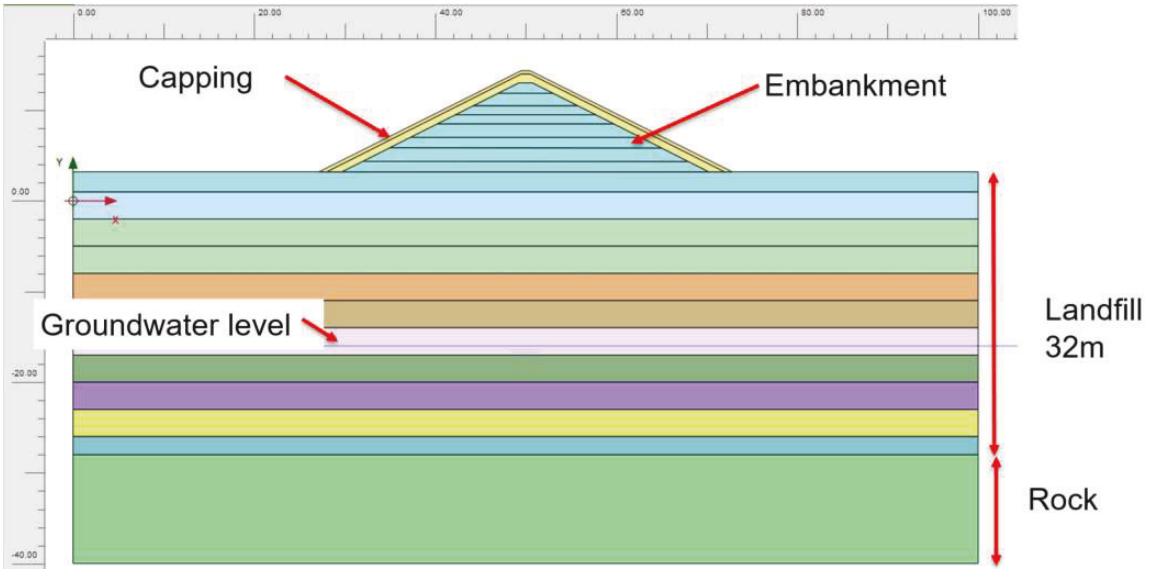

Figure 7.4 Snapshot of PLAXIS 2D model

7.2.6 Validation with settlement at the landfill

In order to validate the settlement prediction, a detailed instrumentation and monitoring plan was implemented at the same location as the site investigation.

Selection of monitoring equipment

The selection of monitoring equipment was required to be remote since the area would be inaccessible in the long term due to opening of adjacent roads. Settlement plates were considered, however they would require ongoing surveying. Strain gauges were considered however they had a small range over which they could measure settlement. Hydrostatic profile gauges were considered for placement underneath the embankment, however, they would require manual monitoring. The chosen options that were installed comprised of settlement cells and extensometers. In addition to the field monitoring instruments, remote monitoring using the interferometric synthetic aperture radar (InSAR) was used to detect and measure surface settlement of the embankment.

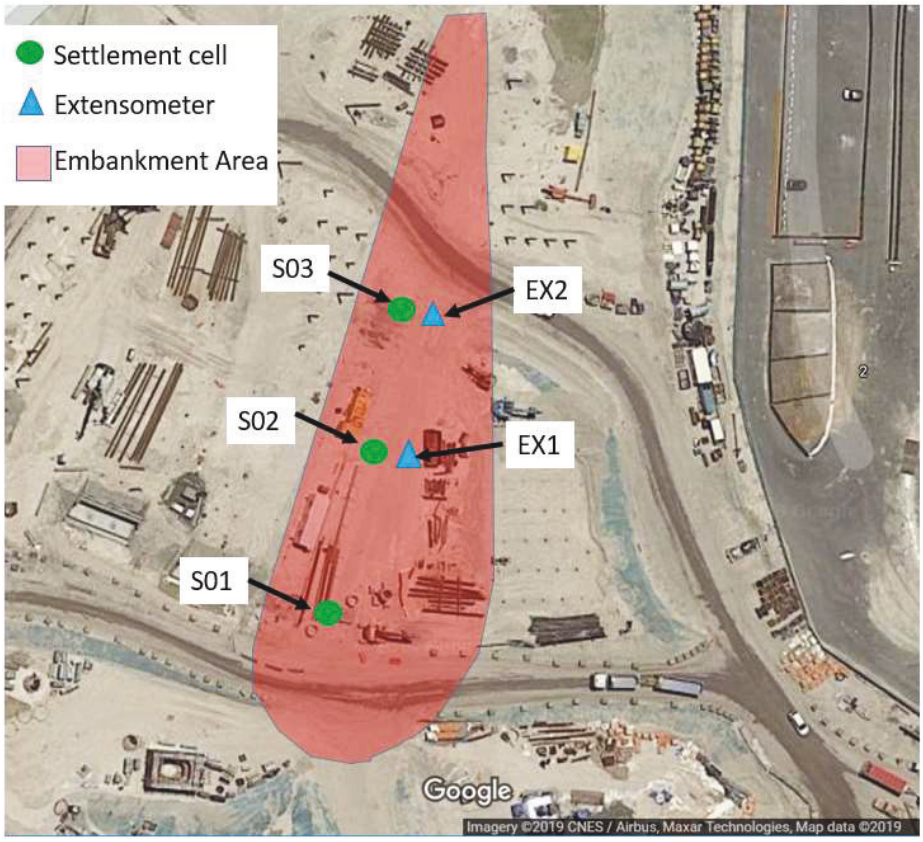

Figure 7.5 Plan view of settlement cell and extensometer locations

Settlement cells

The settlement cell comprises of a pressure transducer. The settlement cell is connected via an electrical cable to a terminal panel and to the liquid reservoir pot via the liquid filled tube. The pressure transducer within the settlement cell measures the pressure created by the head difference between the terminal panel and the settlement cell Figure 7.6. At timed intervals, a vibrating wire signal is sent to the settlement cell to determine the change in pressure. As the settlement cell settles with the surrounding ground, the head difference between the terminal panel and settlement cell increases, creating a higher pressure at the settlement cell. The settlement is calculated by converting the change in pressure to millimetres of liquid head. The liquid settlement cells connected to two boxes, one houses the liquid reservoir pot and the other comprised of the data logger, 12V battery and modem to upload the information to the cloud (refer Figure 7.7). The measurement range of the settlement cell is up to 15m of vertical displacement with an accuracy of 0.1%.

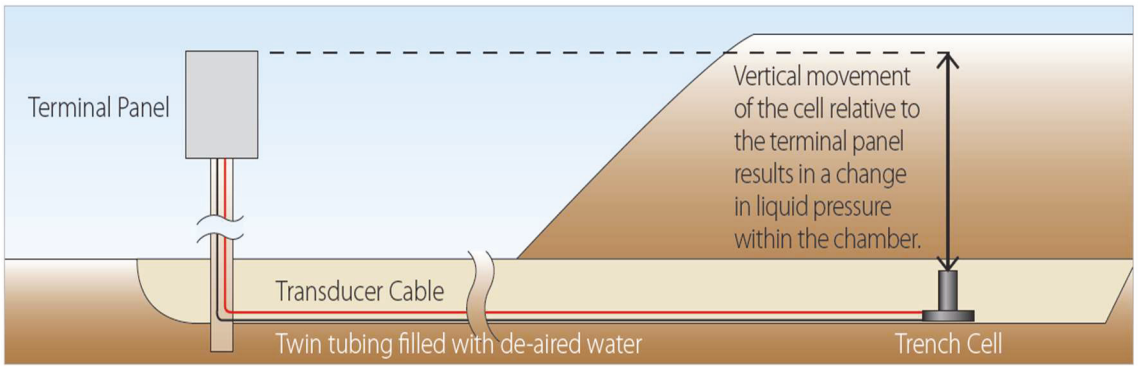

Figure 7.6 Liquid settlement cells function

Three settlement cells were installed at the base of the embankment at the landfill. In order to prevent damage during embankment construction from heavy rollers and dozers, a trench with depth of 1m below the existing ground surface with a width of 600 mm was excavated between the liquid cells and the terminal panel. In addition, liquid cables and electrical cables were pulled through a heavy-duty electrical conduit to provide further protection during embankment construction. Embankment filling occurred within 1 day of completion of installation of the settlement cells.

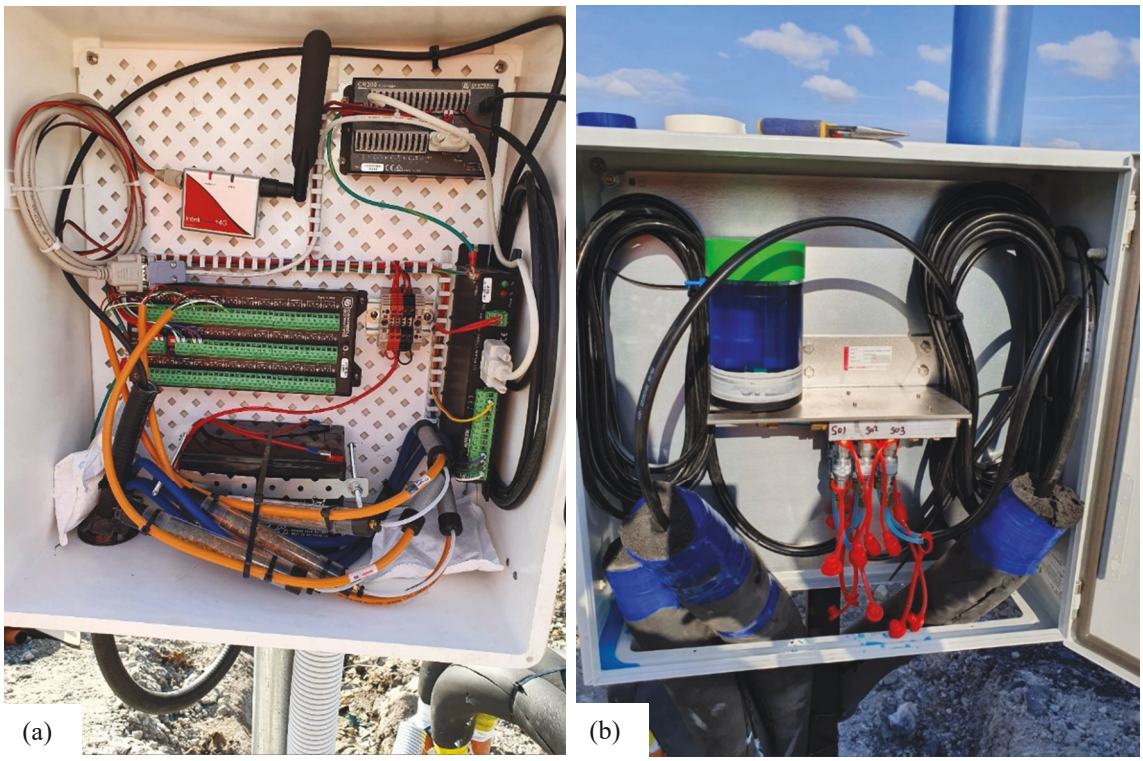

(a) (b)

Figure 7.7 Settlement cells, (a) terminal panel and (b) liquid reservoir pot

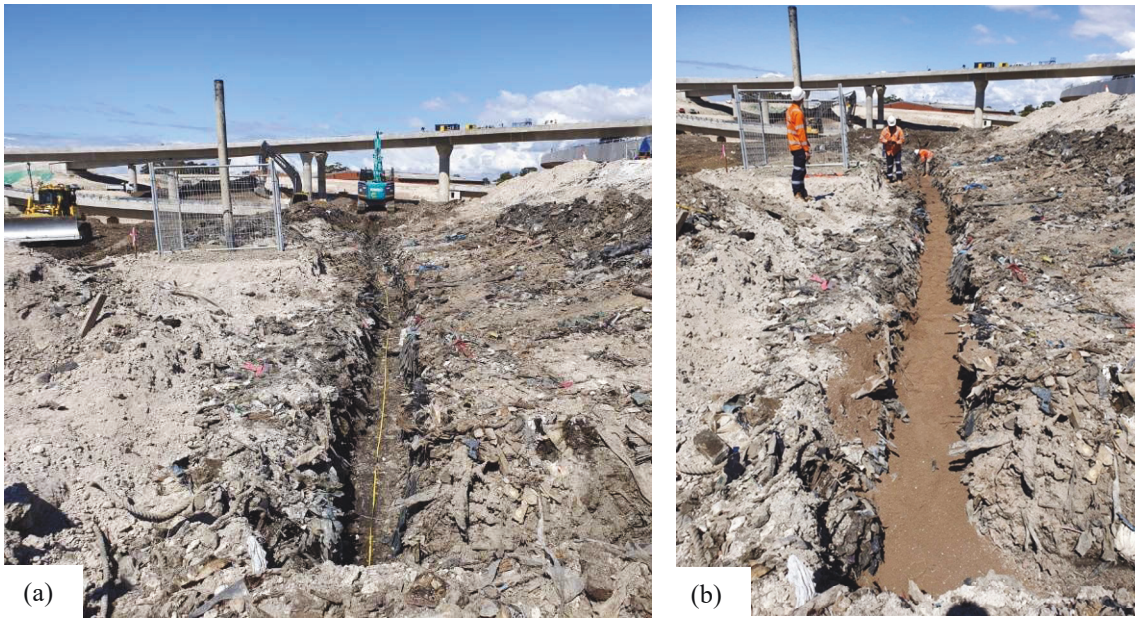

(a) (b)

Figure 7.8 Settlement cells, (a) trench excavation and (b) placement of 100mm thick bedding sand layer within trench

Figure 7.9 Liquid settlement cell installed at base of trench

Embankment construction took place in 1m lift for the first layer, with 600 mm lifts for subsequent layers with a minimum of 8 passes per layer using a 12 tonne pad foot roller with a D65WX bulldozer spreading the material. Photographs before and after embankment construction are presented in Figure 7.10 and Figure 7.11. Since the settlement cells were installed prior to embankment construction.

Figure 7.10 Before embankment construction

Figure 7.11 After embankment construction

Extensometers

Extensometers were selected to obtain settlement profiles at various depths of the landfill. The extensometer comprises of a PVC tube, a spider magnet and a vibrating wire sensor. First a borehole needs to be drilled with diameter large enough to allow for insertion of the PVC pipe, but small enough the ensure the spider magnet legs attach into the surrounding ground. The spider magnet is tied up (refer Figure 7.12), lowered into the borehole and is released at the selected height, when released the spider magnet legs spring open and gain contact with the surrounding ground (refer to Figure 7.13). Within the PVC tube is a vibrating wire sensor, which detect the position of the spider magnet relative to the sensor. As the spider magnet settles with the soil, the location relative to the sensor is known and this change in voltage is converted into a corresponding settlement.

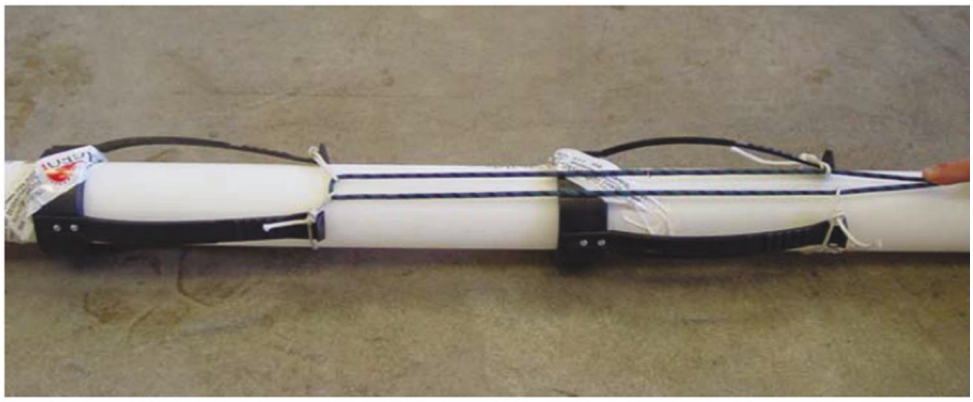

Figure 7.12 Tied up spider magnet

Figure 7.13 Released spider magnet

The sensor comprises of wheels at both ends that align with the grooves within the PVC tube to ensure the extensometer is fixed to move only in the vertical axis (refer Figure 7.14). The sensor within the PVC tube is held in place by a steel wire and has an electrical cable that connects to a terminal panel box with a data logger, power source and modem to upload the data to the cloud (refer to Figure 7.15). The extensometer has a maximum measurement range of 100 mm with an accuracy of 1 mm.

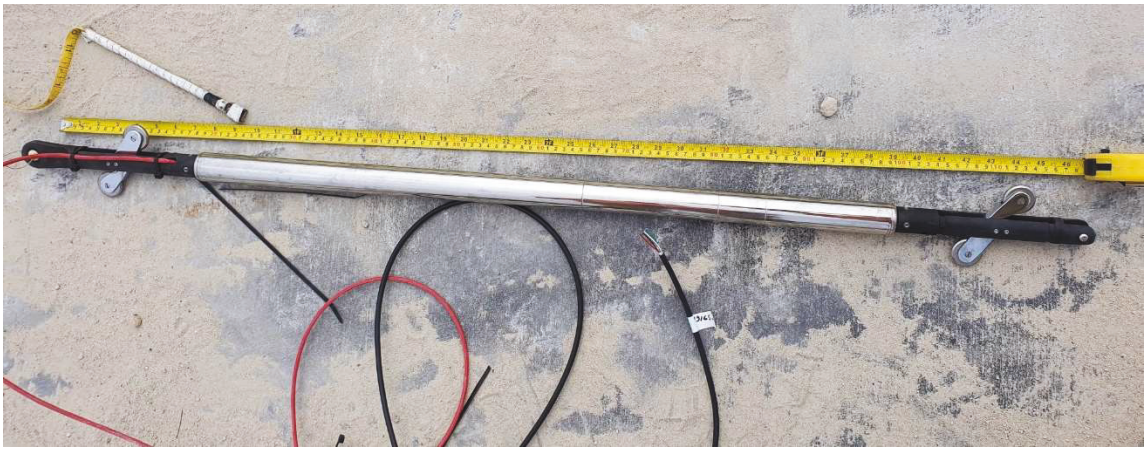

Figure 7.14 Extensometer sensor

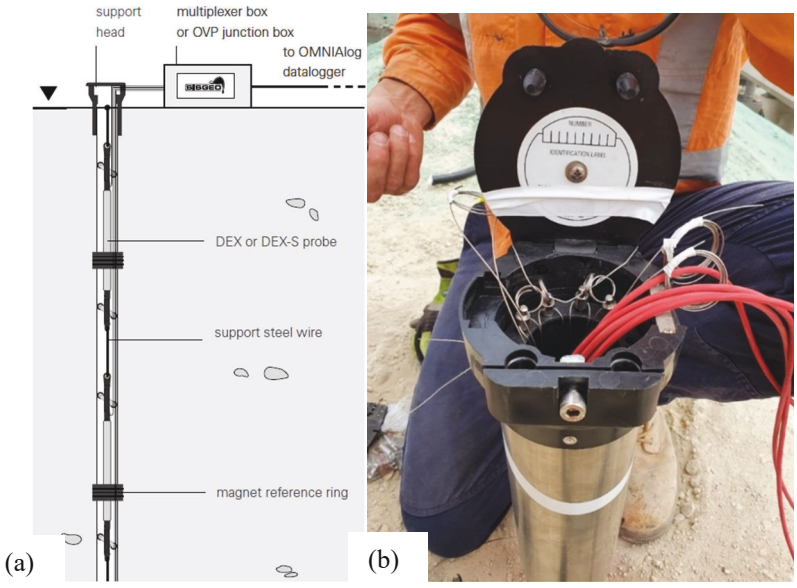

Figure 7.15 Extensometer, (a) field setup and (b) support head with steel cables and electrical cables

Two extensometers were installed at the landfill as per the layout shown in Figure 7.16. One extensometer was a floating extensometer whilst the other was socketed into rock. Extensometers were installed close to the top of the final embankment surface in order to prevent destruction during embankment construction.

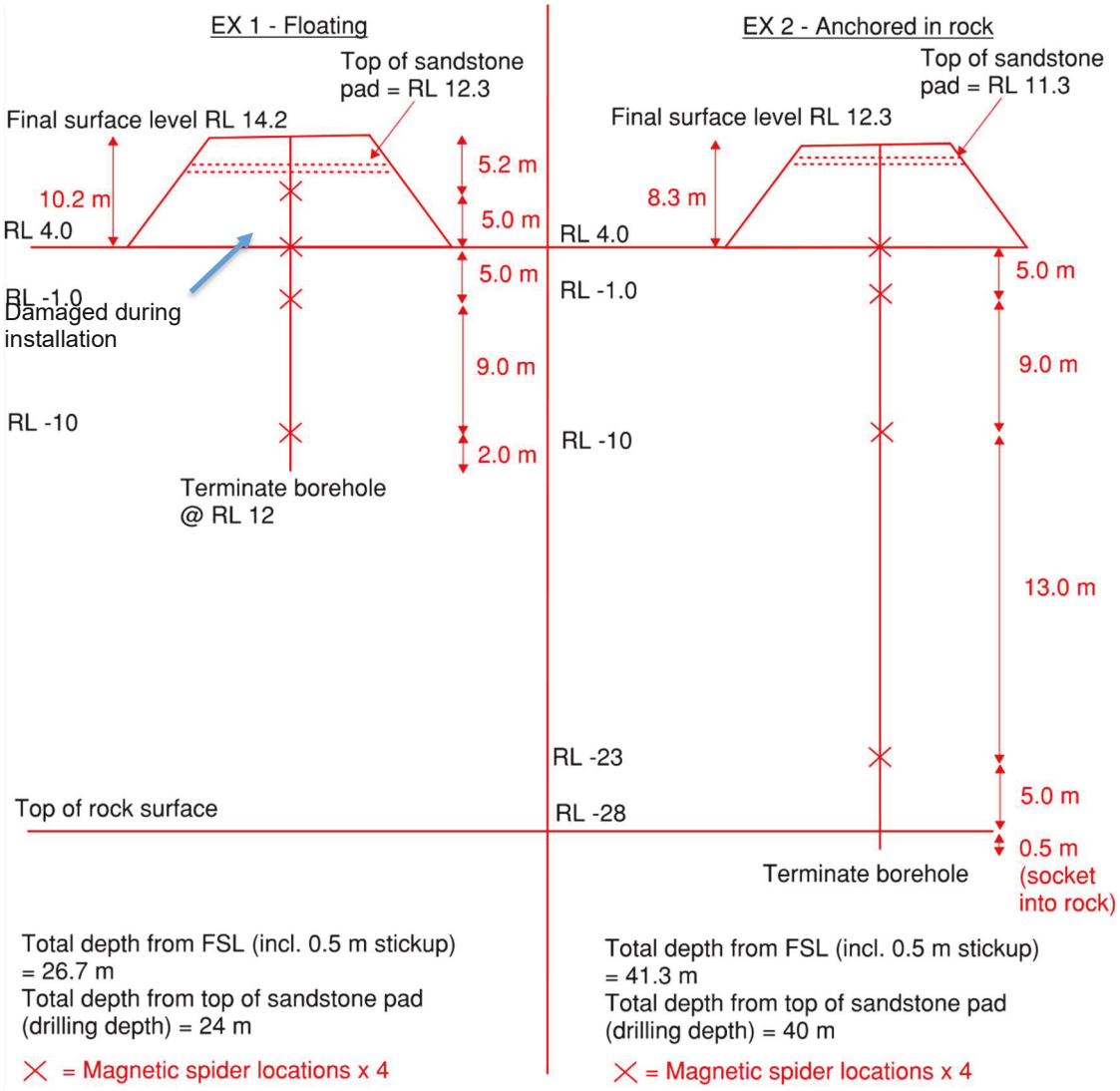

Figure 7.16 Extensometer layout for the landfill

InSAR

Interferometric synthetic aperture radar (InSAR) is a fast, low cost and reasonably accurate method to obtain surface deformation. There are a variety of InSAR processing methods available, the selected version for this case study is differential InSAR (DInSAR) which obtains the surface deformation from two subsequent satellite images obtained from the European Space Agency (ESA) Sentinel-1A satellite (refer Figure 7.17) and is processed using Sentinel Application Platform (SNAP) software. There were a variety of other satellites available with smaller ground pixel sizes than Sentinel-1 (refer Table 7.10), however the cost of obtaining imagery is expensive.

Figure 7.17 Sentinel-1 data acquisition (ESA, 2020)

Table 7.10 Summary of satellites ground pixel size and revisit time

Satellite	Ground pixel resolution	Revisit time (days)
Sentinel 1A and 1B	22m × 3.5m	12
Radarstat-2	8m × 8m	24
Cosmo-skymed	3m × 3m	8
TerraSAR-X (Stripmap)	3m × 3m	11
TerraSAR-X (Spotlight)	1m × 1m	11
TerraSAR-X (Staring spotlight)	0.6m × 0.25m	11

A summary of the InSAR processing flowchart is presented in Figure 7.18. InSAR data downloaded from the ESA was Interometric Wide (IW) swath (land applications) acquisition mode and used the Single Look Complex (SLC). The Sentinel-1 satellite is C-band with a frequency of 5.405 GHz. When downloaded and imported into SNAP, the raw image contains three subswaths and 9 bursts as shown in Figure 7.19.

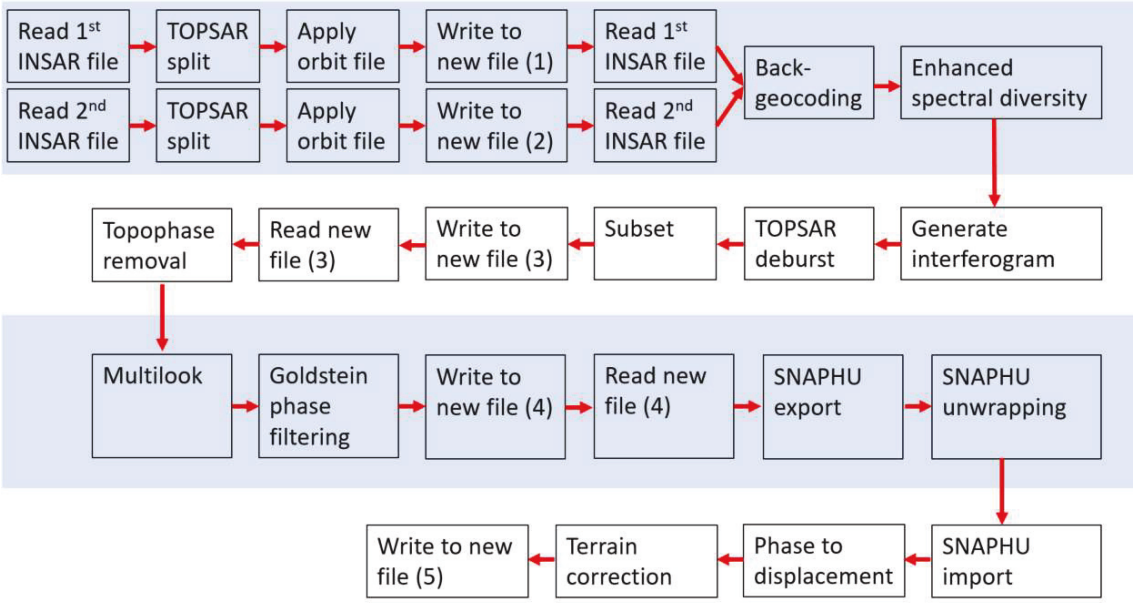

Figure 7.18 InSAR processing methodology

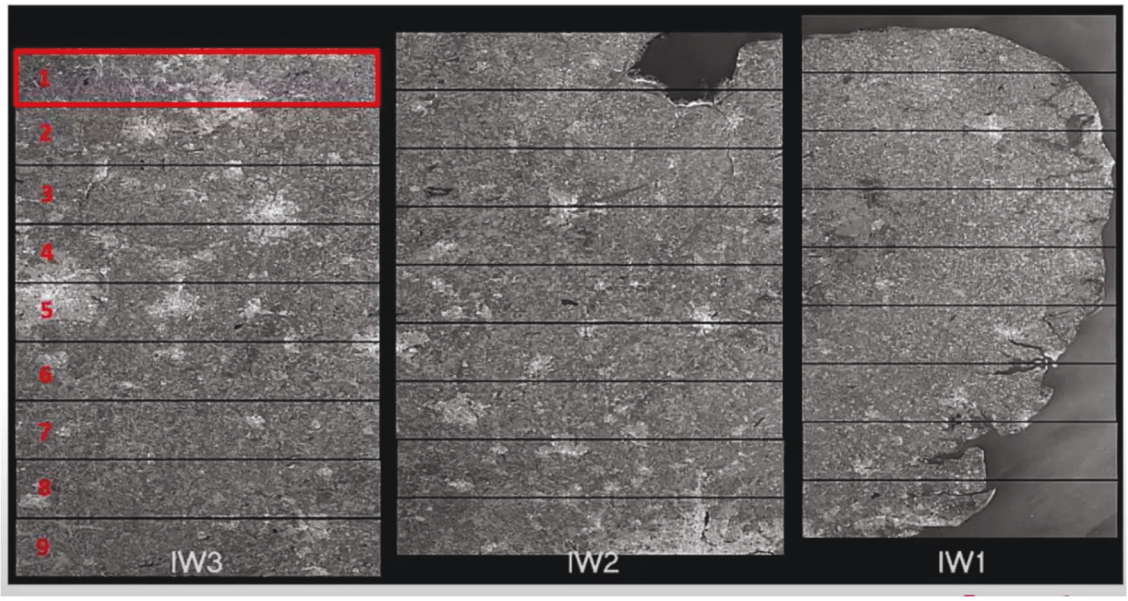

Figure 7.19 Bursts and subswaths for raw InSAR data

Terminology within the processing flowchart to provide a general understanding of the processing is summarised below:

- TOPSAR split – splits the InSAR data into bursts and subswaths
- Apply orbit file – applies the accurate satellite position and velocity info to the InSAR data
- Back-geocoding – overlays two Sentinel-1 images and the digital elevation mesh (DEM)
- Enhanced spectral diversity – corrects two or more bursts within a subswath
- Interferogram – creates and interferogram using the phase and amplitude data
- TOPSAR-deburst – removes and corrects the overlaps of bursts
- Subset – reduces the size of InSAR analysis to a small area
- Topo phase removal – removes the DEM from both interferograms
- Multilook – averages data based on adjacent pixels at the cost of resolution
- Goldstein phase filtering – reduces noise
- SNAPHU – statistical-cost, network flow algorithm for phase unwrapping (SNAPHU)
- SNAPHU export – exports processed data to SNAPHU
- SNAPHU unwrapping – converts the continuous phase data rather than being constrained from pi to –pi
- SNAPHU import – brings the unwrapped phase back into the SNAP program
- Phase to displacement – converts from continuous phase to a displacement in metres
- Terrain correction – corrects orientation of the InSAR data to the right latitude and longitude

Ground pixels from the processing data were overlayed onto an aerial image (refer and points corresponding to settlement cells and extensometers. The ground pixel from the INSAR image falls over an area of 22m x 3.5m. The processed point falls within this zone. The only way to get a higher resolution is by using a satellite such as TerraSAR-X, which has a very small ground pixel size.

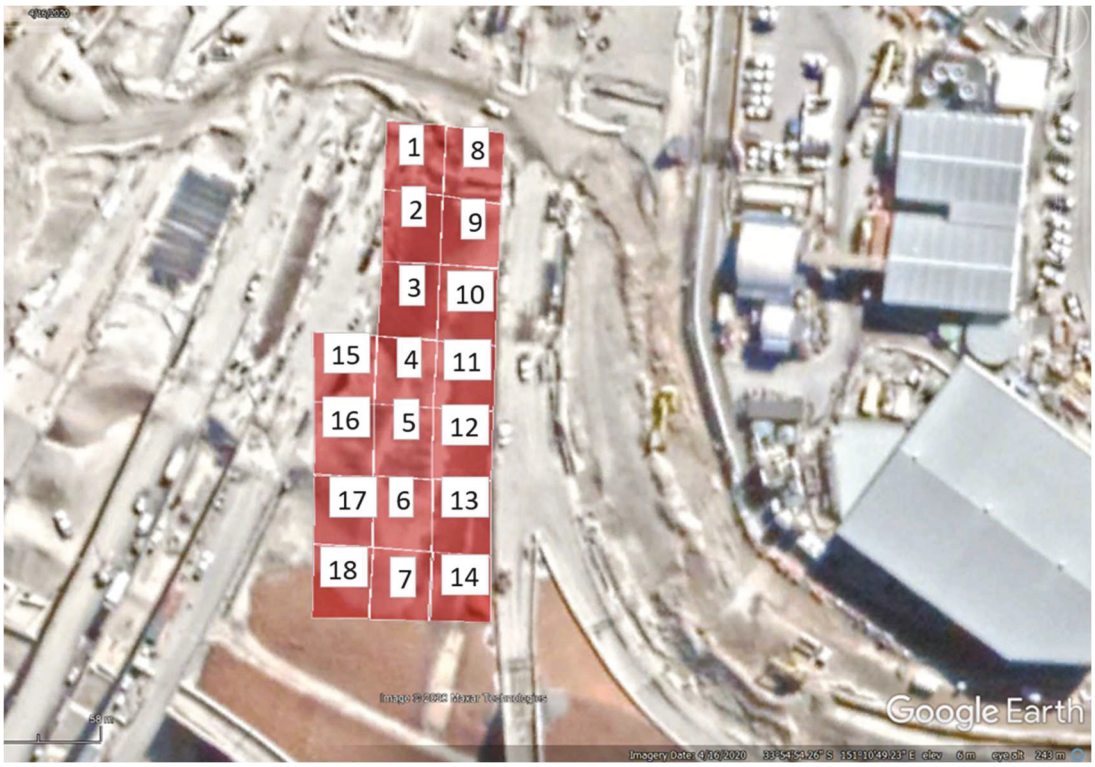

Figure 7.20 Overlay of Sentinel-1 ground pixels onto the landfill

7.3 Results and discussion

The results from field monitoring using settlement cells, extensometers and InSAR processing along with the 1D and PLAXIS 2D settlement predictions are presented in the following sections.

7.3.1 Field monitoring results from the landfill

The settlement at the landfill due to the embankment described in Section 7.2.2 is presented in Figure 7.21 and Figure 7.22. Settlement cell S03 was damaged one day after installation and so results have not been presented. The back calculated creep rate (C_α) assuming a constant void ratio of 1.23 for the entire landfill depth of 32m is estimated to be 0.018 to 0.019. This value is comparable to the findings from site specific laboratory testing described in Section 7.2.3, which has a range of 0.014 to 0.021, with one outlier of 0.053. This demonstrates value in undertaking site specific testing for landfill material to allow for better prediction of long-term landfill settlement. The small spikes and drops in the settlement plots are a result of the change in temperature on the volume of the glycol liquid within the tube

and reservoir pot. The temperature rises during the day and drops at night, causing the spikes in the settlement plot.

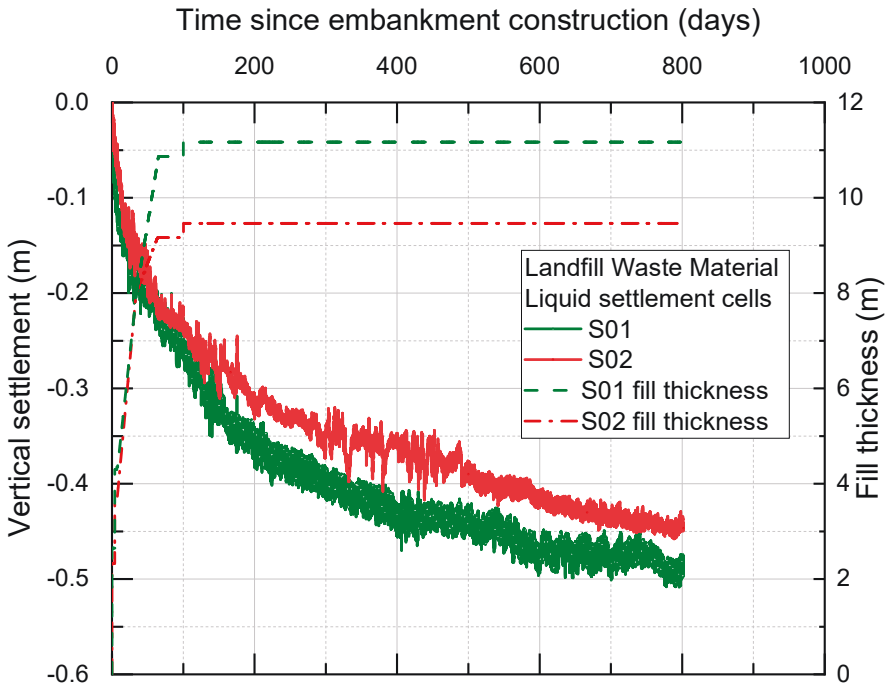

Figure 7.21 Settlement cells S01 and S02 monitoring data on normal time scale

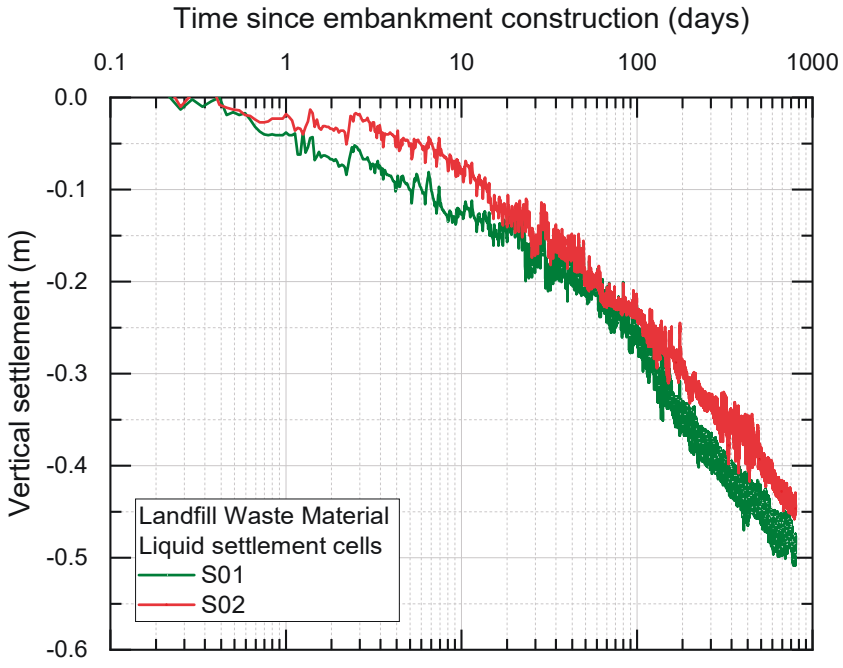

Figure 7.22 Settlement cells S01 and S02 monitoring data on log time scale

Field monitoring data from extensometers installed at the landfill is presented in Figure 7.23 and Figure 7.24. The results appear to be unsuccessful in capturing the actual landfill settlement behaviour at various depths, since there is large jumps and unstable readings. Potential reasons for the poor results could be due to the following:

- Presence of low strength cement bentonite grout (with the consistency of soft clay after hardening) was installed between the extensometer PVC casing and the landfill material. The reason for this installation was to prevent any landfill collapse within the gap, which could potentially knock the spider magnet out of range. The low strength grout may have caused the spider magnet to become rigidly fixed in place.
- Minor grout loss did occur during extensometer installation at the location of the floating extensometer. No grout loss occurred for the rock-socketed extensometer. The grout loss could have seeped through voids and strengthen the landfill material. However, given the low strength nature of grout, even if hardened is not expected to have a major ground strengthening effect.
- Spider magnet release is not visually confirmed other than through retrieval of string tied to magnet. The spider magnet could have been released, but may be stuck within the grout body rather than attaching to the surrounding landfill material. This lack of contact would mean the spider magnet is suspended in place and little to no movement would be observed.
- The PVC tube was installed in 3m lengths with joints that connect each segment together. The connection joint has a larger diameter than the spider magnet. In the event the spider magnet moved to the bottom end of the PVC tube, there would be little to no movement.
- The measurement range of the extensometer is ± 100mm with an accuracy of ± 1mm, however in the figures below, there is a bounce in the results (~20mm) on a daily basis. The only explanation for this bounce is the effect of wind on the top support cap. Sudden drops could be explained through a sudden downward movement of the spider magnet, however sudden raises that are permanent are not indicative of good extensometer results.

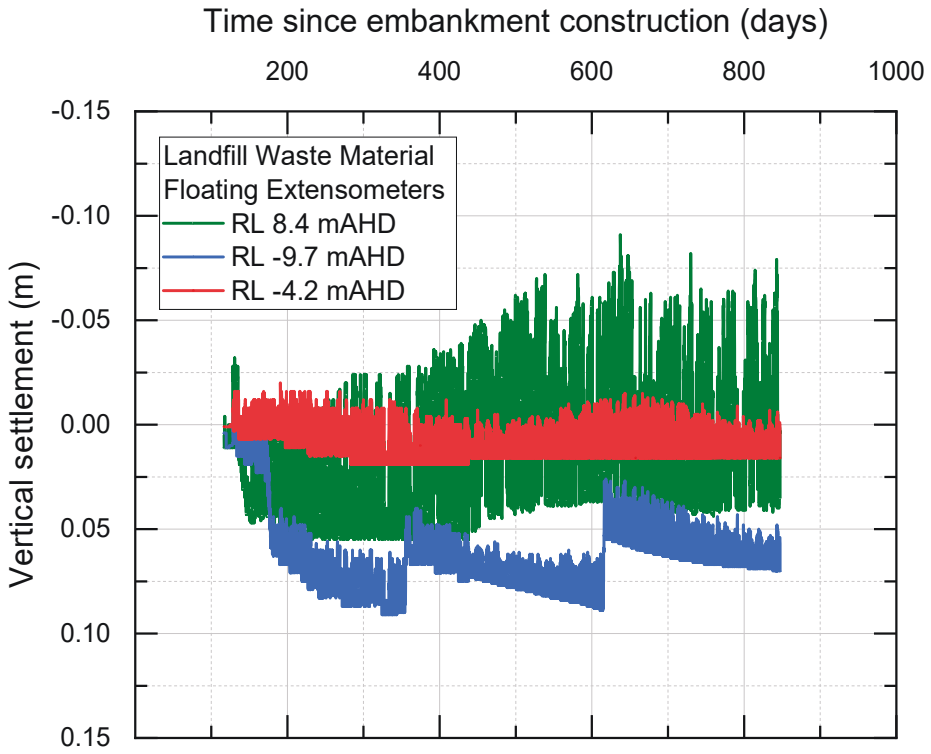

Figure 7.23 Floating extensometer monitoring data

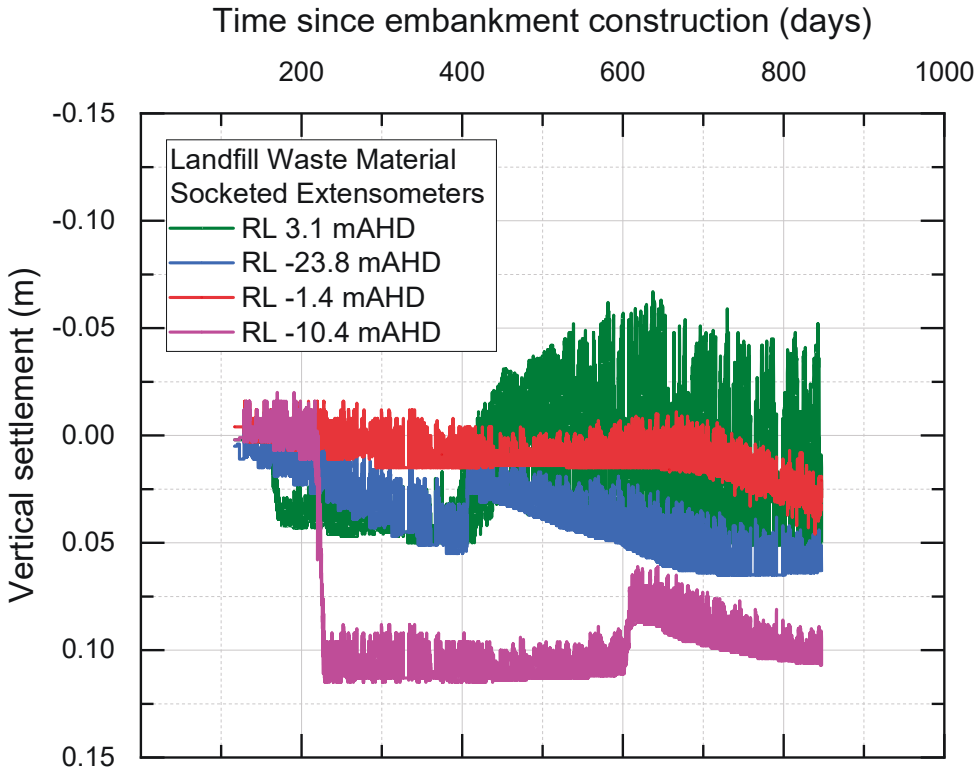

Figure 7.24 Socketed extensometer monitoring data

InSAR was used to determine the surface settlement above the settlement cells S01 and S02, corresponding to points 4 and 5 shown in Figure 7.20. The raw uncorrected settlement data from InSAR shown in Figure 7.25 shows both S01 and S02 are settling at the same rate. InSAR was not able to be undertaken during construction of the embankment since reference height between images was changing in the order of metre and was therefore started after completion of the embankment. After correction of the InSAR data to the settlement cell plots (refer to Figure 7.26 and Figure 7.27), the InSAR data was found to match the trend very well. The difference between the settlement cells and InSAR is approximately 20 mm, which is due to a combination of the embankment settlement and the error, which is known to be up to 5 mm.

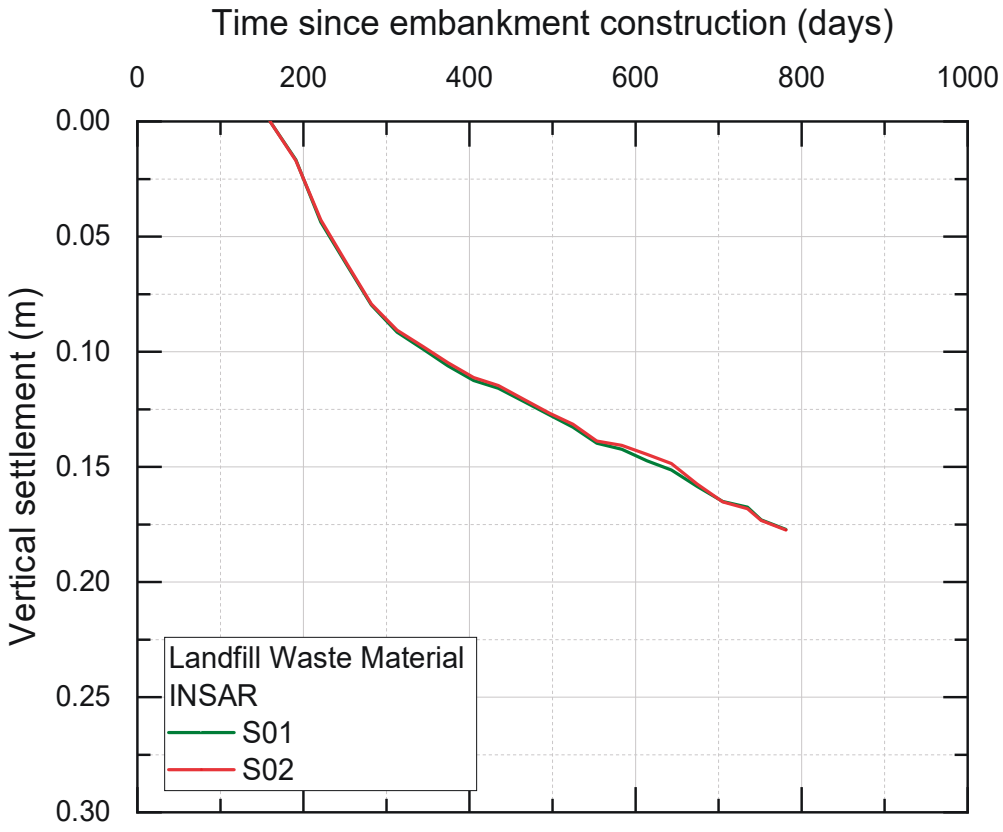

Figure 7.25 Uncorrected InSAR monitoring data

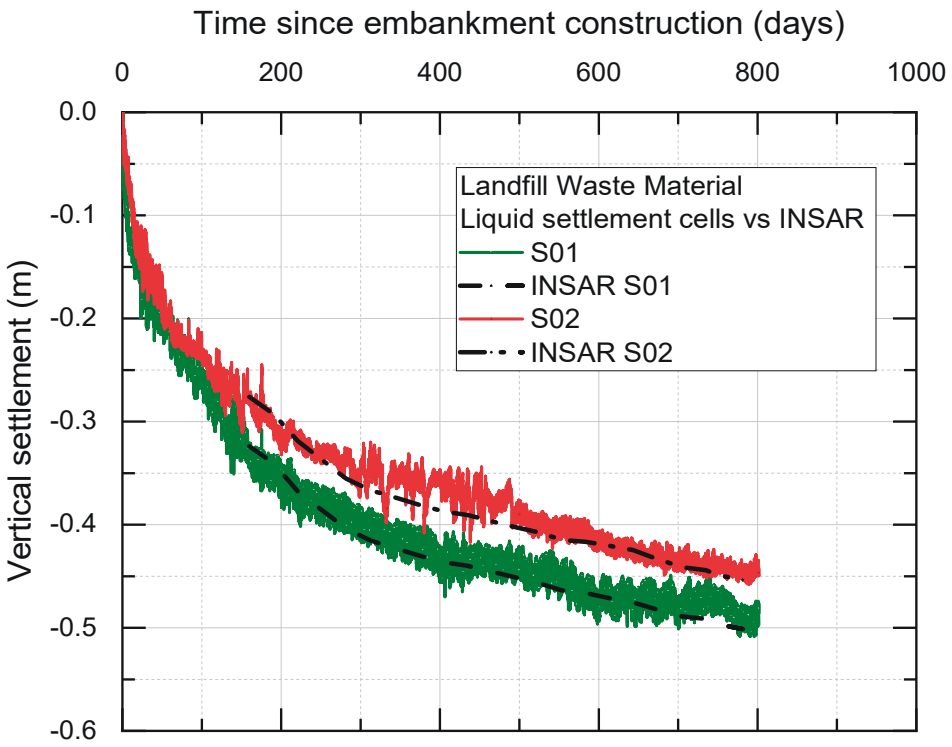

Figure 7.26 Comparison of settlement cells and InSAR on normal time scale

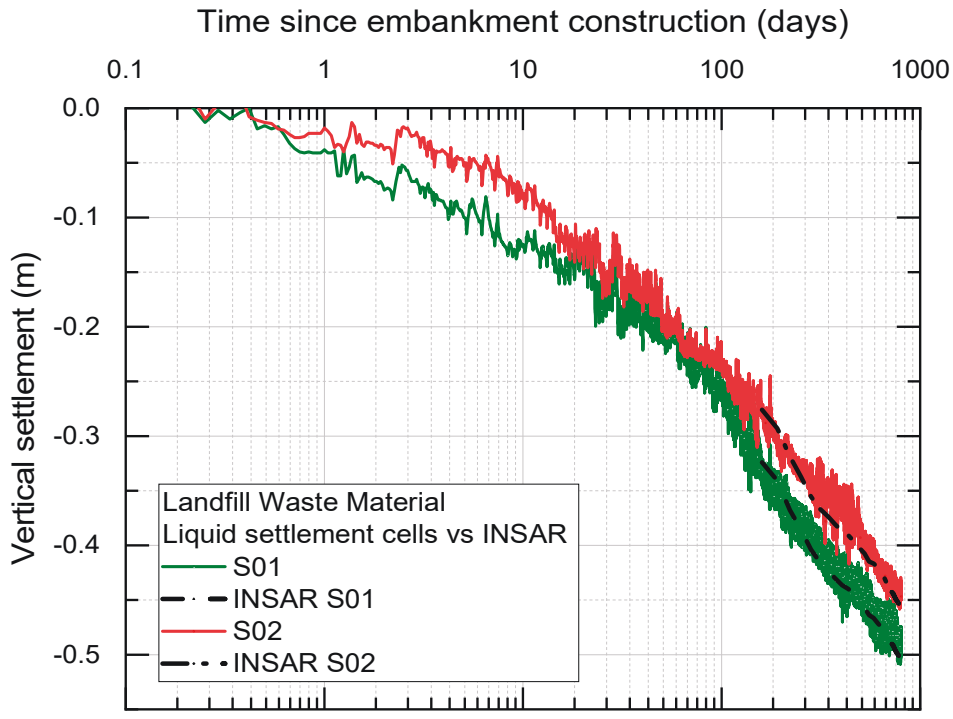

Figure 7.27 Comparison of settlement cells and InSAR monitoring data on log time scale

7.3.2 Prediction with 1D settlement models

Prediction of 1D landfill settlement was undertaken using three models, Sowers, Machado and Gourc. All of these models slightly over-predicted the landfill settlement as shown in Figure 7.28 and Figure 7.30. The over-prediction appears to be largely in the initial stage of embankment construction and so corrected figures were produced as shown in Figure 7.29 and Figure 7.31. The correction of the data involves moving it to match the starting point in the settlement monitoring curve such that the two results The corrected figures match the landfill settlement models with reasonable accuracy.

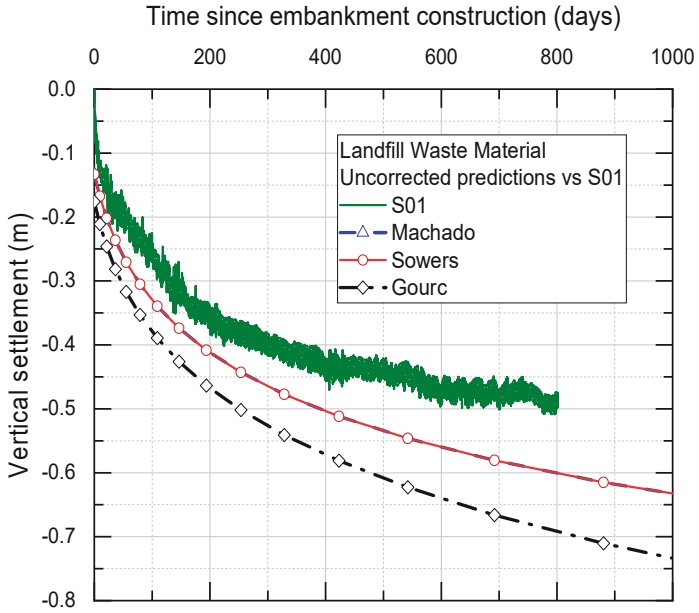

(a)

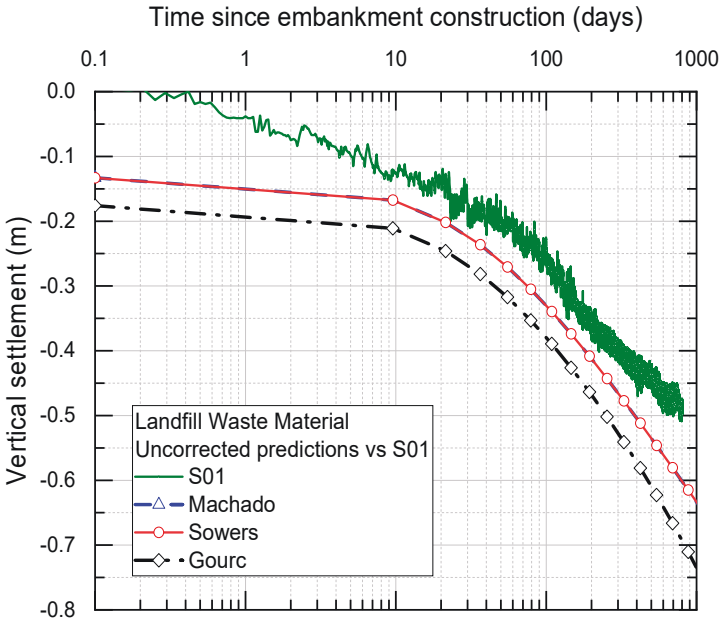

(b)

Figure 7.28 Uncorrected 1D settlement predictions compared against settlement cell S01, (a) normal scale and (b) log scale

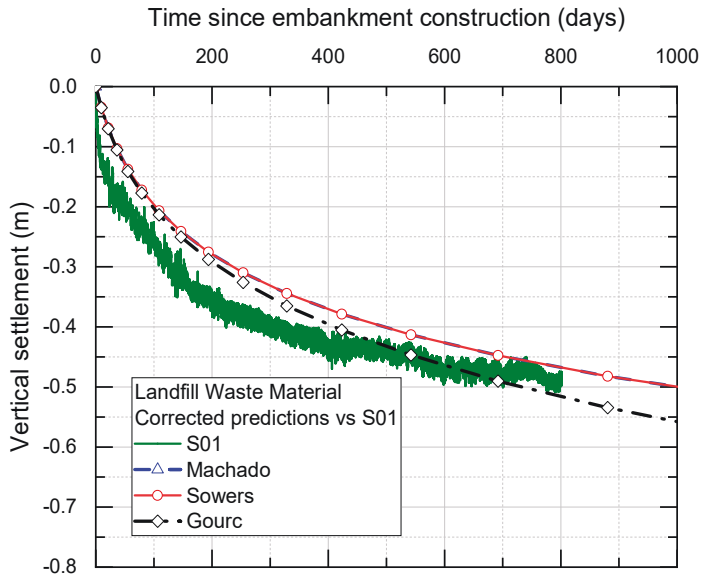

(a)

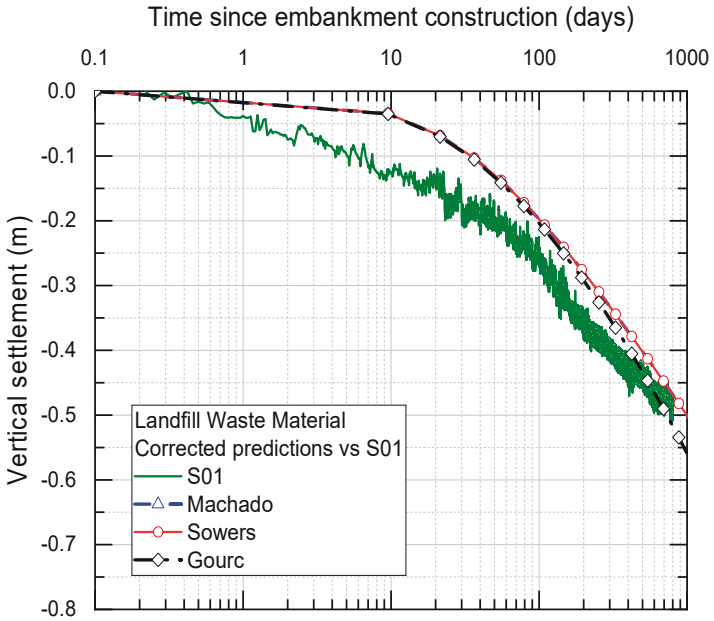

(b)

Figure 7.29 Corrected 1D settlement predictions compared against settlement cell S01 (a) normal scale and (b) log scale

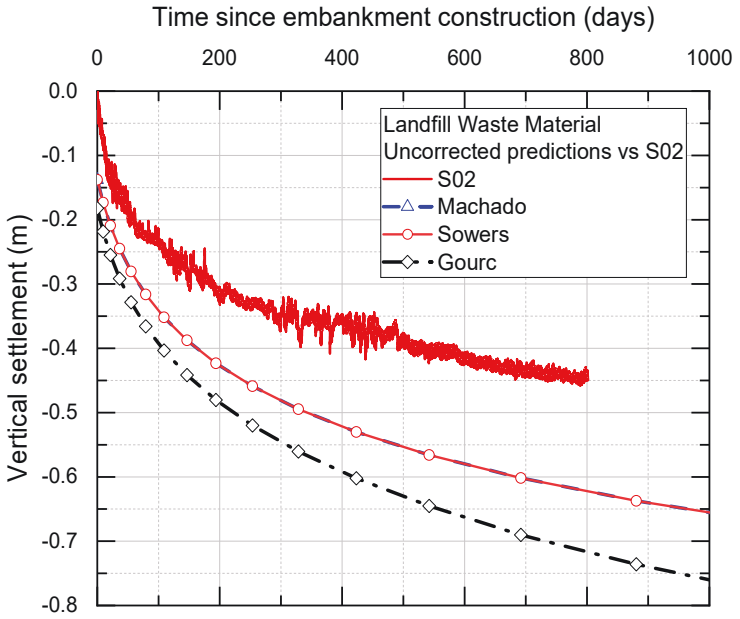

(a)

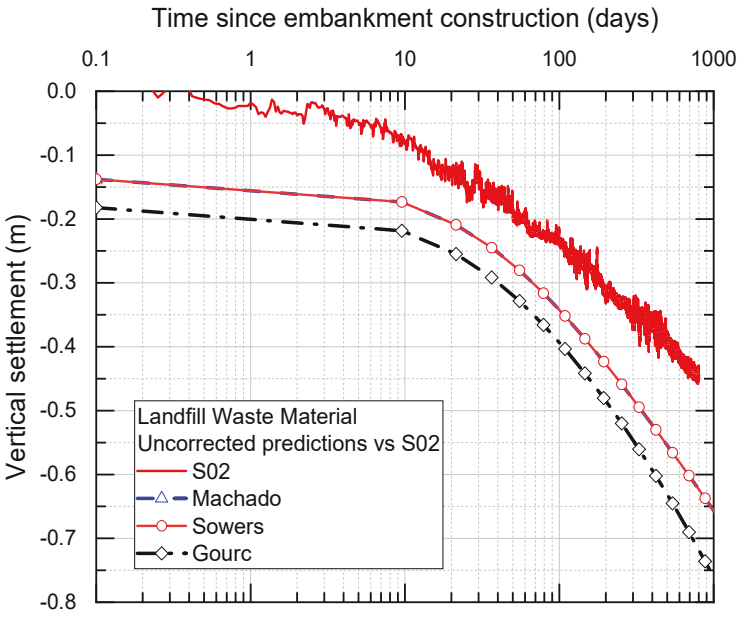

(b)

Figure 7.30 Uncorrected 1D settlement predictions compared against settlement cell S02, (a) normal scale and (b) log scale

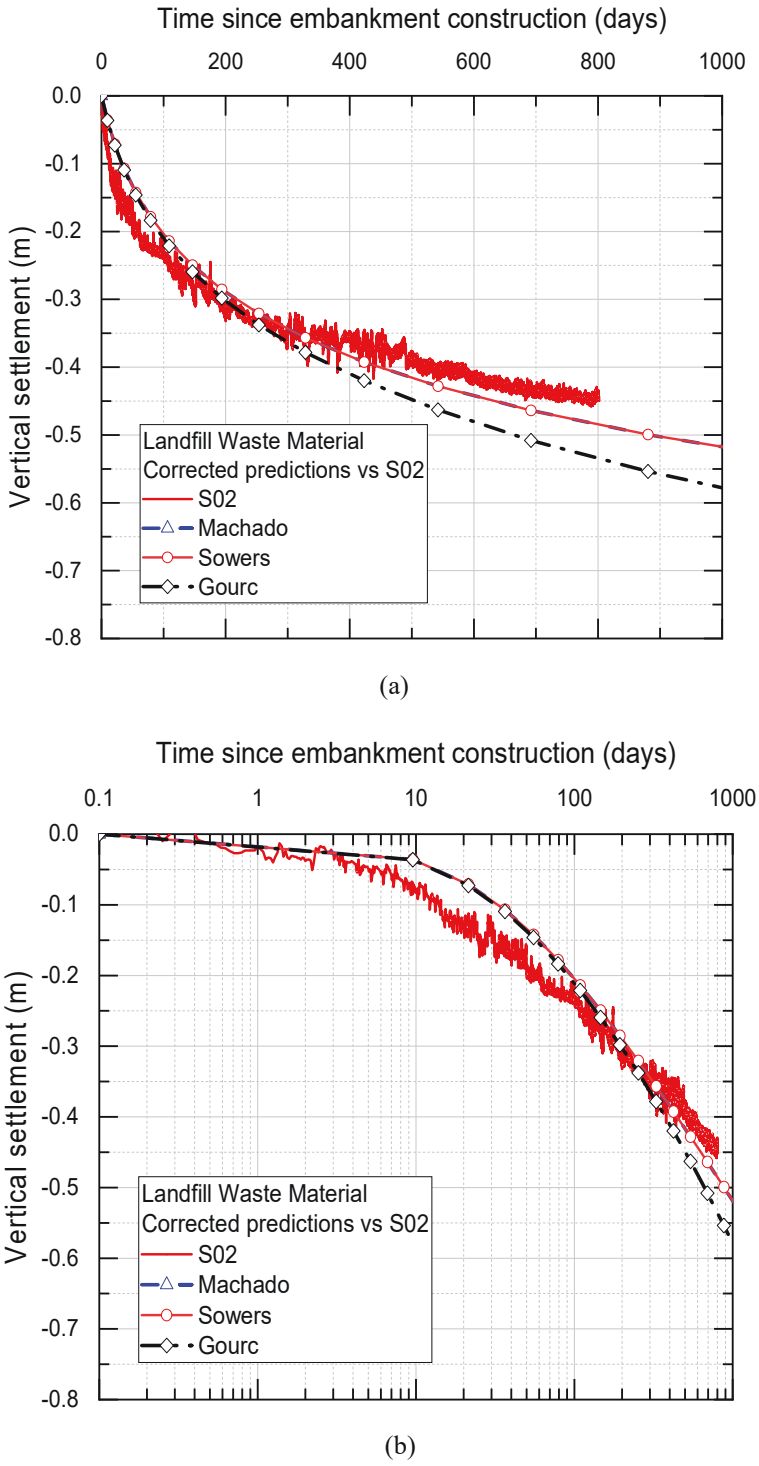

Figure 7.31 Corrected 1D settlement predictions compared against settlement cell S02, (a) normal scale and (b) log scale

Sower's model and Machado's model provided very close results and so both were overlapping. Gourc's model produced a higher settlement. Since the landfill is relatively old, the effect of biodegradation on the settlement is small. A sensitivity analysis was undertaken to determine the critical parameters necessary for geotechnical engineers to predict landfill settlement. The two parameters that were found to have the most significant impact on the settlement were the creep rate (C_α) and primary compression index (C_c) as shown in Figure 7.32 toFigure 7.35 for the Sowers' and Gourc's models. It can be noted that a small primary compression index results in a larger settlement, because the height of material available at the end of primary consolidation is higher with a lower primary compression index.

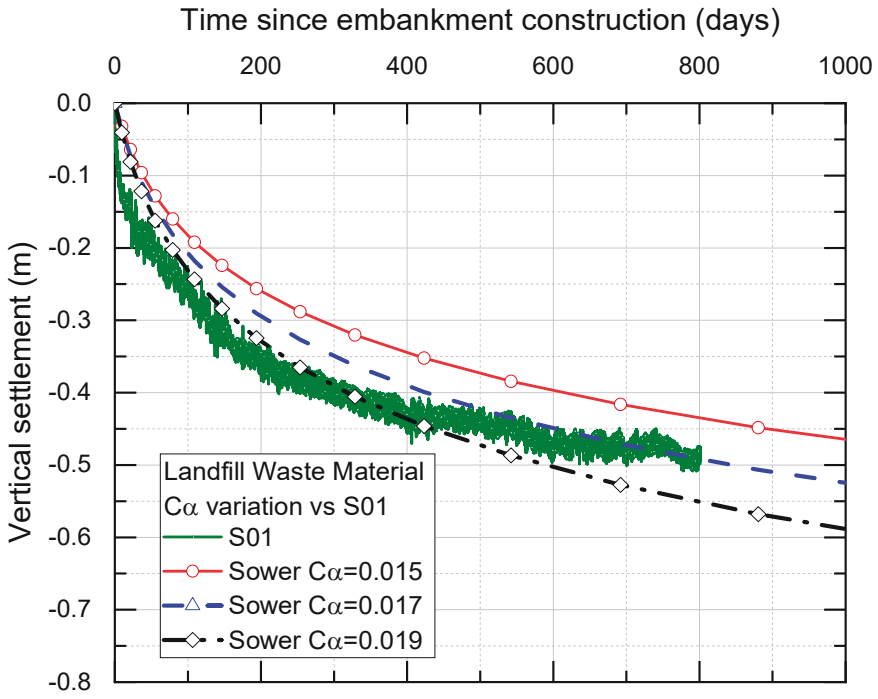

Figure 7.32 Variation effect of C_α on the Sowers 1D settlement prediction model

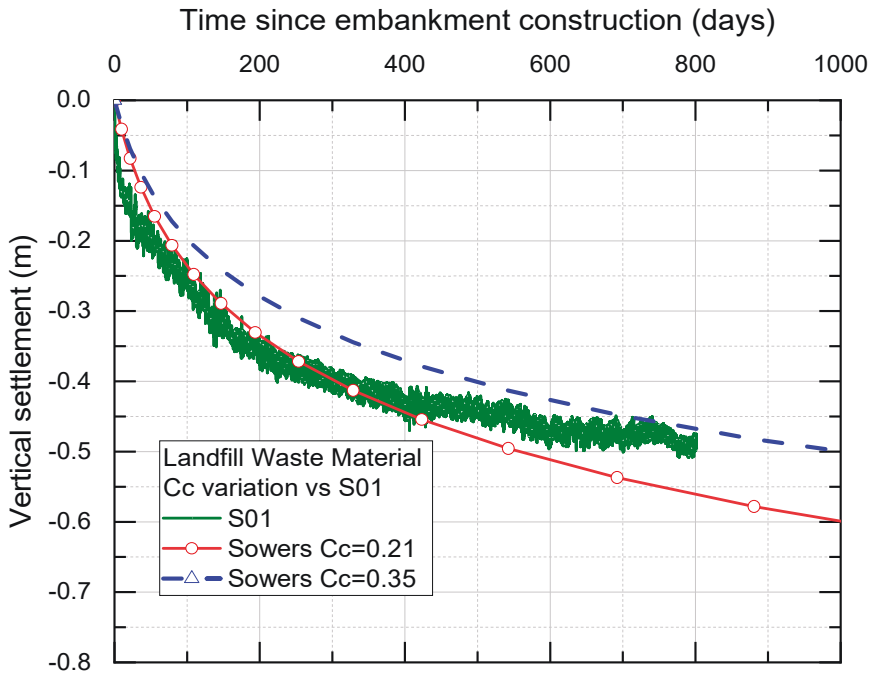

Figure 7.33 Variation effect of Cc on Sowers 1D settlement prediction model

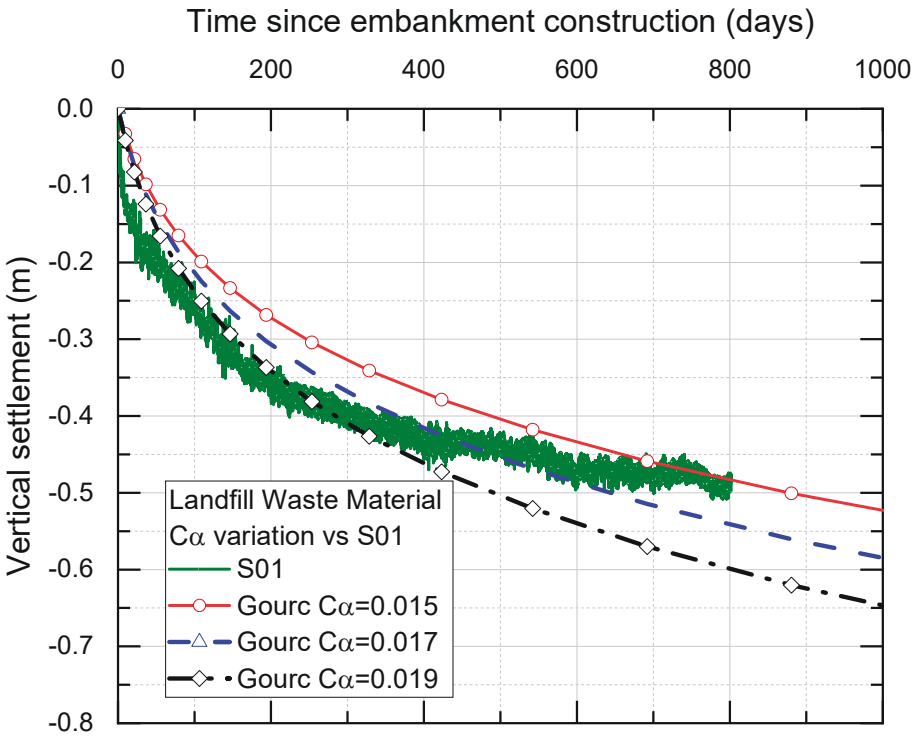

Figure 7.34 Variation effect of C_α on Gourc 1D settlement model

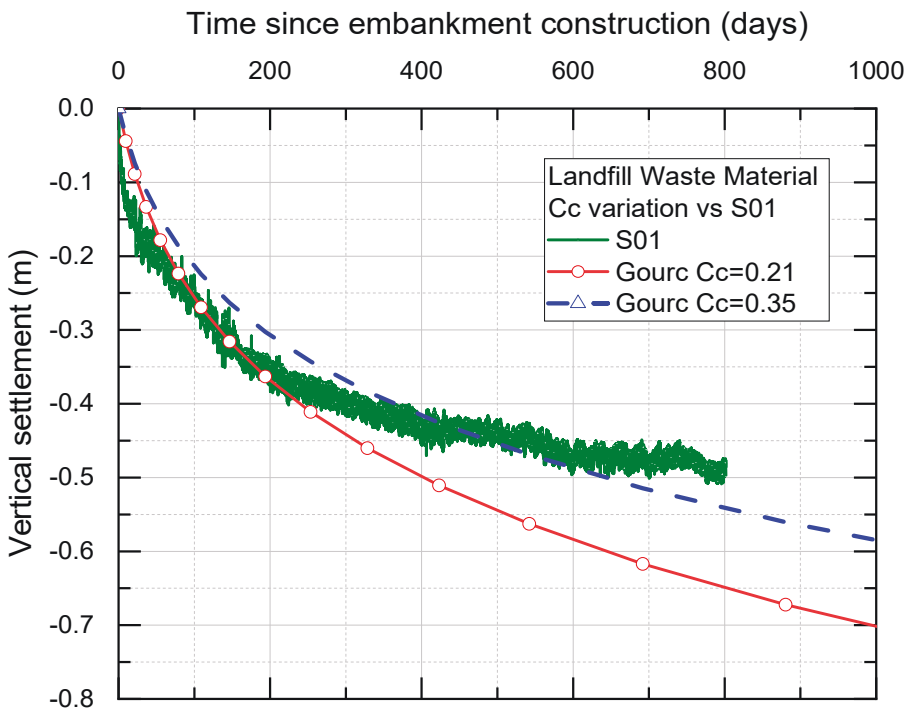

Figure 7.35 Variation effect of Cc on Gourc 1D settlement model

7.3.3 Prediction with PLAXIS 2D

PLAXIS 2D modelling was undertaken with three material models – Mohr Coulomb, soft soil and soft soil creep models. A snapshot of the typical deformed mesh and total displacement profile are presented in Figure 7.36 and Figure 7.37, respectively.

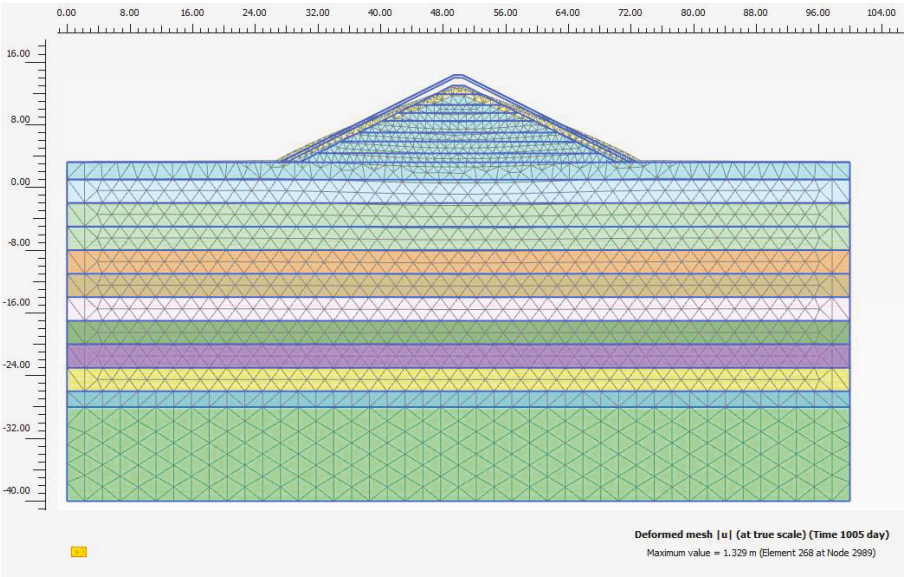

Figure 7.36 Typical deformed mesh under embankment loading

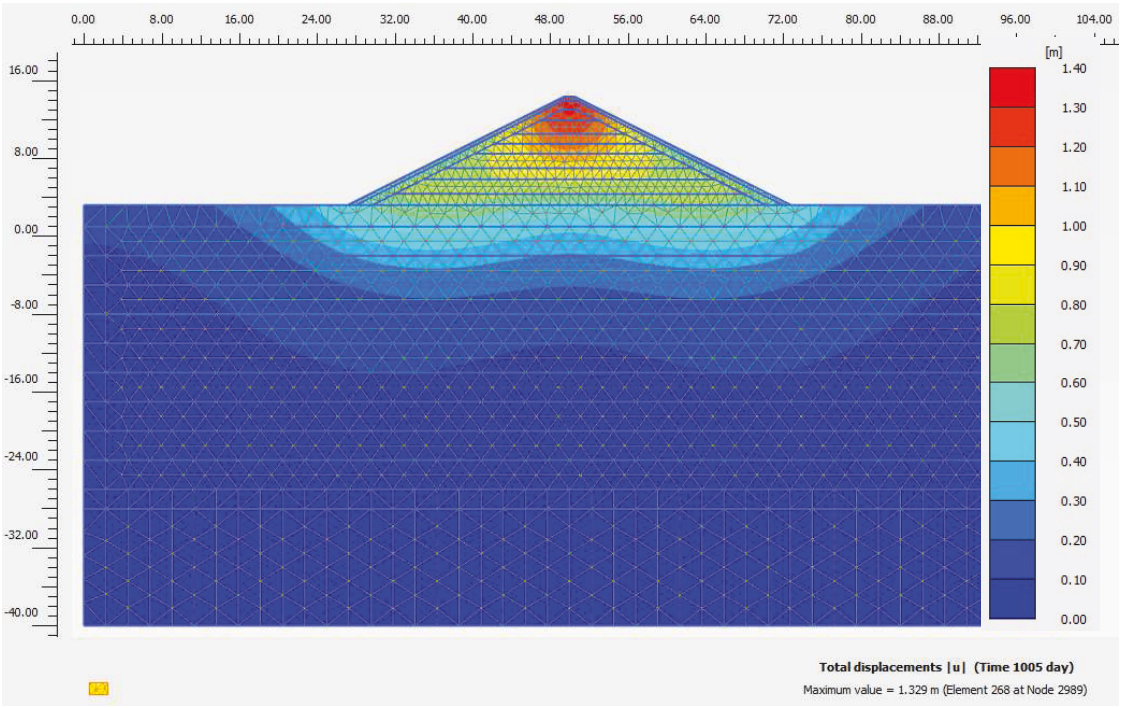

Figure 7.37 Typical displacement contour profile

The Mohr Coulomb and soft soil model do not consider time dependent creep, and so they both significantly underestimate the overall landfill settlement as shown in Figure 7.38 and Figure 7.39. The soft soil creep model when using the same creep rate as the 1D model appears to significantly underestimate the overall landfill settlement. This underestimation is attributed to the lack of consideration of the biodegradation component contributing to landfill settlement, which is considered in the 1D models. A sensitivity of the creep rate using the soft soil model is shown in Figure 7.40. Note that a creep rate of 0.030, which is significantly higher than the field measured creep rate, is necessary to match the soft soil model.

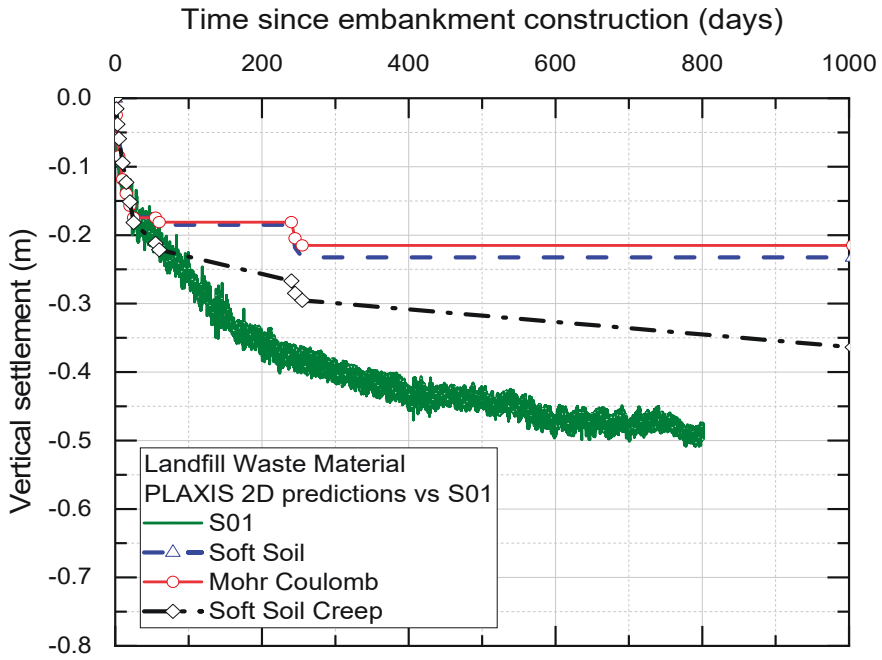

Figure 7.38 PLAXIS 2D settlement prediction and comparison with settlement cell S01

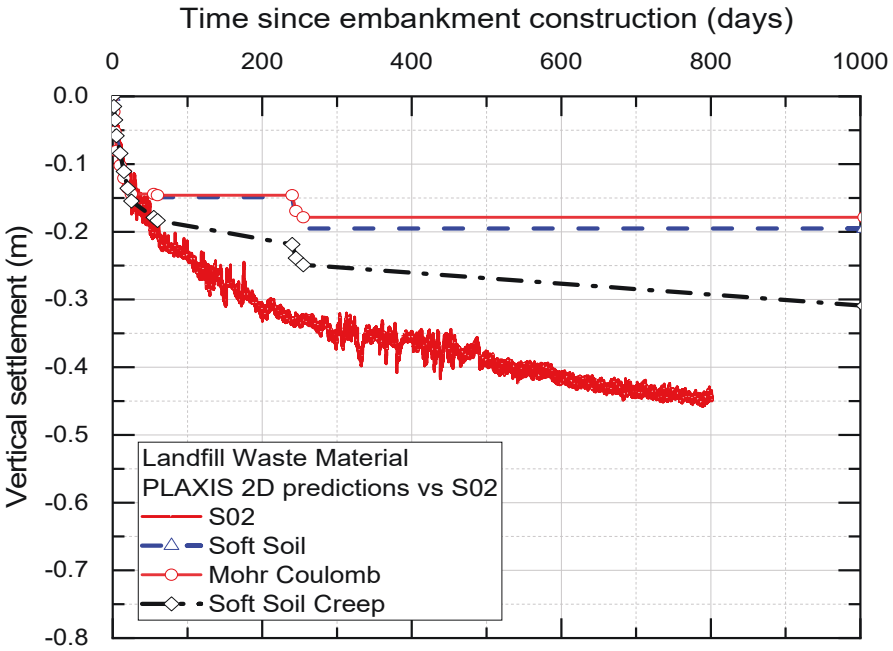

Figure 7.39 PLAXIS 2D settlement prediction and comparison with settlement cell S02

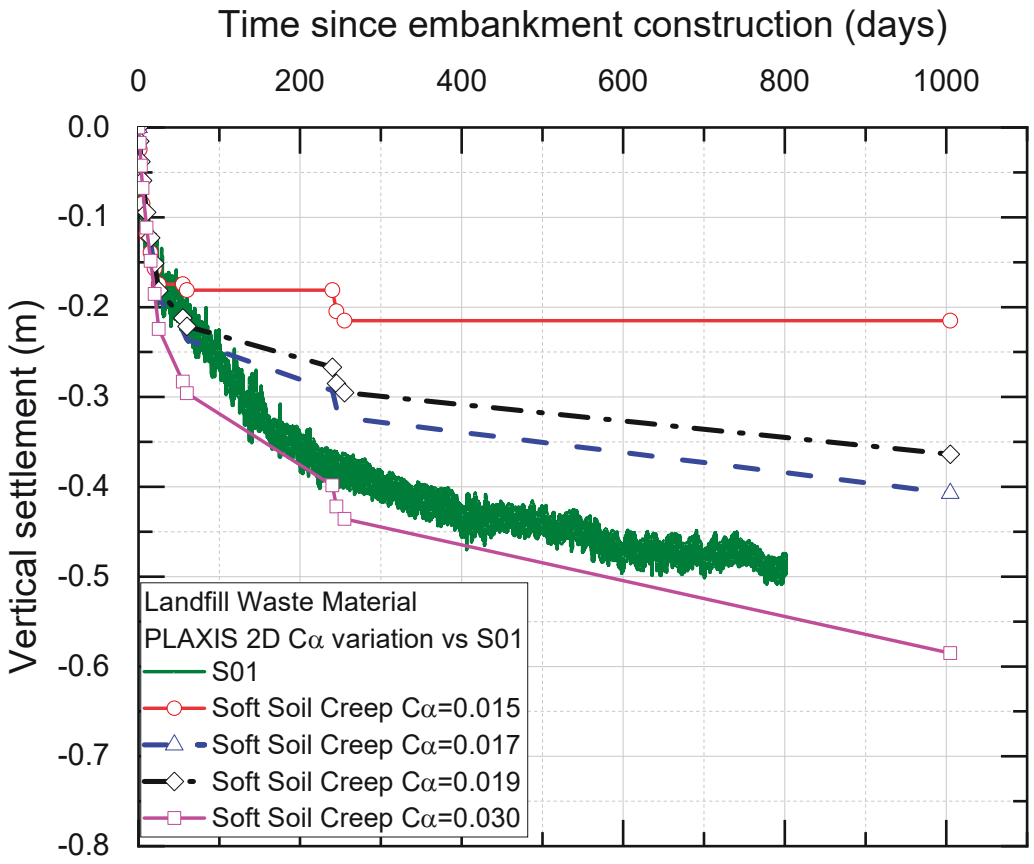

Figure 7.40 Variation effect of C_α on PLAXIS 2D soft soil creep model

7.4 Summary and conclusions

This chapter utilised the site-specific laboratory testing and field testing data to predict landfill settlement to a reasonable accuracy. Landfill settlement predictions were validated through use of field monitoring techniques including settlement cells, extensometers and InSAR techniques. The InSAR monitoring results were accurate in monitoring point data and compared well with settlement cell data. InSAR is a remote monitoring technique that is fast, reliable, accurate and low cost for long term monitoring of landfill settlement. The extensometers were an unsuccessful in monitoring long-term settlement with depth for a number of reasons, postulated to be mainly due to the use of grout between the annulus between the PVC pipe and the landfill.

The uncorrected 1D landfill settlement models by Sowers (1973), Bjarngard & Edgers (1990) and Hossain & Gabr (2005), Machado et al. (2008) and Gourc et al. (2010) all over-predicted the landfill settlement. However, when the initial settlement was corrected,

all the landfill settlement models matched the field landfill settlement profile with reasonable accuracy. The Sower's and Machado's models provided very close results, whilst the Gourc's model provided a higher settlement. The critical parameters identified within the models that are necessary for accurate landfill settlement prediction are the long-term creep and primary compression index as these had the largest impact as shown in the sensitivity charts. The biodegradation components of the models resulted in a minor increase in the settlement, however given the landfill age was 18-32 years old, the impact of biodegradation was significantly less than if it were a fresh landfill.

PLAXIS 2D was used to compare the Mohr-Coulomb, soft soil and soft soil creep models with the field monitoring data. Both the Mohr-Coulomb and soft soil model do not consider time dependent creep and so they under-predict the settlement significantly. The use of the soft soil creep model allowed for time dependent creep, but not biodegradation, and so even with the same inputs from the site specific laboratory testing, the model under-predicts the landfill settlement. Practicing engineers are encouraged to only use PLAXIS 2D for landfill material for short term analysis and rely more so on the 1D models for a more accurate landfill settlement prediction.

The application for future practicing engineers constructing infrastructure above landfills is to undertake site specific testing as this was able to provide a range of values for input into the 1D settlement models. Whilst a correction of the data was still required, this correction in practice can occur after embankment construction whereby the settlement rate is fastest. Understanding the long-term settlement behaviour of the landfill material can provide practicing engineers with the tools to consider ground improvement techniques such as preloading and if long-term maintenance is required rather than defaulting to bored or driven piles to support structures above closed landfills.

Chapter 8 – Conclusions and recommendations

8.1 Summary

In this thesis, practical methodologies for site investigation, laboratory testing and prediction of landfill settlement have been developed for infrastructure built above closed landfills. The site investigation methodology includes a comprehensive set of site investigation techniques undertaken at the landfill comprising of plate load testing, multi-channel analysis of surface waves (MASW), LiDAR and vertical seismic profiling that are able to obtain critical geotechnical parameters for settlement prediction. The critical parameters identified for settlement performance analysis from the field investigations include the unit weight, the moisture content, the organic content, the stiffness parameters and the biodegradation rate.

Furthermore, sampling techniques are described to obtain landfill material with depth and push tube sampling in test pits. These samples were then transported to laboratory and multistage triaxial drained and undrained tests were undertaken. A variety of design parameters for landfill were obtained from the laboratory tests including the long term creep, Young's modulus, the compression and recompression indices, the permeability coefficient and the void ratio.

Parameters from both field investigation and through laboratory testing were used in existing 1D settlement prediction models as well as the finite element analysis, employing PLAXIS 2D software. An embankment at the landfill was instrumented with settlement cells and extensometers and monitored over a period of 2 years. In addition, satellite monitoring using interferometric synthetic aperture radar (InSAR) from the European Space Agency's Sentinel-1 satellite was undertaken to obtain surface settlement. The predictions were compared with the field monitoring results and when initial settlement was corrected, the field settlement matched the predictions with reasonable accuracy. The main outcome of this research is to encourage practicing geotechnical engineers to treat landfill material the same as any other problematic soil and undertake site specific testing to determine landfill design parameters rather than relying heavily on literature. Since prediction methods are reasonable, the use of preloading as a ground improvement technique on landfills to induce settlement can be justified when constructing infrastructure above landfills.

8.2 Concluding remarks

The sections below highlight the conclusions that can be drawn from the present study.

8.2.1 Site investigation and sampling

Landfills are effected by a number of factors therefore site specific field investigation and sampling for laboratory testing is necessary prior to infrastructure being built above closed landfills. A number of field investigation methods were undertaken at the landfill that were able to obtain a number of critical geotechnical design parameters for settlement prediction including:

- Age of waste was determined with depth through LiDAR technology
- Unit weight, moisture content and organic content through test pitting of the landfill surface
- Stiffness was obtained through use of large strain plate load testing and small strain geophysical methods with VSP and MASW
- Biodegradation rate was calculated using landfill gas pumping trial data

8.2.2 Compressibility and strength of reconstituted waste

A reconstituted sample from a depth of 8-10m below the landfill surface was tested in a consolidated drained multistage triaxial test. The main outcomes of this test was to gain compressibility and strength parameters of waste for input into the settlement prediction models. Compression indices, over-consolidation ratio, waste permeability and stiffness were obtained. Long-term creep was obtained through two methods including stress relaxation and consolidation creep. The following trends were observed:

- Permeability was found to increase with void ratio as expected.
- The secondary creep index increased with effective stress in both normally and over-consolidated states.
- A correlation between the over-consolidated and normally consolidated creep indices was establish which can facilitate design preloading for improvement of closed landfills.

8.2.3 Comparison between undisturbed and reconstituted waste

A study was undertaken to determine the difference between undisturbed waste collected using push tube sampling and the same reconstituted sample in terms of strength and compressibility parameters. Multistage consolidated undrained triaxial tests were undertaken in using two tests with the reconstituted sample compacted to the same unit weight as the undisturbed sample. The following trends were observed:

- The testing of the reconstituted sample led to underestimation of landfill creep under 100 kPa effective stress. This underestimation is likely due to the presence of voids and non-uniform compaction of the sample.
- The effect of disturbance for subsequent effective stress stages was found to be negligible.
- For strength parameters, the cohesion was found to be higher in the undisturbed sample, whilst the friction angle was higher in the reconstituted sample.
- The undisturbed sample had a higher stiffness than the reconstituted sample, which is postulated to be formed from structured nature of waste formed over years
- Overall, the undisturbed waste material had a higher creep rate, therefore it is recommended to undertake undisturbed sampling to prevent underestimation of settlement.

8.2.4 Small strain to large strain correlation for landfill waste

A study was undertaken on relatively undisturbed landfill material from the landfill at six varying depths using the UCS test coupled with Hall Effect sensors and bender elements. The outcome of the testing included the following:

- UCS, stiffness and composition were obtained for various depths
- The normalised shear modulus degradation curve decreased with organic content and liquid limit. No trends were observed with depth, specific gravity or UCS values. With the availability of the normalised degradation curve, geotechnical practitioners can either use liquid limit or organic content to determine the small strain to large strain correlation. The use of the correlation allows for small strain data obtained from geophysical testing to be converted into large strain data that is used for settlement assessment. A range of

shear strain data is presented that covers a range of typical structures, including tunnels, retaining walls and foundations.

8.2.5 Landfill settlement prediction and validation through field monitoring

In this thesis, data from laboratory tests and field monitoring were input into existing 1D settlement prediction models and PLAXIS 2D software. An embankment at the landfill was instrumented with settlement cells and extensometers and monitored for a period of 2 years. Satellite monitoring using the InSAR technique was used to monitor surface settlement. Landfill settlement predictions were compared with field monitoring data and the conclusions were as follows:

- InSAR monitoring was proven to be a remote, low cost and accurate long-term measurement for landfill settlement as data compared well with settlement cell monitoring data.
- Uncorrected 1D landfill settlement models overestimated the field settlement.
- Correction of the initial landfill settlement led to a reasonable match with field monitoring data for both settlement cells.
- The back-calculated creep rate from field monitoring data matched well with laboratory testing data.
- The critical parameters identified from the sensitivity analysis is the primary compression index and the secondary creep ratio. The biodegradation component in the models resulted in only a minor increase in settlement since the landfill age was 18-32 years old, this is likely to have a more significant impact for a fresh landfill.
- PLAXIS 2D utilised the Mohr-Coulomb, soft soil and soft soil creep models to estimate the settlement. The Mohr-Coulomb and soft soil models are not recommended for long-term modelling of landfill deposit, since they do not consider the time dependent creep. The soft soil creep model, even with the same creep input values as the 1D settlement models, under-predicts the field settlement. Therefore, the 1D settlement models appear to provide more realistic predictions than PLAXIS 2D for prediction of long-term settlement of closed landfills.
- The usage of parameters from site-specific testing into existing 1D settlement prediction models to estimate landfill settlement has been practically achieved

through this research. Whilst correction of the data was still required, this correction in practice can occur after embankment construction where the settlement rate is fastest.

8.3 Recommendations for further study

This thesis builds on the existing decades of landfill research through practical site investigation methods and laboratory testing to obtain parameters that feed into existing 1D settlement models to predict landfill settlement. This encourages geotechnical engineers to include site specific landfill testing in infrastructure projects constructed above landfills. However, further recommendations to improve this study include:

- Incorporation of the existing 1D settlement prediction models in PLAXIS 2D software. This will allow for geotechnical engineers to implement these landfill specific models easily in readily available software, that can also consider construction staging and ground improvement simulations.
- Incorporation of unsaturated soil mechanics into landfill settlement prediction. Landfill material once placed is not immediately capped and is subject to rainfall over years. This rainfall creates partially saturated material at the time of landfill closure. In some cases, older landfills like the landfill are exposed to groundwater inflow. The incorporation of unsaturated soil mechanics may assist landfill settlement prediction.
- A database of landfill parameters for comparison with site specific testing data. Many researchers have undertaken landfill research studies. However, it is difficult to find one publication or database that covers all testing information. The generation of this database would assist practicing engineers with selection of ball park figures for initial assessments.
- Further undisturbed comparisons with reconstituted samples particularly for creep. The study undertaken demonstrates only one test for comparing disturbed and undisturbed behaviour of landfill material. Further testing to understand this behaviour would assist in justifying the use of undisturbed testing of landfills for site specific testing.
- It is highly recommends to develop and publish a standardised approach for constructing infrastructure above closed landfills. Currently, there is no standard that provides

engineers with options for constructing buildings or transport infrastructures above closed landfill sites.

References

Abmaruzzaman, M., 2010, 'A review on the utilisation of fly ash', *Progress in Energy and Combustion Science*, vol. 36, no. 3, pp. 327-63.

Abreu, A., Gandolfo, O. & Vilar, O., 2016, 'Characterizing a Brazilian sanitary landfill using geophysical seismic techniques', *Waste Management*, vol. 53, pp. 116-27.

Acosta, H.A., 2002, 'Stabilisation of soft subgrade soils using fly ash', University of Wisconsin-Madison, Wisconsin.

Acworth, R.I. & Jorstad, L.B., 2006, 'Integration of multi-channel piezometry and electrical tomography to better define chemical heterogeneity in a landfill leahate plume within a sand aquifer', *Journal of Contaminant Hydrology*, vol. 83, pp. 200-20.

Ajayi, O., Pen, L.L., Zervos, A. & Powrie, W., 2017, 'A behavioural framework for fibre reinforced gravels', *Geotechnique*, vol. 67, no. 1, pp. 56-68.

Akbulut, S. & Saglamer, A., 2002, 'Estimating the groutability of granular soils: a new approach', *Tunnelling and underground space technology*, vol. 17, no. 4, pp. 371-80.

Al-Isawi, R., Idan, I.J., Hassan, A.A., Al-Zubaidi, H.A.M. & Al-Kulabi, N., 2021, 'Evaluation of the hydraulic conductivity for MSW using pilot plant test- A case study of Baghdad city/Iraq', *Environmental and Earth Sciences*, vol. 779, pp. 1-9.

Alexander, A., Burklin, C. & Singleton, A., 2005, *Landfill Gas Emissions Model (LandGEM) Version 3.02 User's Guide*, EPA-600/R-05/047, U.S. Environmental Protection Agency, Washington DC, USA, pp. 1-48.

Ampera, B. & Aydogmus, T., 2005, 'Recent experiences with cement and lime stabilisation of local typical poor cohesive soil', *Geotechnik-Killoquium Freiberg*, vol. Heft 2005-2, pp. 121-44.

Andreas, L., Wikman, K., Berg, M., Sjoblom, R. & Lagerkvist, A., 2003, 'Ash injection for landfill stabilisation', *Proceedings Sardinia 2003, Ninth International Waste Management and Landfill Symposium*, Calgari, Italy.

Arigala, S.G., Tsotsis, T.T., Webster, I.A., Yortsos, Y.C. & Kattapura, J.J., 1995, 'Gas Generation, Transport and Extraction in Landfills', *Journal of Environmental Engineering* vol. 121, no. 1, pp. 33-44.

ASTM, 2003, *Standard test method for bearing capacity of soil for static load and spread footings*, D 1194-94, Philadelphia.

Atkinson, J.H. & Sallfors, G., 1991, 'Experimental determination of soil properties', *Proceedings of the 10th ECSMFE*, vol. 3, Florence, pp. 915-56.

Augustesen, A., Liingaard, M. & Lade, P.V., 2004, 'Evaluation of Time-Dependent Behavior of Soils', *International Journal of Geomechanics*, vol. 4, no. 3, pp. 137-56.

AusGov, 2017, *Waste Management Facilities in Australia*, Geoscience Australia, https://portal.aurin.org.au/.

AusGov, 2020, *Estimating emissions and energy from solid waste and landfill biogas management guideline*, Australian Government - The Clean Energy Regulator, Canberra, Australia, pp. 1-41.

Avalle, D.L. & McKenzie, R.W., 2005, 'Ground improvement of landfill site using the square impact roller', *Australian Geomechanics*, vol. 40, no. 4, pp. 15-22.

Babu, G.L.S. & Ering, P., 2017, 'Role of Stress Deformation behavior of Municipal Solid Waste in landfill design', *Proceedings of the 19th International Conference on Soil Mechanics and Geotechnical Engineering*, International society for soil mechanics and geotechnical engineering, Seoul, pp. 215-30.

Babu, G.S. & Lakshmikanthan, P., 2015, 'Estimation of the components of municipal solid waste settlement', *Waste Management & Research*, vol. 33, no. 1, pp. 30-8.

Bagheri, M., Rezania, M. & Nezhad, M.M., 2019, 'Rate Dependency and Stress Relaxation of Unsaturated Clays', *International Journal of Geomechanics*, vol. 19, no. 12, pp. 1-9.

Balasubramaniam, B., Cai, H., Surarak, C. & Oh, E., 2010, 'Settlement of embankments in soft soil', *Geotechnical engineering journal SEAGS & AGSSEA*, vol. 41, no. 2, pp. 1-19.

Banerjee, A., Puppala, A.J. & Hoyos, L.R., 2020, 'Suction-controlled multistage triaxial testing on clayey silty soil', *Engineering Geology*, vol. 265, pp. 1-15.

Bareither, C.A., Benson, C. & Edil, T., 2013a, 'Compression of Municipal Solid Waste in Bioreactor Landfills: Mechanical Creep and Biocompression', *Journal of Geotechnical and Geoenvironmental Engineering*, vol. 139, no. 7, pp. 1007-21.

Bareither, C.A., Benson, C.H. & Edil, T.B., 2013b, 'Compression behaviour of Municipal Solid Waste: Immediate Compression', *Journal of geotechnical and geoenvironmental engineering*, vol. 138, no. 9, pp. 1047-62.

Bareither, C.A. & Kwak, S., 2015, 'Assessment of municipal solid waste settlement models based on field-scale data analysis', *Waste Management*, vol. 42, pp. 101-17.

Barnard, H.F.T., 2019, 'The importance of plate load tests in geotechnical engineering practice', *Proceedings of the 17th African Regional Conference on Soil Mechanics and Geotechnical Engineering*, International society for soil mechanics and geotechnical engineering Cape Town, South Africa, pp. 345-9.

Bella, G.D., Trapani, D.D., Mannina, G. & Viviani, G., 2012, 'Modeling of perched leachate zone formation in municipal solid waste landfills', *Waste Management*, vol. 32, no. 3, pp. 456-62.

Bjarngard, A. & Edgers, L., 1990, 'Settlement of municipal solid waste landfills', *Proc., 13th Annual Madison Waste Conf.*, Univ. of Wisconsin, Madison, pp. 192–205.

Bo, M.W., Na, Y.M., Arulrajah, A. & Chang, M.F., 2009, 'Densification of granular soil by dynamic compaction', *Proceedings of the Insitution of Civil Engineers Ground Improvement*, vol. 162, no. GI3, pp. 121-32.

Bonaparte, R., Bachus, R.C. & Beth A. Gross, 2020, 'Geotechnical Stability of Waste Fills: Lessons Learned and Continuing Challenges', *Journal of Geotechnical and Geoenvironmental Engineering*, vol. 146, no. 11, pp. 1-24.

Bouazza, A. & Avalle, D.L., 2006, 'Effectiveness of rolling dynamic compaction on an old waste tip', *5th International Congress on Environmental Geotechnics*, Cardiff.

Bouazza, A. & Kavazanjian, E., 2000, 'Characterization of municipal solid waste sites using the continuous surface wave method', paper presented to the *Int. Conf. on Geotechnical & Geological Engineering*, Lancaster USA.

Bray, J.D., Zekkos, D., Kavazanjian, E., Athanasopoulos, G.A. & Riemer, M.F., 2009, 'Shear Strength of Municipal Solid Waste', *Journal of geotechnical and geoenvironmental engineering*, vol. 135, no. 6, pp. 709-22.

Burlingame, M.J., 1985, ' Construction of a highway on a sanitary landfill and its long-term performance', *Transportation Research Record, no. 1031.*

Burlingame, M.J., Egin, D. & Armstrong, W.B., 2007, 'Unit weight determination of landfill waste using sonic drilling methods', *Journal of Geotechnical and Geoenvironmental Engineering*, vol. 133, no. 5, pp. 609-12.

Burnley, S.J., 2007, 'A review of municipal solid waste composition in the United Kingdom', *Waste Management*, vol. 27, pp. 1274-85.

Carlo, L.D., Perro, M.T., Caputo, M.C., Deiana, R., Vurro, M. & Cassiani, G., 2013, 'Characterisation of a dismissed landfill via electrical resistivity tomography and mise-a-la-masse method', *Journal of Applied Geophysics*, vol. 98, no. 1, pp. 1-10.

Carpenter, P.J., Reddy, K.R., ASCE, F. & Thompson, M.D., 2013, 'Seismic imaging of a leachate-recirculation landfill: spatial changes in dynamic properties of municipal solid waste. ', *Journal of Hazardous Toxic Radioactive Waste* vol. 17, no. 4, pp. 331-41.

Castelli, F. & Maugeri, M., 2014, 'Mechanical properties of Municipal Solid Waste by SMDT', *Waste Management*, vol. 34, pp. 256-65.

Chakma, S. & Mathur, S., 2013, 'Postclosure Long-Term Settlement for MSW Landfills', *JOURNAL OF HAZARDOUS, TOXIC, AND RADIOACTIVE WASTE*, vol. 17, no. 2, pp. 81-8.

Chan, A., 2003, 'Determination of the coefficient of consolidation using the least square method', *Géotechnique*, vol. 53, no. 7, pp. 673-8.

Chen, K.S., Chen, R.H. & Liu, C.N., 2012, 'Modeling municipal solid waste landfill settlement', *Journal of Environmental Engineering Science*, vol. 66, no. 8, pp. 2301-9.

Chen, T.H. & Chynoweth, D.P., 1995, 'Hydraulic conductivity of compacted municipal solid waste', *Bioresource Technology*, vol. 51, pp. 205-12.

Chen, Y.M., Zhan, L.T., Wei, H.Y. & Ke, H., 2009, 'Aging and compressibility of municipal solid wastes', *Waste Management*, vol. 29, no. 1, pp. 86-95.

Chiampo, F., Conti, R. & Cometto, D., 1996, 'Morephological characterisation of MSW landfills', *Resources, Conservation and Recycling*, vol. 17, pp. 37-45.

Cho, K. & Mun, S., 2014, 'An analysis of the quality of repeated plate load tests using the harmony search algorithm', *Journal of Applied Mathematics*, pp. 1-5.

Choi, J.H., Dai, S., Lin, J.S. & Seol, Y., 2018, 'Multistage triaxial tests on laboratory-formed methane hydratebearing sediments', *Journal of Geophysical Research: Solid Earth*, vol. 123, pp. 3347–57.

Chouskey, S.K. & Sivakumar Babu, G.L., 2015, 'Constituitive Model for Strength Characteristics of Municipal Solid Waste', *International Journal of Geomechanics*, vol. 15, no. 5, pp. 04014040-1-14.

Chow, Y.K., Yong , D.M., Yong, K.Y. & Lee, S.L., 1992, 'Dynamic compaction analysis', *Journal of Geotechnical Engineering*, vol. 120, no. 8, p. 141.

Cirone, A. & Park, C., 2020, 'MASW survey to estimate the unit weight of municipal solid waste at a landfill in Brazil', *Waste and Resource Management*, vol. 173, no. 1, pp. 1-5.

Clayton, C.R.I. & Khatrush, S.A., 1986, 'A new device for measuring local axial strains on triaxial specimens', *Geotechnique*, vol. 36, no. 4, pp. 593-7.

Clifford, J.M., 1976, 'Impact rolling and construction techniques', *Proceedings of ARRB conference*, Perth, Australia.

Consoli, N.C., Casagrande, M.D.T., Prietto, P.D.M. & Thome, A., 2003, 'Plate Load Test on Fiber-Reinforced Soil', *Journal of geotechnical and geoenvironmental engineering*, vol. 129, no. 10, pp. 951-5.

Consoli, N.C., Montardo, J.l.P., Prietto, P.D.M. & Pasa, G.S., 2002, 'Engineering behaviour of a sand reinforced with plastic waste', *Journal of geotechnical and geoenvironmental engineering*, vol. 128, no. 6, pp. 462-72.

Cossu, R., Andreoletta, G. & Muntoni, A., 1996, *Modelling Landfill Gas Production. Landfilling of Waste: Biogas*, E&FN Spon, London.

Coumoulos, D.G. & Koryalos, T.P., 1997, 'Prediction of attenuation of landfill settlement rates with time', *Proceedings of the 14th International Conference on Soil Mechanics and Foundation Engineering*, vol. 3, ISSMFE, Hamburg, Germany, pp. 1807-11.

de Melo, L., El-Sherbiny, R., Steier, W. & Salem, M., 2012, 'Evaluation of waste compressibility due to preloading at the Fresh Kills landfill', *GeoCongress ASCE*, no. 4184-4193.

DIN 18134, 2012, *Determining the deformation and strength characteristics of soil by the plate loading test*, German Construction Industry Standards Committee, Berlin, Germany.

Diambra, A., Ibraim, E., Muir-Wood, D. & Russell, A.R., 2010, 'Fibre reinforced sands: Experiments and modelling', *Geotextiles and Geomembranes*, vol. 28, no. 3, pp. 238-50.

Dixon, N. & Jones, D., 2005, 'Engineering properties of municipal solid waste', *Geotextiles and Geomembranes*, vol. 23, pp. 205-33.

Dixon, N., Langer, U. & Gotteland, P., 2008, 'Classification and mechanical behavior relationships for municipal solid waste: Study using synthetic wastes', *Journal of geotechnical and geoenvironmental engineering*, vol. 134, no. 1, pp. 79-90.

Dunn, R.J., 1995, 'Design and construction of foundations compatible with solid wastes', *Geotechnical special publication*, vol. 53, pp. 139-59.

Durmusoglu, E., Corapcioglu, M.Y. & Tuncay, K., 2005, 'Landfill Settlement with Decomposition and Gas Generation', *Journal of Environmental Engineering*, vol. 2005, no. 131, pp. 1311-21.

Durmusoglu, E., Sanchez, I.M. & Corapcioglu, M.Y., 2006, 'Permeability and compression characteristics of municipal solid waste samples', *Environmental Geology*, vol. 50, pp. 773-86.

Edil, T., Benson, C., Shafique, S., Tanyu, B., Kim, W. & Senol, A., 2002, 'Field evaluation of construction alternatives for roadway over soft subgrade', *Transportation Research Record Journal of the Transportation Research Board* vol. 1786, no. 1, pp. 36-48.

Edil, T.B., Ranguette, V.J. & Wuellner, W.W., 1990, 'Settlement of municipal refuse', *Geotechnics of waste fills: Theory and practice, STP1070*, eds A. Landva & G.D. Knowles, ASTM, West Conshohocken, pp. 225-39.

El-Fadel, M. & Khoury, R., 2000, 'Modeling Settlement in MSW Landfills: a Critical Review', *Critical Review Environmental Science and Technology*, vol. 30, no. 3, pp. 327-61.

El-Fadel, M., Shazbak, S., Saliby, E. & Leckie, J., 1999, 'Comparitive assessment of settlement models for municipal solid waste landfill applications', *Waste Management Res.*, vol. 17, no. 5, pp. 347-68.

EPA, 2016, *Environmental Guidelines: Solid Waste Landfills*, NSW Environment Protection Authority (EPA), Sydney.

EPA(USA) 2016, *General Crosshole Procedures*, <https://archive.epa.gov/esd/archive-geophysics/web/html/general_crosshole_procedures.html>.

EPA(USA) 2018, *Basic Information about Landfills*, viewed 12 May 2018, <https://www.epa.gov/landfills/basic-information-about-landfills>.

Faour, A.A., Reinhart, D.R. & You, H., 2007, 'First-order kinetic gas generation model parameters for wet landfills', *Waste Management* vol. 27, pp. 946 - 53.

Fatahi, B., 2013, 'Improving geotechnical properties of closed landfills for redevelopment using fly ash and quick lime', Doctoral Dissertation thesis, University of Technology Sydney, Australia.

Fei, X. & Zekkos, D., 2013, 'Factors Influencing Long-Term Settlement of Municipal Solid Waste in Laboratory Bioreactor Landfill Simulators', *Journal of hazardous, toxic, and radioactive waste*, vol. 17, no. 4, pp. 259-71.

Fei, X., Zekkos, D. & Raskin, L., 2016, 'Quantification of parameters influencing methane generation due to biodegradation of municipal solid waste in landfills and laboratory experiments', *Waste Management*, vol. 55, pp. 276-87.

Feng, S.J., 2005, 'Static and dynamic strength properties of municipal solid waste and stability analyses of landfill', *PhD Thesis*, Hangzhou: Zhejiang University.

FHWA 2016, *User guidelines for waste and byproduct materials in pavement construction*, viewed 10 February 2018, <https://www.fhwa.dot.gov/publications/research/infrastructure/structures/97148/cfa53.cfm>.

Fu, Z., Chen, S. & Liu, S., 2016, 'Discrete Element Simulations of Shallow Plate-Load Tests', *International Journal of Geomechanics*, vol. 16, no. 3, pp. 1-12.

Gibson, R.E. & Lo, K.Y., 1961, 'A theory of soils exhibiting secondary compression', *Acta Polytech Scandinavia*, vol. C, no. 10, pp. 1-15.

Gilbert, P.A., 1992, *Effect of sampling disturbance on laboratory-measured soil properties*, US Army Corps of Engineers Miscellaneous Paper GL92-35, Mississippi, USA.

Gomes, C., Lopes, M.L. & Oliveria, P.V., 2013, 'Municipal solid waste shear strength parameters defined through laboratorial and insitu tests', *Journal of the Air and Waste Management Association*, vol. 63, no. 11, pp. 1352-68.

Gomes, C.C., Lopes, M.L. & Oliveira, P.J.V., 2014, 'Stiffness parameters of municipal solid waste', *Bulletin of Engineering Geology and the Environment*, vol. 73, pp. 1073–87.

Gotteland, P., Gourc, J., Alboura, A. & Thomas, S., 2000, 'On site determination of geomechanical characteristics of waste', *Proceedings GeoEng*.

Gourc, J.P., Staub, M.J. & Conte, M., 2010, 'Decoupling MSW settlement into mechanical and biochemical processes - modelling and validation on large scale setups', *Waste Management*, vol. 30, pp. 1556-68.

Graymont New York Materials, 2004, *Lime-treated soil construction manual - Lime stabilisation and lime modification*, National Lime Association, New York.

Grisolia, M., Napoleoni, Q. & Tancredi, G., 1995, 'The Use of Triaxial Tests for The Mechanical Characterization of MSW', *Proceedings of the 5th Sardinia International Landfill Symposium*, Cagliari, Italy, pp. 703-10.

Gruchot, A. & Zydro, T., 2019, 'Shear Strength of Industrial Wastes and Their Mixtures and Stability of Embankments Made of These Materials', *Applied Sciences*, vol. 10, pp. 1-18.

Hamidi, B., Nikraz, H. & Varaksin, S., 2011, 'Dynamic compaction vibration monitoring in a saturated site', *International conference on advances in geotechnical engineering*, Perth, Australia.

He, H., Wu, T., XiaogangWang, Qiu, Z. & Lan, J., 2021, 'Study on Compressibility and Settlement of a Landfill with Aged Municipal Solid Waste: A Case Study in Taizhou', *Sustainability*, vol. 13, pp. 1-13.

Hettiarachchi, C.H., Meegoda, J. & Hettiarachchi, P., 2009, 'Effects of gas and moisture on modeling of bioreactor landfill settlement', *Waste Management*, vol. 29, no. 3, pp. 1018-25.

Horpibulsuk, S., Phojan, W., Suddeepong, A., Chinkulkinjniwat, A. & Liu, M.D., 2011, 'Strength development in blended cement admixed saline clay', *Journal of Materials in Civil Engineering*, vol. 24, no. 2, pp. 184-93.

Hossain, M.S., Gabr, M.A. & Barlaz, M.A., 2003, 'Relationship of compressibility parameters to municipal solid waste decomposition', *Journal of geotechnical and geoenvironmental engineering*, vol. 129, no. 12, pp. 1151-8.

Hossain, M.S., Penmethsa, K.K. & Hoyos, L., 2009, 'Permeability of muncipal solid waste in bioreactor landfill with degradation', *Geotechnical and Geological Engineering*, vol. 27, pp. 43-51.

Hossain, S.M. & Gabr, M.A., 2005, 'Prediction of municipal solid waste landfill settlement with leachate recirculation', *Proceedings of Geo-Frontiers*, vol. 168, Austin, Texas, p. 50.

Houston, S.L., Perez-Garcia, N. & Houston, W.N., 2008, 'Shear strength and shear-induced volume change behavior of unsaturated soils from a triaxial test program', *Journal of Geotechnical and Geoenvironmental Engineering*, vol. 134, no. 11, pp. 1619-32.

Idriss, I.M., Fiegel, G., Hudson, M.B., Mundy, P.K. & Herzig, R., 1995, 'Seismic response of the Operating Industries landfill: Earthquake design and performance of solid waste landfills', *ASCE Geotechnical Special Publication* vol. 54, pp. 83-118.

Incecik, M. & Ceren, I., 1995, 'Cement grouting model tests', *Bulletin of the technical university of Istanbul*, vol. 48, no. 2, pp. 305-17.

IPCC, 2019, *Guidelines for National Greenhouse Gas Inventories: Intergovernmental Panel on Climate Change*, vol. Vol 5-Waste, IGES, Japan.

Ismail, A., 2004, 'Engineering and petrological charestics of clayey silt soils to be used as road base and their improvement by lime and cement', Universitaet Clausthal, Germany.

Ivanov, J., Miller, R.D., Lacombe, P., Johnson, C.D. & Lane, J.W.J., 2006, 'Delineating a shallow fault zone and dipping bedrock strata using multichannal analysis of surface waves with a land streamer', *Geophysics*, vol. 71, pp. A39–A42.

Jastrzębska, M. & Kowalska, M., 2016, 'Triaxial Tests On Weak Cohesive Soils – Some Practical Remarks (Part 2)', *Architecture, Civil Engineering and Environment*, vol. 3, pp. 81-94.

Jessberger, H., 1994, 'Geotechnical Aspects of Landfill Design and Construction,Part 2: Material Parameters and Test Methods', *Proceedings of the Institution of Civil Engineers-Geotechnical Engineering*, vol. 107, no. 2, pp. 105-13.

Karimpour-Fard, M., Machado, S.L., Shariatmadari, N. & Noorzad, A., 2011, 'A laboratory study on the MSW mechanical behavior in triaxial apparatus', *Waste Management*, vol. 31, pp. 1807-19.

Kavazanjian, E., 2001, 'Mechanical properties of municipal solid waste', *Proceedings sardinia*, vol. 1, pp. 415-24.

Kavazanjian, E., Matasovic, N., Bonaparte, R. & Schmertmann, G.R., 1995, 'Evaluation of MSW properties for seismic analysis', *ASCE Geotechnical Special Publication No. 46*, vol. 2, pp. 126-41.

Ke, H., Hua, J., Xu, X.B., Wang, W.F., Chen, Y.M. & Zhan, L.T., 2017, 'Evolution of saturated hydraulic conductivity with compression and degradation for municipal solid waste', *Waste Management*, vol. 65, pp. 63-74.

Kenney, T.C. & Watson, G.H., 1961, 'Multi-stage triaxial for determining c' and phi' of saturated soils', *Proceedings of the 5th International Conference on Soil Mechanics and Foundation Engineering*, Paris, France, pp. 191-5.

Keramati, M., Shahedifar, M., Aminfar, M.H. & Alagipuor, H., 2020, 'Evaluation the Shear Strength Behavior of aged MSW using Large Scale In Situ Direct Shear Test, a case of Tabriz Landfill', *International Journal of Civil Engineering*, vol. 18, pp. 717-33.

Khabbaz, H. & Fatahi., B., 2012, 'Stabilisation of closed landfill sites by fly ash using deep mixing method', *Proceedings of the Fourth International Conference on Grouting and Deep Mixing*, New Orleans, Louisiana, United States.

Kim, D. & Park, S., 2011, 'Relationship between the subgrade reaction modulus and the strain modulus obtained using a plate loading test', paper presented to the *9th world congress on railway research*, France.

Kölsch, F., 1995, 'Material values for some mechanical properties of domestic waste', *Proceedings sardinia*, vol. 95, p. 20.

Konstantaki, L.A., Ghose, R., Draganov, D., Diaferia, G. & Heimovaara, T., 2015, 'Characterization of a heterogeneous landfill using seismic and electrical resistivity data', *Geophysics*, vol. 80, no. 1, pp. EN13-EN25.

Krause, M.J., Chickering, G.W. & Townsend, T.G., 2016, 'Translating landfill methane generation parameters among first-order decay models', *Journal of the Air & Waste Management Association* vol. 66, no. 11, pp. 1084-97.

Kumar, G., Reddy, K.R. & Foster, C., 2021, 'Modeling elasto-visco-bio-plastic mechanical behavior of municipal solid waste in landfills', *Acta Geotechnica*, vol. 16, pp. 1061-81.

Lamborn, J., 2012, 'Observations from using models to fit the gas production of varying volume test cells and landfills', *Waste Management*, vol. 32, pp. 2353-63.

Landpac 2016, *Landpac Intelligent Ground Engineering Services*, viewed 3 February 2018, <http://landpac.com/features-benefits/>.

Landva, A. & Clark, J., 1986a, 'Geotechnical testing of waste fill', *Proceedings, 39th Canadian Geotechnical Conference Ottawa, Ontario*, vol. 3714385.
Landva, A.O. & Clark, J.I., 1986b, *Geotechnicals of Waste Fill - Theory and Practice*, ASTM (American Society for Testing and Materials) STP 1070.
Landva, A.O., Valsangkar, A.J. & Pelkey, S.G., 2000, 'Lateral earth pressure at rest and compressibility of municipal solid waste', *Canadian Geotechnical Journal*, vol. 37, no. 6, pp. 1157-65.
Lapeña, P., Cañizal, J., Castro, J., Da Costa, A. & Sagaseta, C., 2013, 'Mechanical characterisation of MSW using the pressuremeter', *Proceedings of the 18th International Conference on Soil Mechanics and Geotechnical Engineering*, Paris, France.
Lashin, I., Ghali, M., Hussien, M.N., Chekired, M. & Karray, M., 2020, 'Investigation of small- to large-strain moduli correlations of normally consolidated granular soils', *Canadian Geotechnical Journal*, vol. 58, no. 1, pp. 1-22.
Lato, M.J., Anderson, S. & Porter, M.J., 2019, 'Reducing Landslide Risk Using Airborne Lidar Scanning Data', *Journal of geotechnical and geoenvironmental engineering*, vol. 145, no. 9, pp. 1-8.
Leonard, M.L., Floom, K.J. & Brown, S., 2000, 'Estimating Method and Use of Landfill Settlement', *Geotechnical Special Publication*, pp. 1-15.
Leonards, G.A., W.A., C. & Holtz, R.D., 1980, 'Dynamic compaction of granular soils', *Journal of geotechnical enigneering division*, vol. 106, no. 1, pp. 35-44.
Lewis, P.J., Mansfield, J., Ashraf, S. & Zicko, K., 2004, 'Performance of a Highway Embankment Constructed over Landfill Material', *Fifth International Conference on Case Histories in Geotechnical Engineering*, New York.
Lianggang, L., Bing, Z. & Qiang, L., 2014, 'Study on vibration frequency and rock fragmentation effect of sonic drill rig', *Procedia Engineering*, vol. 73, pp. 3-9.
Likitlersuang, S., Surarak, C., Wanatowski, D. & Oh, E., 2013, 'Geotechnical parameters from pressuremeter tests for MRT Blue Line extension in Bangkok', *Geomechanics and Engineering Journal*, vol. 5, no. 2, pp. 99-118.
Lin, C.P. & Lin, C.H., 2016, 'Generalization and Standardization of Multi-station Surface Wave Method for Site Investigation', *5th international conference on geotechnical and geophysical site characterisation*, vol. 1, ISSMGE, Gold Coast, Queensland, Australia, pp. 893-8.
Ling, H.I., Leschchnsky, D., Mohri, I. & Kawabata, T., 1998, 'Estimation of municipal solid waste landfill settlement', *Journal of geotechnical and geoenvironmental engineering*, vol. 124, no. 1, pp. 21-8.
Liu, C.N., Chen, R.H. & Chen, K.S., 2006, 'Unsaturated consolidation theory for the prediction of long term municipal solid waste landfill settlement', *Waste Management Res.*, vol. 24, no. 1, pp. 80-91.
Long, Z., Cheng, Y., Yang, G., Yang, D. & Xu, Y., 2020, 'Study on Triaxial Creep Test and Constitutive Model of Compacted Red Clay', *International Journal of Civil Engineering*, vol. 19, pp. 517-31.
Lukas, R.G., 1986, *Dynamic compaction for highway construction: design and construction guidelines*, US Department of Transportation, Washington.

Machado, S.L., Carvalho, M.F., Gourc, J.-P., Vilar, O.M. & Nascimento, J.C.F.d., 2009, 'Methane generation in tropical landfills: Simplified methods and field results', *Waste Management*, vol. 29, pp. 153-61.
Machado, S.L., Cavalho, M.F. & Vilar, O.M., 2002, 'Constituitive Model for Municipal Solid Waste', *Journal of geotechnical and geoenvironmental engineering*, vol. 128, no. 11, pp. 940-51.
Machado, S.L., Vilar, O.M. & Carvalho, M.F., 2008, 'Constituitive Model for Long Term Municipal Solid Waste Mechanical Behaviour', *Computers and Geotechnics*, vol. 35, no. 5, pp. 775-90.
Machado, S.L., Vilar, O.M., Carvalho, M.F. & Karimpour-Fard, M., 2017, 'A constituitive framework to model the undrained loading of municipal solid waste', *Computers and Geotechnics*, vol. 85, no. 2017, pp. 207-19.
Mair, R.J., 1993, 'Developments in geotechnical engineering research: application to tunnels and deep excavation', *Proceedings of the ICE - Civil Engineering*, vol. 97, pp. 27-41.
Malandraki, V. & Toll, D.G., 2000, 'Drained probing triaxial tests on weakly bonded artificial soil', *Gèotechnique*, vol. 50, no. 2, pp. 141-51.
Marchetti, S., Monaco, P., Totani, G. & Marchetti, D., 2008, 'In situ tests by seismic dilatometer (SDMT)', *ASCE Geotechnical Special Publication* vol. 180, no. 292-311.
Marques, A.C.M., 2001, 'Compaction and compressibility of municipal solid waste', Sao Paulo Univ., Sao Carlos, Brazil.
Marques, A.C.M., Filz, G.M. & Vilar, O.M., 2003, 'Composite compressibility model for municipal solid waste', *Journal of geotechnical and geoenvironmental engineering*, vol. 129, no. 4, pp. 372-8.
Matasovic, N. & Kavazanjian, E.J., 1998, 'Cyclic characterization of OII landfill solid waste', *Journal of Geotechnical and Geoenvironmental Engineering*, vol. 124, no. 3, pp. 197-210.
Mayne, P.W., Jones, J.S. & Dumas, J.C., 1984, 'Ground response to dynamic compaction', *Journal of Geotechnical Engineering*, vol. 110, no. 6, pp. 757-74.
McDougall, J., 2007, 'A hydro-bio-mechanical model for settlement and other behaviour in landfilled waste', *Computers and Geotechnics*, vol. 34, pp. 229-46.
Menard, L. & Broise, Y., 1975, 'Theoretical and practical aspects of dynamic compaction', *Geotechnique*, vol. 25, no. 1, pp. 3-18.
Michalowski, R.L. & Cermak, J., 2003, 'Triaxial compression of sand reinforced with fibres', *Journal of geotechnical and geoenvironmental engineering*, vol. 129, no. 2, pp. 125-36.
Mitchell, A., Lato, M., McDougall, S., Porter, M., Bale, S. & Watson, A., 2017, 'Regional-scale landslide and erosion monitoring utilizing airborne LiDAR change detection analysis', *International Proceedings of the Geological Society of America Annual Meeting*, Geological Society of America, Boulder, Colorado.
Mohamad, R., 2008, *Precompression of soft soils by surcharge preloading - some common pitfalls and misunderstood fundamentals*, Kuala Lumpur.
Mondelli, G., Giacheti, H., Boscov, M. & Elis, V., 2007, 'Geoenvironmental site investigation using different techniques in a municipal solid waste disposal site in Brazil', *Environmental Geology*, vol. 52, pp. 871-87.

Mondelli, G., Giacheti, H.L. & Elis, V.R., 2012, *Geo-Environmental Site Investigation for Municipal Solid Waste Disposal Sites*, Intech, Shanghai.

Muir-Wood, D., 1990, *Soil Behaviour and Critical State Soil Mechanics*, Cambridge Press, Cambridge.

Naveen, B.P., Sivapulliah, P.V., Sitharam, T.G. & Sharma, A.K., 2014, 'Stabilisation of waste dump using fly ash', *National conference on Beneficial Use of Fly Ash in Construction industry and Agriculture*, Bangalore, India.

Nolutshungu, L. & Kalumba, D., 2017, 'Laboratory investigation on shear strength characteristics of soil reinforced with recycled linear low density polyethylene', *Proceedings of the 19th International Conference on Soil Mechanics and Geotechnical Engineering*, International society for soil mechanics and geotechnical engineering Seoul, pp. 467-70.

Okpoli, C.C., 2013, 'Application of 2D Electrical Resistivity Tomography in Landfill. Site: A Case Study of Iku', *Journal of Geological Research*, vol. 1, pp. 1-8.

Ólafsdóttir, E.Á., 2014, 'Multichannel Analysis of Surface Waves: Methods for dispersion analysis of surface wave data', University of Iceland, Iceland.

Oweis, I. & Khera, R., 1986, 'Criteria for geotechnical construction of sanitary landfills', *Int. Symp. on Envir. Geotech.*, ed. H.Y. Fang, vol. 1, Lehigh University Press, Bethlehem, Pa., pp. 205-22.

Oweis, I. & Khera, R., 1998, *Geotechnology of waste management*, PWS, Boston.

Oweis, I.S., 2006, 'Estimate of landfill settlements due to mechanical and decompositional process', *Journal of geotechnical and geoenvironmental engineering*, vol. 132, pp. 644-50.

Park, C.B., Miller, R.D. & Xia, J., 1999, 'Multichannel analysis of surface waves', *Geophysics*, vol. 64, no. 3, pp. 800-8.

Park, H.I. & Lee, S.R., 1997, 'Long-term settlement behavior of landfills with refuse decomposition', *J. Resour. Manage. Technol.*, vol. 24, no. 4, pp. 159-65.

Park, J.-K., Chong, Y.-G., Tameda, K. & Lee, N.-H., 2018, 'Methods for determining the methane generation potential and methane generation rate constant for the FOD model: a review', *Waste Management & Research*, vol. 36, no. 3, pp. 200-20.

Pelkey, S.A., Valsangkar, A.J. & Landva, A., 2001, 'Shear displacement dependent strength of municipal solid waste and its major constituent', *Geotechnical Testing Journal*, vol. 24, no. 4, pp. 381-90.

Penmethsa, K.K., 2007, 'Permeability of municipal solid waste in bioreactor landfill with degradation', Unversity of Texas Arlington, Texas.

Pinard, M.I., 1999, 'Innovative developments in compaction technology using high energy impact compactors', *Proceedings 8th Australia New Zealand Conference on Geomechanics*, Hobart.

Powrie, W., Xu, X.-B., Richards, D., Zhan, L.-T. & Chen, Y.-M., 2019, 'Mechanisms of settlement in municipal solid waste landfills', *Journal of Zhejiang University-SCIENCE A (Applied Physics & Engineering)*, vol. 20, no. 12, pp. 927-47.

Prakash, K. & Sridharan, A., 1989, 'Lime stabilisation and curing effects on the index and compaction characteristics of a montmorllonitic soil', *Journal of Southeast Asian Geotechnical Society*, vol. 20, no. 1, pp. 39-47.

Qubain, B.S., Seksinsky, E.J. & Li, J.C., 2000, 'Transporation research record. Incorporating subgrade lime stabilisation into pavement design', *Geomaterials*, vol. 1721, pp. 3-8.

Raj, P.P., 2011, *Ground improvement techniques*, 7th edn, University Science Press, New Dehli.

Rakic, D., Basaric, I., Caki, L. & Coric, S., 2020, 'Contribution to the geotechnical classification of municipal waste landfills in Serbia', *Environmental Geotechnics*, vol. 7, no. 7, pp. 501-11.

Ramaiah, B.J., Ramana, G.V. & Kavazanjian, E., 2014, 'Undrained Response of Municipal Solid Waste Collected from a Waste Site in Delhi, India', *Geoenvironmental Engineering GSP 241 ASCE*, pp. 130-9.

Reddy, K.R., Gangathulasi, J., Parakalla, N.S., Hettiarachchi, H., Bogner, J.E. & Lagier, T., 2009a, 'Compressibility and shear strength of municipal solid waste under short-term leachate recirculation operations', *Waste Management & Research*, vol. 27, no. 6, pp. 578-87.

Reddy, K.R., Hettiarachchi, C.H., Parakalla, N., Gangathulasi, J., Bogner, J. & Lagier, T., 2009b, 'Hydraulic conductivity of MSW in landfills', *Journal of environmental engineering*, vol. 135, no. 8, pp. 677-83.

Reddy, K.R. & Kumar, G., 2018, 'Modelling Coupled Hydro-Bio-Mechanical Processes in Bioreactor Landfills: Framework and Validation', *International Journal of Geomechanics*, vol. 18, no. 9, pp. 04018102-20.

Rogers, J.D., 2006, 'Subsurface exploration using the standard penetration test and the cone petrometer test', *Environmental and Engineering Geoscience*, vol. 12, no. 2, pp. 161-79.

Roscoe, K.H. & Burland, J.B., 1968, 'On the generalised stress strain behaviour of 'wet clay'', *Engineering plasticity*, eds J. Heyman & F.A. Leckie, Cambridge University Press, pp. 535-609.

Sahoo, J.P., Sahoo, S. & Yadav, V.K., 2010, 'Strength characteristics of fly ash mixed with lime stabilised soil', *Indian Geotechnical Conference, GEOtrendz*, Mumbai.

Seneversa 2012, *Landfill Site Investigation - Allotment 36A, Griffiths Street, Port Fairy*, viewed 4 March 2018, <http://www.moyne.vic.gov.au/files/assets/public/documents/our-community/environment/reports/groundwaterassessmentreport2012.pdf>.

Senol, A., Bin-shafique, M.S., Edil, T.B. & Benson, C.H., 2002, 'Use of class C fly ash for stabilisationof soft subgrade', *Fifth International Congress on Advances in Civil Engineering*, Istanbul, Turkey.

Serridge, C.J. & Synac, O., 2006, 'Application of the rapid impact compaction (RIC) technique for risk mitigation in problematic soils', *10th Congress of the International Association for Engineering Geology and the Environment (IAEG)*, Nottingham, U.K.

Sharma, B., Sridharan, A. & Talukdar, P., 2016, 'Static Method to Determine Compaction Characteristics of Fine-Grained Soils', *Geotechnical Testing Journal*, vol. 39, no. 6, pp. 1048-55.

Sharma, H.D. & De, A., 2007, 'Municipal Solid Waste Landfill Settlement: Postclosure Perspectives', *Journal of geotechnical and geoenvironmental engineering*, vol. 133, no. 6, pp. 619-29.

Sharma, M.S.R., Baxter, C.D.P., Moran, K., Vaziri, H. & Narayanasamy, R., 2011, 'Strength of weakly cemented sands from drained multistage triaxial tests', *Journal of geotechnical and geoenvironmental engineering*, vol. 137, pp. 1202-10.

Sheriff, R.E. & Geldart, L.P., 1982, *Exploration seismology, Data-processing and interpretation*, Cambridge Univ. Press., New York.

Shi, J., Qian, X., Liu, X., Sun, L. & Liao, Z., 2016, 'The behavior of compression and degradation for municipal solid wasteand combined settlement calculation method', *Waste Management*, vol. 55, pp. 154-64.

Shi, J., Shu, S., Ai, Y., Jiang, Z., Li, Y. & Xu, G., 2020, 'Effect of elevated temperature on solid waste shear strength and landfill slope stability', *Waste Management & Research*, vol. 39, no. 2, pp. 351-9.

Singh, M.K., Sharma, J.S. & Fleming, I.R., 2009, 'Shear strength testing of intact and recompacted samples of municipal solid waste', *Canadian Geotechnical Journal*, vol. 46, pp. 1133-45.

Sivakumar Babu, G.L., Reddy, K.R., Chouskey, S.K. & Kulkarni, H.S., 2010, 'Prediction of Long-Term Municipal Solid Waste Landfill Settlement Using Constitutive Model', *Practice Periodical of Hazardous, Toxic, and Radioactive Waste Management*, vol. 14, no. 2, pp. 139-50.

Sormunen, K., Laurila, T. & Rintala, J., 2013, 'Determination of waste decay rate for a large Finnish landfill by calibrating methane generation models on the basis of methane recovery and emissions', *Waste Management & Research*, vol. 31, pp. 979-85.

Sowers, G.F., 1973, 'Settlement of waste disposal fills', *Proc., 8th Int. Conf. on Soil Mechanics and Foundation Engineering*, vol. 2, Moscow, pp. 207-10.

Splajt, T., Ferrier, G. & Frostick, L.E., 2003, 'Application of ground penetrating radar in mapping and monitoring landfill sites', *Environmental Geology*, vol. 44, no. 8, pp. 963-7.

Stark, T.D., Huvaj-Sarihan, N. & Li, G., 2009, 'Shear strength of municipal solid waste for stability analyses', *Environmental Geology*, vol. 57, pp. 1911-23.

Staub, M., Galietti, B., Oxarango, L., Khire, M.V. & Gourc, J.P., 2009, 'Porosity and hydraulic conductivity of MSW using laboratory scale tests', *Third international workshop Hydro-Physio-Mechanics of landfills*, Braunschweig, Germany.

Stoltz, G., Gourc, J.-P. & Oxarango, L., 2010a, 'Liquid and gas permeabilities of unsaturated municipal solid waste under compression', *Journal of Contaminant Hydrology*, vol. 118, pp. 27-42.

Stoltz, G. & Gourc, J.P., 2007, 'Infuence of compressibility of domestic waste on fluid permeability', *Proceedings of the 11th International Waste Management and Landfill Symposium*, Environmental Sanitary Engineering Centre CISA, Calgari, Italy pp. 1-8.

Stoltz, G., Gourc, J.P. & Oxarango, L., 2010b, 'Characterization of the physic-mechanical parameters of MSW', *Waste Management*, vol. 30, no. 8-9, pp. 1439-49.

Tahmoorian, F. & Khabbaz, H., 2020, 'Performance comparison of a MSW settlement prediction model in Tehran landfill', *Journal of Environmental management*, vol. 254, pp. 1-12.

Taylor, D.W., 1948, *Fundamentals of Soil Mechanics*, J. Wiley and Sons, New York.

Tchobanoglous, G. & Kreith, F., 2002, *Handbook of solid waste management*, 2nd Ed. edn, McGraw-Hill, New York.
Thomas, Z.G. & White, D.J., 2003, 'Engineering properties of self-cemeenting fly ash subgrade mixtures', *Proceedingsof the International Ash Utilisation Symposium*, Lexington.
Timoshenko, S. & Goodier, J.N., 1951, *Theory of Elasticity*, McGraw-Hill Book Co., New York.
Trapani, D.D., Bella, G.D., Mannina, G. & Nicosia, S., 2015, 'Influence of the Height of Municipal Solid Waste Landfill on the Formation of Perched Leachate Zones', *Journal of Environmental Engineering*, vol. 141, no. 8, pp. 1-7.
Tsai, C., Kishida, T. & Kuo, C., 2019, 'Unified correlation between SPT–N and shear wave velocity for a wide range of soil types considering strain-dependent behavior', *Soil Dynamics and Earthquake Engineering*, vol. 126, pp. 1-12.
Van Impe, W.F., 1994, *Soil improvement techniques and their evolution*, A.A., Balkema, Rotterdam.
Van Impe, W.F. & Bouazza, A., 1996, 'Densification of domestic waste fills by dynamic compaction', *Canadian Geotechnical Journal*, vol. 33, pp. 879-87.
Viggiani, G. & Atkinson, J.H., 1995, 'Stiffness of fine-grained soil at very small strains', *Geotechnique*, vol. 45, no. 2, pp. 249-65.
Vilar, O.M. & Carvalho, M.F., 2004, 'Mechanical properties of municipal solid waste', *Journal of testing and evaluation*, vol. 32, no. 6, pp. 438-49.
Visontay, E. 2020, 'Lendlease to buy back up to 841 homes at 'sinking' Jordan Springs East site in Sydney', *The Guardian*, 15 Dec 2020.
Wall, D.K. & Zeiss, C., 1995, 'Municipal Landfill Biodegradation and Settlement', *Journal of Environmental Engineering ASCE*, vol. 121, no. 3, pp. 214-23.
Wang, L., Wang, S., Li, G. & Wang, L., 2020, 'Construction of 3D Creep Model of Landslide Slip-Surface Soil and Secondary Development Based on FLAC3D', *Advances in Civil Engineering*, vol. 9, pp. 1-15.
Wang, Y., Zhang, Z., Xu, H., Wu, D., He, X., Fang, Y. & Zhang, Y., 2021, 'Testing the hydraulic conductivity of degraded municipal solid waste in China', *Environmental Geotechnics*, vol. 8, no. 6, pp. 408-15.
Watts, K.S. & Charles, J.A., 2002, ' Initial assessment of a new rapid impact ground compactor', *Proceedings of the 4th International Conference on Engineered Fills*, Kuala Lumpur, Malaysia.
Wichtmann, T., Kimmig, I. & Triantafyllidis, T., 2017, 'On correlations between “dynamic” (small-strain) and “static” (large-strain) stiffness moduli – An experimental investigation on 19 sands and gravels', *Soil Dynamics and Earthquake Engineering*, vol. 98, pp. 72-83.
Wickland, B.E., Wilson, G.W. & Wijewickreme, D., 2010, 'Hydraulic conductivity and consolidation response of mixtures of mine waste rock and tailings', *Canadian Geotechnical Journal*, vol. 47, pp. 472-85.
Witowski, M., 2019, 'Local measurements of axial and radial strains using magnetic encoders in triaxial apparatus', *E3S Web of Conferences*, vol. 92, EDP Sciences, Glasgow, Scotland, pp. 1-4.

Wong, C.T., Leung, M.K., Wong, M.K. & Tang, W.C., 2013, 'Afteruse development of former landfill sites in Hong Kong', *Journal of Rock Mechanics and Geotechnical Engineering*, vol. 5, pp. 443-51.

Woodward, J., 2005, *An introduction to geotechnical processes*, Spon Press, Oxon, U.K.

Xie, M., Aldenkortt, D., Wagner, J.F. & Rettenberger, G., 2006, 'Effect of plastic fragments on hydraulic characteristics of pretreated municipal solid waste', *Canadian Geotechnical Journal*, vol. 43, no. 12, pp. 1333-43.

Yang, R., Xu, Z., Chai, J., Qin, Y. & Li, Y., 2016, 'Permeability test and slope stability analysis of municipal solid waste in Jiangcungou Landfill, Shaanxi, China', *Journal of Air & Waste Management*, vol. 66, no. 7, pp. 655-62.

Yen, B.C. & Scanlon, B.S., 1975, 'Sanitary landfill settlement rates.'", *Journal of Geotechnical engineering*, vol. 101, no. 5, pp. 475-87.

Yin, K., Tong, H., Giannis, A., Wang, J. & Chang, V.W.C., 2017, 'Multiple geophysical surveys for old landfill monitoring in Singapore', *Environmental Monitoring Assessment*, vol. 189, no. 20, pp. 1-13.

Yin, Z.H., Zhu, Q.Y., Yin, J.H. & NI, Q., 2014, 'Stress relaxation coefficient and formulation for soft soils', *Geotechnique Letters* vol. 4, pp. 45-51.

Young, A., 1989, 'Mathematical modeling of landfill degradation', *J. Chem. Technol. Biotechnol.,*, vol. 46, no. 189-208.

Zekkos, D., 2005, 'Evaluation of static and dynamic properties of municipal solid waste', A dissertation submitted in partial satisfaction of the requirements for the degree of Doctor of Philosophy in Geotechnical Engineering thesis, University of California, Berkeley.

Zekkos, D., Bray, J.D., Jr., E.K., Matasovic, N., Rathje, E.M., Riemer, M.F. & II, K.H.S., 2006, 'Unit Weight of Municipal Solid Waste', *Journal of Geotechnical and Geoenvironmental Engineering*, vol. 132, no. 10, pp. 1250-61.

Zekkos, D., Bray, J.D. & Riemer, M.F., 2008, 'Shear modulus and material damping of municipal solid waste based on large-scale cyclic triaxial testing', *Canadian Geotechnical Journal*, vol. 45, pp. 45-58.

Zekkos, D., Bray, J.D. & Riemer, M.F., 2012, 'Drained response of municipal solid waste in large-scale triaxial shear testing', *Waste Management*, vol. 32, pp. 1873-85.

Zekkos, D. & Fei, X., 2017, 'Constant load and constant volume response of municipal solid waste in simple shear', *Waste Management*, vol. 63, pp. 380-92.

Zekkos, D., Jr., E.K., Bray, J.D., Matasovic, N. & Riemer, M.F., 2010, 'Physical Characterization of Municipal Solid Waste for Geotechnical Purposes', *Journal of geotechnical and geoenvironmental engineering*, vol. 136, no. 9, pp. 1231-41.

Zekkos, D., Kabalan, M. & Flanagan, M., 2013, 'Lessons learned from case histories of dynamic compaction at municipal solid waste sites', *Journal of geotechnical and geoenvironmental engineering*, vol. 139, no. 5, pp. 738-51.

Zekkos, D., Matasovic, N., El-Sherbiny, R., Athanasopoulos-Zekkos, A., Towhata, I. & Maugeri, M., 2011, 'Dynamic Properties of Municipal Solid Waste', *Geotechnical characterization, field measurement and laboratory testing of municipal solid waste*, vol. 41146, no. 209 GSP, pp. 112–34.

Zekkos, D. & Riemer, M.F., 2006, 'Shear modulus reduction and material damping relations for municipal solid waste', *Proceedings of the 8th U.S. National Conference on Earthquake Engineering*, San Francisco, California, USA, pp. 1-11.

Zekkos, D., Sahadewa, A., Woods, R.D. & II, K.H.S., 2014, 'Development of Model for Shear-Wave Velocity of Municipal Solid Waste', *Journal of geotechnical and geoenvironmental engineering*, vol. 140, pp. 04013030-1-14.

Zhao, Y., Ling, X., Gong, W., Li, P., Li, G. & Wang, L., 2020, 'Mechanical Properties of Fiber-Reinforced Soil under Triaxial Compression and Parameter Determination Based on the Duncan-Chang Model', *Journal of Applied Sciences*, vol. 10, no. 9043, pp. 1-16.

Appendices

Appendix A – Summary of site investigation techniques

Investigation method	Geophysical[2]	Boreholes	Test Pits	SPT	CPT / CPTu / RCPTu / SCPTu	SMDT	Pressuremeter
Intrusive / non-intrusive	Intrusive / non-intrusive	Intrusive	Intrusive	Intrusive	Intrusive	Intrusive	Intrusive
Effective depth	Up to **100 m**	Limited to base of landfill lining system	Typically **3 m**	Limited to base of landfill lining system / refusal from landfill waste	Limited to base of landfill lining system / refusal from landfill waste	Previous literature to depth of **20 m** below ground level	Limited to borehole depth / base of landfill lining system
Parameters obtained	Geological profile, Shear velocity & Shear modulus	Refer Note [1]	Refer Note [1]	Refer Note [1]	Resistivity, pH, temperature, pore pressure, shear wave velocity & shear modulus	Shear velocity & Shear modulus	Shear modulus & Inaccurately shear velocity
Availability of previous case studies on landfills	Numerous case studies	Numerous case studies	Numerous case studies	Numerous case studies	Numerous case studies	Limited case studies	Limited case studies
Physical samples obtained and laboratory testing required	No	Yes	Yes	Yes	No	No	No
Key benefits	Most methods are non-intrusive	Physical samples collected allow for accurate parameters to be determined	Physical samples collected allow for accurate parameters to be determined	Can be completed concurrently to borehole	A lot of data obtained from single penetration	Cheap and fast, no waste disposal requirements	Cheap and fast, no waste disposal requirements
Key limitations	Difficult to interpret data obtained from testing	Expensive to drill, sample disposal is expensive & can fail to capture heterogeneous nature of waste	Limited investigation depth & sample disposal is expensive	requires borehole therefore expensive & sample is highly disturbed	Likely to hit refusal & investigation is localised to penetration	Limited information obtained & difficult to interpret testing data	Limited information obtained & difficult to interpret testing data

Notes:

1. Physical samples obtained from testing methods are sent to be tested in laboratory conditions. Lab tests for landfills can comprise of waste classification and composition (by dry material weight), direct shear strength, particle size distribution, Atterberg limits, California Bearing Ratio (CBR), chemical suite (for soils and ground water) and moisture content. Note that collection and testing of landfill samples in laboratory conditions can be expensive to transport and dispose. Sample accuracy is typically greater for laboratory samples than field measurements.
2. Geophysical methods consist of a range of individual methods. Information presented in the table is for MASW, electrical resistivity, GPR & cross hole tomography.

Appendix B – Summary of settlement models

Model name	Settlement considered		Basis for equations (large scale landfill, experiment or theory)	Benefits	Limitations
	Primary	Secondary			
Soil Mechanics					
Sowers (1973)	Yes	Yes	Based on data collected from a number of landfills	Simple calculation method	Difficult to attain accurate site specific landfill compression ratios Does not properly address secondary settlement
Hossain & Gabr (2005)	No	Yes	Field experiment on a landfill		
Empirical Models					
Logarithmic function (Yen & Scanlon, 1975)	No	Yes	Based on data collected from a number of landfills	Simple calculation method	Very simplified equations which do not accurately capture landfill specific properties Difficult to obtain compression factors Does not properly address secondary settlement
Power creep model (Edil et al., 1990)	Yes	Yes			
Hyperbolic equation (Ling et al., 1998)	Yes	Yes			
Attenuation equation (Coumoulos & Koryalos, 1997)	No	Yes			
Rheological models					
Gibson & Lo (1961)	Yes	Yes	Theory based equation	Comparison of landfill waste to peaty soils for modelling settlement	Difficult to obtain compression factors
Biodegradation models					
Park and Lee model (1997)	No	Yes	Theory based equation	Consider biodegradation factors in equations	Difficult to attain parameters required for equations Calculations are tedious and time consuming
Hettiarachchi model (2009)	Yes	Yes			
Marques model (2001)	Yes	Yes	Based on data collected from a number of landfills	Considers waste lift thickness Simple calculation method	Significant landfill records required for accurate calculation – likely to be unavailable for older landfills
Marques model (2003)	Yes	Yes			

Model name	Settlement considered		Basis for equations (large scale landfill, experiment or theory)	Benefits	Limitations
	Primary	Secondary			
Gourc (2010)	No	Yes	Theory based equation with supporting experimental data	Simple calculation method	Difficult to obtain compression factors Does not consider pH & temperature of waste
Bareither model (2012)	Yes	Yes	Field experiment on a landfill	Simple calculation method	Does not consider previous literature factors, rather proposes new method which still requires validation
Constitutive Models					
Machado (2002)	Yes	Yes	Theory based equation with supporting experimental data	Practical with parameters able to be determined from lab tests	Large number of parameters, however they are all obtainable from simple triaxial compression and oedometer tests Requires further validation using field data
Machado (2008)	Yes	Yes			
Machado (2017)	Yes	Yes			
Sivakumar Babu (2010)	Yes	Yes	Theory based equation with supporting experimental data	Considers mechanical, creep and biodegradation	Requires further validation using field data
Chouskey & Sivakumar Babu (2015)	Yes	Yes		Considers elastic, plastic, creep and biodegradation	
HBM model (2018)	Yes	Yes	Theory based equation with supporting experimental data	Considers mechanical, creep, biodegradation, unsaturation	Model uses Mohr-Coulomb criteria, which is not the best representation for landfill settlement
Note: All methods still have variability and difficulty in obtaining secondary compression elements (where compression factors or ratios are used). Constitutive equations have shown the best reliability and accuracy for determining landfill settlement. The most practical method due to obtainable parameters from simple testing methods, with a considerable number of landfill input factors is the Machado (2017) model.					

Appendix C – Summary of ground improvement techniques

	Dynamic compaction	**Rapid impact Compaction**	**Preloading**	**High Energy Impact Compaction**	**Vibro Compaction and vibro replacement**	**Chemical stabilisation**	**Geocells**
Design intent	Densification of waste by applying high energy impacts	Densification of waste by applying energy	Densification of waste by applying surcharge load	Densification of waste by applying energy	Compaction via vibration techniques	Fill voids (permeability grouting) or compaction grouting	Reduce load impact on landfill
Depth of application	**4 – 9 m** below landfill surface (depending on applied energy)	**2 – 4 m** below landfill surface (depending on applied energy)	Up to **20 m** below landfill surface (depending on surcharge)	Up to **2 m** below landfill surface	Unlimited	Unlimited	On landfill surface
Cost and time factors	Fast method, however requires multiple passes, and craters to be backfilled with material	Faster than dynamic compaction, still requires multiple passes and craters to be backfilled	Preloading material cost, typical surcharge period ranges between 3 – 12 months	Very fast method, however only effective for shallow landfill compaction, requires multiple passes	Costly for material replacement, difficult to vibro compact waste so additional time considerations required	Costly for supply of chemical additives, requires installation of perforated pipes for chemical insertion	Labour intensive for initial layout of geocells, filling geocell pockets can be time consuming
Suitability for landfills	Not suitable for shallow (< 2m) or very deep (>10m) applications	Effective for densifying waste, not deep applications	Effective for densifying waste, not for shallow applications	Effective for densifying waste at shallow level only	Not suitable for landfills due to installation difficulty	Suitable, however limited ground improvement effectiveness	Suitable for limiting load related settlement on landfill
Labour and equipment requirements	Dynamic compaction rig and small excavator / loader	RIC rig with small excavator / loader	Loaders and rollers	HEIC rig and roller (if smooth surface required)	Vibration probe, pressured air/water supply and replacement material	Continuous supply of chemical additive, mixing equipment and borehole rig (for pipe installation)	Manual labour for geocell installation, filling with excavator and roller for compaction
Potential methods for monitoring effectiveness	Surface wave analysis, settlement plates, hydrostatic pressure gauges, periodic site survey, intrusive ground techniques (CPT, boreholes or CBR samples) or geophysical methods. Note surface wave analysis has proven to be effective as a non-intrusive method of determining effectiveness of ground improvement on landfills.						
Key limitations	Environmental pollution (dust, noise, air) Import material cost (if required)	Environmental pollution (dust, noise, air) Import material cost (if required)	Waiting period for settlement Import material cost (if required)	Only suitable for shallow applications	Not suitable for landfills due to installation difficulty	Effect of ground improvement is minimal	Does not address primary, secondary or creep landfill settlement
Previous experience	Numerous successful landfill applications	Numerous successful landfill applications	Numerous successful landfill applications	Numerous successful landfill applications	Not commonly used for landfill application	Not commonly used for landfill application	Not commonly used for landfill application